

https://dspace.org/

Prognostic influence of myc aberrations and other clinicopathological factors of aggressive b-cell non-Hodgkin lymphomas

Pather, Sugeshnee

2024

https://hdl.handle.net/10539/37605

Downloaded from a DSpace repository. https://dspace.org/

PROGNOSTIC INFLUENCE OF *MYC* ABERRATIONS AND OTHER CLINICOPATHOLOGICAL FACTORS OF AGGRESSIVE B-CELL NON-HODGKIN LYMPHOMAS

DR. SUGESHNEE PATHER

Thesis statement: A thesis submitted to the Faculty of Health Sciences, University of the Witwatersrand, Johannesburg, in fulfilment of the requirements for the degree of Doctor of Philosophy (ANAP9000).



(signature)

Johannesburg, 2023.





DECLARATION

I, Sugeshnee Pather, declare that this research is my own, unaided work, which is being submitted for the degree of Doctor of Philosophy (Ph.D.), to the University of the Witwatersrand, Johannesburg. This thesis has not been submitted for any other degree or examination at this or any other University.



24/01/2023

Signature **Date**

DEDICATION

I sincerely dedicate this thesis to

the patients at Chris Hani Baragwanath Academic Hospital,

my heroic colleagues at the frontline,

my dedicated colleagues at the laboratory,

my supportive family,

all the teachers who contributed to my education

and the Almighty Lord.

Thank you for infusing this research with immense inspiration.

For decades you have inspired me to

pitch up with a positive attitude,

pay attention

and persevere.

PUBLICATIONS ARISING FROM THIS STUDY

Pather S., Mashele T., Willem P., et al. (2021) *MYC* status in HIV-associated plasmablastic lymphoma: dual-colour-CISH, FISH and immunohistochemistry. *Histopathology* 79(1): 86-95.

Pather S. and Patel M. (2022) HIV-associated DLBCL: Clinicopathological factors including dual-colour chromogenic *in situ* hybridisation to assess *MYC* gene copies. *Annals of Diagnostic Pathology* 58: 151913. https://doi.org/10.1016/j.anndiagpath.2022.151913

ABSTRACT

Introduction: Up to 30% of cancers in Africa are linked to infectious agents and in the context of the aggressive B-cell non-Hodgkin lymphomas (NHL), human immunodeficiency virus (HIV) infection is an established risk factor. Aggressive B-cell NHLs are frequently confirmed at the Chris Hani Baragwanath Academic Hospital due to the high seroprevalence of HIV infection. Therefore, an array of clinicopathological characteristics of these tumours was evaluated with the aim of identifying poor prognostic factors.

Materials and methods: HIV-associated plasmablastic lymphoma (PBL), HIV-associated diffuse large B-cell lymphoma (DLBCL) and DLBCL, not otherwise specified (NOS) were included from October 2013 to June 2017. Formalin-fixed paraffin-embedded tissue sections were subjected to c-MYC immunohistochemistry (IHC), dual-colour chromogenic and fluorescence *in situ* hybridisation (CISH and FISH) for assessment of *MYC* gene rearrangement and *MYC* gene copy number enumeration. Thereafter, the clinicopathological characteristics were explored.

Results: The study included 67 PBL patients and 63/64 (98%) were HIV-seropositive. HIV-associated PBL was typified by a mean age of 41 (standard deviation [SD] ± 10.1) years and a 54% female predominance. The patients received combination antiretroviral therapy (c-ART) prior to, or shortly after, the lymphoma diagnosis was confirmed. The median CD4 count was 170 (interquartile range [IQR] 249) cells/mm^3 and 37% of the patients had CD4 counts <100 cells/mm^3. The median viral load was 55 587 (IQR 273 582) copies/mL and 15% of patients had a lower than detectable limit viral load. Advanced stage of lymphoma, i.e., Ann Arbor stage III-IV, occurred in 77% of the patients and there was a predominance of extra-oronasal topographic involvement. A starry-sky (SS) appearance was documented in 33% of these tumours, mainly in association with monomorphic morphology (P=0.02). Expression of c-MYC protein (i.e., ≥40%) occurred in 81% of PBL. Epstein-Barr virus (EBV) latent infection was detected in 90% of these tumours by utilising CISH. *MYC* gene aberrations included *MYC* rearrangement (70%) and a low-level increase in *MYC* gene copy numbers (43%). Concurrent *MYC* rearrangement with increased *MYC* gene copy numbers (49%) were also detected. In addition, there was low-level polysomy of chromosome (C) 8 (6%). *MYC* aberrations in HIV PBLs were significantly associated with a SS appearance (P=0.01), monomorphic morphology (P=0.03), c-MYC protein expression (P=0.03) and mortality (P=0.03). The median overall survival (OS) for HIV PBL was 75 days (95% CI 14–

136). *MYC* aberrations in HIV PBL did not significantly influence the median OS [*MYC*+ 65 days (95% CI 0–143 days) and *MYC*- 71 days (95% CI 3–139 days), *P*=0.61].

There were 22 HIV seronegative DLBCL, NOS patients (19%) with a mean age of 57 (SD ±16.7) years and a 59% male predominance. There were 93 patients (81%) with HIV-associated DLBCL, typified by a mean age of 42 (SD ±10.8) years and a 55% male predominance. The HIV seropositive patients were significantly younger at the time of presentation with lymphoma (*P* <0.01). c-ART was commenced prior to, or shortly after, the lymphoma diagnosis was confirmed. The median CD4 count was 162 (IQR 215) cells/mm^3 and 33% of the patients had CD4 counts <100 cells/mm^3. The median viral load was 217 (IQR 182 981) copies/mL and 30% of the patients had a lower than detectable limit viral load. An advanced stage of lymphoma, i.e., stage III-IV, at presentation occurred in 87% of the patients. HIV DLBCL demonstrated a germinal centre (GC) and non-germinal centre (NGC) immunophenotypic cell of origin (COO) in 53% and 47%, respectively. Expression of c-MYC protein occurred in 58% of the HIV DLBCLs and this was significantly associated with a SS appearance (*P*=0.04) and high tumour proliferation indices, i.e., Ki-67 ≥90%, (*P*<0.01). Double expression of c-MYC and BCL2 proteins were significantly associated with the NGC COO immunophenotype (*P*<0.01). *MYC* aberrations included a low-level increase of *MYC* gene copy numbers (57%) and *MYC* rearrangements (12%). Infrequently, C8 polysomy, *MYC* gene clusters and concurrent *MYC* rearrangement with increased *MYC* gene copies were also identified in HIV DLBCL. The median OS was 228 days (95% CI 54–402) and 825 days (95% CI 309–1341) in the HIV seropositive and seronegative DLBCL groups, respectively (*P*=0.08). Compared with the HIV seronegative DLBCL group, an inferior median OS outcome occurred in the HIV seropositive group when the CD4 counts were <100 cells/mm^3 (*P*=0.04) and when the Internal Prognostic Index (IPI) was 3–5 (*P*=0.01). *MYC* aberrations did not significantly influence the median OS [*MYC*+ DLBCL 155 days (95% CI 0–356) and *MYC*- DLBCL 154 days (95% CI 53–256), *P*=0.67]. In the multivariate regression analysis, the presence of concomitant infections negatively impacted the overall survival (hazard ratio 4.01 [95% CI 1.86–12.20], *P*=0.02).

Conclusion: An array of clinicopathological features of aggressive B-cell NHLs was explored. Greater awareness of these aggressive tumours, early and accurate diagnosis, timeous referral and appropriate treatment, may improve the outcome of the patients who tend to present with advanced

stage disease, IPI scores of 3-5 and low CD4 counts. In many regions of the world, the timeous implementation of c-ART has led to a noteworthy reduction in the incidence of HIV-associated NHL. Accordingly, a decline in the incidence of aggressive HIV-associated B-cell NHL in SA is optimistically anticipated.

ACKNOWLEDGEMENTS

Professor Moosa Patel has inspired many generations of healthcare workers with his outstanding medical expertise, remarkable empathy towards patients and saintly humility. I sincerely thank Professor Patel for his invaluable contribution to this research. Working with such a dedicated expert is indeed a privilege for which I am very grateful.

Professor Martin J. Hale encouraged me to embark on this doctoral journey within Anatomical Pathology. His kindness, empathy and academic support are appreciatively acknowledged.

The staff within the Division of Anatomical Pathology at CHBAH provided essential support and assistance, which I truly appreciate.

The supplier, Roche, and their staff provided technical guidance and consistent support during troubleshooting and optimisation of the dual-colour CISH staining procedure.

The researcher appreciatively acknowledges the staff bursaries that were received from the University of the Witwatersrand and the National Health Laboratory Service.

FUNDING ACKNOWLEDGEMENTS

The researcher appreciatively acknowledges the funding grants that were received from:

- National Health Laboratory Service Research Trust (grant number 004_ 94538).
- University of the Witwatersrand, Faculty Research Committee for Individual Research (grant number 001.283.8462101.5121105.5152).
- University of the Witwatersrand, Faculty of Health Sciences Seed Funding (grant number 001 251 8462101 5121105 000000 0000000000 4550).
- The Division of Anatomical Pathology, School of Pathology, Faculty of Health Sciences, at the University of the Witwatersrand.
- The researcher also acknowledges the invaluable biostatistical and epidemiology training that occurred due to scholarship support from the South African Tuberculosis AIDS Training / Fogarty International Centre (grant number 3U2RTW007370-05S1).

LIST OF FIGURES

Figure 2.1: DLBCL cytomorphology: centroblastic (A), immunoblastic (B) and anaplastic (C)..19

Figure 3.1: c-MYC immunohistochemistry on external control tissue sections demonstrating positive nuclear staining in keratinocytes (A) and DLBCL (D). No nuclear immunoreactivity noted in salivary gland parenchyma (B) and (C) eccrine glands (magnification x200)…...…….52

Figure 3.2: Dual-colour CISH displaying intranuclear black signals of *MYC* and red signals of CEN8 in the external control epithelial cells (A) and (B) [magnification x400]..……....60

Figure 4.1: Starry-sky appearance in PBL [arrows denoting tingible body macrophages] (H&E-stained section, x100 magnification) 72

Figure 4.2: Plasmablastic lymphoma displaying monomorphic (A) and (B) plasmacytic cytomorphology (H&E-stained sections, x400 magnification). 73

Figure 4.3: c-MYC protein immunoexpression in PBL (IHC-stained, x200 magnification). 75

Figure 4.4: Dual-colour CISH demonstrating intranuclear *MYC* signals (black) and CEN8 signals (red) in the squamous epithelium and dermal fibroblasts (x400 magnification). 77

Figure 4.5: PBL (P46) displaying increased *MYC* gene copy numbers (black signals) and not-increased CEN 8 (red signals) within tumour nuclei (CISH-stained section by light microscopy, x400 magnification). 78

Figure 4.6: PBL (P55) displaying increased *MYC* gene copy numbers (black signals) and increased CEN8 (red signals) within tumour nuclei (CISH-stained section under light microscopy, x400 magnification). 79

Figure 4.7: 4′,6-diamidino-2-phenylindole (DAPI)-stained nuclei (P35) hybridised with the Vysis LSI MYC dual-colour break-apart probe. Arrowed nuclei show increased *MYC* signals, involving both the intact *MYC* locus seen as a fusion (F), (overlap of SpectrumOrange and SpectrumGreen probes encompassing the 5’ and 3’ regions of the *MYC* gene, respectively) and rearranged *MYC* loci seen as separate orange (O) and green signals (G). 81

Figure 4.8: PBL (P35) displaying diffusely positive nuclear signals of EBER by ISH (x200 magnification). 87

Figure 4.9: Kaplan Meier survival estimates for HIV PBL with c-MYC expression (green) and without c-MYC expression (blue). 89

Figure 4.10: Kaplan Meier survival estimates for HIV PBL with *MYC* aberrations (green) and without *MYC* aberrations (blue). 90

Figure 4.11: Centroblastic morphology (A), immunoblastic morphology (B) and anaplastic morphology (C) in DLBCL (H&E, x200 magnification). 97

Figure 4.12: Positive nuclear immunoreactivity for c-MYC in DLBCL (D4 and D60 at x200, D112 at x400). 99

Figure 4.13: Ki-67 immunohistochemistry demonstrating a lower proliferation index in HIV-DLBCL (A) and a higher proliferation index in (B) HIV+ DLBCL (x400 magnification). 101

Figure 4.14: Kaplan Meier survival estimates for HIV+ DLBCL by COO. 104

Figure 4.15: Double expression of c-MYC and BCL2 proteins in DLBCL [case D10] (x200 magnification). 106

Figure 4.16: Dual-colour CISH demonstrating intranuclear *MYC* signals (black dots and transparent arrows) and CEN8 signals (red dots and white arrows) in the internal control endothelial cells and fibroblasts (x400 magnification). 108

Figure 4.17: Case D60 displaying increased *MYC* gene signals (black dots/white arrows) and not increased CEN8 signals (red dots) [dual-colour CISH at x400 magnification]..... 109

Figure 4.18: Case D112 displaying increased *MYC* gene signals (black dots) and increased CEN8 signals (red dots) denoted by white arrows [dual-colour CISH at x400 magnification]. 111

Figure 4.19: *MYC* gene clusters in case D52 (dual-colour CISH at x400 magnification)..... 112

Figure 4.20: Kaplan Meier survival curves depicting HIV+ DLBCL with IPI 0-2 and 3-5..... 117

Figure 4.21: Kaplan Meier survival curves depicting HIV+ DLBCL and HIV- DLBCL..... 118

Figure 4.22: Kaplan Meier survival curves of DLBCL by HIV status, CD4 counts <100 cells/mm^3 and CD4 counts ≥100 cells/mm^3..... 119

Figure 4.23: Kaplan Meier survival curves of HIV+ DLBCL with and without CCI. 120

LIST OF TABLES

Table 2.1: Review of c-MYC and BCL2 expression in DLBCL……...…….23

Table 2.2: IPI prognostic scoring system for aggressive NHL……..……29

Table 2.3: Revised IPI for DLBCL……..……..……30

Table 2.4: Differential diagnosis for tumours displaying plasmablastic morphology……..……35

Table 3.1: Details of the primary antibodies utilised for DLBCL and PBL…….…….49

Table 4.1: Concomitant conditions that occurred with PBL..... 69

Table 4.2: PBL - Topographic sites of biopsy 71

Table 4.3: Immunophenotypic analysis of PBL..... 76

Table 4.4: PBL with increased *MYC* copy numbers 82

Table 4.5: Clinicopathological characteristics of PBL and *MYC* aberrations..... 85

Table 4.6: PBL - Analysis of immunohistochemistry and *MYC* aberrations..... 86

Table 4.7: Clinicopathological characteristics of DLBCL patients 92

Table 4.8: Concomitant conditions documented for DLBCL patients 95

Table 4.9: Immunophenotypic analysis of DLBCL..... 100

Table 4.10: c-MYC protein expression in HIV+ and HIV- DLBCL. 103

Table 4.11: Analysis of c-MYC and BCL2 co-expression in HIV+ and HIV- DLBCL. 107

Table 4.12: Increased *MYC* gene copy numbers and c-MYC protein expression in DLBCL .. 110

Table 4.13: Bivariate analysis of clinicopathological factors and *MYC* gene copies. 113

Table 4.14: *MYC* aberrations in DLBCL. 115

Table 4.15: Clinicopathological factors of DLBCL and median overall survival outcome 121

Table 4.16: Univariate and multivariate Cox regression analysis of selected clinicopathological factors associated with overall survival 123

LIST OF ABBREVIATIONS

ABC	Activated B-cell
ACS	American Cancer Society
AID	Activation-induced cytidine deaminase
AIDS	Acquired immunodeficiency syndrome
AP	Anaplastic
ART	Antiretroviral therapy
BCL2	B-cell lymphoma 2
bcl-6	B-cell lymphoma 6
BFM	Berlin Frankfurt Munster
BL	Burkitt lymphoma
BLIMP1	B-lymphocyte-induced maturation protein 1
c-ART	Combination antiretroviral therapy
C8	Chromosome 8
CB	Centroblastic
CC/s	Concomitant condition/s
CC1	Cell conditioning 1
CC2	Cell conditioning 2
CCI	Concomitant condition infection
CCR5	C-C chemokine receptor type 5
CD	Cluster of differentiation
CD40L	Cluster of differentiation 40 ligand
CDC	Center of Disease Control
CDK	Cyclin-dependent kinase
CDW	Corporate Data Warehouse
CEN8	Centromere of chromosome 8
CHBAH	Chris Hani Baragwanath Academic Hospital
CHL	Classic Hodgkin lymphoma
CHOP	Cyclophosphamide, hydroxydaunorubicin, vincristine and prednisone

CHOEP	Cyclophosphamide, hydroxydaunorubicin, vincristine, etoposide and prednisone
CI	Confidence interval
CISH	Chromogenic *in situ* hybridisation
CKI	Cyclin dependent kinase inhibitor
CMJAH	Charlotte Maxeke Johannesburg Academic Hospital
c-MYC	Cellular homolog myelocytomatosis oncogene
COO	Cell of origin
CRP	C-reactive protein
DE	Double expression
DIG	Digoxigenin
DISA	Data Intensive Systems and Applications
DLBCL/s	Diffuse large B-cell lymphoma/s
DLBCL NOS	Diffuse large B-cell lymphoma, not otherwise specified
DNA	Deoxyribonucleic acid
DNP	Dinitrophenol
E2F	E2 transcription factor
EON	Extra-oronasal
Eμ	Intron enhancer region of immunoglobulin
E-box	Enhancer box
EBER	Epstein-Barr virus encoded small RNA
EBER ISH	EBER *in situ* hybridisation
EBV	Epstein-Barr virus
ELISA	Enzyme-Linked Immunosorbent Assay
FFPE	Formalin-fixed paraffin-embedded
FISH	Fluorescence *in situ* hybridisation
FOXP1	Forkhead box P1
GC	Germinal centre
GCB	Germinal centre B-cell
GCET1	Germinal centre B-cell-expressed transcript 1
GEP	Gene expression profiling

GLUT1	Glucose transporter 1
HAART	Highly active antiretroviral therapy
H&E	Haematoxylin and eosin
HHV8	Human herpesvirus-8
HIF	Hypoxia inducible factor
HIV	Human immunodeficiency virus
HIV+	Human immunodeficiency virus seropositive
HIV-	Human immunodeficiency virus seronegative
HPF	High-power field
HR	Hazard ratio
HREC	Human Research Ethics Committee
HRP	Horseradish peroxidase
IARC	International Agency for Research on Cancer
IB	Immunoblastic
IG	Immunoglobulin
IgH	Immunoglobulin heavy chain
IHC	Immunohistochemistry
IL6	Interleukin 6
INK	Inhibitor of kinase
IQR	Interquartile range
IPI	International Prognostic Index
ISH	*In situ* hybridisation
Ki-67	Marker of proliferation or labelling index
LABTRAK	Laboratory Trak information system
LDH	Lactate dehydrogenase
LDL	Lower than detectable limit
LMO2	LIM domain only 2 protein
MAD	Mitotic arrest deficient
MALT	Mucosa associated lymphoid tissue
MALT1	MALT lymphoma translocation protein 1
MAX	MYC-associated factor X

MC29	Myelocytomatosis retrovirus avian (chicken) strain
MHC	Major-histocompatibility-complex
MIB-1	Molecular Immunology Borstel
miRNA	MicroRNA
MGA	MAX gene-associated
MNT	MAX network transcriptional repressor
mRNA	Messenger ribonucleic acid
MUM1	Multiple myeloma oncogene 1
MXD	MAX dimerisation protein
MYC	Myelocytomatosis proto/oncogene
NADPH	Nicotinamide adenosine dinucleotide phosphate hydrogen
NCR	National Cancer Registry
NGC	Non-germinal centre
NGS	Next generation sequencing
NHLs	Non-Hodgkin lymphomas
NHLS	National Health Laboratory Service
ON	Oronasal
OS	Overall survival
PAX5	Paired box 5
PBL/s	Plasmablastic lymphoma/s
P13K	Phosphatidylinositol-3-kinase
PRDM1	Positive regulatory domain 1
PTEN	Phosphatase and tensin homolog deleted on chromosome 10
RB	Retinoblastoma susceptibility protein
R	Rituximab
R-CHOP	Rituximab, cyclophosphamide, hydroxydaunorubicin, vincristine, prednisone
RNA	Ribonucleic acid
R-IPI	Revised International Prognostic Index
SA	South Africa
SISH	Silver *in situ* hybridisation
SIV	Simian Immunodeficiency Virus

SNOMED	Systematised Nomenclature of Medicine
SS	Starry-sky
SSA	Sub-Saharan Africa
T58	Threonine 58
TAD	Transcriptional activation domain
Tat	Transactivator of transcription
TP53	Tumour protein 53
USA	United States of America
XBP1	X-box-binding protein 1

TABLE OF CONTENTS

DECLARATION ii
DEDICATION iii
PUBLICATIONS ARISING FROM THIS STUDY iv
ABSTRACT v
ACKNOWLEDGEMENTS viii
FUNDING ACKNOWLEDGEMENTS ix
LIST OF FIGURES x
LIST OF TABLES xii
LIST OF ABBREVIATIONS xiii
TABLE OF CONTENTS xviii
1 CHAPTER ONE 1
1.1 Introduction 1
2 CHAPTER TWO 1
Literature review 1
2.1 HIV infection and aggressive B-cell NHLs: A riotous association 1
2.1.1 Salient historic aspects of HIV 1
2.1.2 HIV-induced crisis in sub-Saharan Africa 2
2.1.3 Immunopathogenesis of HIV: laconic overview relevant to B-cell stimulation 2
2.1.4 Chronic HIV: Persistent cytokine-production and B-cell proliferation 4
2.1.5 HIV exerts a direct influence on B-cell lymphomagenesis 5
2.2 Myelocytomatosis and the cellular homolog 5
2.2.1 *MYC* proto-oncogene 6
2.2.2 c-MYC protein: transcription factor 7
2.2.3 Structure of c-MYC protein 7
2.2.4 c-MYC and the cell cycle 8
2.2.5 c-MYC and apoptosis 9
2.2.6 c-MYC induced metabolism of glucose and glutamine 9
2.2.7 c-MYC and miRNA 11
2.2.8 *MYC* and oncogenesis 11
2.2.9 *MYC* and B-cell lymphomagenesis 13
2.3 Diffuse large B-cell lymphoma 15
2.3.1 DLBCL: Age and gender 15
2.3.2 DLBCL: HIV viral load, CD4 count and ART 15
2.3.3 DLBCL: Morphology 17
2.3.4 DLBCL: What is the relevance of the cell of origin subtype? 20

2.3.5 DLBCL: c-MYC protein expression 22
2.3.6 DLBCL: BCL2 and c-MYC co-expression 25
2.3.7 DLBCL: Ki-67 expression 25
2.3.8 DLBCL: *MYC* aberrations (rearrangement and/or copy number increase) 27
2.3.9 DLBCL: Stage and extranodal involvement 28
2.3.10 DLBCL: IPI and R-IPI score 29
2.3.11 DLBCL: Treatment and survival outcome 31
2.4 Plasmablastic lymphoma 32
2.4.1 PBL: HIV and severity of immunosuppression 32
2.4.2 PBL: Age and gender 33
2.4.3 PBL: Topographic sites of involvement 33
2.4.4 PBL: Morphology 33
2.4.5 PBL: Immunophenotype 34
2.4.6 PBL: Epstein–Barr virus 36
2.4.7 PBL: Molecular features and *MYC* status 37
2.4.8 PBL: Stage 38
2.4.9 PBL: Treatment 38
2.4.10 PBL: Survival outcome 39
2.5 Research questions: 41
2.6 Research aims: 41
2.7 Research objectives: 41
3 CHAPTER THREE 43
Methodology and materials 43
3.1 Research protocol inception 43
3.2 Ethics approval 43
3.3 Study design and funding 43
3.4 Target cases 43
3.5 Sample size 44
3.6 Case detection and retrieval 44
3.7 Exclusion criteria 44
3.8 Included tumours 45
3.9 Confidentiality of the patients 45
3.10 Clinical data collection 46
3.11 Laboratory data collection 46
3.11.1 Pathology data of DLBCL 46
3.11.2 Pathology data of PBL 47

3.12 Histopathology laboratory investigation: c-MYC IHC 50
3.12.1 c-MYC IHC: methodology 53
3.12.2 c-MYC IHC: adequacy of staining 54
3.12.3 c-MYC IHC: interpretation 54
3.13 Histopathology laboratory investigation: *MYC* and CEN8 dual-colour CISH 56
3.13.1 Dual-colour CISH: methodology 58
3.13.2 Dual-colour CISH: adequacy of staining and signal visualisation 61
3.13.3 Guidelines for interpreting *MYC* SISH signals 61
3.13.4 Dual-colour CISH: Evaluation and interpretation 62
3.13.5 Definition of increased CISH signals 64
3.13.6 CISH-defined subcategorisation of DLBCL and PBL 64
3.14 FISH on DLBCL and PBL 66
3.15 Statistical analysis 66
4 CHAPTER FOUR 68
4.1 RESULTS: PLASMABLASTIC LYMPHOMA 68
4.1.1 PBL: Included cases 68
4.1.2 PBL: Age of patients 68
4.1.3 PBL: Gender of patients 68
4.1.4 PBL: HIV status 68
4.1.5 PBL: CD4 count and immunosuppression 69
4.1.6 PBL: Concomitant conditions 69
4.1.7 PBL: Stage of lymphoma 70
4.1.8 PBL: Topographic site of biopsy 70
4.1.9 PBL: Morphology 72
4.1.10 PBL: Immunophenotype 74
4.1.11 PBL: CISH 77
4.1.12 PBL: FISH 80
4.1.13 PBL: Average number of *MYC* copies by CISH and FISH 83
4.1.14 PBL: *MYC* aberrations 83
4.1.15 PBL: EBV ISH 86
4.1.16 PBL: Treatment 87
4.1.17 PBL: Survival outcome 88
4.2 RESULTS: DIFFUSE LARGE B-CELL LYMPHOMA 91
4.2.1 DLBCL: Included cases 91
4.2.2 DLBCL: Age of patients 91
4.2.3 DLBCL: Gender of patients 93

4.2.4 DLBCL: HIV status 93
4.2.5 DLBCL: CD4 count and immunosuppression 94
4.2.6 DLBCL: Concomitant conditions 94
4.2.7 DLBCL: Stage of lymphoma 95
4.2.8 DLBCL: Topographic site of biopsy 96
4.2.9 DLBCL: Starry-sky appearance and cytomorphology 96
4.2.10 DLBCL: Immunophenotype 98
4.2.11 DLBCL: IHC-defined COO 104
4.2.12 DLBCL: Double expression of c-MYC and BCL2 proteins 105
4.2.13 Increased *MYC* copy numbers detected using FISH and CISH 108
4.2.14 DLBCL: FISH for *MYC* rearrangement and *MYC* copy numbers 114
4.2.15 DLBCL: *MYC* aberrations 114
4.2.16 DLBCL: Treatment 116
4.2.17 DLBCL: IPI score 117
4.2.18 DLBCL: Survival outcome 118
5 CHAPTER FIVE 124
DISCUSSION 124
5.1 Age and gender 124
5.2 HIV status and severity of immunosuppression depicted by CD4 counts 125
5.3 Concomitant conditions 126
5.4 IPI score 128
5.5 Topographic sites of biopsy 128
5.6 Starry-sky appearance 129
5.7 Cytomorphology 130
5.8 Immunophenotype 131
5.9 Double expression (DE) of c-MYC and BCL2 in DLBCL 133
5.10 *MYC* rearrangement 133
5.11 *MYC* gene copy number increases 134
5.12 Dual-colour CISH on FFPE specimens 136
5.13 *MYC* aberrations in DLBCL and PBL 136
5.14 Stage of lymphoma 137
5.15 Survival outcome 138
5.16 DLBCL in a paediatric patient 139
5.17 Latent EBV infection in PBL 139
5.18 Limitations of this study 140
6 CHAPTER SIX 142

CONCLUSION 142
REFERENCES 144
APPENDICES 175
I: Ethics certificates 175
II: Title amendments 177
III. DLBCL data collection spreadsheet 179
IV: PBL data collection spreadsheet 180
V: CISH interpretation tools 181
VI: Turn-it-in 182

1 CHAPTER ONE

1.1 Introduction

A substantial fraction of a working day in Anatomical Pathology is directed towards the diagnostic confirmation of malignancies. In accordance herewith, for the year 2018 more than 17 million new cases of cancer were diagnosed globally and approximately 9.6 million cancer-related deaths occurred worldwide. Prior to the Covid-19 pandemic, approximately 1 in 6 human deaths was attributable to cancer, making cancer the second leading cause of death globally. Moreover, cancer is expected to become the leading cause of death within many countries during the 21st century (Bray et al., 2018; World Health Organization, 2018). In support of the premise of an alarming increase in the incidence of cancer, in the United States of America (USA) during 2020, there were more than 1.8 million newly diagnosed cancer cases and approximately 600 000 cancer-related deaths occurred (Siegel et al., 2020). Aligned with the worldwide cancer trend, according to the Globocan 2020 report, within the southern region of Africa, the cancer incidence was 116 391 with a cancer-related mortality of 61 659 (World Health Organization, 2020). Furthermore, for the year 2030 it is projected that in Africa, an astounding 1.27 million cancer cases and 970 000 cancer deaths could occur (Sylla and Wild, 2012).

Non-Hodgkin lymphoma (NHL) is a malignancy that derives from mature or immature B-lymphocytes, T-lymphocytes and/or natural killer cells. Within the NHL category, the mature B-cell subtypes constitute >90% of the lymphoid neoplasms worldwide (Jaffe et al., 2017). During 2018, NHL ranked 13th on a global list of 36 cancers as it accounted for an alarming 509 590 new cases worldwide and 248 724 cancer related deaths (Bray et al., 2018).

According to the South African National Cancer Registry (NCR) of 2017, there were 2 633 confirmed cases of NHL, hereby establishing this malignancy as the 7th and 9th leading cancer in males and females, respectively (National Health Laboratory Service, 2018). Due to the high seroprevalence of human immunodeficiency virus (HIV), aggressive B-cell NHLs are frequently documented in South Africa (Patel, 2007; Abayomi et al., 2011; Pather et al., 2013b; Meer et al., 2020; Cassim et al., 2020; Magangane et al., 2020).

The high incidence of aggressive B-cell NHL within SA is attributable to several influential factors, acting in synergy with advancements in diagnostic modalities.

Diffuse large B-cell lymphoma, not otherwise specified (DLBCL, NOS), HIV-associated DLBCL and HIV-associated plasmablastic lymphoma (PBL) are aggressive high-grade B-cell NHLs (Jaffe and Pittaluga, 2011; Gascoyne et al., 2017b; Said et al., 2017). An array of clinicopathological factors may contribute to an inferior survival outcome in the context of these aggressive tumours (Miller et al., 1994; Hans et al., 2004; Nyman et al., 2007; Dunleavy et al., 2010; Ott et al., 2010; Salles et al., 2011; Olszewski et al., 2015; Rosenwald et al., 2019). In this thesis, increased *MYC* gene copy numbers, *MYC* rearrangement and c-MYC protein expression are explored in depth within HIV positive and negative DLBCLs and PBL. Other factors such as demographic characteristics, tumour morphology, immunophenotypic features, tumour proliferation indices, topographic site of biopsy, Ann Abor stage of lymphoma at presentation, International Prognostic Index (IPI) score, HIV status, CD4 counts and viral load at lymphoma presentation, concomitant conditions, treatment and survival outcome are also explored and analysed. These factors harbour tremendous potential to create vexing challenges during the diagnostic process and the management of the afflicted patients. Therefore, research that scrutinises the clinicopathological diversity of the aforementioned tumours at the largest hospital in Africa is warranted with the aim of identifying poor prognostic factors. The findings may lead to heightened awareness of these malignancies and possible modification, enhancement or targeted treatment regimens in future.

The abovementioned clinicopathological characteristics of DLBCL, NOS, HIV-associated DLBCL and HIV-associated PBL are presented and elaborated upon in the literature review that follows.

2 CHAPTER TWO

LITERATURE REVIEW

2.1 HIV infection and aggressive B-cell NHLs: A riotous association

Up to 30% of cancers in Africa are linked to infectious agents. In the setting of B-cell NHL specifically, HIV is identified as a risk factor of high public health relevance (Parkin et al., 2008; Sylla and Wild, 2012).

2.1.1 Salient historic aspects of HIV

During the early 1980's a novel T-lymphotropic retrovirus was isolated from patients that developed the acquired immunodeficiency syndrome (AIDS) and demised from unusual opportunistic infections and malignancies (Centre for disease control., 1981). This virus was subsequently classified as HIV (Gottlieb et al., 1981; Barre-Sinoussi et al., 1983; Gallo et al., 1983). The existence of HIV for decades prior to its formal documentation was solidified when this virus was retrospectively demonstrated in lymph node and plasma specimens that were sampled during 1959 to 1960 from patients in Leopoldville, Belgian Congo [now Kinshasa, Democratic Republic of the Congo] (Zhu et al., 1998). A monumental historic perspective of HIV infection was hereby contributed. The origin of HIV is linked to the cross-species zoonotic transmission of non-human simian immunodeficiency virus (SIV) to humans that likely occurred during primate hunting, capture, butchering, trade and the keeping of primate pets in the regions of Western and Central Africa (Gao et al., 1999; Hahn et al., 2000). HIV-1 group M is the strain that is the notorious causative agent of a devastating infectious disease that has exerted far reaching life-threatening effects on millions of patients throughout the world (NAM AIDS map, 2021; Sharp and Hahn, 2011).

2.1.2 HIV-induced crisis in sub-Saharan Africa

For several decades, many regions of the world have been ravaged by the HIV epidemic. On a daily basis, an estimated 6000 new cases of HIV infection are confirmed globally, and two of every three patients thereof are likely to be located in sub-Saharan Africa [SSA] (Kharsany and Karim, 2016). SSA is the most severely affected region, as it is home to approximately 70% of patients who are living with HIV worldwide (World Health Organisation, 2017; Del Rio, 2017). In SA, the estimated prevalence of HIV is 20.6% in the age group 15-49 years and this country is home to 7.5 million people, the highest worldwide, who are living with HIV. Although the incidence of HIV has decreased by 53% since 2010, during 2019 approximately 200 000 new HIV cases were confirmed and 72 000 AIDS-related deaths were documented (Human Sciences Research Council 2018; UNAIDS, 2021).

Heterosexual transmission is the dominant mode of spread of HIV in SSA and 56% of new infections are documented in females within this region (UNAIDS, 2016; Del Rio, 2017). Consequently, the epidemic of HIV also involves paediatric patients due to vertical transmission of the virus (Kharsany and Karim, 2016).

2.1.3 Immunopathogenesis of HIV: laconic overview relevant to B-cell stimulation

In the context of sexual transmission, infection commences after exposure to HIV occurs when it is transmitted across a mucosal barrier in the form of a cell-free virus, via an infected cell or a virion that is attached to a dendritic cell, macrophage or Langerhans cell (Haase, 2005). HIV characteristically infects CD4-positive lymphocytes causing proliferation and destruction thereof, that leads to increased T-lymphocytic turnover (Hellerstein et al., 1999). Although this process results in a reduction in the CD4 T-lymphocytic half-life, it masterfully drives viral replication by generating activated T-cell targets (Grossman et al., 1998) that express the C-C chemokine receptor type 5 [CCR5]. CCR5 acts as a potent co-receptor for HIV-1 viral entry (Tan et al., 2013). HIV subsequently migrates rapidly to lymphoid tissue of the gastrointestinal tract at which massive propagation initially manifests within activated CD4 T-lymphocytes in the lamina propria (Guadalupe et al., 2003; Moir et al., 2011).

The high levels of viraemia that follow allows for widespread dissemination of HIV to several lymphoid tissue sites, predominantly lymph nodes, at which stable viral reservoirs are established. At these sites, viral replication persists (Haase, 2005). The replication of HIV is an inherently mutagenic process (Jarrett, 2006) which entails integration of a viral intermediate into the host cell deoxyribonucleic acid [DNA] (Goff, 2001). The defining feature of untreated progressive HIV infection is chronic systemic immune activation that manifests as polyclonal B-lymphocytic activation, increased B-cell turnover, hypergammaglobulinaemia, elevated serum levels of cytokines or chemokines and T-lymphocytes with an activated phenotype (Lane et al., 1983; Valdez and Lederman, 1997; Douek et al., 2009; Carroll and Garzino-Demo, 2015). Progressive depletion of CD4+ T-lymphocytes is an immunological hallmark of untreated HIV infection (Moir et al., 2011). It is firmly established that a low baseline CD4 count is strongly associated with the probability of progression to AIDS or death (Egger et al., 2002; Braitstein et al., 2006). The immunopathogenesis is a complex and potent interplay between the immune system and HIV, which leads to loss of immune control. Untreated, this process inevitably manifests as susceptibility to overwhelming life-threatening pathogenic infection and neoplasia (Douek et al., 2009).

Many factors contribute to the development of B-cell NHL in HIV seropositive patients and these factors may influence the oncogenic process in a synergistic manner. Influential factors include the severity and duration of immunosuppression, impaired immune surveillance, concomitant infection by oncogenic viruses such as Epstein-Barr virus (EBV) or human herpesvirus-8 (HHV-8), cytokine-induced B-cell proliferation and advancing age (Knowles, 2003; Dolcetti et al., 2016). The persistent uncontrolled stimulation of B-lymphocytes leads to immunological deregulation that predisposes HIV afflicted patients to cumulative genetic alterations through somatic hypermutation or aberrant immunoglobulin (IG) class switch recombination (Carroll and Garzino-Demo, 2015). Hereby, a monoclonal population emerges with subsequent development of an aggressive B-cell NHL (Powles et al., 2000; Grogg et al., 2007; Dolcetti et al., 2016).

2.1.4 Chronic HIV: Persistent cytokine-production and B-cell proliferation

The risk of developing DLBCL is increased in the presence of a condition that stimulates B-cell proliferation (Chihara et al., 2015). In the setting of chronic HIV-1 infection, the capsid protein p24, matrix protein p17 and the envelope glycoprotein gp120 persist in the germinal centres of lymph nodes. This occurs despite the absence of detectable viral replication, even after a prolonged timeframe of antiretroviral therapy (ART). These viral proteins have the potential to interact with the mononuclear cells of the immune system to enhance or induce cytokine production and cellular proliferation (Popovic et al., 2005). In support hereof, despite the administration of ART for up to 24 months, serum levels of interleukin 6 (IL-6) and C-reactive protein (CRP) remained elevated in a cohort of HIV-seropositive males (Regidor et al., 2011).

IL-6 is a cytokine that stimulates B-lymphocytic proliferation by promoting immunoglobulin heavy chain (*IgH*) class switching and by exerting an antiapoptotic effect. Due to its stimulatory influence on B-lymphocytes, persistently elevated levels of IL-6 are associated with the development of B-cell lymphoma in the era of ART (Regidor et al., 2011; Carroll and Garzino-Demo, 2015). Moreover, despite ART the HIV-1 matrix protein p17 plays an influential role in angiogenesis, hereby contributing to a favourable microenvironment for the growth, maintenance and spread of HIV-related lymphomas (Caccuri et al., 2012; Caccuri et al., 2014; Basta et al., 2015). Variants of p17, such as S75X, have also been shown to influence B-lymphocytic proliferation and malignant transformation by interacting with phosphatase and tensin homolog deleted on chromosome 10 (PTEN) and the phosphatidylinositol-3-kinase (PI3K/Akt) pathway (Giagulli et al., 2011). The microenvironment for lymphoma development is furthermore influenced by the transactivator of transcription (Tat) protein of HIV that enhances production of IL-6 and IL-10 (Scala G et al., 1994). There is subsequent binding to and deregulation of the oncosuppressor protein pRb2/p130 within B-lymphocytes (Lazzi et al., 2002) which facilitates angiogenesis (Kundu et al., 1999; Dolcetti et al., 2016). These stimulatory influences promote the development of B-cell neoplasia.

2.1.5 HIV exerts a direct influence on B-cell lymphomagenesis

Due to the presence of immune suppression, HIV was classically thought to exert an indirect influence on lymphomagenesis (Grogg et al., 2007). However, convincing evidence has emerged in favour of its direct contribution to lymphomagenesis, by acting on B-lymphocytes. Activated T-lymphocytes express the CD40 ligand (CD40L) and when the HIV-1 particles bud from these infected cells, the CD40L inserts at the surface of the virions. The insertion of CD40L confers potent B-cell stimulating properties (Martin et al., 2007; Imbeault et al., 2011). Stimulated B-cells express activation induced cytidine deaminase (AID), a DNA modifying enzyme, that facilitates chromosome translocation, immunoglobulin gene class switch recombination and somatic hypermutation (Robbiani et al., 2009; Graham et al., 2010; Vendrame et al., 2014). AID induces DNA double-strand breaks throughout the genome (Robbiani et al., 2009) and from this fertile field emerges the potential for genetic aberrations within B-cell NHL. Notably, increased expression of AID has been demonstrated in the context of HIV infection, in advance of the development of NHL (Epeldegui et al., 2007). Moreover, AID expression is documented more frequently in HIV-associated DLBCL than the HIV seronegative counterpart (Shponka et al., 2020), hereby supporting the notion that AID may play a direct role in HIV-associated B-cell lymphomagenesis. Aberrant expression of AID may be responsible for the *IgH* and c-*MYC* (hereafter referred to as *MYC*) genetic recombination that is demonstrated in some germinal-centre derived B-cell (GCB) NHLs (Robbiani et al., 2008; Robbiani et al., 2009). Noteworthy, Pasqualucci et al. (2008) contributed that AID deficiency prevents the development of GCB NHL. The aggressive HIV-associated B-cell NHLs may harbour aberrations of the *MYC* gene which potentially exerts a negative influence on the survival outcome (Chisholm et al., 2015).

2.2 Myelocytomatosis and the cellular homolog

The MYC abbreviation derives from myelocytomatosis. During 1964, the MC29 strain of an avian myelocytomatosis retrovirus was propagated from a chicken that demised of anaemia and promyelocytic solid tumours. The MC29 strain differed from other avian leukosis viruses as it predisposed to the manifestation of solid or diffuse haematopoietic tumours rather than leukaemia (Ivanov et al., 1964; Lautenberger et al., 1981). Subsequently, it was established that the influence of the MC29 virus was linked to a cellular homolog of the retroviral oncogene v-*MYC*, that became

known as c-*MYC*. *MYC* is a cellular proto-oncogene, that occurs intrinsically within avian and other vertebrate sources (Bishop, 1978; Sheiness and Bishop, 1979; Vennstrom et al., 1982). These pioneering findings spearheaded the goal to define and elucidate *MYC*-associated oncogenesis.

2.2.1 *MYC* proto-oncogene

The enigmatic *MYC* oncogene family is implicated in diverse malignancies (Ryan and Birnie, 1996). The location of *MYC* on the long arm of chromosome 8 was formally documented during 1982 within a sentinel publication that was based on a Southern blotting technique, a *MYC* gene-specific DNA probe and somatic hybrids between human Burkitt lymphoma (BL) cells and rodent cells (Dalla-Favera et al., 1982a). Cloning and sequencing of the human *MYC* gene ensued (Dalla-Favera et al., 1982b; Battey et al., 1983). The *MYC* proto-oncogene has an exact cytogenetic location of 8q24.21 and is encoded in three exons (Battey et al., 1983). Expression occurs in many eukaryotic cells as *MYC* plays a diversely influential role that extends from embryonic development and differentiation to apoptosis (Miller et al., 2012).

In non-neoplastic cells, *MYC* expression is meticulously controlled by mitogenic signals that serve to drive the process of cellular proliferation. *MYC* is an immediate early gene that is rapidly induced in response to growth factor signalling (Tansey, 2014). The transcription of *MYC* is stringently regulated at the level of initiation and release of the ribonucleic acid (RNA) polymerase II. The proliferative influence of *MYC* in normal cells is furthermore curtailed by the short lifespan of *MYC* messenger ribonucleic acid (mRNA) and translational modulation that results from the influence of microRNA (miRNA). In turn, regulatory signals result in reduced *MYC* transcription and low c-MYC protein levels (Blackwood and Eisenman, 1991; Dang, 1999a; Miller et al., 2012; Dang, 2012; Karpathiou et al., 2016). *MYC* over-expression in normal cells may induce cellular growth, DNA replication and polypoidy (Blackwood and Eisenman, 1991; Beer et al., 2004; Gabay et al., 2014). Hence, *MYC* is renowned for its neoplastic potential (Dang, 1999a; Chen et al., 2018).

2.2.2 c-MYC protein: transcription factor

The MYC oncoproteins, deemed "super transcription factors" (Dang et al., 2006), include c-MYC that is encoded from the *MYC* oncogene as a helix-loop-helix leucine zipper transcription factor. The c-MYC transcription factor localises within nuclei, has a molecular weight of 65 kilodalton (Persson and Leder, 1984) and plays a regulatory role in cellular proliferation, differentiation, growth, metabolism and apoptosis (Sakamuro and Prendergast, 1999; Sander et al., 2008; Madden et al., 2021).

2.2.3 Structure of c-MYC protein

The c-MYC protein contains a transcriptional activation domain (TAD) that is located at the amino-terminus (N-terminal). When the TAD region is bound to a heterologous DNA binding domain, *MYC* gene induction occurs (Kato et al., 1990). The TAD region also harbours instantaneous potential to function as a degron from which signalling for ubiquitin-mediated proteolytic degradation of c-MYC manifests (Salghetti et al., 1999). At the N-terminal of the c-MYC protein there are sequences called MYC boxes I, II and III which are instrumental in the activation and repression of MYC target genes. MYC boxes also play an influential role in protein stability and protein interaction (Adhikary and Eilers, 2005). c-MYC protein stability is linked to the presence of two phosphorylation sites in the N-terminal region. One of these sites is threonine 58 (T58) and phosphorylation thereof leads to degradation of c-MYC (Junttila and Westermarck, 2008). c-MYC protein stability is enhanced within some lymphomas due to the presence of mutations of a hot spot region in which T58 is located. Such mutations lead to a reduction of c-MYC phosphorylation and a reduction in proteasome mediated degradation (Bahram et al., 2000).

At the carboxyl terminus (C-terminal) of the c-MYC protein, there is a DNA binding domain that comprises a basic helix-loop-helix-leucine zipper region (Blackwell et al., 1990). Dimerisation of c-MYC with MYC-associated factor X (MAX), a stable ubiquitously expressed protein, results in heterodimer formation. Subsequent transcriptional activation manifests when binding to the DNA sequences of target genes occurs. The MYC/MAX heterocomplex specifically utilises the 5′-CACGTG-3′ DNA motive sequence (Fisher et al., 1993), which belongs to the E-box class of binding sequences, for transcriptional activation or transformation of genes (Blackwell et al., 1990;

Blackwood and Eisenman, 1991; Eilers et al., 1991; Philipp et al., 1994; Dang, 1999a; Grandori et al., 2000).

In the human genome, the 5′-CACGTG-3′ E-box is one of the most frequent DNA binding motive sequences (Eilers et al., 1991; Dang, 2012). Expression of c-MYC tends to correlate with cellular proliferation, as an immediate early response to mitogenic influences. Stringent homeostatic control thereof occurs at many steps in response to growth suppressive signals (Dang et al., 1999b; Grandori et al., 2000; Klapproth and Wirth, 2010). By means of its ability to activate transcription that is mediated by RNA polymerases I, II and III, c-MYC contributes to ribosome biogenesis. Therefore, a gain of c-MYC function is associated with enhanced cell growth (Dang, 2013).

c-MYC also plays a participant role in transcriptional repression of genes (Mateyak et al., 1999). The MYC/MAX interaction is regulated by the binding of MAX to other basic helix-loop-helix leucine zipper proteins such as MAX dimerisation protein (MXD) 1-4, MAX network transcriptional repressor (MNT) and MAX gene-associated protein (MGA) by which antagonistic transcriptional repressor action is imposed (Hurlin et al., 1997; Grandori et al., 2000; Madden et al., 2021). Cellular differentiation and growth arrest are associated with increased expression of the MYC/MXD proteins, hereby highlighting its role as a tumour suppressor protein (Dang et al., 1999b). The stability of the c-MYC protein in unison with its short half-life in proliferating cells, contributes to regulation of the *MYC* gene. The c-MYC protein has a half-life of fifteen to twenty minutes and it is subject to numerous methods of post-translational modifications such as ubiquitylation and degradation, glycosylation or phosphorylation that influence its functional activity (Miller et al., 2012; Dang, 2012; Tansey, 2014).

2.2.4 c-MYC and the cell cycle

c-MYC protein plays a regulatory role in the machinery of the cell cycle by serving as a link between growth factor stimulation and cell proliferation at the G1 (pre-synthesis) or G1/S (DNA synthesis) transition of the cell cycle (Amati et al., 1993; Dang et al., 1999b; Dang, 2012). While c-MYC expression is evident in cells which progress through the cell cycle, c-MYC protein levels rapidly decrease in resting and differentiated cells (Klapproth and Wirth, 2010). Progression through various phases of the proliferative cycle is controlled by proteins called cyclins, enzymes which are known as cyclin-dependent kinases (CDK) and inhibitors thereof. The CDK, when

activated by binding to cyclins, promote progression of the cell cycle by phosphorylating the retinoblastoma susceptibility protein (RB). Thereafter, the release and activation of the transcription factor E2F manifests. Transcription of target genes such as cyclin E and DNA polymerases, among others, that drive the cell through the proliferative phase of the cell cycle subsequently occurs. CDK4 and CDK6 are activated by the D-type cyclins and expression of D-cyclins occurs as an early event in response to growth factors (Mateyak et al., 1999). By phosphorylating the RB protein, the cyclin D/CDK4 complex and the cyclin E/CDK2 complex contribute to the regulation of the G1 to S1 transition in the cell cycle. c-MYC indirectly represses the transcription of the cyclin D1 gene, a function that occurs independently of the MYC/MAX complex, while increasing the expression of cyclin E. Consequently, by sustaining cyclin E and CDK2 activity, c-MYC is able to prevent growth arrest (Philipp et al., 1994; Perez-Roger et al., 1997; Mateyak et al., 1999). The inhibitor of kinases (INK) family of cyclin dependent kinase is active on CDK4 and CDK6 and the inhibitory binding thereof occurs independently of the cyclin proteins. c-MYC expression is linked to a reduction in the levels and functioning of p27 which is a cyclin dependent kinase inhibitor [CKI] (Karn et al., 1989; Mateyak et al., 1999).

2.2.5 c-MYC and apoptosis

c-MYC has physiological potential to trigger rapid apoptosis (Amati et al., 1993), possibly as a protective mechanism to counteract oncogenic proliferation. It is postulated that the increased DNA replication that occurs due to over-expression of c-MYC, leads to DNA damage which subsequently triggers a tumour protein 53 (TP53) pathway to apoptosis. c-MYC may downregulate anti-apoptotic proteins such as BCL2 and upregulate proapoptotic proteins (Dang et al., 2005; Hemann et al., 2005). In the context of gene expression, deregulation of c-MYC is aptly described as producing an ‘avalanche’ type of effect that contributes to neoplasia (Hummel et al., 2006; Horn et al., 2013).

2.2.6 c-MYC induced metabolism of glucose and glutamine

The growth and proliferation of mammalian cells is fuelled by the catabolism of glucose and glutamine (Wise et al., 2008). By directly activating genes that are involved in mitochondrial

biogenesis, glycolysis and glutaminolysis, c-MYC can influence and regulate energy metabolism. c-MYC plays both an indirect and a direct role in regulating glucose metabolism genes such as *lactate dehydrogenase-A* (LDH) A and the *glucose transporter* (GLUT1). These genes are transactivated and stimulated by hypoxia inducible factor-1 (HIF) in the setting of hypoxic conditions, while c-MYC asserts its influence on glucose metabolism genes under aerobic conditions (Shim et al., 1997; Kim et al., 2006). During hypoxia, c-MYC is usually suppressed by HIF. However, when c-MYC is expressed in a deregulated manner, collaboration with HIF manifests and this serves to drive glycolytic gene expression in tumour cells (Dang, 2012). It is via c-MYC that altered cellular metabolism is linked to tumorigenesis. When tumour cells are located greater than 150μm from a blood supply, chronic hypoxia manifests and cellular adaptation is required for the tumour cells to survive and progress (Dang et al., 1999b). c-MYC contributes to the Warburg effect in cancer cells that encompasses an increased uptake and conversion of glucose to pyruvate. Pyruvate is subsequently converted to lactate by the enzyme LDH-A. It is likely that in the microenvironment of a tumour, c-MYC over-expression by tumour cells drives glycolysis in an aerobic setting and a moderately hypoxic setting. The latter occurs in unison with HIF, thus providing the energy required for cellular proliferation and growth (Dang, 1999a). The c-MYC-related glucose metabolic reprogramming confers the advantage of growth, survival and tissue invasion by tumour cells (Kroemer and Pouyssegur, 2008; Tansey, 2014). In contrast, glucose deprivation or the exposure to glucose antimetabolites induces apoptosis in c-MYC transformed cells. Knowledge hereof creates the potential for metabolite-targeted therapy of MYC-associated tumours (Shim et al., 1998).

Glutamine is considered to be an essential nutrient for cell growth or viability and its metabolism is enhanced by c-MYC. Within c-MYC transformed cells, glutamine transporters and glutaminase are induced along with LDH-A. In these cells, glutaminolysis is instrumental in the maintenance of the mitochondrial tricarboxylic acid cycle activity and mitochondrial integrity. The marked increase in glutamine utilisation and catabolism that occurs in this setting has been described as a c-MYC-induced cellular addiction to glutamine. Glutaminolysis leads to the production of nicotinamide adenosine dinucleotide phosphate hydrogen (NADPH), which is a source of bioenergy for cells. Within MYC transformed cells, the production of optimal quantities of NADPH from glutamine degradation supplies energy that is needed to sustain the process of cellular proliferation (Wise et al., 2008; Tansey, 2014). In contrast, glutamine deprivation of c-

MYC overexpressing cells stimulates apoptosis (Dang, 2012) and knockdown of glutaminase expression induces a marked reduction in the growth of prostatic cancer cells and lymphoma (Gao et al., 2009). Glutamine addiction within c-MYC transformed cells harbours potential for targeted therapeutic intervention of c-MYC-associated tumours.

2.2.7 c-MYC and miRNA

MiRNAs are non-protein coding single-stranded RNA, that specifically inhibit mRNA translation or marks it for cleavage by a nuclease. At the post-transcriptional level, MiRNAs regulate gene expression and have the potential to act as tumour suppressors due to their influence on cell proliferation, apoptosis and differentiation (Leucci et al., 2008). It was on lymphoma models which were *MYC*-dependent, that the link between miRNAs and tumorigenesis was established (He et al., 2005; O'Donnell et al., 2005). Direct upregulation of the protumorigenic miR-17-92 cluster is induced by c-MYC. Moreover, when activated c-MYC binds to miRNA promotors, there is widespread repression of expression of miRNA. It is established that deregulation of miRNA appears to be a fundamental element of the tumorigenic program of c-MYC (Chang et al., 2008; Sander et al., 2008). Notably, down-regulation of miRNA such as hsa-mir-34b is documented in cases of BL that lack *MYC* translocations. The upregulation of c-MYC protein, that occurs independently of gene alterations, is likely due to deregulated miRNA. MiRNA deregulation leads to gene modulation which contributes to oncogenesis (Chang et al., 2008; Leucci et al., 2008; Sander et al., 2008; Klapproth and Wirth, 2010:).

2.2.8 *MYC* and oncogenesis

Constitutive activation and aberrant expression of *MYC* occurs in approximately 70% of human malignancies (Klapproth and Wirth, 2010; Madden et al., 2021). In addition to tumour initiation, *MYC* is documented to also play a role in the maintenance of tumours (Arvanitis and Felsher, 2006; Dang, 2012; Gabay et al., 2014). Accordingly, the *MYC* gene may be viewed as a central oncogenic switch and over-expression is often associated with aggressive tumour behaviour and poor survival outcome (Spencer and Groudine, 1991; Dang et al., 1999b).

Over-expression of *MYC* may occur by mechanisms that include chromosomal translocation, chromosome 8 polysomy, amplification of the *MYC* oncogene due to increased *MYC* gene copy numbers, regulatory region single nucleotide polymorphism, upstream signalling pathway mutations or mutations that facilitate the stability of the c-MYC protein by prolonging its half-life (Stasik et al., 2010; Lin et al., 2012; Dang, 2012). It is noteworthy that alterations in the coding sequence of *MYC* are not a prerequisite for its oncogenic potential to manifest (Tansey, 2014).

MYC oncogene amplification was initially demonstrated within a human leukaemia cell line HL-60 (Collins and Groudine, 1982). When *MYC* over-expression occurs in proliferating neoplastic cells, there is a reduction in growth factor requirements, inhibition of exiting from the cell cycle, cellular enlargement and an acceleration of cell division (Karn et al., 1989; Grandori et al., 2000). Lin et al. (2012) demonstrated that throughout the cancer cell genome, in the context of *MYC* over-expression, there is an accumulation of c-MYC in the promoter regions of active genes that results in transcriptional amplification. This in turn increases the levels of transcripts within the gene expression program of the cancer cell. In other words, when deregulated expression of *MYC* occurs in cancers, it is likely that a sustained increase in c-MYC protein expression manifests throughout the cell cycle, thus contributing to tumorigenesis. Moreover, c-MYC associated tumorigenesis is linked to the evasion of tumour suppressing check points such as proliferative arrest, apoptosis and senescence (Gabay et al., 2014).

It is argued that by its own unaided influence, deregulated expression of c-MYC is unlikely to force cellular transition through the proliferative cycle. However, when deregulated expression of c-MYC is present in unison with other oncogenic events, such as loss of p53 or B-cell lymphoma 2 (BCL-2) over-expression, it may contribute to tumorigenesis in a synergistic manner (Gabay et al., 2014).

Over-expression of the MYC family of oncoproteins has been demonstrated in a multitude of malignancies such as small cell carcinoma of the lung and carcinomas of the breast, prostate and colon. c-MYC over-expression is also documented in myeloma, melanoma, neuroblastoma and lymphoma (Dang, 2012; Tansey, 2014). Within cells of the haematopoietic lineage, c-MYC over-expression promotes tumorigenesis and the level of over-expression plays an influential role in the onset of malignant transformation (Klapproth and Wirth, 2010). Moreover, the expression of c-MYC within DLBCL patients who received rituximab with cyclophosphamide,

hydroxydaunorubicin, vincristine and prednisone (R-CHOP) treatment is reported to be an adverse prognostic factor (Gupta et al., 2012). Conversely, the inactivation of c-MYC in tumour cells of the haematopoietic lineage leads to proliferative arrest, differentiation and senescence with subsequent intense apoptosis (Felsher and Bishop, 1999). Hereby, the potential for therapeutic intervention emerges. Therapeutic strategies that target the inhibition of c-MYC may induce tumour regression. Although theoretically feasible and promising, such strategies are currently evolving (Soucek et al., 2008).

2.2.9 *MYC* and B-cell lymphomagenesis

Cellular proliferation is a complex process which is highly regulated by an interplay of genes that promote growth, such as *MYC*, and the suppression of genes that inhibit growth. An altered expression of genes in favour of cell proliferation, leads to uncontrolled malignant proliferation (Adams et al., 1985). The prime example of *MYC*-induced lymphomagenesis is BL.

In 1958, a surgeon named Denis Parsons Burkitt, who worked as a missionary in equatorial Africa, documented a series of rapidly growing, fatal tumours of the jaw that distorted the facial region of African children and also involved the abdominal region (Burkitt, 1958; Coakley, 2006; Andrade-Filho, 2014). Although this tumour was initially described as a sarcoma, it was subsequently recognised as a very aggressive malignant lymphoma which is infamously known as BL (O'Conor and Davies, 1960; Burkitt and O'Conor, 1961; O'Conor, 1961). BL is often associated with EBV infection and it may afflict adults or paediatric patients worldwide as sporadic, endemic or HIV-associated subtypes (Epstein et al., 1964; Leoncini et al., 2008; Klapproth and Wirth, 2010).

MYC induced lymphomagenesis is classically evident in BL. The defining translocation that involves the immunoglobulin gene loci of the heavy chain (μ) or light chains [kappa(κ) or lambda (λ)], may be viewed as a characteristic cancer initiating event. These translocations in BL lead to constitutive *MYC* oncogene activation in the setting of a simple karyotype which lacks additional rearrangements (Zech et al., 1976; Dalla-Favera et al., 1982a; Erikson et al., 1982; Taub et al., 1982).

The *MYC* and immunoglobulin gene translocations in BL are usually mediated by class switch recombination or aberrant somatic hypermutation in the presence of AID within germinal centre

B-cells (Robbiani et al., 2008; Pasqualucci et al., 2008; Allday, 2009). The perspicacious finding of the frequent development of fatal B-cell lymphoma in transgenic mice in which *MYC* was coupled to the intron enhancer region of immunoglobulin (Eμ), was instrumental to the understanding of B-cell lymphomagenesis (Adams et al., 1983; Adams et al., 1985).

c-MYC immunoexpression has been reported in a diverse array of NHLs which are predominantly but not exclusively of B-cell subtypes such as BL, DLBCL, PBL, high-grade B-cell lymphoma with *MYC, BCL2* and/or *BCL6* rearrangements, transformed lymphoma, ALK-positive large B-cell lymphoma and lymphoblastic lymphoma (Yano et al., 1992; Ott et al., 2013; Chisholm et al., 2015; Kluk et al., 2016; Ye et al., 2016; Mihashi et al., 2017). c-MYC expression within >50% of tumour cells tends to occur predominantly in BL, DLBCL, high-grade B-cell lymphoma with *MYC, BCL2* and/or *BCL6* rearrangements and PBL in association with a high concordance of *MYC* rearrangements which are confirmed using fluorescence *in situ* hybridisation [FISH] (Chisholm et al., 2015). Within aggressive B-cell NHLs, which are driven by *MYC* aberrations, c-MYC protein expression within at least 40% of tumour cells is likely to be a poor prognostic factor (Horn et al., 2013; Cook et al., 2014; Bigras, 2016).

2.3 Diffuse large B-cell lymphoma

DLBCL is the most common subtype of NHL which may develop de novo, from transformation of a low-grade B-cell lymphoma and due to HIV infection (Campo et al., 2017). This tumour accounts for approximately 35% of the malignancies of lymphoid origin (Gascoyne et al., 2017b). In developing regions of the world such as SA, DLBCL accounts for up to 43% of NHL due to a high seroprevalence of HIV (World Health Organization, 2020; Patel et al., 2015). In the ART era, DLBCL persists as one of the main types of cancer in the HIV seropositive population (Gibson et al., 2014; Dolcetti et al., 2016) and it displays high-grade characteristics. HIV-associated DLBCL manifests at a younger age and demonstrates a propensity towards advanced stage of disease that includes involvement of the perinodal soft tissues, bone marrow, liver, central nervous system and the gastrointestinal tract (Dolcetti et al., 2016; Magangane et al., 2020; Cassim et al., 2020).

2.3.1 DLBCL: Age and gender

DLBCL, NOS has a propensity to occur in adult patients of median age 55 to 71 years and demonstrates a slight male predominance (Anderson et al., 1998; Ott et al., 2010). In contrast, HIV-associated DLBCL tends to manifest approximately two decades earlier with a median age at presentation of 36 to 41 years (Patel et al., 2015; Machailo, 2016; Cassim et al., 2020). The gender distribution in HIV DLBCL varies from being male predominant to a relatively equal distribution between males and females (Baptista et al., 2015; Magangane et al., 2020; Machailo, 2016). Infrequently, DLBCL is documented in paediatric or adolescent patients and a male predominance is reported (Oschlies et al., 2006).

2.3.2 DLBCL: HIV viral load, CD4 count and ART

In the era predating ART, the incidence of NHL was 60 to 200 times higher in the HIV seropositive population (Beral et al., 1991; Levine, 1993; Rabkin, 1994; Grogg et al., 2007). Due to the presence of high levels of HIV viraemia and low CD4 counts, NHL was documented in

approximately 10% of patients who were afflicted with AIDS (Goedert et al., 1998; Carbone, 2002). A substantial increased risk for NHL occurs when the CD4 count is <50 cells/mm^3 and HIV RNA levels are >100 000 copies/µL (Zoufaly et al., 2009; Bower et al., 2009; Engels et al., 2010).

In accordance with the World Health Organisation (WHO) guidelines of "test and treat" implementation of ART is currently recommended as soon as HIV infection is confirmed, irrespective of the baseline CD4 count (World Health Organisation, 2016; Kitahata et al., 2009; Sterne et al., 2009). The implementation of antiretroviral therapy has led to a notable reduction in the incidence of NHL (Besson et al., 2001; Engels et al., 2008; Franceschi et al., 2010; Hleyhel et al., 2013). Most of the HIV-1 infected patients who receive effective ART will experience immune recovery in the form of restoration of a normal CD4 T-lymphocytic count [i.e., CD4 >500 cells/mm^3] (Battegay et al., 2006). Therefore, there was worldwide determination to reach the 90-90-90 treatment target by 2020, whereby 90% of people who are living with HIV know their status, 90% of whom are on ART and 90% subsequently experience viral suppression (World Health Organisation, 2016). SA has reached and exceeded two of these targets and currently has the largest ART program worldwide. According to 2019 data, SA has provided 75% of patients with ART and is presently striving to rollout to at least 90% of its HIV seropositive population (UNAIDS, 2021).

Unfortunately, up to one third of patients who receive effective ART may experience persistently low levels of CD4+ T-lymphocytes, despite the presence of virological suppression and long-term duration of therapy (Battegay et al., 2006). An important predictor of incomplete CD4 recovery or restoration is the presence of a profoundly low CD4 count (i.e., <200 cells/mm^3) at the time of commencing ART (Braitstein et al., 2006; Kelley et al., 2009). Incomplete CD4 restoration following effective ART may also be due to HIV-induced exhaustion or destruction of lymphoid tissue (Mauser et al., 2021), loss of regenerative potential and thymic dysfunction (Moir et al., 2011). The cumulative viraemia that occurs during ART, is proven to be a strong independent risk factor for developing HIV-associated lymphoma (Zoufaly et al., 2009). Compared with the general population, there is a persistent 9 to 11 times increased risk of NHL developing in HIV patients who receive ART (Hleyhel et al., 2013; Gibson et al., 2014; Shiels et al., 2018). The

aggressive B-cell NHLs that develop despite the influence of ART (Grulich, 1999; Carbone et al., 2014), have a direct influence on HIV-associated morbidity and mortality (Gopal et al., 2013).

ART-induced immune reconstitution is not always sufficient to prevent the progression of disease in patients who are living with HIV (Totonchy and Cesarman, 2016). Although AIDS-defining malignancies are decreasing due to the influence of ART (Bouvard et al., 2009; Smith et al., 2014), in SA HIV-associated high-grade B-cell NHL remains a malignancy of dire public relevance (Pather et al., 2013b; Patel et al., 2015; Machailo, 2016; Cassim et al., 2020; Magangane et al., 2020). Severe HIV-induced immunosuppression at the time of the lymphoma diagnosis has a negative impact on survival outcome and the likelihood of achieving complete remission. In HIV DLBCL, a CD4 count of <150 cells/mm^3 is associated with an inferior overall survival outcome (Cassim et al., 2020). Moreover, when the CD4 count is <100 cells/mm^3 complete remission of aggressive B-cell NHL is less likely to occur than if the CD4 count is >200 cells/mm^3 (Ramos et al., 2020).

Despite the presence of immune reconstitution that is induced by combination ART, the persistent risk of HIV-seropositive patients developing an aggressive B-cell NHL (Gibson et al., 2014; Dolcetti et al., 2016) leads us to question whether the complex interaction of the aforementioned factors could be shrouding other entities that are contributing to lymphomagenesis. Consequently, NHL continues to contribute significant morbidity and mortality in the HIV seropositive population (Dolcetti et al., 2016).

2.3.3 DLBCL: Morphology

DLBCL comprises tumour cells which are medium to large in size. Based on whether the tumour nuclei are larger than or equal in size to the nuclei of non-neoplastic macrophages, the size of the tumour cells is assigned. Non-neoplastic lymphocytes may also be used as an intrasectional reference structure by which to gauge the cell size. If the tumour nuclei are more than twice the size of non-neoplastic nuclei, a large tumour cell size is assigned with reasonable reliability (Gascoyne et al., 2017b).

Due to the presence of high rates of cellular proliferation and turnover, some cases of DLBCL may display a starry-sky (SS) appearance, similar to that which occurs in BL. Three common

morphological variants of DLBCL are recognised, in addition to several rare variants. The common variants are labelled as centroblastic (CB) when >90% of the tumour comprises centroblasts, immunoblastic (IB) when >90% of the tumour comprises immunoblasts and anaplastic (AP) which is defined by the presence of bizarre cytological features (Ott et al., 2010). CB, IB and AP cytological features are depicted below within Figure 2.1

In a prospective multicentre clinical trial, comprising 949 DLBCL patients, the CB morphological variant was documented seven times more frequently than the IB variant and twenty-seven times more frequently than the AP variant. Importantly therein, IB morphology which also included plasmablastic or plasmacytic features, had proven to be an adverse prognostic factor (Ott et al., 2010). The prognostic influence thereof is most likely linked to the IB variant being a morphological clue and "major reservoir" for the presence of *MYC* rearrangement, which is demonstrable in 33% of this variant (Horn et al., 2015). The IB variant of DLBCL is reported to occur more frequently in advanced HIV than the centroblastic variant (Dolcetti et al., 2016). Furthermore, CB and IB morphological variants may be associated with germinal centre B-cell-like [GCB] and nongerminal centre [NGC] or activated B-cell-like [ABC]-subtypes of DLBCL, respectively (Rosenwald et al., 2002; Gascoyne et al., 2017b).

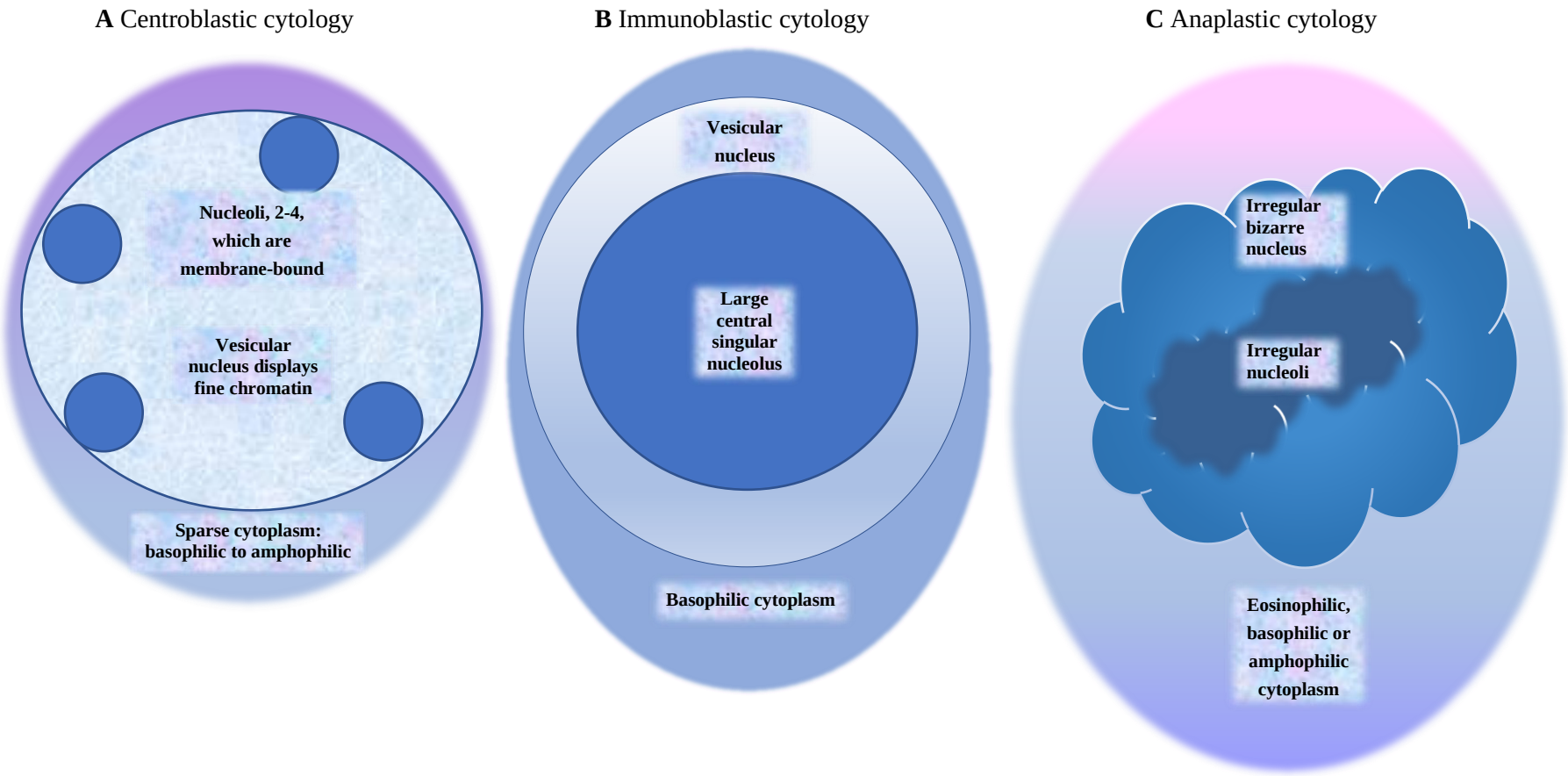


Figure 2.1: DLBCL cytomorphology: centroblastic (A), immunoblastic (B) and anaplastic (C).

2.3.4 DLBCL: What is the relevance of the cell of origin subtype?

The molecular stratification of DLBCL continues to evolve. There is supportive evidence that genomic analysis of DLBCL may detect prognostic factors of significance (Lacy et al., 2020) with vulnerability to targeted therapy in an emerging era of precision medicine (Wright et al., 2020). Molecular subtyping of DLBCL by gene expression profiling (GEP), which is considered the gold standard thereof, has facilitated the segregation of DLBCL into three major categories comprising GCB, ABC and primary mediastinal B-cell lymphoma. These categories are predictive of survival outcome (Alizadeh et al., 2000; Rosenwald et al., 2002; Rosenwald et al., 2003; Pasqualucci et al., 2011; Schmitz et al., 2018; Chapuy et al., 2018; Chen et al., 2019).

The GCB subtype expresses cluster of differentiation 10 (CD10) and B-cell lymphoma 6 (bcl-6) proteins in association with somatic hypermutations and mutations of the *Ig* genes. In contrast, an ABC subtype is characterized by upregulation and activation of multiple myeloma oncogene 1 (MUM1), B-cell receptor signalling and the nuclear factor–kappa B (NF-κB) antiapoptotic pathway. However, up to 10% of DLBCL may defy molecular subtyping by GEP (Alizadeh et al., 2000; Davis et al., 2010).

Identification of the molecular COO of DLBCL has clinical relevance, as the presence of a GCB-subtype confers a survival advantage over an ABC-subtype (Alizadeh et al., 2000; Hans et al., 2004). The persistently inferior survival outcome and high relapse rates of the ABC-subtype, despite CHOP and Rituximab (anti-CD20 monoclonal antibody) regimens, led to exploration of the molecular characteristics and therapeutic targeting thereof. Advancement of treatment strategies subsequently ensued with the addition of newer agents to a doxorubicin-based regimen. The addition of bortezomib, that targets the NF-κB pathway, to dose adjusted infusional etoposide and CHOP has improved the survival outcome of the ABC subtype of DLBCL (Dunleavy et al., 2009). Other agents such as ibrutinib, lenalidomide, idelalisib or venetoclax, when used with R-CHOP are also promising armaments for the treatment of the ABC-subtype (Mathews Griner et al., 2014).

GEP for determining the COO may be performed on formalin-fixed paraffin-embedded (FFPE) tumour specimens (Scott et al., 2014). However, the routine implementation of GEP assessment for all cases of DLBCL is currently not feasible. This modality is not widely available and there are limiting factors regarding cost, technical challenges and scarcity of interpretational expertise.

In contrast, IHC is an essential component of the histopathological confirmation of DLBCL. Accordingly, IHC is recognised as an acceptable alternative and surrogate technique for the subclassification of DLBCL into the aforementioned categories (Gascoyne et al., 2017b).

After performing GEP subtyping on DLBCL, a classic COO IHC-defined algorithm for DLBCL was published approximately two decades ago by Hans et al. (2004). Routinely available immunomarkers such as CD10, bcl-6 and MUM1 were utilised with positive staining defined as expression in ≥30% of tumour cells. GCB-type DLBCL was defined CD10+, bcl-6+/-, MUM1 +/- or bcl-6+, CD10-, MUM1-. The NGC-type DLBCL is characteristically CD10-, bcl-6+/- and MUM1+.

Several other algorithmic substratifications of DLBCL have been created by including immunomarkers such as BCL2, forkhead box P1 (FOXP1), germinal centre B-cell-expressed transcript 1 (GCET1) and/or LIM domain only 2 (LMO2). Although variable concordance and disparities between the IHC and GEP subclassifications have been documented, the value of IHC in the COO subtyping of DLBCL appears to be convincingly applicable to the routine diagnostic workup of DLBCL (Muris et al., 2006; Nyman et al., 2007; Choi et al., 2009; Meyer et al., 2011). In HIV-associated DLBCL, consensus appears to be lacking regarding the COO distribution and its influence on survival outcome. ABC subtype based on the Tally algorithm, was reported to occur more frequently in HIV DLBCL with an inferior overall survival (Morton et al., 2014). However, Dunleavy et al. (2010) documented the GCB subtype more frequently in HIV DLBCL and this was significantly associated with progression free disease. Notably, there are also several reports of a relatively equal GCB and ABC subtype distribution in HIV DLBCL without significant differences in the overall survival outcome (Chadburn et al., 2009; Pather et al., 2013b; Machailo, 2016; Cassim et al., 2020). B-lymphocyte-induced maturation protein 1 (BLIMP1) expression in DLBCL denotes the acquisition of a partial plasmablastic phenotype in DLBCL, which is associated with aggressive clinical behaviour (Montes-Moreno et al., 2010). Based on the Hans-defined algorithm, IHC will be utilised to determine the COO subtypes of HIV positive and negative DLBCL subgroups. The influence of the COO on the overall survival outcome will be explored.

2.3.5 DLBCL: c-MYC protein expression

c-MYC protein expression occurs in 13-64% of DLBCL as summarised within Table 2.1. An inferior survival outcome is predicted when c-MYC expression occurs in >50% of DLBCL tumour cells (Kluk et al., 2012). A close correlation has been demonstrated between high levels of c-MYC protein expression, i.e. ≥70-80%, within DLBCL and *MYC* rearrangements (Green et al., 2012a; Kluk et al., 2016). Hence, we are led to accept the convincing evidence that high expression of c-MYC by immunohistochemistry is likely to be a suitable screening modality for predicting the presence of *MYC*-driven aggressive B-cell lymphoma (Nwanze et al., 2017). Nonetheless, concomitant FISH analysis is still warranted for confirmation of *MYC* rearrangement. When *MYC* rearrangement is confirmed, further investigations for *BCL2* and *BCL6* rearrangements are also indicated.

Over-expression of c-MYC protein may occur in DLBCL in which *MYC* translocations are not evident (Kluk et al., 2016). High levels of c-MYC protein expression within DLBCL due to increased copy numbers of the *MYC* gene has been documented in the absence of *MYC* translocation (Stasik et al., 2010; Kluk et al., 2012; Valentino et al., 2013). However, a slight lack of alignment is evident in isolated reports which have not demonstrated a statistically significant association between increased *MYC* gene copy numbers and c-MYC protein expression (Kluk et al., 2016). Hereby highlighted, is the need for an in-depth exploration of *MYC* gene copy number increases in DLBCL, lacking *MYC* translocation, that may be associated with expression of c-MYC protein.

Table 2.1: Review of c-MYC and BCL2 expression in DLBCL

IHC	+ Tumours	Rearrangement/No. tumours	Author	Year
≥70% MYC ≥50% BCL2 MYC & BCL2	28/98 (29%) 68/98 (69%) 34/98 (35%)	21/98 (21%) 28/98 (29%)	Ma *et al*	2020
≥40% MYC ≥50% BCL2 MYC & BCL2	HIV DLBCL: 14% HIV DLBCL:48% HIV DLBCL: 10%		Cassim *et al*	2020
>40% MYC BCL2 MYC & BCL2	18/61 (HIV DLBCL: 30%) 32/61 (53%) 9	8/29 (28%) 1/24 (4%)	Ramos *et al*	2020
>40% MYC >50% BCL2 MYC & BCL2	29/217 (13%) 115/217 (53%) 10/217 (5%)		Jesionek-Kupnicka *et al*	2019
≥40% MYC ≥50% BCL2	264/2383 (11%)	94 *MYC*/*IG* locus translocation 82/264 (*MYC & BCL2* + 31%)	Rosenwald *et al*	2019
>50% MYC	0/10 (DLBCL)	1/10 (10%)	Nwanze *et al*	2017
>50% MYC	32/176 (18%)	37/176 (21%)	Kluk *et al*	2016
≥90% MYC 50% or 70% BCL2	23/50 (46%) 37/50 (74%)	51/574 (9%) (24 *MYC/IG* [4%] & 26 *MYC/nonIG* [5%]) 19/51 [37%] *MYC & BCL2*)	Copie-Bergman *et al*	2015
≥40% MYC ≥50% BCL2 MYC & BCL2 +	65/135 (48%) 98/117 (84%) 54/135 (40%)	32/131 (24%) 39/117 (33%) 16/131 (12%) 34/131 (26%) multiple *MYC* copies	Wang *et al*	2015

IHC	+ Tumours	Rearrangement/No. tumours	Author	Year
>70-95% MYC	52% (mean expression)	39/432 (9%) 3 tumours *MYC* gains	Tzankov *et al*	2014
MYC ≥40%	27/198 (14%)	13/69 (19%)	Cook *et al*	2014
MYC >40%	90/283 (32%)	36/407 (9%)	Horn *et al*	2013
40% MYC 70% BCL2 MYC & BCL2	300/466 (64%) 233/4 66 (50%) 157/466 (34%)	 10/394 (3%)	Hu *et al*	2013
≥50% BCL2	178/327 (54%)	60/327 (18%) 27/327 (8%) *MYC* 8/327 (3%) *BCL2 & MYC*	Visco *et al*	2013
MYC ≥40%	59/132 (45%)	11/121 (9%) *MYC* Increased *MYC* copies 114/132 (83%)	Valentino *et al*	2013
≥70% MYC	35/205 (17%)	25/212 (12%) (23/207 primary DLBCL) (2/5 secondary DLBCL)	Green *et al*	2012
30% MYC	12/24 (50%)	3/29 (10%)	Gupta *et al*	2012
≥40% MYC ≥50% BCL2 MYC & BCL2	100/307 (33%) 160/304 (53%) 35/167 (21%)	34/290 (12%) *MYC* 68/287 (24%) *BCL2* 14/290 (5%) *MYC* & *BCL2*	Johnson *et al*	2012
>30% BCL2 & bcl-6	-	12/135 (9%)	Savage *et al*	2009
≥10% BCL2	110/168 (66%) 15/17 (88%)	14/156 (9%) *MYC* 11/156 (7%) increased *MYC* copies 5/145 (3%) *BCL2*	Yoon *et al*	2008

Abbreviations: DLBCL – diffuse large B-cell lymphoma, IHC – immunohistochemistry HIV – human immunodeficiency virus

2.3.6 DLBCL: BCL2 and c-MYC co-expression

While c-MYC protein is associated with neoplastic cellular proliferation and transformation, inhibition of apoptosis is primarily the function of BCL2 (Wang et al., 2015). A subset of de novo and relapsed DLBCL, which constitutes 5-40% thereof, demonstrates over-expression of c-MYC and BCL2 proteins which are detected by utilising IHC. A summary of c-MYC and BCL2 protein expression within DLBCL is presented within Table 2.1 The terminology 'double-positive, dual expressor or double expression (DE) DLBCL is applicable (Wang et al., 2015; Herrera et al., 2017; Rosenwald et al., 2019). DE tends to occur in the ABC subtype of DLBCL (Johnson et al., 2012; Hu et al., 2013; Jesionek-Kupnicka et al., 2019) and its presence is confirmed by c-MYC and BCL2 protein co-expression of ≥40% and ≥50%, respectively in the absence of concomitant *MYC* and *BCL2* translocations (Johnson et al., 2012; Horn et al., 2013; Perry et al., 2014; Wang et al., 2015; Rosenwald et al., 2019). Such rearrangements are the defining components of high-grade B-cell non-Hodgkin lymphoma with *MYC* and *BCL2* rearrangements (Johnson et al., 2012; Green et al., 2012b; Hu et al., 2013), which frequently expresses c-MYC and BCL2 proteins, predominantly in the context of a germinal centre phenotype or genotype in association with a dismal survival outcome (Snuderl et al., 2010; Li et al., 2012a). DE DLBCL is more common than the translocation-defined category and DE may also occur in HIV seropositive patients (Ramos et al., 2020; Cassim et al., 2020). DE LBCL tends to correlate with an inferior survival outcome and has proven to be refractory to R-CHOP treatment regimens (Staiger et al., 2017; Ma et al., 2020).

2.3.7 DLBCL: Ki-67 expression

A nonhistone nuclear and nucleolar protein, i.e., Ki-67 antigen/pKi-67, is expressed in normal and neoplastic cells within active phases of the cell cycle (i.e., G_1, S and G_2) and during mitosis of proliferating cells. Assessment of the growth fraction proliferation activity of NHL tumour cells, i.e. beyond G_0 and early G_1, has evolved from utilising flow cytometry and snap-frozen tissue to protein expression that is detectable by IHC on FFPE tumour specimens (Gerdes et al., 1984; Bauer et al., 1986; Grogan et al., 1988; Miller et al., 1994). When an antibody such as Molecular Immunology Borstel 1 (MIB-1) targets this protein in proliferating cells, the term "proliferation marker" is applicable (Gerdes et al., 1983; Gerdes et al., 1991; Scholzen and Gerdes, 2000; Endl and Gerdes, 2000; Brown and Gatter, 2002). Due to its strict expression beyond G0 of the cell

cycle and the co-expression with other markers of proliferation, Ki-67 plays a pivotal role in cellular proliferation (He et al., 2014).

The value of Ki-67 in assessing the growth fraction within NHL was highlighted during the 1980's when expression exceeding 70-80% was established as a pre-treatment independent factor of poor survival outcome (Bauer et al., 1986; Gerdes et al., 1987; Grogan et al., 1988). Broyde et al. (2009) subsequently proposed a 45% cut off to distinguish aggressive from indolent disease and demonstrated that expression of at least 70% in DLBCL could predict a poor outcome. Aggressive NHLs are typified by a high proliferation index in which Ki-67 often exceeds 75% (Miller et al., 1994; Savage et al., 2009).

The prognostic value of the Ki-67 proliferation index in lymphoma has subsequently been labelled as inconclusive, inconsistent and intermittently contradictory. Some researchers have not demonstrated a significant prognostic impact (Jerkeman et al., 2004), while others have documented an inverse impact on survival outcome such that a low proliferation index may negatively impact the survival outcome of DLBCL (Hasselblom et al., 2008; He et al., 2014). In contrast, several reports have supported the notion that high Ki-67 expression of >80-85% in DLBCL is a predictor of poor survival outcome (Zaiem et al., 2020), higher relapse rates and inferior event free survival in the R-CHOP era (Yoon et al., 2010). In the rituximab era, a significant correlation between poor survival outcome and high Ki-67 expression has been demonstrated (Salles et al., 2011). However, this may be limited to the NGC-subtype of DLBCL (Li et al., 2012b; Koh et al., 2015) and when the age of patients exceeds 70 years (Koh et al., 2015).

HIV+ DLBCLs tend to have higher Ki-67 expression than HIV- DLBCLs (Cassim et al., 2020). Chadburn et al. (2009) have suggested that Ki-67 expression which exceeds 90% within HIV+ DLBCLs, is associated with an improved survival outcome. This may be due to an improved response to therapy, in the context of high proliferation indices within HIV+ DLBCLs. The proliferative driving force within these tumours might be further enhanced by the presence of *MYC* aberrations.

2.3.8 DLBCL: *MYC* aberrations (rearrangement and/or copy number increase)

Constitutive activation of *MYC* in DLBCL has been consistently documented when this gene is translocated and juxtaposed to an immunoglobin gene on chromosomes 2, 14 or 22 (Croce, 1993; Leoncini et al., 2008) or a non-immunoglobulin locus such as *BCL6,* paired box 5 (*PAX5), BCL11A, ICAROS49, ZBTB5* or *ZCCHC7* (Bertrand et al., 2007; Barrans et al., 2010; Tzankov et al., 2014; Rosenwald et al., 2019). To reiterate, aggressive B-cell lymphomas harbouring translocations of *MYC* and *BCL2* and/or *BCL6* are now classified as high-grade B-cell lymphomas with *MYC* and *BCL2* and/or *BCL6 rearrangements* and these have proven to be refractory to current standard therapy (Swerdlow et al., 2016; Kluin et al., 2017).

Approximately 4-16% of de novo DLBCL may harbour *MYC* translocations (Yoon et al., 2008; Savage et al., 2009; Aukema et al., 2011) which tends to occur in association with a GC cell of origin subtype (Klapper et al., 2008; Yoon et al., 2008; Horn et al., 2013; Visco et al., 2013; Copie-Bergman et al., 2015; Rosenwald et al., 2019). *MYC* translocations also have a tendency to occur as a secondary event in DLBCL, often in the setting of complex karyotypic aberrations (Nguyen et al., 2017). *MYC* translocations tend to correlate with advancing age of patients, high-grade phenotype, progression of the lymphoma, poor response to certain treatment regimens such as CHOP or R-CHOP and an inferior overall survival (Yano et al., 1992; Akasaka et al., 2000; Yoon et al., 2008; Boerma et al., 2009; Savage et al., 2009; Barrans et al., 2010; Horn et al., 2013; Copie-Bergman et al., 2015). Therefore, intensified therapy such as a BL-treatment protocol, radiation or targeted novel therapy may be warranted in this context (Savage et al., 2009; Sehn, 2012; Zhou et al., 2014; Tzankov et al., 2014).

By utilising FISH, increased *MYC* gene copy numbers have been astutely documented in DLBCL (Yoon et al., 2008; Tzankov et al., 2014; Wang et al., 2015; Lu et al., 2015). During recent decades, advancement in diagnostic modalities has rendered an option of evaluating gene copies within FFPE specimens of malignancies. The forerunner thereof is the human epidermal growth factor receptor oncogene (*HER2*) which is amplified within a subset of breast carcinomas. *HER2* gene copies can now be evaluated in combination with chromosome 17 centromere numbers by utilising dual-colour brightfield chromogenic *in situ* hybridisation (CISH) on FFPE breast carcinomas (Arnould et al., 2003; Todorović-Raković et al., 2007; Nitta et al., 2008; Wolff et al., 2018). Subsequently, dual-colour CISH and comparative genomic hybridisation techniques have been

utilised to demonstrate increased copies of the *MYC* gene in 3-83% of DLBCLs. Very few of these tumours were noted to concurrently harbour *MYC* translocation (Stasik et al., 2010; Testoni et al., 2011; Valentino et al., 2013; Kluk et al., 2012). Increased *MYC* gene copies in DLBCLs are associated with c-MYC protein over-expression and the latter correlates with a poor overall survival (Valentino et al., 2013). Lu et al. (2015) further demonstrated that *MYC* copy number aberrations, i.e., gains (3-4 copies) or amplification (≥5) in DLBCL, NOS conferred an inferior median OS and an inferior progression free survival. Although gains of *MYC* are more common in DLBCL than *MYC* amplification, the former might not influence the survival outcome (Ott et al., 2013). The presence of increased *MYC* gene copy numbers in HIV seropositive DLBCL has yet to be explored in depth.

2.3.9 DLBCL: Stage and extranodal involvement

Standardisation of the oncological care of lymphoma patients necessitated the development of a staging system. The Ann Arbor staging system was originally developed for patients with Hodgkin lymphoma. Subsequently, it was established as the basis from which the anatomic stage of NHL could also be assigned (Carbone et al., 1971). However, there are fundamental differences in the disease patterns of CHL and NHL, regarding nodal or extra-nodal involvement and the frequent bone marrow infiltration by some types of NHL. Hereby, the shortcomings of the clinical applicability of this staging classification to NHL were highlighted (Armitage, 2005). Nonetheless, this staging classification remains the globally adopted method for the anatomic staging of NHL. Early-stage disease (i.e., I-II) includes the involvement of a single lymph node region or lymphoid structure and the involvement of two or more lymph node regions on the same side of the diaphragm. In contrast, advanced-stage disease (i.e., stage III-IV) refers to the involvement of lymph node regions or structures on both sides of the diaphragm or the involvement of extranodal structures other than a contiguous extranodal site or proximal to a known nodal site (Carbone et al., 1971). Cotswold modifications of this staging were subsequently implemented and included the designation of bulky disease with the use of the suffix 'X', among other changes (Lister et al., 1989). HIV-associated aggressive B-cell lymphomas have a strong tendency towards advanced stage (i.e., Ann Arbor stage III or IV) at presentation and extranodal involvement, both of which are poor prognostic factors (Patel, 2007; Lu et al., 2014; Patel et al., 2015; Chen et al.,

2019). The stage of lymphoma and extranodal involvement are factors that contribute towards formulating the IPI score.

2.3.10 DLBCL: IPI and R-IPI score

Based on a multivariate analysis of 2031 adult patients in Canada, USA and Europe who had aggressive NHLs for which treatment included doxorubicin-based chemotherapy, a model that was predictive of long-term survival was proposed. This model comprised a pentad of factors such as the patients' age (>60 years), Ann Arbor stage of tumour (III/IV), the presence of more than one extranodal disease site, Eastern Cooperative Oncology Group (ECOG) performance status ≥2 and LDH concentration greater than the upper limit of normal within the serum. Based on the total score rendered by this model, four risk groups were generated. A three-year overall survival of 91% was documented for the low-risk group and a three-year overall survival of 59% was documented for the high-risk group as shown in Table 2.2. This model was labelled the International Prognostic Index (IPI) score and it was found to be more accurate in predicting the long-term survival than the Ann Arbor staging classification (International Non-Hodgkin's Lymphoma Prognostic Factors Project, 1993; Ruppert et al., 2020).

Table 2.2: IPI prognostic scoring system for aggressive NHL

Risk Factors/Score	**Risk Category**	**3-year OS Percentage**
0 – 1	Low	91%
2	Low-intermediate	81%
3	High-intermediate	65%
4-5	High	59%

Abbreviations: IPI – International Prognostic Index, OS – overall survival

An age adjustment of the IPI score is applicable when patients are 60 years of age or younger. In this age adjusted context, the tumour stage, LDH level and performance status were shown to be independent prognostic factors (International Non-Hodgkin's Lymphoma Prognostic Factors Project, 1993). The addition of immunotherapy to the CHOP regimen to treat DLBCL in HIV-patients has led to a consistent improvement of the survival outcome and cure rate. The IPI score has proven to retain its predictive value in the era of anti-CD20 (rituximab) immunotherapy by distinguishing fewer risk groups (Sehn et al., 2006; Ziepert et al., 2010). Redistribution of the IPI factors into a revised IPI (R-IPI) provided a more clinically relevant prediction of outcome in the era of immunochemotherapy. Therefore, with the aim of improving the risk stratification of newly diagnosed DLBCL patients who received R-CHOP therapy, the IPI score was modified and revised by Sehn et al. (2006) to comprise three risk groups as shown in Table 2.3

Table 2.3: Revised IPI for DLBCL

Revised IPI	Number of IPI Factors	4-year OS percentage DLBCL
Very good	0	94%
Good	1-2	79%
Poor	3-5	55%

Abbreviations: IPI – International Prognostic Index, OS – overall survival

Although the predictive value of IPI scores in HIV-associated DLBCL is deemed controversial (Kimani et al., 2021; Dunleavy and Wilson, 2012), Mounier et al. (2006) contributed that IPI scores and HAART were prognostic factors that influenced the survival outcome of HIV-associated DLBCL patients.

2.3.11 DLBCL: Treatment and survival outcome

DLBCL is potentially curable with chemotherapy (Armitage and Weisenburger, 1998) and immunotherapy (Mounier et al., 2003; Dunleavy et al., 2010; Johnson et al., 2012; Shah et al., 2014). However, in the developing regions of the world, the survival outcome of HIV DLBCL is still progressively evolving. Reports from the southern regions of Africa have attested that when ART and CHOP treatment regimens are used for HIV-DLBCL, the overall survival outcome might not be influenced by HIV infection. Moreover, the survival outcome might be similar to that achieved in the USA and Europe (Painschab et al., 2019; de Witt et al., 2013). It is further suggested that HIV DLBCL may be associated with longer or similar disease-free survival (Baptista et al., 2015) to that of HIV seronegative DLBCL and possibly an excellent overall survival (Coutinho et al., 2014).

Rituximab is an anti-CD20 monoclonal antibody which was initially approved for the treatment of B-cell follicular lymphoma (McLaughlin et al., 1998; Colombat et al., 2001). When rituximab binds to the CD20 antigen that is expressed in B-cell lymphoma and non-neoplastic B-lymphocytes, cytotoxicity occurs due mechanisms of direct induction of apoptosis, complement-dependent or antibody-dependent pathways and direct growth arrest (Jazirehi and Bonavida, 2005). Improvement in the survival outcome of HIV- DLBCL patients that was documented since the CHOP regimen was augmented with anti-CD20 immunotherapy has been described as an extraordinary revolution in the prognosis (Held et al., 2006; Sonet and Bosly, 2009). Even in the context of relapsed and refractory DLBCL, the standard of care includes salvage chemotherapy with rituximab, high-dose therapy and autologous stem cell transplant for chemosensitive patients (Vardhana et al., 2017). Rituximab may be included in the treatment regimen of HIV-associated DLBCL (Ribera et al., 2008; Barta et al., 2013) with c-ART for curability that matches that of the HIV seronegative counterpart. Notably, ART in the context of AIDS-related lymphoma, is shown to significantly increase the median survival (Mounier et al., 2006). However, balancing effective cytotoxic treatment with the insult on immune function and potentially life-threatening infections, are significant clinical challenges which are heavily influenced by the baseline CD4 counts (Dunleavy and Wilson, 2012).

2.4 Plasmablastic lymphoma

Banks et al. (1978) reported a case of a solitary extramedullary diffuse large cell lymphoma that demonstrated immunoblastic and plasmablastic features, but otherwise lacked cell surface markers. PBL is an exceptionally aggressive NHL that was originally documented in the oral cavity region of HIV-seropositive homosexual males. This tumour was initially considered to be a variant of DLBCL until the PBL nomenclature was proposed in 1997 by Delecluse et al. (1997). PBL was subsequently recognised as a distinct diagnostic category (Campo et al., 2017) that constitutes approximately 3% of NHL (Carbone, 2002; Castillo et al., 2015).

There is worldwide consensus that the majority of these tumours develop in the context of immunodeficiency (Chetty et al., 2003; Dong et al., 2005; Castillo et al., 2008; Cattaneo et al., 2015; Meer et al., 2020). Due to the high seroprevalence of HIV in SA, PBL constitutes 23% of NHLs at Chris Hani Baragwanath Academic Hospital [CHBAH] (Patel et al., 2015) and 32% of head and neck NHLs reported at Charlotte Maxeke Academic Hospital [CMJAH] (Alli and Meer, 2017), both of which are tertiary academic institutes in the Johannesburg region.
In those who are seronegative for HIV (Han et al., 2017), PBL is usually reported in the context of a concurrent autoimmune disorder or due to immunosuppression following organ transplantation, cancer therapy or advancing age (Borenstein et al., 2007; Castillo et al., 2010a; Castillo et al., 2011b; Brahmania et al., 2011; Zimmermann et al., 2012; Black et al., 2013; Chen et al., 2015; Elyamany et al., 2015; Liu et al., 2015; Gui et al., 2016; Han et al., 2017; Bouchla et al., 2018). Rarely, PBL is reported in non-elderly immunocompetent patients (Matikas et al., 2014; Huang et al., 2015).

2.4.1 PBL: HIV and severity of immunosuppression

HIV PBL most often develops in the setting of severe immunosuppression when the CD4 count is less than 100-200 cells/mm^3 (Castillo et al., 2010b; Ibrahim et al., 2014), in the presence of a variable viral load (Bogusz et al., 2009).

2.4.2 PBL: Age and gender

HIV PBL has a propensity to develop in the 39-49 year age group and it is reported predominantly in males (Castillo et al., 2010b; Morscio et al., 2014; Tchernonog et al., 2017; Rodrigues-Fernandes et al., 2018). The male gender predilection of PBL may be linked to homosexual risk groups or intravenous drug usage risk groups. However, in regions of southern Africa, a relatively equal male to female ratio is evident among patients who have PBL (Zuze et al., 2018; Meer et al., 2020). PBL develops infrequently in paediatric patients (Misra et al., 2017) who may be HIV seropositive (Radhakrishnan et al., 2005; Chabay et al., 2009; Pather et al., 2013a; Vaubell et al., 2014; Goedhals et al., 2014).

HIV seronegative PBL patients are generally older by approximately two decades at presentation and the male predominance persists in this category (Li et al., 2016).

2.4.3 PBL: Topographic sites of involvement

PBL develops in the oronasal (ON) and the extra-oronasal (EON) topographic regions. The latter may include unusual anatomical sites such as the female genital tract (Pather et al., 2015; Galvao Ferreira et al., 2017; Hadzisejdic et al., 2017; Hwang et al., 2017), breast (Wang et al., 2008; Matikas et al., 2014; Liang et al., 2014), male genital tract (Sun et al., 2011; Sugimoto et al., 2011), the central nervous system (Shuangshoti et al., 2008; Ustun et al., 2009; Urrego et al., 2011; Zhang et al., 2012; Gao et al., 2013; Romero et al., 2016; Ma et al., 2017) or heart (Miller et al., 2007; Qing et al., 2016). Very rarely, PBL may develop in the immediate vicinity of *in situ* medical devices such as a cardiac pacemaker (Zarifi et al., 2018) or a peritoneal dialysis catheter (Chen et al., 2007).

2.4.4 PBL: Morphology

HIV PBL is a high-grade tumour that may display a SS appearance in association with large malignant cells that exhibit monomorphic (i.e., immunoblastic or plasmablastic) or plasmacytic morphological features (Gujral et al., 2008; Kane et al., 2009). Rarely, clear cell change, multinucleated giant cells or pseudo-alveolar features may also be present in PBL (Mwazha et al.,

2020). Apoptotic debris of tumour cells is usually present and coagulative necrosis may also be evident within this neoplasm.

The ultrastructure of PBL, by electron microscopy, is typified by well-developed concentric arrangements of the rough endoplasmic reticulum (Goedhals et al., 2006).

2.4.5 PBL: Immunophenotype

PBL is defined by the absent or limited expression of leukocyte common antigen (LCA) and pan B-cell markers such as cluster of differentiation 20 (CD20), cluster of differentiation 79a (CD79a) and PAX5. Instead MUM1, cluster of differentiation 138 (CD138), cluster of differentiation 38 (CD38) , VS38c, BLIMP1 and X-box-binding protein 1 (XBP1) are frequently expressed in PBL (Montes-Moreno et al., 2010; Lopez and Abrisqueta, 2018; Teruya-Feldstein et al., 2004; Boy et al., 2015; Montes-Moreno et al., 2017). c-MYC protein over-expression may be detectable in 61-100% of these tumours (Loghavi et al., 2015), with or without *MYC* rearrangement. Aberrations such as *MYC* amplification or chromosome 8 polysomy may account for over-expression of c-MYC protein in PBL. PBL is typified by very high proliferation indices which may exceed 90%, as assessed by utilising Ki-67 immunohistochemistry (Wang et al., 2017).

Aberrant expression of T-cell markers, such as CD3, CD4 and CD7, is reported in PBL (Tzankov et al., 2005; Suzuki et al., 2010; Sun et al., 2011; Iliadis et al., 2016; Mishra et al., 2017) and expression may be confined to the cytoplasm of tumour cells (Pan et al., 2018).

Infrequently, HIV PBL displays clinicopathological features resembling plasmablastic or anaplastic myeloma or plasmablastic extramedullary plasmacytoma. Monoclonal light chain restriction, lytic bone lesions, EBV infection, CD56 immunoexpression and *MYC* rearrangement with an *IG* gene partner may be present in PBL (Vega et al., 2005; Boy et al., 2010; Taddesse-Heath et al., 2010). By definition, PBL does not express HHV-8 and ALK-1.

A list of tumours that may display plasmablastic morphology is presented in Table 2.4.

Table 2.4: Differential diagnosis for tumours displaying plasmablastic morphology

TUMOUR	MORPHOLOGY	IMMUNOPHENOTYPE	ANCILLARY INVESTIGATIONS
Plasmablastic lymphoma	Monomorphic plasmablastic morphology with or without plasmacytic differentiation	CD45 +/- BLIMP1 + MUM1 + CD138+ CD38+ VS38c+ CD20 and CD79a - or focally + PAX5 - CD56 variably + Ki-67 very high	EBER ISH + Light chain restriction by ISH may be present *MYC* rearrangement + Clonal *IgH* rearrangement
HHV8+ diffuse large B-cell lymphoma	Confluent sheets of large tumour cells with background multicentric Castleman disease	HHV8 latency-associated nuclear antigen + CD38 + CD138 – CD20 variable expression	IgM lambda light chain restriction + EBER ISH -
ALK+ large B-cell lymphoma	Diffuse immunoblastic-like or plasmablastic cells and multinucleated tumour giant cells	ALK1 + (cytoplasmic predominantly, nuclear and nucleolar staining infrequently) EMA + BLIMP1 + XBP1 + MUM1 + CD30 - CD20 - CD45 -/weak+ c-MYC+	Clonal immunoglobulin gene rearrangement. *ALK* translocation +
Primary effusion lymphoma, extracavitary	Immunoblastic, plasmablastic or anaplastic features	CD45+ CD138+ CD38+ VS38c+ HHV8+ CD20+/- Aberrant expression of T-cell markers	EBER ISH + Clonal immunoglobulin gene rearrangement
Anaplastic variant of myeloma	Diffuse sheets of plasmablastic tumour cells	MUM1+ CD138+ CD38+ CD56+ HHV8- CD45- CD20 may be expressed Ki-67 variable expression	Light chain restriction (kappa and lambda ISH). *IgH* may be rearranged as detected by PCR. EBER ISH usually negative. *MYC* rearrangement + t(4;14), t(11;14)(q13;q32), t(14;16)(q13;q32), t(14;20), del(17p13), trisomy 3, 7, 9, 11, 15 or 17 in addition to other cytogenetic aberrations
Carcinoma with plasmacytoid morphology	Discohesive and/or cohesive tumour cells displaying plasmacytoid morphology	Pan-keratin+ EMA + CD138+ GATA 3 + (urothelial and breast carcinoma)	Electron microscopy – closely apposed and variably interdigitating cell membranes with junctional complexes, desmosomes and aggregates of intermediate filaments in the cytoplasm

Abbreviations: CD – cluster of differentiation, HHV8 – human herpes virus 8, ALK – anaplastic lymphoma kinase, EMA – epithelial membrane antigen. EBER ISH – Epstein-Barr virus encoded small RNA.

2.4.6 PBL: Epstein–Barr virus

EBV was originally documented within cultured cells of Burkitt lymphoma (BL) by electron microscopy and the finding thereof was published during 1964 (Epstein et al., 1964). EBV is classified as a double-stranded DNA γ-1 herpes virus which belongs to the family Herpesviridae and subfamily Gammaherpesvirinae (Yao et al., 1985; Ok et al., 2015).

EBV is shed in the oral secretions of a seropositive host and new infection occurs when the virus comes into contact with the oropharyngeal epithelial cells of a naïve host (Yao et al., 1985; Cohen, 2000). Due to its ubiquitous nature, more than 90% of the human population are carriers of EBV (Ok et al., 2015). There has been lively, yet contentious, debate about the target cell of primary EBV infection. Following the infection of epithelial cells, EBV infection of B-lymphocytes was thought to occur as a secondary phenomenon by means of the major viral envelope glycoprotein, gp 350, which binds to CD21/Cd3 complement receptor-2 (Fingeroth et al., 1984). However, it is now established that B-cells are the primary target of EBV infection (Anagnostopoulos et al., 1995; Niedobitek et al., 1997). During the process of EBV infection of B-lymphocytes, the major-histocompatibility-complex (MHC) class II molecule plays the role of a cofactor (Li Q, 1997). The virus enters the host via oropharyngeal epithelial cells that harbour immunoglobulin A (IgA) receptors to which the EBV/IgA complex binds (Sixbey et al., 1984). Lytic replication of the virus then manifests at this site (Castillo et al., 2014).

EBV infection in humans induces both cellular and humoral immunity to the virus. The cellular immune response plays an important role in the control of EBV infection. During latency, there is markedly diminished expression of viral genes which enables EBV to evade cytotoxic T-lymphocytes due to a reduction in the expression of viral proteins within infected cells (Cohen, 2000). Hallmarks of EBV infection include B-lymphocytic tropism, latent infection and B-lymphocytic transforming capacity (Ok et al., 2015). Lifelong latent EBV infection is linked to this virus and its unique interaction with resting memory B-lymphocytes which serve as a viral reservoir (Babcock et al., 1998; Linke-Serinsoz et al., 2017).

By utilising EBV-encoded small RNA *in situ* hybridisation [EBER ISH] (Ambinder and Mann, 1994), EBV latent infection is evident in 70-93% of HIV PBL (Castillo et al., 2010a; Loghavi et

al., 2015; Tchernonog et al., 2017; Meer et al., 2020). Recently, in a South African based PBL cohort, EBV latency type 0 was identified in 73% of the tumours (Ramburan et al., 2022).

EBV latent infection tends to occur in association with *MYC* rearrangement (Castillo and Reagan, 2011a; Laurent et al., 2016; Ramburan et al., 2022). It is postulated that within *MYC* rearranged and EBV-positive PBL, oncogenic *MYC* prevents cellular apoptosis while plasmablastic differentiation of B-cells is driven by EBV (Castillo et al., 2015). Latent EBV infection occurs less frequently in HIV seronegative PBL (Loghavi et al., 2015). In PBL, EBV positive and negative alike, the strategy of immune escape includes several pathways with upregulated expression of immune check-point proteins such as programmed cell death-1, programmed cell death-ligand 1, CD163 predominantly within microenvironment cells and to a lesser extent within tumour cells (Laurent et al., 2016).

2.4.7 PBL: Molecular features and *MYC* status

Our understanding of the molecular characteristics of PBL is steadily evolving. Monoclonal rearrangements of *IgH* or light chain restriction may be detected in PBL (Rafaniello Raviele et al., 2009; Sarode et al., 2010). Aligned with the initial premise of PBL being a variant of DLBCL, Chang et al. (2009) utilised array comparative genomic hybridisation to demonstrate that PBL had significant overlapping genomic lesions with AIDS and non-AIDS related DLBCL and 40% thereof were segmental gains of 1p36.11-1p36.33, 1p34.1-1p36.13, 1q21.1-1q23.1, 7q11.2-7q11.23, 11q12-11q13.2 and 22q12.2-22q13.3. However, the transcriptional profile of PBL was subsequently shown to differ from DLBCL due to downregulation of B-cell receptor signalling genes, upregulation of mitochondrial genes and upregulation of c-MYC transcription factor (Chapman et al., 2015).

MYC translocations are identified in approximately 50% of PBL, most often with an *IG* gene partner of which 85% are *IgH* (Valera et al., 2010; Dawson et al., 2007; Miao et al., 2020) with a complex karyotype. *MYC* aberrations are reported in 60-100% of HIV PBL (Taddesse-Heath et al., 2010; Boy et al., 2011; Morscio et al., 2014; Loghavi et al., 2015; Meer et al., 2020) with *MYC* translocation occurring more frequently in HIV PBL and EBV-positive tumours (Valera et al., 2010; Laurent et al., 2016; Miao et al., 2020). *MYC* RNA expression occurs in PBL in association

with c-MYC protein expression (Chapman et al., 2015). *MYC* copy number alterations are reported in 33% of PBL (Ramburan et al., 2022) and rarely gains of the *MYC* gene are noted in a PBL which harbours *MYC* translocation (Valera et al., 2010).

While PBL lacks rearrangements of *BCL2, BCL6, PAX5* and *MALT lymphoma translocation protein 1* (*MALT1)* genes (Valera et al., 2010), the molecular histogenesis of HIV PBL includes recurrent somatic hypermutation of the *IG* variable heavy chain (Gaidano et al., 2002) and recurrent somatic mutations in the *positive regulatory domain 1* (*PRDM1)* gene. The latter accounts for BLIMP1 protein expression and may occur concurrently in tumours which harbour *MYC* translocations. *PRDM1* likely contributes to *MYC* oncogenicity in PBL (Montes-Moreno et al., 2017). Other translocations such as t(4;7) and t(9;13) in HIV seronegative PBL are linked to loss of p16 expression (Matsuki et al., 2011). The genomic landscape of HIV PBL was further explored recently when whole exome and deep-targeted sequencing were performed on a large cohort of tumours in SA (Liu et al., 2020).

2.4.8 PBL: Stage

At presentation, PBL often exhibits an advanced stage of disease (i.e., Ann Arbor stage III or IV) irrespective of the HIV status (Castillo et al., 2010b; Loghavi et al., 2015; Liu et al., 2015; Han et al., 2017; Rudresha et al., 2017).

2.4.9 PBL: Treatment

The treatment of this malignancy is challenging. As the optimal therapeutic approach is progressively developing, contemporary appropriate treatment may be required for each PBL patient. Antiviral treatment for HIV PBL and doxorubicin-based chemotherapy with etoposide, high-dose methotrexate or rituximab, with or without radiotherapy, may lead to a good response being achieved with prolonged disease-free survival (Noy et al., 2016; Tchernonog et al., 2017). The addition of the newer agents, such as bortezomib or lenalidomide, to the chemotherapy regimen appears promising with overall response rates of 90-100% documented (Saba et al., 2013; Hirosawa et al., 2015; Yanamandra et al., 2016; Guerrero-Garcia et al., 2017; Kobayashi and Miyagi, 2017; Pretscher et al., 2017; Schmit et al., 2017; Dittus et al., 2018; Marrero et al.,

2018). Thus far, bortezomib-induced tumour lysis syndrome is rarely reported (Lipstein et al., 2010). Elotuzumab may also prove effective as a therapeutic agent for HIV PBL (Shi et al., 2019). Daratumumab is an anti-CD38 monoclonal antibody which is currently being investigated in conjunction with dose-adjusted etoposide, prednisone, vincristine, cyclophosphamide and doxorubicin (DA-EPOCH) (Tan et al., 2019). The options of combined chemotherapy and autologous stem cell transplantation or surgical resection of a localised tumour are utilised infrequently (Dawson et al., 2007; Matikas et al., 2014; Tchernonog et al., 2017; Goto et al., 2011). Mammalian target of rapamycin (mTOR) inhibitors and vitamin D3 for growth inhibition as a component of the treatment armoury of PBL requires further exploration (Mine et al., 2017; Gascoyne et al., 2017a). Rarely, spontaneous regression of PBL is reported, with or without ART (Nasta et al., 2002; Igawa et al., 2015).

2.4.10 PBL: Survival outcome

Based on 135 PBL patients in Belgium and France, Tchernonog et al. (2017) demonstrated a median OS of 32 months. Moreover by univariate analysis, HIV seropositivity and EBV infection were associated with better OS when compared with HIV seronegative status. It is noteworthy that although PBL is defined by lack of expression of CD20, rituximab therapy may be utilised as immunotherapy (Witte et al., 2020). Rituximab for PBL may be associated with a good response and an improved event free survival (Yan et al., 2014; Tchernonog et al., 2017). When limited stage disease is treated with aggressive doxorubicin-based chemotherapy followed by radiotherapy, a favourable outcome may ensue (Pinnix et al., 2016). In the elderly patients with PBL, the clinical course may be more indolent with a better overall survival reported (Liu et al., 2012).

Unfortunately, the OS outcome of most patients with HIV PBL is inferior to that of HIV BL and HIV DLBCL. The OS is approximately six to fifteen months (Guan et al., 2010; Castillo et al., 2010b; Ibrahim et al., 2014; Schommers et al., 2015; Koizumi et al., 2016; Harmon and Smith, 2016; Guerrero-Garcia et al., 2017; Arora et al., 2019). An age at presentation of ≥50 years, advanced stage of disease, high IPI score, lymph node involvement and EBV-positive status may adversely impact the overall survival (Loghavi et al., 2015; Tchernonog et al., 2017; Rodrigues-Fernandes et al., 2018).

Notably, CD4 counts that are >100 cells/mm^3 at diagnosis and first-line chemotherapy-induced complete remission are reported to be associated with an improved PBL outcome (Koizumi et al., 2016).

Valera et al. (2010) contributed that the median OS in PBL was not significantly influenced by the presence of *MYC* rearrangements. However, the prognostic influence was subsequently explored in depth. The presence of *MYC* rearrangements in HIV PBL are suggested to portend an aggressive clinical course and an inferior survival outcome (Bogusz et al., 2009; Miao et al., 2020). Recently, when PBL was assessed regarding *MYC* rearrangements and compared with *MYC* wild-type with *MYC* amplification, the former was found to be a significant prognostic indicator of inferior OS and progression free survival (Witte et al., 2020).

Transformation of low-grade B-cell malignancies such as follicular lymphoma or small lymphocytic lymphoma/chronic lymphocytic leukaemia to PBL is a rare occurrence. Transformed PBL is documented in HIV seronegative patients, tends to lack EBV infection and may acquire a *MYC* rearrangement (Robak et al., 2001; Ramalingam et al., 2008; Ouansafi et al., 2010; Martinez et al., 2013; Pan et al., 2013; Ise et al., 2018). Very infrequently, a CD20-positive DLBCL may co-exist with or transform to PBL and the survival outcome thereof is dismal (Marini et al., 2016).

2.5 Research questions:

1. What is the prognostic influence of *MYC* aberrations, as detected by FISH and dual-colour *MYC* and chromosome 8 centromere (CEN8) chromogenic *in situ* hybridisation (CISH), on the survival outcome of patients with aggressive B-cell NHLs such as DLBCL and PBL at CHBAH?
2. Does immunophenotypic subclassification of DLBCL into germinal centre and nongerminal centre subtypes have prognostic value in HIV seropositive patients?
3. Will the co-expression of BCL2 and c-MYC protein in DLBCL, that occurs in the context of HIV seropositive DLBCL, be associated with an inferior survival outcome? In the setting of an inferior survival outcome, is there an association with the severity of immunodeficiency as depicted by the CD4 count at presentation of the lymphoma?

2.6 Research aims:

This research aimed to affirm and establish prognostic factors of DLBCL and PBL, in the setting of high HIV seroprevalence, at the largest hospital in Africa. Clinicopathological characteristics, that might necessitate more rigorous treatment regimens, would be identified and explored.

2.7 Research objectives:

1. To examine and describe the morphological and immunophenotypic characteristics of DLBCL and PBL.
2. To document the presence of concomitant conditions.
3. To determine the prognostic influence of IHC-defined GC and NGC subtypes of DLBCL in HIV seropositive and seronegative patients.
4. To investigate c-MYC protein expression in DLBCL and PBL by using IHC and to document the proportion of immunoreactive tumour cells.
5. To investigate the influence of c-MYC protein expression on survival outcome in DLBCL and PBL.

6. To investigate the influence of the co-expression of c-MYC and BCL2 proteins, as detected by IHC, on survival outcome in DLBCL.
7. To assess *MYC* aberrations in DLBCL and PBL by utilising dual-colour CISH and FISH.
8. To elucidate the influence of *MYC* aberrations on survival outcome of DLBCL and PBL.

3 CHAPTER THREE

METHODOLOGY AND MATERIALS

3.1 Research protocol inception

The research protocol was designed during a timeframe which extended from September 2015 to January 2016. The protocol was subsequently reviewed and approved during February 2016 by the Postgraduate Research Committee of the School of Pathology in the Faculty of Health Sciences at the University of the Witwatersrand.

3.2 Ethics approval

This study was granted ethics approval during March 2016 from the Human Research Ethics Committee (HREC) [Medical] of the University of the Witwatersrand. The original ethics clearance certificate number is M151017 (Appendix I) and the renewal extension thereof is M2010122 (Appendix I). Data collection commenced after ethics approval was received for this project.

3.3 Study design and funding

Retrospective observational research comprising descriptive, comparative and inferential components was conducted on patients who presented at CHBAH with DLBCL and PBL. This project was funded by the NHLS Research Trust and the University of the Witwatersrand with a contribution from the Division of Anatomical Pathology at the School of Pathology.

3.4 Target cases

Included cases derived from adult and paediatric patients from whom tissue specimens were submitted for the histopathological confirmation of DLBCL and PBL at the Division of

Anatomical Pathology, National Health Laboratory Service (NHLS) at CHBAH, Soweto, South Africa. These tumours were histopathologically confirmed during a timeframe of 45 consecutive months which extended from October 2013 to June 2017. Follow-up of the PBL patients occurred until December 2020 and follow up of the DLBCL patients occurred until December 2021.

3.5 Sample size

The sample size calculation was based on the formula $Z^2\,2p(1\text{-}p)/2e^2$. From the published findings regarding increased *MYC* copy numbers in DLBCL by Stasik et al. (2010) and Valentino et al. (2013), p was assigned 85% for this study, Z was equal to 1.96 and e was equal to 0.05. This formula yielded a requirement of 196 tumours for this study.

3.6 Case detection and retrieval

A systematised nomenclature of medicine (SNOMED) search of the NHLS DISA and LABTRAK laboratory information systems was conducted during 2016 and 2017 with the assistance of the NHLS Corporate Data Warehouse (CDW) using M-codes (M95903 – malignant lymphoma and M95953 – malignant lymphoma diffuse). Intra-laboratory IHC log sheets were also scrutinised to consistently detect the confirmed cases of DLBCL and PBL. Two hundred and nine (N=209) tumours comprising 73 PBL and 136 DLBCL were initially found. The paraffin-embedded tissue blocks and the slides of all the cases were retrieved from the Histopathology NHLS archival storage area at CHBAH by the researcher, who was intermittently assisted by the laboratory staff. These study materials were then methodically stored within the researchers' office, access to which was controlled and monitored by closed circuit television surveillance at the NHLS. All the cases were evaluated by the researcher for suitability and inclusion in this study.

3.7 Exclusion criteria

Cases were excluded from this study if any of the following occurred or were present -

- Tissue blocks were irretrievable from the archival storage site.

- Limited residual tissue remaining in the cassette, limited viable tumour due to extensive necrosis or extensive crush and/or smearing artefacts within the tumour.
- Low-grade B-cell NHL or Hodgkin lymphoma that transformed to DLBCL.
- Anaplastic variant of myeloma.
- Primary effusion lymphoma.
- ALK-positive large B-cell lymphoma.
- HHV8-positive diffuse large B-cell lymphoma, NOS.
- Burkitt lymphoma.
- High-grade B-cell lymphoma with *MYC* and *BCL2* and/or *BCL6* rearrangements.
- B-cell lymphoma, unclassifiable, with features intermediate between DLBCL and classic Hodgkin lymphoma (CHL).
- Variants of DLBCL other than DLBCL, NOS and DLBCL associated with HIV infection.

3.8 Included tumours

The study subsequently comprised 190 tumours of which 67 were PBL and 123 were DLBCL.

3.9 Confidentiality of the patients

Anonymity of the patients within this study was strictly preserved. A linked-code study case number was assigned as P01-P67 for PBL and D01-D123 for DLBCL. The data spreadsheets were password encrypted and stored on a password protected computer. Only the researcher and a supervisor of this project had access to the master copies of the spreadsheets. All personal identifying information such as names, surnames, hospital folder numbers, identity numbers, physical addresses, contact numbers, specimen episode numbers and/or specimen accession numbers were omitted from the tables and spreadsheets that were utilised for statistical analysis, presented within this thesis and published in manuscripts that derived from this thesis.

3.10 Clinical data collection

Information such as the gender, treatment regimens, stage of the lymphoma, IPI score, concomitant conditions and the survival status, in days since lymphoma was confirmed, and duration of follow up were retrospectively retrieved from the patients' folders in close collaboration with the Department of Clinical Haematology and the Department of Paediatric Oncology at CHBAH. Data were captured within Excel spreadsheets of Microsoft 365 (Appendices III-IV).

3.11 Laboratory data collection

DISA and LABTRAK laboratory information systems were utilised for the retrospective documentation of age, HIV serological status, viral load, CD4 count and FISH findings regarding *MYC*, *BCL2* and/or *BCL6* rearrangements of the included patients. If multiple CD4 counts were available within 6 months of the lymphoma diagnosis, the CD4 count that was sampled nearest to the time of the lymphoma diagnosis was documented.

All the haematoxylin and eosin-stained (H&E) slides, IHC and EBER ISH slides were reviewed by the researcher to confirm that the diagnoses aligned with the diagnostic criteria for PBL, DLBCL, NOS and DLBCL associated with HIV infection as specified in the 2017 WHO Classification of Tumours of Haematopoietic and Lymphoid Tissue (Campo et al., 2017; Gascoyne et al., 2017b; Said et al., 2017).

3.11.1 Pathology data of DLBCL

The topographic site of the biopsy specimen, morphology of DLBCL regarding centroblastic, immunoblastic, anaplastic or mixed features and the presence or absence of concomitant conditions for each case were documented in the DLBCL datasheet (Appendix III).

CD20, CD10, BCL2, bcl-6, MUM1, Ki-67 IHC was performed routinely and FISH for *MYC* gene rearrangement was performed on some of the tumours at the time of the primary diagnosis of DLBCL. These tests were conducted in the presence of adequate control sections, in accordance with the manufacturer's specifications. IHC-stained sections were semiquantitatively interpreted according to the proportion of tumour cells that stained positively. Ideally, fifty tumour cells were

assessed per high power field (HPF) at x400 magnification. Ten high power fields were assessed such that 500 tumour cells were interpreted for each IHC-stained section. The overall positive proportion of immunoreactivity within tumour cells was then assigned from 0-100% and documented in the DLBCL datasheet (Appendix III). CD20, CD10, bcl-6 and MUM1 were interpreted as positive if at least 30% of tumour cells (i.e., ≥30%) displayed immunoreactivity within appropriate cellular components such as the cell membrane, cytoplasm or nucleus. A 30% cut-off was selected to align with the Hans-defined IHC algorithm regarding CD10, bcl-6 and MUM1 expression (Hans et al., 2004). BCL2 was interpreted as positive if at least 50% of the tumour cells demonstrated cytoplasmic immunoreactivity. When Ki-67 IHC was interpreted, the hot-spot areas of nuclear immunoreactivity were targeted within the tumour. The highest percentage of staining was deemed the proliferation index regarding the number of positive tumour cells versus the number of negative tumour cells within at least 500 nuclei at x400 magnification (Kinra and Malik, 2020).

A positive external control section was included on every slide of each IHC test that was performed during the diagnostic work-up. Automated staining occurred with heat-induced antigen unmasking and cell conditioning 1 (CC1), in accordance with the manufacturer's specifications. Details of the primary antibodies are specified in Table 3.1.

3.11.2 Pathology data of PBL

The topographic site of the biopsy specimen, morphology of PBL regarding the presence of monomorphic or plasmacytic features and the presence concomitant conditions for each case were documented in the PBL datasheet (Appendix IV).

CD20, MUM1, CD138, HHV8 and ALK1 IHC were performed at the time of the primary diagnostic work-up of PBL, in the presence of adequate control sections, in accordance with the manufacturer's specifications. Details of the primary IHC antibodies are specified in Table 3.1. IHC stained sections were interpreted according to the proportion of tumour that stained positively from 0-100%, similar to the aforementioned method in 3.11.1. CD20, CD138 and MUM1 IHC were interpreted as positive if at least 40% of the tumour cells (i.e., ≥40%) displayed immunoreactivity within appropriate cellular components such as the cell membrane or the nucleus. Ki-67 IHC was interpreted as described in 3.11.1. A positive external control section

was included on every slide for every IHC test of PBL. The proportion of tumour cells that stained positively (i.e., 0-100%) was entered into the PBL datasheet (Appendix IV).

Table 3.1: Details of the primary antibodies utilised for DLBCL and PBL

PRIMARY ANTIBODY	SUPPLIER SOURCE	CLONE	DILUTION	INCUBATION TIME and TEMPERATURE	IMMUNO-REACTION	EXTERNAL + CONTROL SECTION
CD20	Roche/ Ventana	L26	Ready to use (RTU)	32 minutes, Room temperature (RT)	Cell membrane	B-cells within lymph node
CD10	Roche/ Ventana	SP67	RTU	48 minutes, RT	Cell membrane	B-cells of lymph node germinal centres (GC)
BCL2	Roche/ Ventana	124	RTU	48 minutes, RT	Cytoplasmic	Lymph node: Interfollicular lymphocytes
bcl-6	Roche/ Ventana	GI191E / A8	RTU	48 minutes, RT	Nuclear	Lymph node: GC lymphocytes
MUM1	Roche/ Ventana	MRQ-43 SP114	RTU	30 minutes, RT	Nuclear	Plasmacytoma and plasma cells in a lymph node
Ki-67	Roche/ Ventana	30-9	RTU	20 minutes, RT	Nuclear	Lymph node: GC and interfollicular lymphocytes
CD138	Roche/ Ventana	SP152	RTU	10 minutes, RT	Cell membrane	Plasmacytoma and plasma cells in a lymph node
ALK1	Dako	CD246/ ALK1	RTU	30 minutes, RT	Cytoplasmic and/or nuclear	Anaplastic large cell lymphoma, ALK-positive
HHV8	Roche/ Ventana	13B10	RTU	32 minutes, RT	Nuclear	Kaposi sarcoma within skin and soft tissue
c-MYC	Roche/ Ventana	Y69	RTU	16 minutes, RT	Nuclear	c-MYC+ DLBCL or epidermis of skin
Negative reagent control	Roche/ Ventana	Monoclonal Neg control Ig	RTU	20 minutes, RT	No reaction	DLBCL

The INFORM EBER Probe (Ventana Medical Systems, Inc., Tucson, AZ, USA, Roche Diagnostics, Mannheim, Germany) was utilised for EBER ISH and automated staining was conducted in a Ventana BenchMark XT instrument. Dark blue intranuclear signals within tumour cells indicated a positive staining reaction. The presence of latent EBV infection was hereby confirmed. Any proportion (i.e., 0-100%) of intranuclear staining within tumour cells was considered a positive staining reaction. An external positive control tissue section such as an EBV-associated neoplasm (i.e., EBV-associated smooth muscle tumour or EBV-positive nasopharyngeal carcinoma) was included in each batch run of EBER ISH.

3.12 Histopathology laboratory investigation: c-MYC IHC

c-MYC IHC was performed on all the included DLBCL and PBL tumours for the purposes of this study. The anti-c-MYC (clone Y69) rabbit monoclonal primary antibody that targets the N-terminus of the c-MYC transcription factor was utilised to yield a positive nuclear staining pattern within tumours which expressed this protein. The nuclear expression was detected by light microscopic examination. This antibody required a Ventana detection kit and was utilised on a Ventana BenchMark XT automated slide stainer instrument.

The Ventana *ultra*View universal diaminobenzidine (DAB) detection kit is an indirect biotin-free system for detecting a rabbit primary antibody, i.e., anti-c-MYC, in this context. The staining principle was based on a horseradish peroxidase multimer hapten detection system in which the enzyme of the multimer molecule was directly conjugated to a secondary antibody by long-arm linkers. Utilisation of the reagents and kits occurred, prior to the expiration dates, on histopathology specimens of DLBCL and PBL that were originally fixed in 10% neutral buffered formalin.

Optimisation of the staining protocol was performed according to the manufacturer's recommendation for anti-c-MYC (Y69) by subjecting several tissue sections to the staining procedure as outlined below in 3.12.1. The tissue sections comprised skin (i.e., epidermis and dermis), salivary gland acini, salivary gland ducts and adipocytes. The c-MYC immunostained sections were then assessed and scored independently by the researcher and a histotechnician or a histotechnologist, as good, adequate or inadequate nuclear staining. Optimisation was deemed

successful when brown nuclear staining of moderate intensity was identified within the basal and suprabasal keratinocytes of the epidermis and when staining was not detected within cells of the dermis, salivary gland parenchyma, adipocytes or skeletal muscle.

Validation of the staining results of the anti-c-MYC (Y69) IHC assay subsequently occurred. Tissue sections were prepared from skin, salivary gland, adipocytes, skeletal muscle and DLBCL tumours. All of these specimens were originally fixed in 10% neutral buffered formalin and underwent standardised processing within the Histopathology laboratory of the NHLS at CHBAH. One of the DLBCL cases harboured increased copies of the *MYC* gene as detected by FISH, which was performed at a referral cytogenetics laboratory at which a validated assay was used at the time of the primary diagnosis. Tissue sections, 3µm in thickness, were subjected to the anti-c-MYC (Y69) staining protocol within the Ventana BenchMark XT automated slide stainer. The case of DLBCL with *MYC* aberration demonstrated diffuse nuclear staining of strong intensity due to c-MYC protein over-expression. Immunoreactivity was not evident within the fibroblasts and non-neoplastic lymphocytes within that tumour. Nuclear staining of moderate intensity was present in the basal and suprabasal keratinocytes of the skin specimen. Staining was not evident within fibroblasts of the dermis, salivary gland parenchyma (Figure 3.1), adipose, skeletal muscle and some of the tumours.

A limited fragment of tissue, measuring <5mm in greatest dimension, of the DLBCL tumour that displayed diffuse nuclear immunoreactivity (Figure 3.1) was subsequently used as a positive reagent control and an external positive control for c-MYC IHC testing in this study.

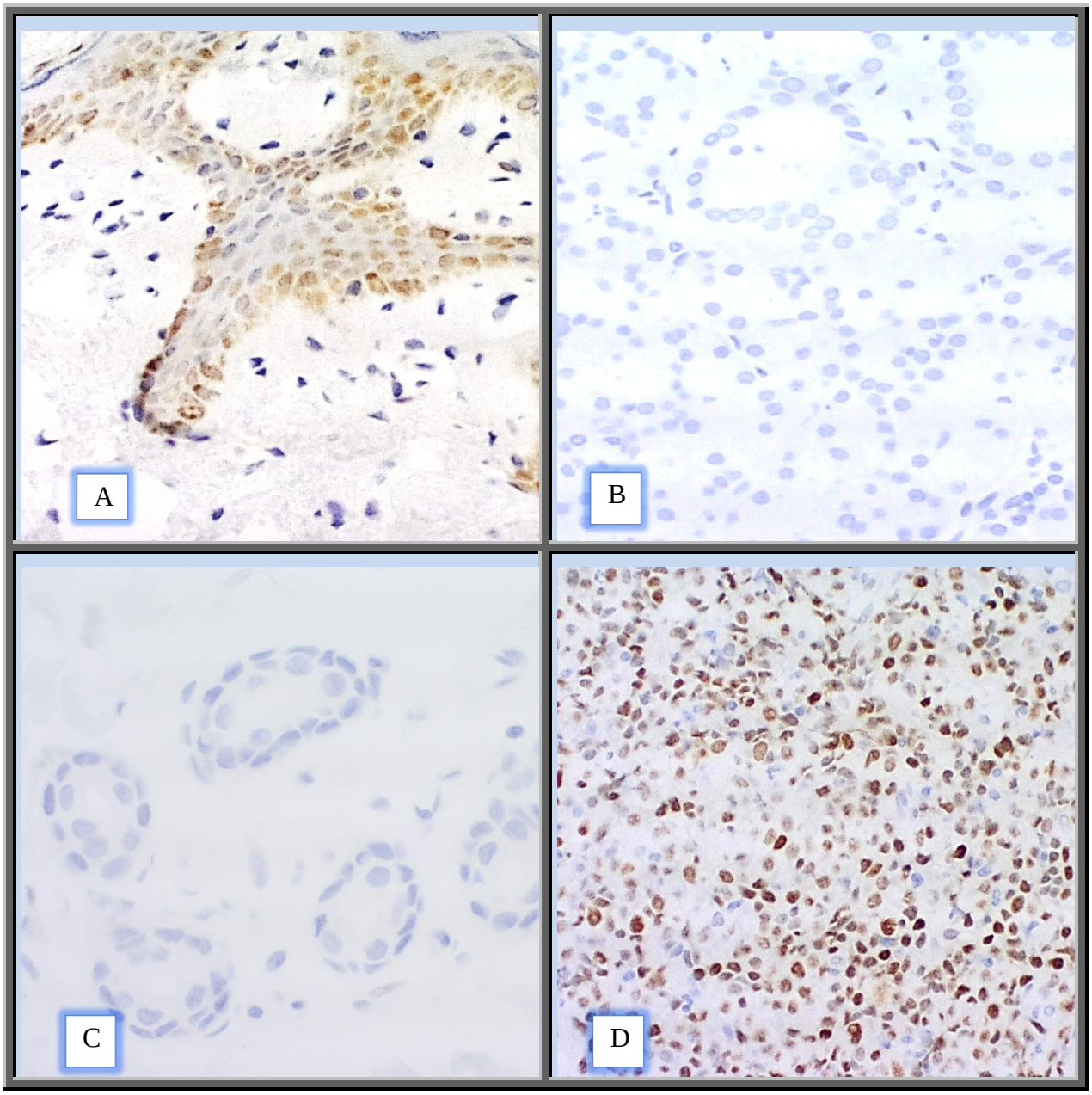


Figure 3.1: c-MYC immunohistochemistry on external control tissue sections demonstrating positive nuclear staining in keratinocytes (A) and DLBCL (D). No nuclear immunoreactivity noted in salivary gland parenchyma (B) and (C) eccrine glands (magnification x200).

3.12.1 c-MYC IHC: methodology

i. Microtomy was conducted on a microtome (Leica Rotary RM2125 RTS, Leica Biosystems Inc. GmbH, Wetzlar, Germany) by the researcher under the supervision, guidance and assistance of experienced histopathology microtomists, to obtain tissue sections that were 3µm in thickness from the paraffin-embedded tissue blocks of DLBCL, PBL and the control tissues. Whole tissue sections were hereby made available for testing. Each slide contained an external positive control tissue section (i.e., skin or c-MYC+ DLBCL), an external negative control tissue section (i.e., salivary gland) and tumour section/s.

ii. The tissue sections were set afloat on a water bath (Vogel-Wasserbad, Germany), the optimal temperature of which was 45°C. Mounting of the sections on Superfrost Plus slides (Menzel-Glaser, USA) that were appropriately labelled with the coded-link study case number (i.e., P01-67 or D01-123), was followed by drying of the slides by incubation in a Labex-Labcon incubator for 60 minutes at temperatures of 60°C or 37°C when incubation occurred overnight.

iii. Barcoded slide labels were printed using the Benchmark XT printer and applied to the appropriate slides thereafter.

iv. Automated staining occurred as soon as possible after the incubation period, to preserve the antigenicity of the tissue.

v. The slides were loaded into the Benchmark XT automated slide stainer instrument to stain for 6 hours according to the manufacturers recommended protocol.

vi. The automated staining procedure entailed deparaffinisation and cell conditioning or antigen unmasking with CC1 solution by standard application.

vii. The primary antibody [anti-c-MYC (Y69)] application occurred for 16 minutes at 37°C.

viii. Amplification and counterstaining with haematoxylin II occurred for 12 minutes, followed by post counterstaining with a bluing agent of ammoniated water for 4 minutes.

ix. Insertion of the glass coverslips occurred as an automated procedure.

x. A negative reagent control was included for each case of DLBCL and PBL. Hereby, the presence of non-specific reactivity was excluded in the tumour sections.

xi. Prior to the use of new reagents in this study, the validation of the staining results was repeated. The tested sections were assessed and scored independently by the researcher and a histotechnician or a histotechnologist.

xii. Inter-lot reproducibility of the antibody and inter-run reproducibility on the BenchMark instrument also occurred by testing several tissue sections, cut onto one slide, of which the staining reactions were known to be positive and negative. After the staining was confirmed to be appropriately positive and negative, further IHC testing of tumour sections in this study proceeded. To reiterate, validation of the staining results was repeated for each new lot of reagents and when troubleshooting occurred.

3.12.2 c-MYC IHC: adequacy of staining

i. Positive control sections on each c-MYC stained slide were evaluated for adequacy of immunostaining. This occurred independently by a histotechnician or histotechnologist and by the researcher. Each slide was assessed as having good, adequate or inadequate staining within the external positive control section.

ii. Evaluation of staining adequacy routinely commenced with a detailed assessment of the external control tissue sections. The slide was deemed adequately stained when nuclear immunoreactivity was present within the external positive control tissue section, when nuclear immunoreactivity was not present in the external negative control tissue section and when nuclear immunoreactivity was not present in the fibroblasts and non-neoplastic lymphocytes of the tumour sections at x400 magnification.

iii. When the control tissues were assessed as inadequately stained, the cases and controls were recut and subjected to the staining procedure once again.

iv. All slides that displayed good or adequate staining were issued to the researcher for interpretation in this study.

3.12.3 c-MYC IHC: interpretation

i. The H&E sections of each tumour were reviewed by the researcher immediately prior to interpreting the c-MYC slides of the tumours. The coded-link study case numbers on the IHC slides were also cross checked with those specified in the data spreadsheets. These

steps confirmed that the immunostained tumour sections matched the H&E sections and the coded-link study case numbers.

ii. Microscopic examination of the entire c-MYC slide commenced at x100 magnification using an Olympus system microscope model BX40F4 (Olympus Optical Co, Japan) or a Zeiss Primo Star microscope (Göttingtin, Germany).

iii. External control tissue sections (i.e., positive and negative) as shown in Figure 3.1 were always examined before the test section was interpreted.

iv. Magnification at x200 enabled the researcher to detect heterogeneity of c-MYC expression, if heterogeneity was present within the tumour.

v. Areas of highest c-MYC expression within each tumour, that were located away from the edges of the tissue section, were identified and selected for interpretation. The peripheral boundary of the areas of highest immunoexpression was manually marked by the researcher using a permanent waterproof marker for glass (Faber-Castell Multimark 1525, Germany). Such markings were applied to the free surface of the glass coverslip of the c-MYC slide.

vi. Detailed interpretation of 500 tumour cells (i.e., 50 cells per HPF and 10 HPFs per case) occurred at x400 magnification. Tumour cells that displayed nuclear immunoreactivity were manually and semi-quantitatively scored in 10% increments.

vii. A positive proportion or positive percentage (0-100%) was allocated according to the number of tumour cells that stained positively within several contiguous, non-overlapping, fields.

viii. The c-MYC positive proportion, of every adequately stained tumour, was then entered into the DLBCL and PBL datasheets (Appendices III and IV).

ix. If c-MYC protein immunoexpression was detected within at least 40% (i.e., ≥40% proportion stained) of the tumour cells, irrespective of the staining intensity, that tumour was categorised as positive for c-MYC expression.

3.13 Histopathology laboratory investigation: *MYC* and CEN8 dual-colour CISH

In situ hybridisation (ISH) generally employs the use of probes, which are labelled, to detect the presence of specific DNA or RNA target sequences within tissue sections. For this study, *MYC* and CEN8 dual-colour CISH were performed with silver and red chromogens, respectively on FFPE tissue sections in the Ventana BenchMark XT automated slide stainer. The Ventana *ultra*View silver *in situ* hybridisation (SISH) dinitrophenol (DNP) detection kit, *MYC* DNP probe, Ventana red ISH digoxigenin (DIG) detection kit, CEN8 DIG probe (980-1220), accessory reagents and the XT dual-colour open probe staining procedure were utilised in this study.

The DNP detection kit is based on an indirect method for visualisation of a labelled target as a black precipitate due to specific antibodies that are bound to antigens. The *MYC* probe is a DNP probe that spans an approximately 496 kilobase region of chromosome 8 which includes the *MYC* gene. The *MYC* reaction was visualised with silver detection chemistry that was evident as black dots within the nuclei of cells, when the stained slide was examined by using conventional light microscopy. Ventana red ISH DIG detection kit is also based on an indirect method to detect DIG-labelled targets. This kit identifies targets by chromogenic red ISH of FFPE tissue sections. The CEN8 DIG probe (980-1220) is an analyte specific reagent that was designed to hybridise to chromosome 8 DNA.

After acquiring the reagents, probes and kits, utilisation thereof occurred prior to the expiration dates, on histopathology specimens of DLBCL and PBL that were originally fixed in 10% neutral buffered formalin.

According to the manufacturer's guidelines, the *MYC* DNP probe was diluted to 20µg/ml by using a ISH probe diluent (760-4409) which was inserted into a user fillable probe dispenser. The *MYC* DNP probe was combined with the CEN8 DIG probe within one dispenser, hereby allowing for dilution of both probes and dual-colour staining using a single dispenser. The dual-colour open probe staining procedure occurred in this study, according to the manufacturer's recommendations as elaborated in the subsection 3.13.1. Hereby, CEN8 CISH occurred simultaneously and the CEN8 reaction was visualised as red dots within the nuclei of cells by using conventional light microscopy.

The validation of *MYC* and CEN8 CISH in this study required the implementation of quality control procedures that included assay verification and positive control specimens. Prior to the initial use of the kits, probes and during episodes of troubleshooting, assay verification occurred by utilising a positive reagent control of DLBCL that contained increased copies of the *MYC* gene, as originally detected by FISH during the diagnostic workup. This was repeated for each new lot of reagents, kits and probes.

At the outset, assay verification occurred by subjecting tissue sections, of which the CISH performance characteristics was known, to the staining protocol and procedure. The tissue sections comprised tonsil, in which squamous mucosa and lymphocytes were present, salivary gland parenchyma and a case of DLBCL that was known to contain increased copies of the *MYC* gene.

When the staining protocol and procedure were completed, the performance of the reagents was verified by the presence of 1-2 red signals of CEN8 and 1-2 silver signals of *MYC*. These signals were identified within the nuclei of normal cells such as the squamous epithelium, fibroblasts, non-neoplastic lymphocytes as well as within the nuclei of tumour cells. Hereby, the CISH assay was verified for testing in this study.

The limited fragment of the abovementioned DLBCL, which harboured increased *MYC* gene copies, subsequently constituted a positive reagent control that was run during future assay verification of CISH and troubleshooting in this study.

The staining of positive and negative control sections occurred routinely during assay verification, troubleshooting and for each new lot of reagents. A laboratory-specific positive external control specimen, i.e., tonsil, was included on all slides that underwent CISH staining. The positive external control was originally fixed in 10% neutral buffered formalin and underwent standardised processing within the Histopathology laboratory of the NHLS at CHBAH. This control specimen served to confirm that the reagents and the instrument had functioned appropriately when 1-2 red signals of CEN8 and 1-2 silver signals of *MYC* were visualised within the epithelium, fibroblasts or lymphocytes. For every CISH test that was performed, a tonsil or DLBCL external positive tissue control section and a salivary gland external negative tissue control section were included on each slide.

3.13.1 Dual-colour CISH: methodology

i. Microtomy was conducted on a microtome (Leica Rotary RM2125 RTS, Leica Biosystems' Inc. GmbH, Wetzlar, Germany) by the researcher and highly experienced histopathology microtomists, to obtain tissue sections that were 2µm in thickness from the paraffin-embedded tissue blocks of DLBCL, PBL and the control tissues. Whole tissue sections were hereby made available for testing.

ii. The tissue sections were set afloat on a water bath (Vogel-Wasserbad, Germany), the optimal temperature of which was 45°C. Mounting of the sections on Superfrost Plus slides (Menzel-Glaser, USA) that were appropriately labelled with the linked-code study case numbers (i.e., P1-67 or D1-123), was followed by incubation in a Labex-Labcon incubator for 60 minutes at temperatures of 60°C or 37°C when incubation occurred overnight.

iii. Thereafter, barcoded slide labels were printed using the Benchmark XT printer and applied to the appropriate slides.

iv. Each slide contained the test sections of tumour, an external negative control tissue section (i.e., salivary gland) and an external positive control tissue section (i.e., tonsil). The control tissue sections would stain simultaneously with the tumours.

v. Staining ensued soon after the tissue sections were prepared to reduce the likelihood of diminished quality of the nuclear acid target.

vi. Within the Ventana BenchMark XT automated slide stainer, the sections were hybridised with the DNP-labelled probe.

vii. Incubation occurred with a rabbit anti-DNP antibody that binds to the DNP hapten on the probe.

viii. A multimer solution of a goat anti-rabbit secondary antibody with a horseradish peroxidase (HRP) enzyme was applied to detect the rabbit anti-DNP antibody.

ix. Visualisation of the bound secondary antibody was accomplished by means of a HRP-enzyme catalysed deposition of silver which produced a black precipitate.

x. Silver ions (Ag+) from the SISH DNP chromogen A (silver A) solution were reduced by hydroquinone from the SISH DNP chromogen B (silver B) solution to metallic silver ions (Ag0). This reaction was fuelled by HRP substrate hydrogen peroxide (silver C) and the

silver precipitate was deposited in the nuclei of cells. The target sequence was visualised as a black dot and counterstaining with haematoxylin II allowed for visualisation by using conventional light microscopy at x200 and x400 magnification.

xi. The staining procedure comprised several steps of reagent incubation at variable temperatures, according the to the manufacturer specifications. After each incubation step, the sections were washed and thereafter a liquid coverslip was applied.

xii. Within the automated slide stainer deparaffinisation of the sections occurred by Extended II at 72°C, followed by 3 cycles at 12 minutes per cycle, of cell conditioning using Cell Conditioning 2 (CC2) solution at 80°C.

xiii. Enzyme application using ISH protease 3 occurred for 32 minutes, followed by denaturing at 80°C for 12 minutes.

xiv. Hybridisation incubation then occurred at 44°C for 6 hours.

xv. Stringency wash incubation time entailed 3 cycles, at 8 minutes per cycle, at 72°C.

xvi. The silver detection incubation time and silver chromogen application occurred for 20 and 8 minutes, respectively.

xvii. The CEN8 red detection had an incubation time of 20 minutes and the red chromogen application occurred for 8 minutes.

xviii. Counterstaining with haematoxylin II occurred for 8 minutes and post counterstaining using a bluing reagent occurred for 4 minutes.

xix. A successful staining reaction was characterised by 1-2 red signals of CEN8 and 1-2 silver or black signals of *MYC* within the nuclei of normal and neoplastic cells as shown in Figure 3.2.

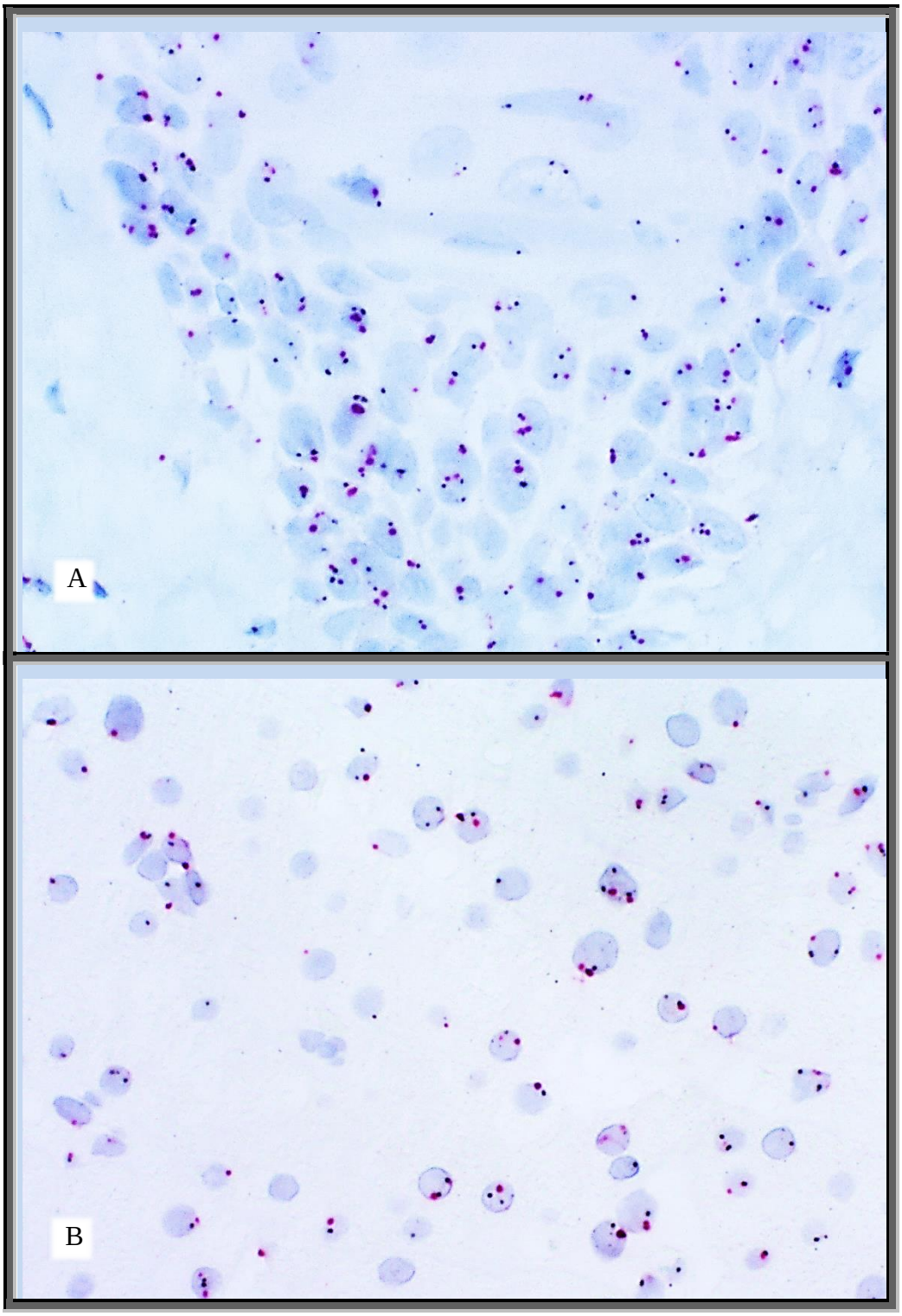


Figure 3.2: Dual-colour CISH displaying intranuclear black signals of *MYC* and red signals of CEN8 in the external control epithelial cells (A) and (B) [magnification x400].

3.13.2 Dual-colour CISH: adequacy of staining and signal visualisation

The positive control specimens contained 1-2 copies of the *MYC* gene and 1-2 signals of CEN8 per nucleus. These signals were visible by light microscopy at x200 or x400 magnification.

The CISH-stained slides were adequate for signal enumeration when the following two criteria were met:

i. Internal positive controls and tumour nuclei contained positive black and red nuclear signals that were clearly enumerable.

   The internal positive controls comprised non-neoplastic cells such as epithelial cells, endothelial cells, fibroblasts or lymphocytes within the tumour section. In other words, every adequately stained section contained an internal positive control as *MYC* and CEN8 CISH signals are present within normal cells. These cells constituted the true positive control.

ii. Several target areas of viable tumour were available for enumeration of the signals. Assessment of signals was not performed in areas of necrosis, when the nuclei were overlapping, compressed, bubbled and distorted by traction or crush artefacts.

iii. The dual-colour CISH tests were targeted towards *MYC* and CEN8 copy numbers. *MYC* rearrangement was not detectable using this method.

iv. The CISH stained slides were deemed adequate for enumeration, independently by the researcher and a histotechnician. All adequately stained CISH slides were issued to the researcher for enumeration, interpretation and analysis in this study. After the slides were deemed adequate for enumeration, interpretation occurred in accordance with the following guidelines regarding the *MYC* SISH signals.

3.13.3 Guidelines for interpreting *MYC* SISH signals

a. *MYC* SISH signals were visualised as single or multiple copies when discrete black dots were present within a nucleus. The size of these dots needed to be similar to those within the internal control cells.

b. The limitation of assessing a three-dimensional nucleus by using a two-dimensional visual method could lead to the finding of less than 2 black signals within some of the nuclei. This would occur due to variability in the plane of sectioning.
c. Two adjacent signals would be counted as two signals if the distance between the signals was greater than or equal to the diameter of a single signal.
d. A *MYC* cluster was defined as multiple closely packed or overlapping signals within the tumour nuclei that could not be separately enumerated.
e. Assessment of *MYC* signals was not performed when the nuclei lacked signals and when the nuclei contained only one colour signal (i.e., only red signals or only black signals).
f. Assessment of *MYC* signals was not performed when the signals were located outside of the nuclear membrane and when the SISH signals were weak.

3.13.4 Dual-colour CISH: Evaluation and interpretation

i. Evaluation and interpretation of all the CISH stained slides was performed by the researcher. Evaluation routinely commenced with a detailed assessment of the external control tissue sections as shown in Figure 3.2, internal positive control cells and the tumour cells to confirm that black dots of *MYC* signals and red dots of CEN8 signals were present in all of these sections. The presence of signals in all of these sections indicated that the *MYC* DNP probe had hybridised to the *MYC* gene region and that CEN8 DIG probe had hybridised to the centromere of C8.
ii. The c-MYC IHC slide of each tumour was reviewed by the researcher immediately prior to interpreting the CISH-stained tumour section. The coded-link study case numbers on the CISH slides were cross checked with those specified on the c-MYC IHC slides and with those within the data spreadsheets, to ensure that interpretation occurred appropriately for each case.
iii. Detailed microscopic interpretation of the CISH sections occurred in the areas that matched the areas of highest c-MYC immunoexpression. The latter was previously marked on the c-MYC IHC-stained slide of each PBL and DLBCL as outlined in step v of subsection 3.12.3.

iv. At a magnification of x400, CISH signals within tumour nuclei were manually enumerated in the areas containing the highest number thereof. Based on previous studies by Valentino et al. (2013) and Stasik et al. (2010), the researcher opted to assess 50 tumour nuclei of every tumour that was adequately CISH-stained in this study.

v. Each selected field of tumour was visually divided into four quadrants according to the face of a clock, i.e., 12-3, 3-6, 6-9 and 9-12 o'clock, as shown in Appendix V(a). Two tumour cells that displayed clearly discernible red and black nuclear signals, were randomly selected within each of the quadrants and from the central area of that HPF. Hereby, 10 tumour cells per HPF were consistently selected for enumeration. This visual method of tumour cell selection ensured that erratic reselection and recounting of tumour cells did not occur within a HPF.

vi. A CISH interpretation tool, shown in Appendix V(b), was created by the researcher by utilising Excel of Microsoft 365, for the methodical documentation and accurate summation of *MYC* and CEN8 signals within 50 tumour cells of each PBL and DLBCL, that was adequately stained. This tool was also used for documenting the presence of *MYC* clusters per 50 tumour cells, for assessing the external control cells and the internal control cells of each tumour.

vii. Ten tumour nuclei within 5 non-overlapping HPFs at x400 magnification were interpreted, hereby constituting 50 tumour cells for each case of PBL and DLBCL.

viii. For each HPF interpreted as per Appendix V(a) the number of *MYC* and CEN8 signals that were identified in the selected tumour cells were entered into the appropriate tiles of the CISH interpretation tool [Appendix V(b)].

ix. After 10 tumour cells in a HPF were evaluated and interpreted, automated summation occurred of the signal numbers within the *MYC* and CEN8 columns of that field in the Excel-based tool.

x. After 50 tumour cells of the case were evaluated and interpreted, an overall summation occurred of the figures specified within the *MYC* and CEN8 rows that were located at the base of the tool. Hereby, the overall number of *MYC* and CEN8 signals within 50 tumour nuclei of each PBL and DLBCL case was consistently ascertained.

xi. Due to the variable plane of tissue sectioning, less than 100 signals per 50 tumour cells were intermittently detected for *MYC* and CEN 8.

3.13.5 Definition of increased CISH signals

Ideally, a normal tumour nucleus would display 2 signals of *MYC* and 2 signals of CEN8. Increased *MYC* signals and increased CEN 8 signals were defined by the presence of signals that were more than 10% above that which is normal for 50 tumour nuclei (Stasik et al., 2010; Valentino et al., 2013). Therefore, in this study, the presence of more than 110 black signals of *MYC* per 50 tumour nuclei and the presence of more than 110 red signals of CEN8 per 50 tumour nuclei, were classified as increased signals. If the number of signals of *MYC* or CEN8 was close to 110 (i.e., 107 to 112) for a case, re-enumeration of the signals of that case ensued. The final number of CEN8 and *MYC* signals were then transferred to the data spreadsheets of PBL and DLBCL (Appendices IV and III, respectively).

3.13.6 CISH-defined subcategorisation of DLBCL and PBL

Based on the CISH findings, subcategorisation of DLBCL and PBL subsequently occurred as follows:

No increase in *MYC* and no increase in CEN8 signals
(≤110 *MYC* signals/50 tumour nuclei and
≤110 CEN8 signals/50 tumour nuclei).

Increased *MYC* signals and no increase in CEN8 signals
(>110 *MYC* signals/50 tumour nuclei and
≤110 CEN8 signals/50 tumour nuclei).

Increased *MYC* signals and increased CEN8 signals (i.e., C8 polysomy)
(>110 MYC signals/50 tumour nuclei and
>110 CEN8 signals/50 tumour nuclei).

MYC clusters were present when clustered signals were noted in at least 20% of the tumour cells enumerated. The tumour was deemed positive for *MYC* clusters when these were present within ≥10/50 cells assessed.

Histopathology images were captured by utilising a Carl Zeiss Axiocam ERc 5s (Göttingen, Germany).

3.14 FISH on DLBCL and PBL

FISH for *MYC* rearrangement was performed on some cases of DLBCL during the diagnostic work up. FISH occurred at a referral cytogenetics laboratory, at CMJAH, and a validated assay was used at the time of the primary diagnosis. To reiterate, tumours that concurrently harboured *MYC*, *BCL2* and/or *BCL6* rearrangements were excluded from this study.

FISH for *MYC* rearrangement was performed in this study on a subset of PBL tumours that were c-MYC+ by IHC. This occurred at the abovementioned referral cytogenetics laboratory. The Vysis LSI *MYC* dual-colour, break apart rearrangement probe (Abbot Molecular, IL, USA), specific for the identification of *MYC* rearrang84ement on chromosome sub-band 8q24, was used on FFPE tissue sections of PBL that were 3µm in thickness. A normal interphase nucleus showed two fusion signals, while an abnormal case with a simple translocation will have one fusion, one green and one orange signal. Fifty nuclei were analysed and at least 10% of the cells were required to show positive signals (i.e., break apart or dual fusion) for a positive result regarding *MYC* rearrangement. The FISH findings on PBL were initially interpreted by a competent scientist and thereafter the findings were doublechecked by the Head of the Somatic Cell Genetics Unit at CMJAH. The FISH findings and selected images of the PBL tumours were subsequently included and analysed in this study.

3.15 Statistical analysis

Data analysis was performed with the aid of IBM SPSS Statistics versions 26.0, 27.0 and 28.0 software and the Statistica application 13 software. Statistical analyses that generated probabilities (*P*-values) of less than significance level alpha 0.05 (i.e., $P<0.05$), were interpreted as significant. Analyses were performed at the 95% confidence interval. Descriptive and inferential statistical methods were utilised.

Continuous data variables such as age, CD4 count and HIV viral load were assessed for normality using the graphical method such as a histogram graph and a numerical method, i.e., the Shapiro-Wilk W test for normality. When the histogram graph was bell-shaped and symmetric about the mean, that variable was normally distributed. When the *P*-value of the Shapiro-Wilk W test for normality was >0.05, that continuous variable was normally distributed and it was presented as a

mean value with the standard deviation. When the *P*-value of the Shapiro-Wilk W test for normality was <0.05, that particular continuous variable was not normally distributed and the median value with an inter-quartile range was presented. Mann-Whitney U test was used for comparisons of medians of the non-normal distributed continuous variables. The independent *t*-test was used for normal distributed continuous variables for comparison of means (Ghasemi and Zahediasl, 2012; Mishra et al., 2019).

The categorical data variables in this study comprised the patients' gender, HIV status, concomitant conditions including infections, stage of lymphoma, IPI score, topographic site of biopsy, SS appearance, cytomorphology, IHC COO, DE of BCL2 and c-MYC in DLBCL, Ki-67 proliferation index, EBER ISH status of PBL, *MYC* rearrangement, *MYC* copy numbers, combined *MYC* aberrations and mortality. Frequencies, proportions or percentages thereof were generated. Associations between categorical variables were assessed using Pearson Chi-square test or Fisher's exact test (2-sided). The latter was used when the expected frequencies in 20% of the cells was <5%. Mortality was based the number of patients who had demised by the end of the study timeframe, i.e., December 2020 for the PBL patients and January 2021 for the DLBCL patients.

The median overall survival (OS) time, applicable from the date of lymphoma diagnosis to death from any cause, was assessed using the Kaplan Meier survival estimate method and presented with 95% confidence intervals. Survival outcome comparison among the subgroups was compared using the Log rank test. Data were right censored as some patients were alive at the end of the study and others were lost to follow up.

Cox proportional hazards regression analysis was performed for DLBCL to determine the factors that contributed to time to death. In other works, the Cox proportional hazards model was developed to determine potential associations of the prognostic factors with survival outcome. Univariate analysis was performed initially. Hazard ratios (HR) were generated and presented with 95% confidence intervals (CI). Factors with a *P* value ≤0.02, or those which are clinically relevant, were selected as the covariates for multivariate analysis.

4 CHAPTER FOUR

4.1 RESULTS: PLASMABLASTIC LYMPHOMA

4.1.1 PBL: Included cases

Seventy-three cases of PBL were initially retrieved from the database from October 2013 to June 2017. Three cases were excluded due to irretrievable tissue blocks and an additional three cases were excluded due to insufficient residual tumour within the tissue blocks. Thereafter, 67 cases of PBL (N=67) were included in this study. These tumours were confirmed at the Histopathology Laboratory of the NHLS at CHBAH.

4.1.2 PBL: Age of patients

The age variable was normally distributed with a mean of 40 years and a standard deviation (SD) of ± 10.2 years. The minimum and maximum ages were 18 and 64 years, respectively. The HIV seropositive patients had a mean age of 41 (SD 10.1) years.

4.1.3 PBL: Gender of patients

There were 35 females (52%) and 32 males (48%). The male to female ratio was 1:1.1 in the overall PBL group. Of the HIV seropositive patients, there were 34 females (54%) with a male to female ratio of 1:1.2.

4.1.4 PBL: HIV status

The HIV status of 64 patients was confirmed, using the Enzyme-Linked Immunosorbent Assay (ELISA) assay, to be seropositive for 63 (98%), seronegative for a 24-year-old immunocompetent male and unknown for 3 patients. The HIV viral load was available for 46 patients, within one to five months of the PBL diagnosis. The median viral load was 55 587 copies/mL with an interquartile range (IQR) of 273 582 copies/mL. The minimum HIV viral load

was lower than the detectable limit (LDL) and the maximum was 6 797 265 copies/mL. The former was evident in 15% (7 of 46) of the patients and for purposes of statistical analysis LDL that was serologically <20 copies/mL, was assigned a numerical value of 19 copies/mL.

4.1.5 PBL: CD4 count and immunosuppression

The CD4 count was available for 54 patients within one to five months of the PBL diagnosis. The median CD4 count was 170 cells/mm^3 and the IQR was 249 cells/mm^3. The minimum and maximum CD4 counts were 4 cells/mm^3 and 787 cells/mm^3, respectively. The CD4 count was <200 cells/mm^3 for 57% (31 of 54) of the patients and 37% (20 of 54) had CD4 counts <100 cells/mm^3.

4.1.6 PBL: Concomitant conditions

Concomitant conditions (CCs) were documented in 23% (7 of 31) of the PBL patients, for whom data was available. CCs comprised infections predominantly and one patient developed ocular surface squamous cell carcinoma as listed in Table 4.1.

Table 4.1: Concomitant conditions that occurred with PBL

PBL patients	Concomitant conditions
6	**Infections**
1	Hepatitis B and pulmonary tuberculosis
1	Botryomycosis and hepatitis C
1	Anogenital and oral herpes simplex infection
1	Neurocysticercosis
1	Necrotising fasciitis
1	Septic shock
1	**Neoplasia**
1	Ocular surface squamous cell carcinoma

Abbreviations: PBL – plasmablastic lymphoma

CCs were not significantly associated with mortality (P=0.88) and CCs did not significantly impact the median OS (CCs+ 65 [95% CI 0-134] and CCs- 122 days [95% CI 27-217], P=0.74, Log rank test).

4.1.7 PBL: Stage of lymphoma

The Ann Arbor stage of lymphoma was available for 31 patients who were referred to the Clinical Haematology Department at CHBAH. There was a predominance of advanced stage disease, i.e. Ann Arbor stage III-IV at presentation in 23 of 30 (77%) HIV seropositive patients. Twenty-two (73%) HIV seropositive patients had stage IV lymphoma at presentation. The HIV seronegative patient presented with stage IV lymphoma. The stage of PBL was not significantly associated with ON/EON topography (P=1.0, Fischer's exact test), increased *MYC* gene copy numbers (P=0.19, Chi Square test), *MYC* rearrangement (P=0.60, Fischer's exact test) or *MYC* aberrations (P=1.0 Fischer's exact test).

4.1.8 PBL: Topographic site of biopsy

Three patients had PBL confirmed at two topographic sites during the primary diagnostic workup. Therefore, PBL was confirmed at 70 topographic sites of which the extra-oronasal (EON) region predominated (53 of 70, 76%). Twenty-four percent of PBLs were confirmed at oronasal (ON) regions. The topographic regions of biopsy are shown in Table 4.2. Bone marrow involvement by PBL occurred in 10% (7 of 41) of the patients, as detected at the initial diagnosis and during the staging of NHL. Based on the haematological workup and multidisciplinary review of these patients, myeloma was deemed unlikely due to the presence of HIV seropositivity, low CD4 counts, high proliferation indices and positive EBER ISH status within the tumours.

Table 4.2: PBL - Topographic sites of biopsy

Anatomical sites	70	
Oronasal site at diagnosis*	17 (24%)	
Soft or hard palate		4
Oropharynx		1
Gingiva		3
Tonsil		1
Oral region, not otherwise specified		1
Nasal		7
Extra-oronasal site at diagnosis**	53 (76%)	
Gastrointestinal tract	16	
Anorectal region		11
Colon		1
Small intestine		2
Stomach		1
Oesophagus		1
Liver	1	
Lymph node	9	
Soft tissue	8	
Breast	4	
Skin	4	
Bone	4	
Bone marrow	3	
Urinary bladder	1	
Cervix or vagina	2	
Pelvis, not otherwise specified	1	

*PBL was confirmed at 2 oronasal sites in 2 patients:
P4 (oropharynx and posterior nasal region),
P33 (gingiva and tonsil).
**PBL confirmed at 2 extra-oronasal sites for P39 (lymph node and femur).

4.1.9 PBL: Morphology

A SS appearance (Figure 4.1) was identified in 31% of the tumours (20 of 65) and was unassessable in two cases. SS appearance was evident in 20 of 61 (33%) HIV PBLs.

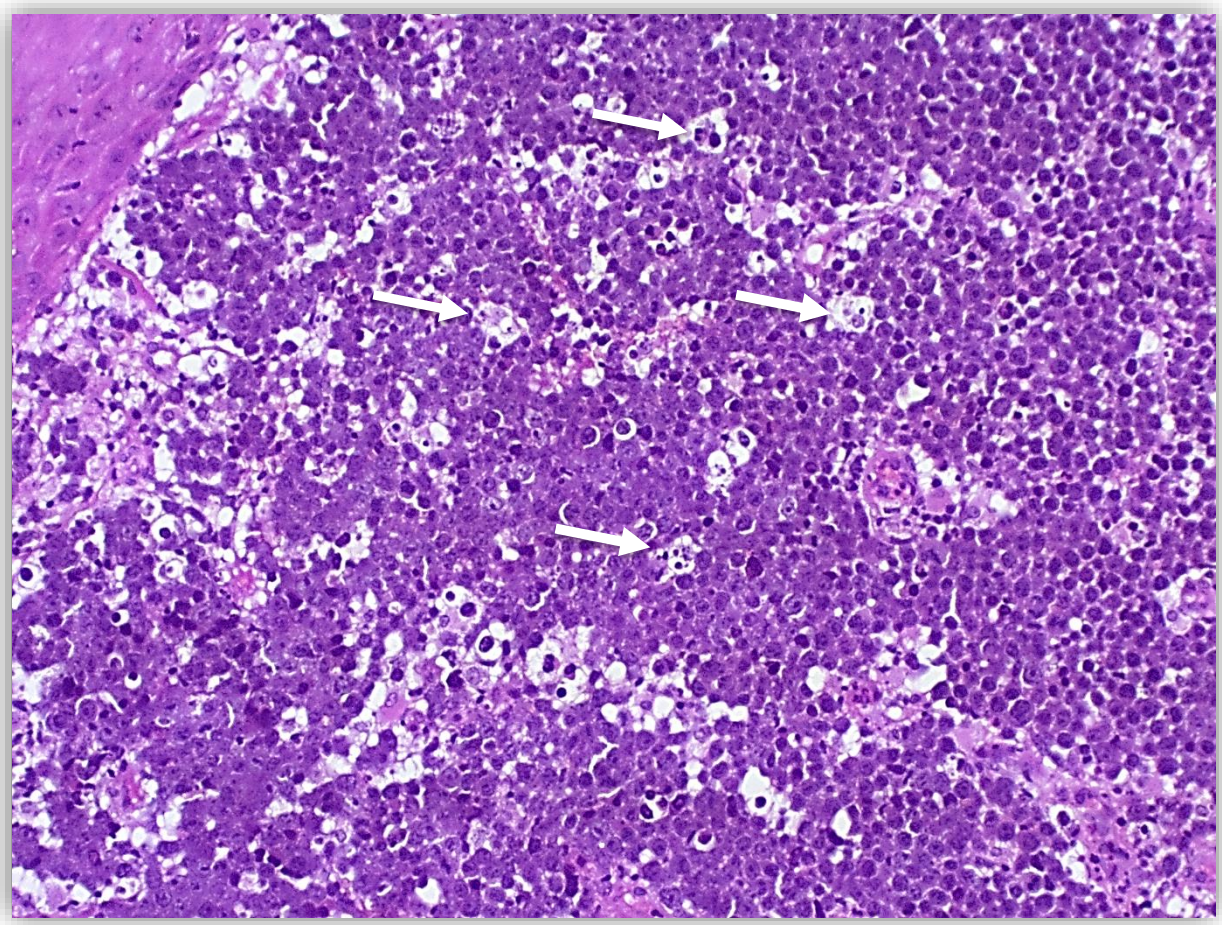


Figure 4.1: Starry-sky appearance in PBL [arrows denoting tingible body macrophages] (H&E-stained section, x100 magnification)

Monomorphic morphology (Figure 4.2A) was documented in 31 of 63 (49%) and plasmacytic differentiation (Figure 4.2B) occurred in 32 of 63 (51%) HIV PBLs. In the HIV PBLs, a SS occurred mainly in the context of monomorphic plasmablastic morphology (14 of 20, 70%, P=0.02). There was no significant association between morphology and topography (P=0.82, Chi-Square test).

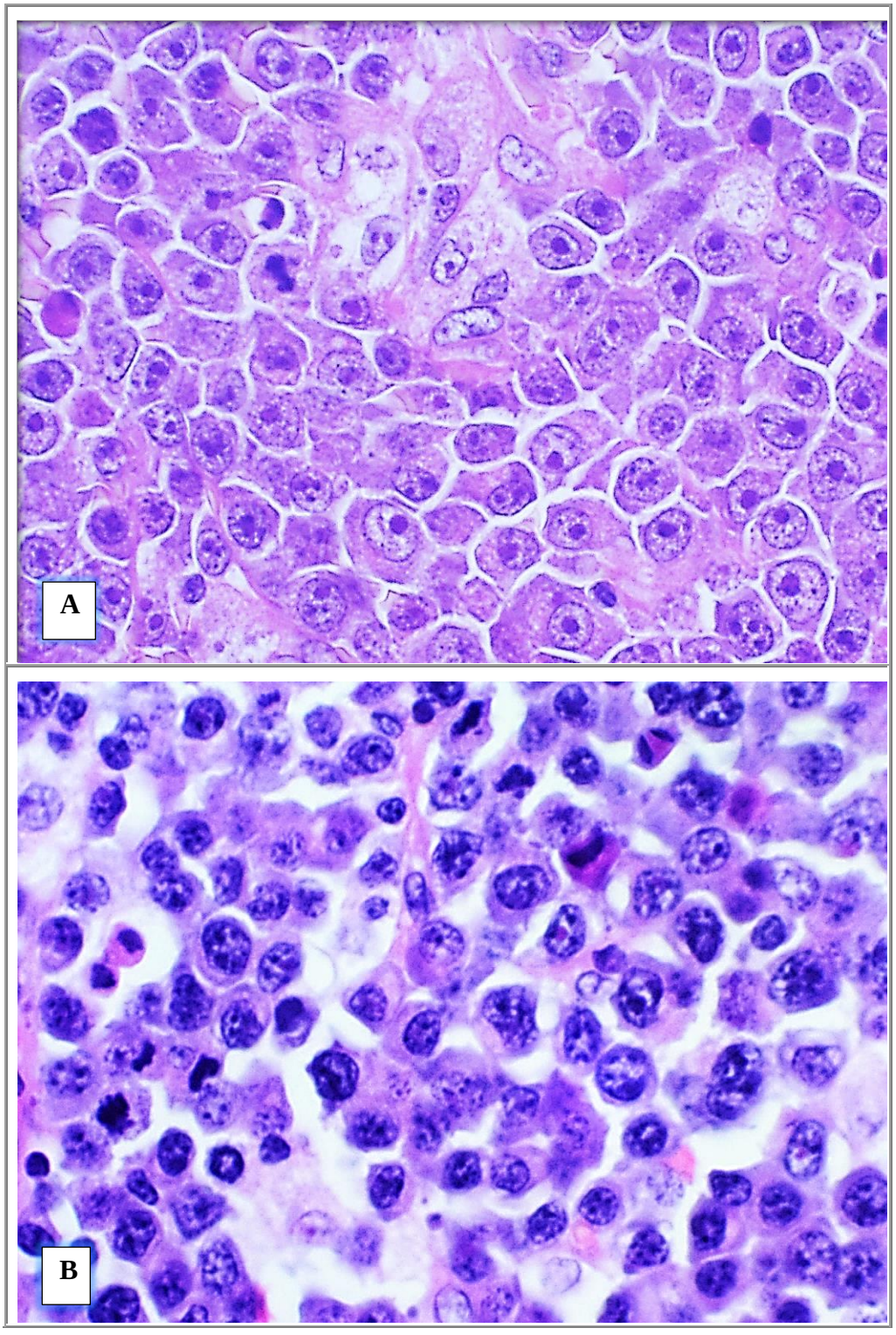


Figure 4.2: Plasmablastic lymphoma displaying monomorphic (A) and (B) plasmacytic cytomorphology (H&E-stained sections, x400 magnification).

4.1.10 PBL: Immunophenotype

c-MYC immunohistochemistry was successfully performed on all PBLs and 81% (54 of 67) demonstrated positive nuclear expression of at least 40% (Figure 4.3). c-MYC protein expression was detected in 51 of 63 (81%) HIV PBLs and this was significantly associated with EON topography (44 of 51, 86%, $P=0.03$).

All the PBLs displayed diffuse MUM1 and CD138 expression.

There were very high proliferation indices, with an average expression of 93% within PBL. The Ki-67 proliferation index (i.e., <90% and ≥90%) in PBL was not significantly associated with c-MYC protein expression ($P=0.57$, Fischer's exact test).

The tumours were negative for CD20 as expression thereof was not ≥40%. Two PBL cases had CD20 immunoreactivity of 30% and one tumour displayed 10% expression.

The PBLs were negative for ALK1 and HHV8.

An immunophenotypic analysis and summary of PBL is presented in Table 4.3.

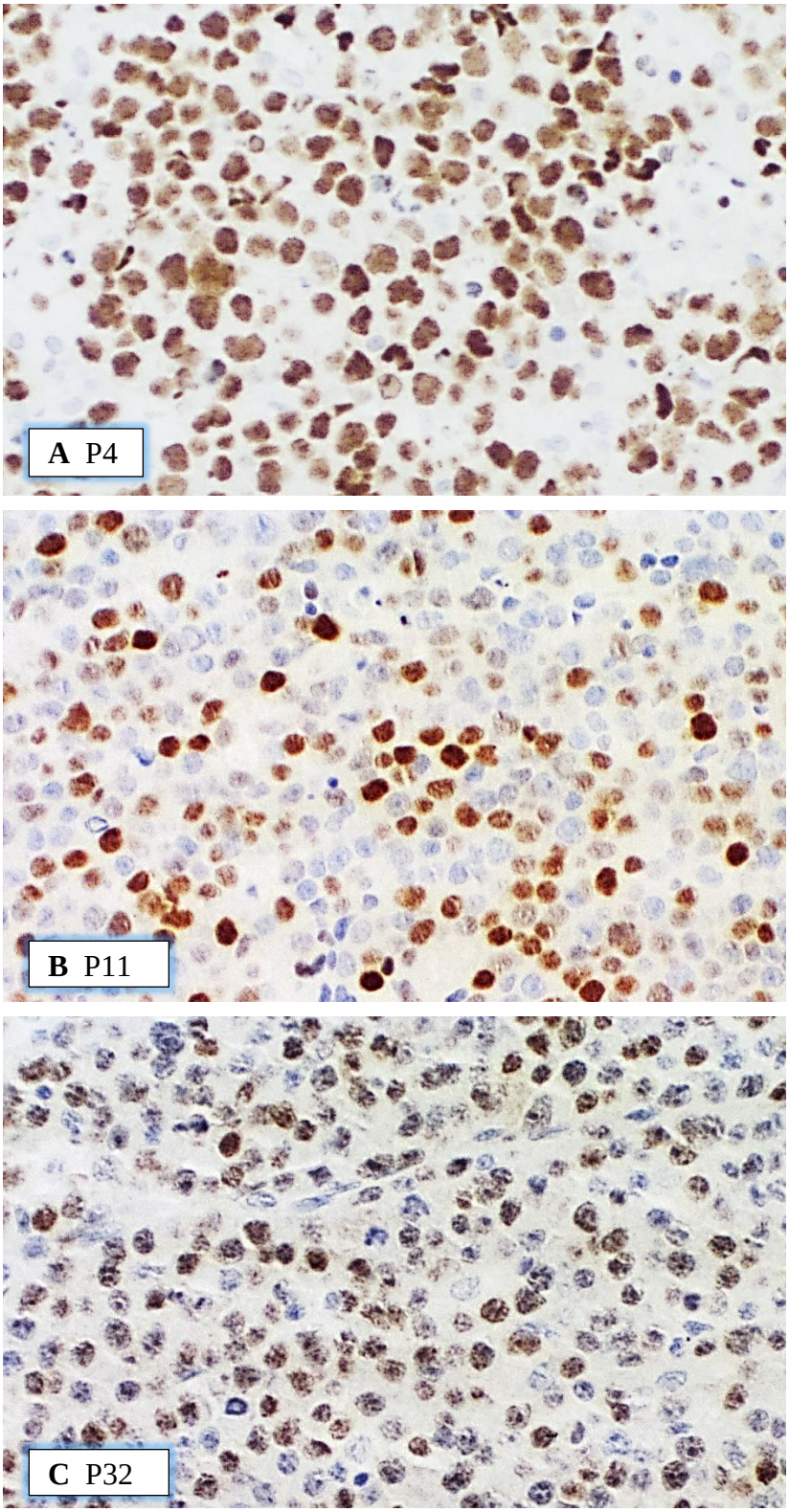


Figure 4.3: c-MYC protein immunoexpression in PBL (IHC-stained, x200 magnification).

Table 4.3: Immunophenotypic analysis of PBL

Immunohistochemistry	**PBL (N=67)**
c-MYC+ +proportion (min-max) average proportion+	54 of 67 (81%) 40-95% 63%
MUM1+ +proportion (min-max) average proportion+	67 of 67 (100%) 60-100% 97%
CD138+ +proportion (min-max) average proportion+	53 of 64 (83%) 50-100% 74%
Ki-67 +proportion (min-max) average proportion+	 80-95% 93%
HHV8 negative	 51 of 51
ALK1 negative	 36 of 36
CD20 negative	 67 of 67

Abbreviations: CD – cluster of differentiation,
HHV8 – human herpes virus-8,
ALK – anaplastic large cell lymphoma kinase,
PBL – plasmablastic lymphoma.

The Ki-67 proliferation index (i.e., <90% and ≥90%) in PBL was not significantly associated with c-MYC protein expression (P=0.57, Fischer's exact test), the presence of *MYC* translocation (0.19, Fischer's exact test), increased *MYC* copy numbers (P=0.79, Fischer's exact test) or combined

MYC aberrations (*P*=1.0, Fischer's exact test). The proliferation index did not significantly impact the median OS (*P*=0.88, 95% CI 32-158, Log rank test).

4.1.11 PBL: CISH

Dual-colour CISH was successful on 73% (49 of 67) of the PBLs. The internal positive control cells included squamous epithelium and fibroblasts as shown in Figure 4.4, glandular epithelium, endothelial cells, macrophages and non-neoplastic lymphocytes.

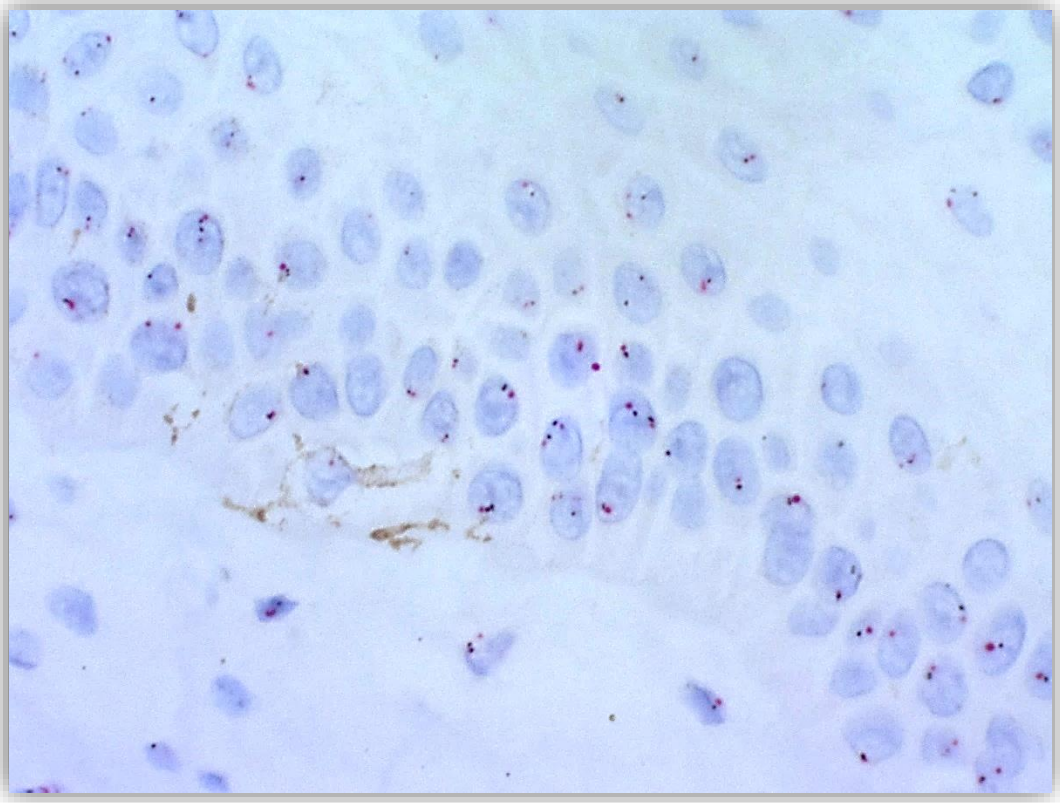


Figure 4.4: Dual-colour CISH demonstrating intranuclear *MYC* signals (black) and CEN8 signals (red) in the squamous epithelium and dermal fibroblasts (x400 magnification).

Low-level increase in *MYC* gene copy numbers, as shown in Figure 4.5, was identified in 29% (14 of 49) of PBL.

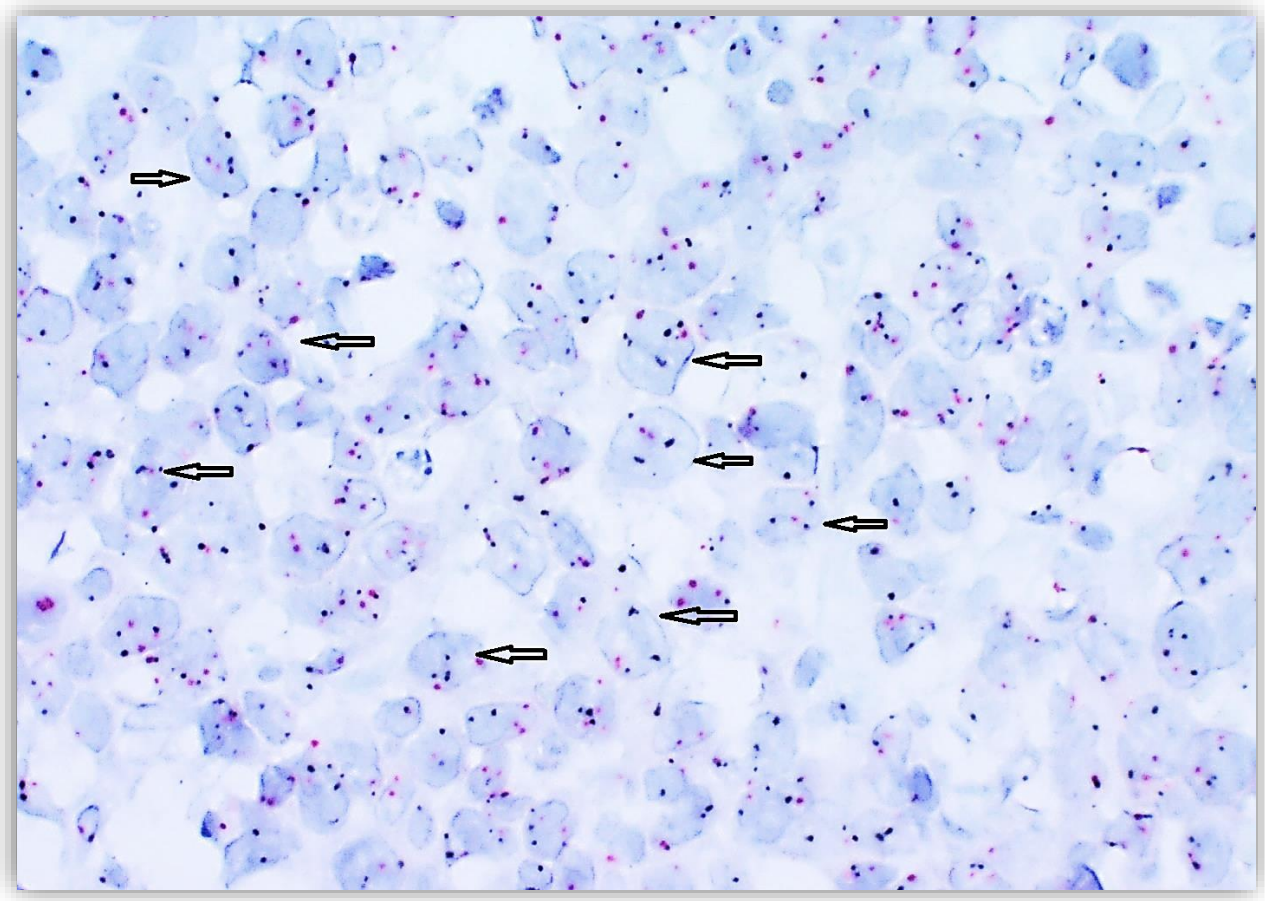


Figure 4.5: PBL (P46) displaying increased *MYC* gene copy numbers (black signals) and not-increased CEN 8 (red signals) within tumour nuclei (CISH-stained section by light microscopy, x400 magnification).

Three HIV PBLs displayed increased *MYC* gene copy numbers and increased CEN8 signals as shown in Figure 4.6, in keeping with C8 polysomy.

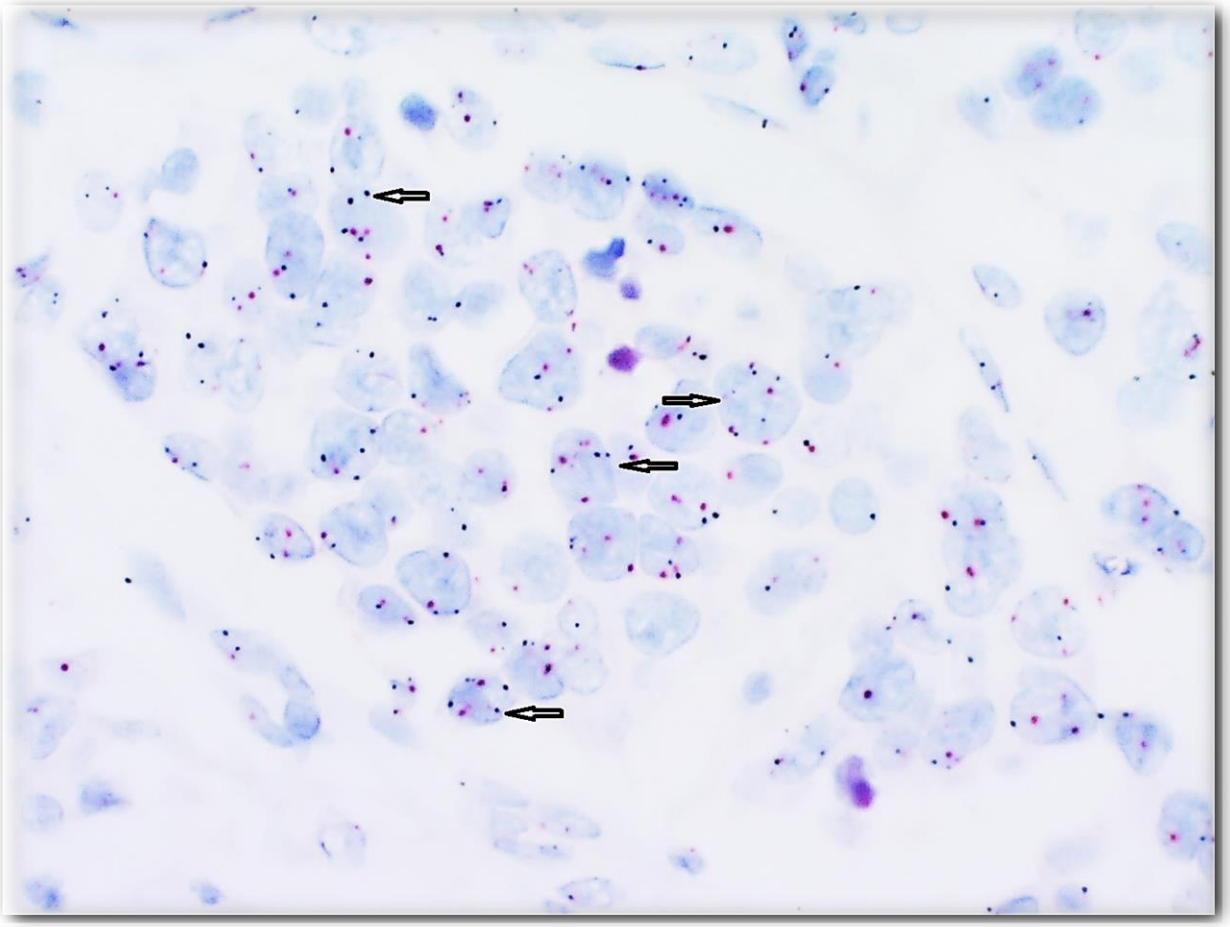


Figure 4.6: PBL (P55) displaying increased *MYC* gene copy numbers (black signals) and increased CEN8 (red signals) within tumour nuclei (CISH-stained section under light microscopy, x400 magnification).

CISH was deemed unsuccessful on 27% (18 of 67) of PBLs due to sparse or absent *MYC* signals within internal control cells and the tumour cells (five tumours), technical challenges with the autostainer instrument (nine tumours) and sparse residual tumour cells in the biopsy fragments after IHC was performed (four tumours).

4.1.12 PBL: FISH

Based on the presence of adequate residual tumour within the tissue blocks, 41 PBLs which demonstrated positive c-MYC immunoexpression or increased numbers of *MYC* gene copies by dual-colour CISH, were subsequently evaluated for *MYC* rearrangement and *MYC* gene copies by utilising FISH.

FISH was successful and interpretable for 88% (36 of 41) of the tumours (33 HIV+, 1 HIV- and 2 of unknown HIV status).

MYC rearrangement was identified in 25 tumours. Twenty three of 33 (70%) HIV PBLs harboured *MYC* rearrangement. *MYC* rearrangement was not significantly associated with a SS appearance (*P*=0.63, Chi-Square test), tumour morphology (*P*=0.27, Fischer's exact), c-MYC immunoexpression (*P*=0.52, Fischer's exact), Ki-67 [<90 versus ≥90%] (*P* =0.19, Fischer's exact), EBER ISH status (*P*=1.0, Fischer's exact), stage of lymphoma (*P*=0.60, Fischer's exact) and mortality (*P*=0.47, Fischer's exact). The median OS was 65 days (95% CI 0-149) when *MYC* rearrangement was present in PBL. This was not significantly different from the median OS of 32 days (95% CI 13-51) when *MYC* rearrangement was not present (*P*=0.91, Log rank test).

Concurrent *MYC* rearrangement and increased *MYC* gene copy numbers, as shown in Figure 4.7 and Table 4.4, were identified in 16 HIV PBLs (of 33, 49%, *P*= 0.98, Chi-Square test).

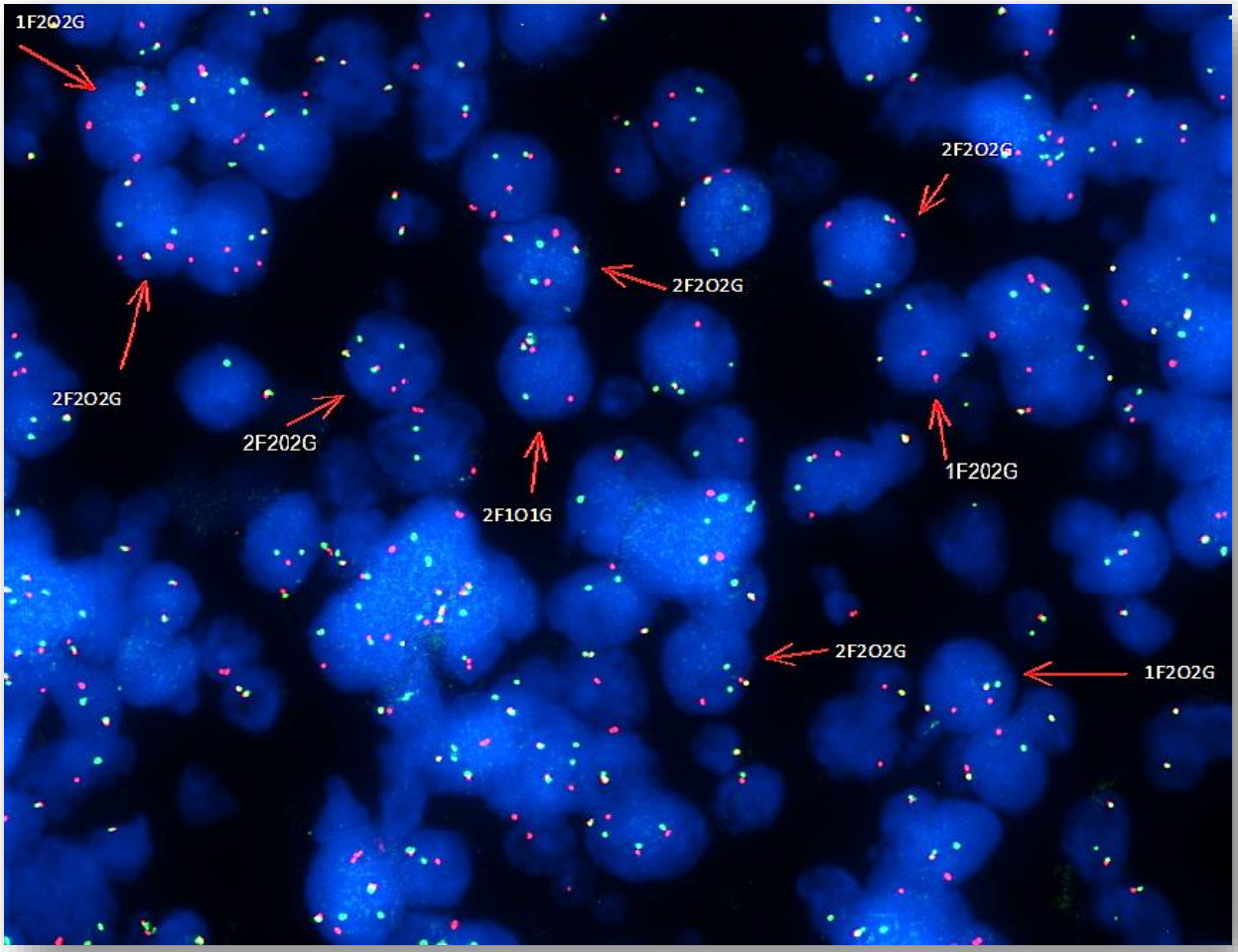


Figure 4.7: 4′,6-diamidino-2-phenylindole (DAPI)-stained nuclei (P35) hybridised with the Vysis LSI MYC dual-colour break-apart probe. Arrowed nuclei show increased *MYC* signals, involving both the intact *MYC* locus seen as a fusion (F), (overlap of SpectrumOrange and SpectrumGreen probes encompassing the 5' and 3' regions of the *MYC* gene, respectively) and rearranged *MYC* loci seen as separate orange (O) and green signals (G).

Table 4.4: PBL with increased *MYC* copy numbers

No.	PBL study no.	*MYC* signals per 50 nuclei; per nucleus of tumour	CEN8 signals per 50 nuclei; per nucleus of tumour	c-MYC IHC (proportion stained)	*MYC* rearranged +/-	EBER ISH +/-/ NP*
1.	P4	112; 2.24	˚	95%	+	-
2.	P5	112; 2.24	˚	95%	+	+
3.	P6	122; 2.44	81; 1.62	90%	+	+
4.	P11	128; 2.56	83; 1.66	70%	-	*
5.	P13	118; 2.36	94; 1.88	60%	+	+
6.	P14	119; 2.38	90; 1.80	95%	+	+
7.	P16	146; 2.92	87; 1.74	30%	-	+
8.	P18	125; 2.50	˚	80%	+	+
9.	P19	129; 2.58	88; 1.76	70%	-	+
10.	P30	116; 2.32	˚	95%	+	+
11.	P33	136; 2.72	89; 1.78	80%	-	+
12.	P35	133; 2.66	100; 2.00	60%	+	+
13.	P36	117; 2.34	92; 1.84	90%	+	+
14.	P37	120; 2.40	˚	90%	+	+
15.	P38	125; 2.50	˚	90%	+	*
16.	P39**	171; 3.42	122; 2.44	70%	-	+
17.	P40	126; 2.52	101; 2.02	95%	+	+
18.	P42	164; 3.28	129; 2.58	80%	+	+
19.	P46	145; 2.90	87; 1.74	95%	+	+
20.	P52***	181; 3.62	99; 1.98	60%	-	+
21.	P55	173; 3.12	129; 2.58	70%	+	-
22.	P57	117; 2.34	78; 1.56	30%	+	+
23.	P61	130; 2.60	97; 1.94	50%	-	*
24.	P63	155; 3.10	˚	40%	-	+

Abbreviations: IHC- immunohistochemistry, CEN8- centromere of chromosome 8, EBER- EBV small RNA ISH
*NP - not performed.
**PBL was confirmed within two sites of P39: lymph node (P39a) and femur (P39b). The latter showed extensive coagulative necrosis.
*** HIV seronegative patient. ˚not assessed / CEN8 signals not assessed using FISH.
+ present/positive finding, - not detected/negative.
<100 CEN8 signals per 50 nuclei is due to the variable plane of sectioning of three-dimensional nuclei.

4.1.13 PBL: Average number of *MYC* copies by CISH and FISH

By utilising FISH and CISH, *MYC* gene copy numbers were assessed in 87% (58 of 67) of the PBLs (54 HIV+, 1 HIV- and 3 of unknown HIV status). Forty one percent (24 of 58) were confirmed to have increased *MYC* gene copy numbers, i.e., >110 *MYC* signals per 50 tumour nuclei.

Twenty-three HIV PBLs (23 of 54, 43%) displayed a low-level increase in *MYC* gene copy numbers as shown in Table 4.4. There were 3 HIV PBLs (of 54, 6%) with C8 polysomy. *MYC* gene clusters were not identified.

Increased *MYC* gene copy numbers were not significantly associated with tumour morphology (P= 0.05, Chi-Square), a SS appearance (P=0.22, Chi-Square), EBER ISH status (P=1.00, Chi-Square), c-MYC protein expression (P=0.27, Fischer's exact), Ki-67 [<90 versus ≥90%] (P=1.00 Fischer's exact), stage of lymphoma (P=0.20, Chi-Square) and mortality (P=0.25, Chi-Square). The median OS was 95 days (95% CI 7-183) when increased *MYC* gene copy numbers were present. This was not significantly different from the median OS of 71 days (95% CI 11-131) when *MYC* gene copies were not increased (P=0.95, Log rank).

4.1.14 PBL: *MYC* aberrations

MYC aberrations such as *MYC* rearrangements and/or increased numbers of *MYC* gene copies were identified in 33 of 58 (57%) of the overall PBLs by utilising dual-colour CISH and FISH. Clinicopathological features and immunophenotypic analysis of the overall PBLs, with and without *MYC* aberrations, are shown in Table 4.5. and Table 4.6. No significant difference was demonstrated in the median OS of HIV PBL with *MYC* aberrations [65 days (95% CI 0-143 days)] and HIV PBL without *MYC* aberrations [71 days (95% CI 11-131 days)] (Log rank test P=0.61).

Fifty-six percent (30 of 54) of HIV PBLs harboured *MYC* aberrations. The average *MYC* gene copy numbers were significantly higher in the HIV PBL subgroup containing *MYC* aberrations (125 copies/50 nuclei) than those without *MYC* aberrations (83 copies/50 nuclei) [$p < 0.001$]. *MYC* aberrations in HIV PBLs were significantly associated with a SS appearance (P=0.01), monomorphic morphology (P=0.03) and c-MYC protein expression of ≥40% (P=0.03).

The EBER ISH status was not significantly associated with *MYC* aberrations (P=0.68).

The Ki-67 proliferation index (i.e., <90% and ≥90%) in PBL was not significantly associated with the presence of *MYC* translocation (0.19, Fischer's exact test), increased *MYC* copy numbers (*P*=0.79, Fischer's exact test) or combined *MYC* aberrations (*P*=1.0, Fischer's exact test).

Table 4.5: Clinicopathological characteristics of PBL and *MYC* aberrations

Clinicopathological parameters	***+MYC* aberrations**	***-MYC* aberrations**	***P*-value**
PBL tumours	33/58 (57%)	25/58 (43%)	
Age years (mean ± SD)	38.7 ± 9.7	41.2 ± 10.2	0.34 (Mann-Whitney U test)
Gender	F=17; M=16	F=12; M=13	0.79 (Chi-Square test)
HIV status Seropositive Seronegative Unknown	 30 1 2	 24 0 1	0.38 (Chi-Square test)
Viral load copies/mL median (IQR; min*- max)	117 000 (369 965; LDL – 6 797 265	57 412 (327 786; LDL – 2 100 000)	0.80 (Mann-Whitney U test)
CD4 cells/mm^3 median (IQR; min-max) 0-100 101-199 200-349 350-499 500-800 Unavailable	190 (350; 4-787) 9 4 6 1 5 8	154 (192; 10-511) 8 5 6 1 1 4	0.49 (Mann-Whitney U test)
Stage Early (I-II) Advanced (III-IV)	 5 (29%) 12 (71%)	 2 (22%) 7 (78%)	1.0 (Fischer's exact test)
Mortality (Data available for 33 patients) Demised	 20	 10	**0.02 (Chi-Square test)**
Median overall survival (OS) time (days) 95% confidence interval	95 19-171	71 3-139	0.77 (Log rank test)
Topographic site of biopsy Oronasal site at diagnosis Extra-oronasal site at diagnosis	 9/12 24/46	 3/12 22/46	0.16 (Chi Square)
Morphology Starry-sky appearance Monomorphic features Plasmacytic features	 47% (15/32) 64% (21/33) 36% (12/33)	 16% (4/25) 32% (8/25) 68% (17/25)	 **0.01** (Chi-Square test) **0.03** (Chi-Square test)

Abbreviations: *LDL – lower than detectable limit was <20 copies/mL; assigned numerical value 19 for statistical analysis. M-male, F-female, SD – standard deviation, IQR – interquartile range

Table 4.6: PBL - Analysis of immunohistochemistry and *MYC* aberrations

Immunohistochemistry	**PBL +*MYC* aberration** (n=33)	**PBL -*MYC* aberration** (n=25)	***P*-value**
c-MYC+	31 (94%)	17 (68%)	
+proportion (min-max)	40-95%	40-95%	
average proportion+	74%	51%	0.01 (*t*-test)
MUM1+	33 (100%)	25 (100%)	
+proportion (min-max)	80-100	60-100%	
average proportion+	99%	94%	0.20 (*t*-test)
CD138+	33 (100%)	25 (100%)	
+proportion (min-max)	80-100	60-100	
average proportion+	69%	79%	0.20 (*t*-test)
Ki-67			
+proportion (min-max)	80-95	80-95	
average proportion+	94%	93%	0.69 (*t*-test)

Abbreviations: CD – cluster of differentiation,
HHV8 – human herpes virus-8,
ALK – anaplastic large cell lymphoma kinase.

4.1.15 PBL: EBV ISH

Latent EBV infection was detected by utilising EBER ISH as shown in Figure 4.8 in 91% of the overall PBLs and in 90% (46 of 51) of HIV PBLs.

In HIV PBLs, positive EBER ISH and *MYC* rearrangement (Figure 4.7) occurred in 67% (18 of 27), positive EBER ISH and increased *MYC* copies occurred in 41% (18 of 44) and positive EBER ISH with *MYC* aberrations were present in 52% (23 of 44). Dual positivity for EBER ISH and c-MYC IHC was present in 73% (37 of 51) of the HIV PBLs.

No significant associations of EBER ISH positivity was demonstrated regarding topography (P=0.9, Chi-Square test), a SS appearance (P=1.0, Fischer's exact test), morphology (P=0.58, Chi-Square test), Ki-67 proliferation index [<90 versus ≥90%] (P=0.57, Chi-Square test), c-MYC IHC (P=0.29, Chi-Square test), *MYC* aberration (P=0.68, Chi-Square test), *MYC*

rearrangement (P=0.38, Fischer's exact test), increased *MYC* gene copy numbers (P=0.86, Fischer's exact test), stage of PBL (P=0.61, Chi-Square test) and mortality (P=0.66, Chi-Square test). The median OS was 102 days (95% CI 30-174) when the EBER ISH status was positive in PBL (P=0.95, Log rank test).

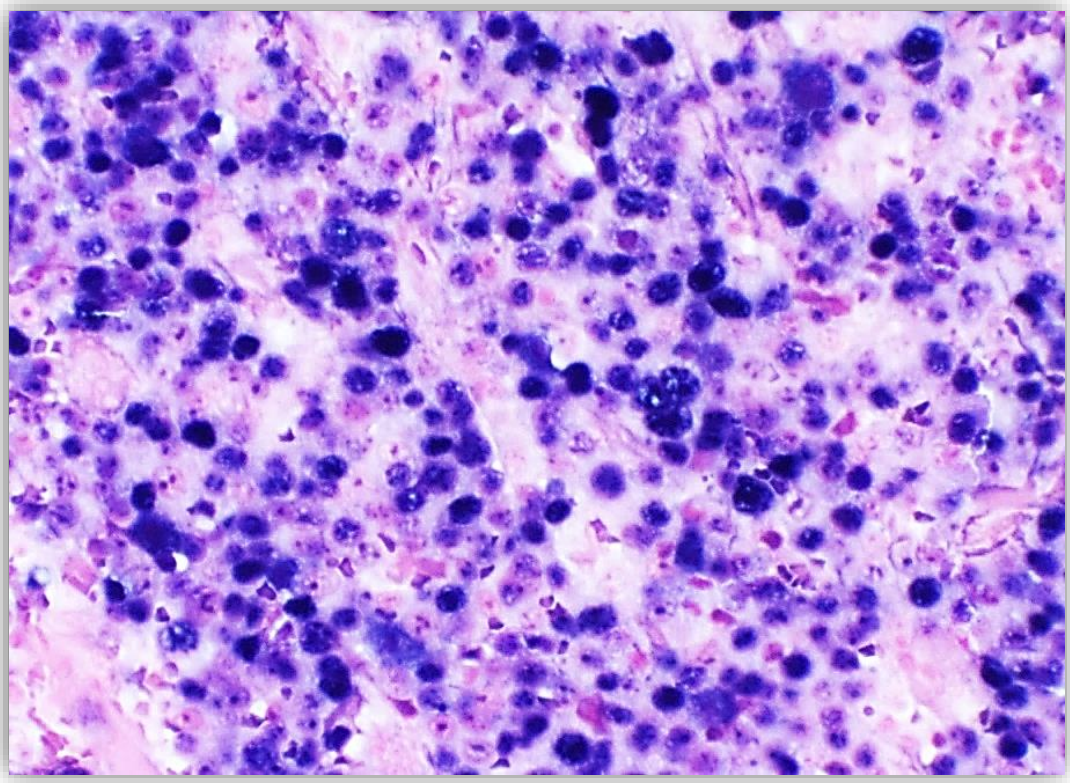


Figure 4.8: PBL (P35) displaying diffusely positive nuclear signals of EBER by ISH (x200 magnification).

4.1.16 PBL: Treatment

Treatment data were available for 38 patients who were referred to the Clinical Haematology Unit at CHBAH. Treatment included c-ART, cyclophosphamide, vincristine, adriamycin, prednisone (CHOP) or CHOP and etoposide (CHOEP). For refractory patients, rituximab-

CHOEP and salvage therapies including methotrexate, platinum compounds or cytosine arabinoside were used, with or without radiation. Rituximab-CHOEP was administered to 7 patients and 3 patients received radiation therapy. Patient-specific therapy for concomitant conditions was administered accordingly.

4.1.17 PBL: Survival outcome

Survival outcome data were available for 33 PBL patients, who were referred for treatment to the Clinical Haematology Department at CHBAH. The follow-up timeframe spanned from the month of the lymphoma diagnosis to the last month of this study, i.e., October 2013 to December 2020. The median follow-up time for the PBL patients was 193 days (95% CI 0 - 689 days). Nineteen of the HIV PBL patients with *MYC* aberrations (19) demised and 10 of the HIV PBL patients without *MYC* aberrations (13) demised (P=0.03). The median OS for HIV PBL was 75 days [95% confidence interval (CI) 14-136 days]. No significant difference was demonstrated in the median OS of HIV PBL with c-MYC protein expression [121 days (95% CI 0-360 days)] and HIV PBL without c-MYC protein expression [153 days (95% CI 77-229 days)] (P=0.80 Log rank test) as shown in Figure 4.9.

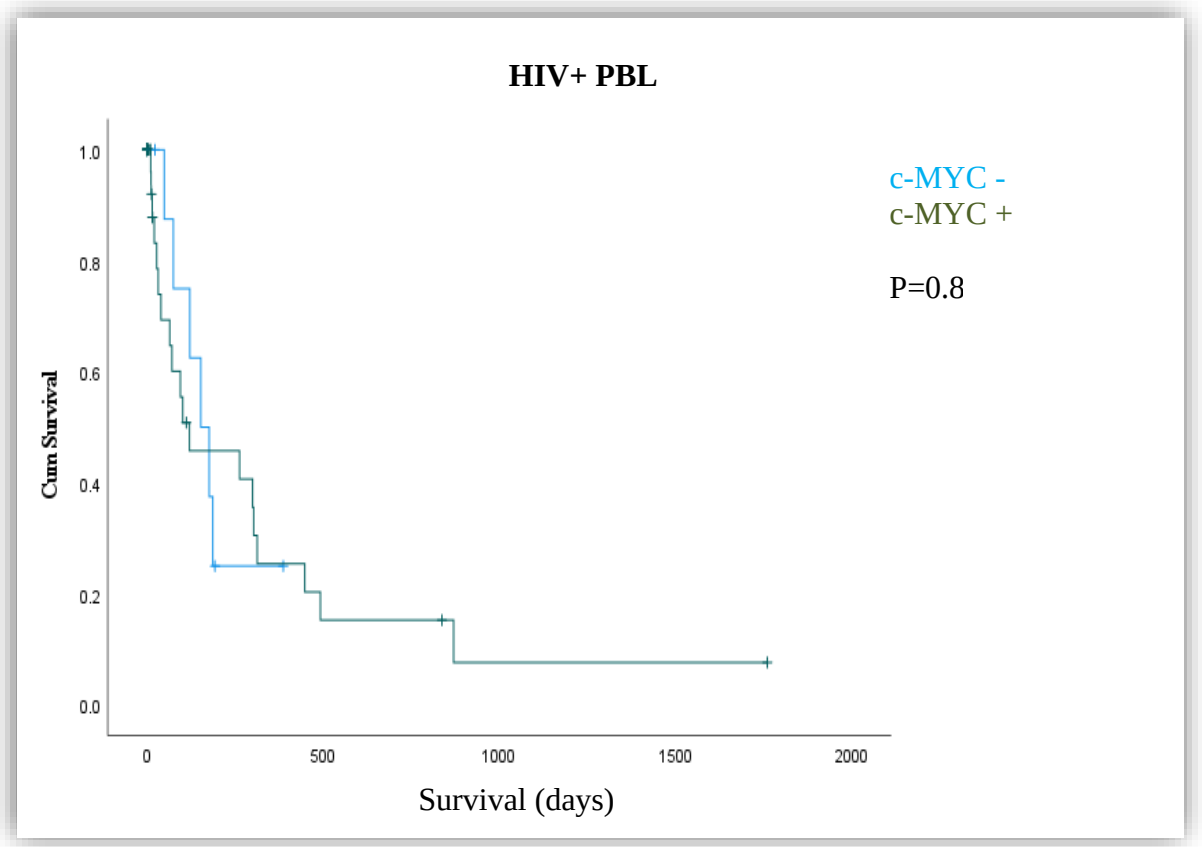


Figure 4.9: Kaplan Meier survival estimates for HIV PBL with c-MYC expression (green) and without c-MYC expression (blue).

No significant difference was demonstrated in the median OS of HIV PBL with *MYC* aberrations [65 days (95% CI 0-143 days)] and HIV PBL without *MYC* aberrations [71 days (95% CI 3–139 days days)] (*P*=0.61, Log rank test). Kaplan Meier survival estimate curves of HIV PBL with and without *MYC* aberrations are shown in Figure 4.10.

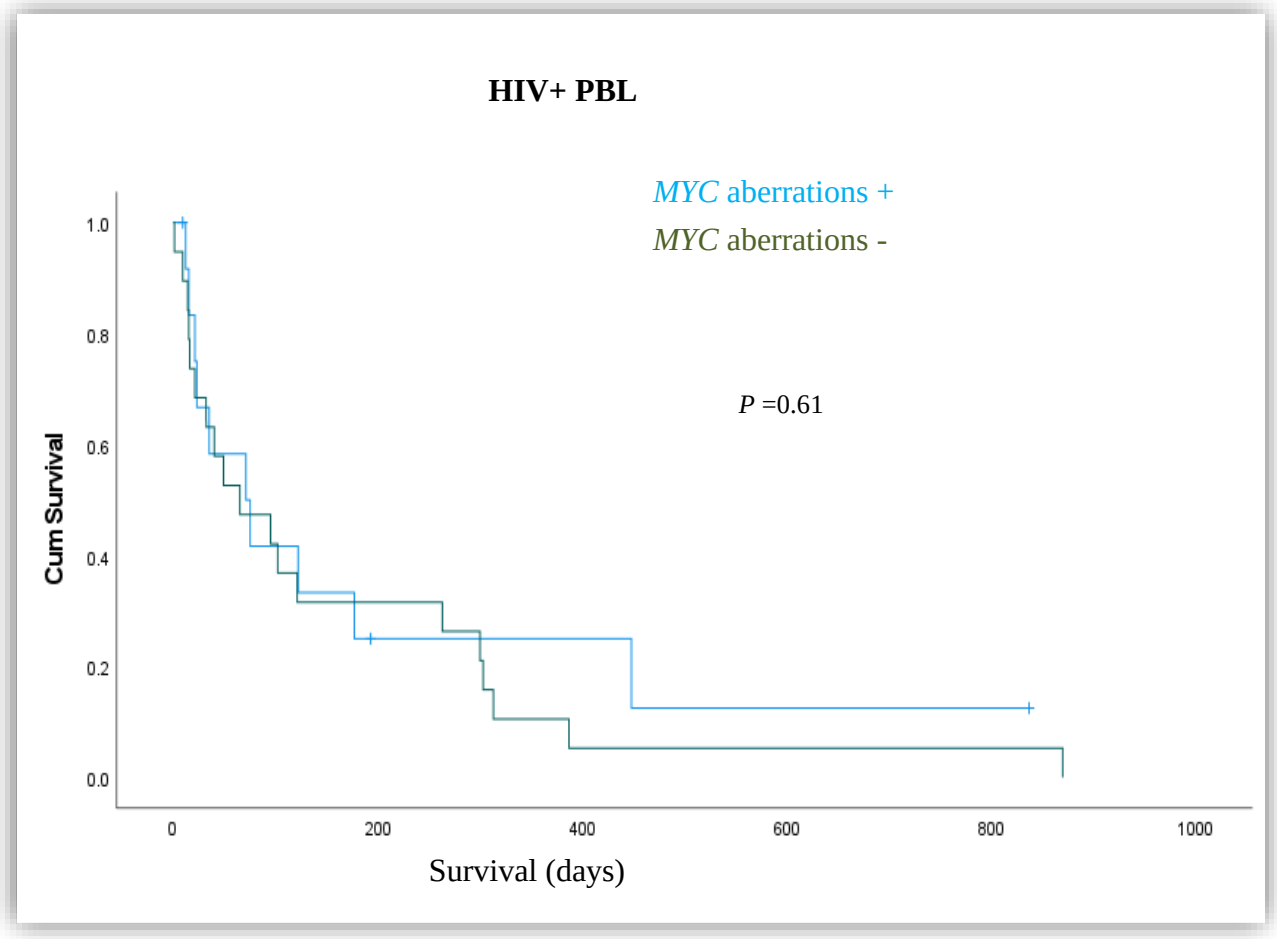


Figure 4.10: Kaplan Meier survival estimates for HIV PBL with *MYC* aberrations (green) and without *MYC* aberrations (blue).

The Ki-67 proliferation index (i.e., <90% and ≥90%) in PBL did not significantly impact the median OS (*P*=0.88, 95% CI 32-158, Log rank test).

4.2 RESULTS: DIFFUSE LARGE B-CELL LYMPHOMA

4.2.1 DLBCL: Included cases

One hundred and thirty-six (n=136) cases of DLBCL were initially retrieved from October 2013 to June 2017. Two cases were excluded due to extensive necrosis and insufficient residual tissue within the tissue blocks, which precluded further histopathology investigations. During review of the tumours, eleven additional cases were excluded due to the presence of criteria that deviated from the diagnosis of DLBCL NOS or HIV associated DLBCL. Thereafter, 123 cases of DLBCL (N=123) were retrospectively included in this study. These tumours were confirmed at the Histopathology Laboratory of the NHLS at CHBAH, over a timeframe of 45 consecutive months. Clinicopathological characteristics of the DLBCL patients are shown in Table 4.7.

4.2.2 DLBCL: Age of patients

The age was available for all the patients. The age variable was normally distributed with a mean value of 46 [standard deviation (SD) ±13.4] years. The minimum and maximum ages were 12 and 88 years, respectively. In the HIV seropositive and seronegative groups, the mean ages were 42 (SD ±10.8) and 57 (SD ±16.7) years, respectively. The HIV seropositive patients were significantly younger at the time of presentation with DLBCL ($P<0.01$).

Table 4.7: Clinicopathological characteristics of DLBCL patients

	Overall DLBCL	**HIV+ DLBCL**	**HIV- DLBCL**	***P*-value**
Number of patients	N=123	n=93	n=22	
HIV status: Seropositive (p) Seronegative (n) Unknown (u)	 8	 93/115 (81%)	 22/115 (19%)	
Age (years; mean) <60 years patients ≥60 years patients	46 (SD 13.4) 106 (86%) 17 (14%)	42 (SD 10.8) 88 (95%) 5 (5%)	57 (SD 16.7) 12 (55%) 10 (45%)	**0.001** (Indep samples *t*-test) **<0.001** (Chi-square test)
Gender: Male Female	66 (54%) 57 (46%)	51 (55%) 42 (45%)	13 (59%) 9 (41%)	0.72 (Chi-square test)
Viral load copies/mL Available Median IQR Minimum Maximum LDL		 78 patients 217 182 981 LDL 10 000 000 23 (30%)		
CD4 cells/mm^3 Available Median IQR Min-Max <100 ≥100 <150 <200 200-349 350-499 ≥500 Unavailable		 86 patients 162 215 6-1429 28 (33%) 58 (67%) 39 (45%) 53 (62%) 20 (23%) 6 (7%) 7 (8%) 7 (8%)		
Bone marrow infiltration Available Positive Negative	 87 6 (7%) 81 (93%)	 70 5 (7%) 65 (93%)	 15 1 (7%) 14 (93%)	1.00 (Fischer's exact test)
Stage Available Early (I-II) Advanced (III-IV)	 69 12 (17%) 57 (83%)	 55 7 (13%) 48 (87%)	 14 5 (36%) 9 (64%)	**0.04** (Chi-square test)
IPI score Available 0-2 3-5	 55 14 (26%) 41 (74%)	 48 12 (25%) 36 (75%)	 7 2 (29%) 5 (71%)	1.00 (Fischer's exact test)

	Overall DLBCL	HIV+ DLBCL	HIV- DLBCL	*P*-value
Infection concomitant conditions (CCI)				0.15 (Fischer's exact test)
Present	27/42 (64%)	24/33 (73%)	2/8 (25%)	
Biopsy topography				0.46 (Fischer's exact test)
Available	122	92	22	
Nodal	43 (35%)	35 (38%)	6 (27%)	
Extranodal	79 (65%)	57 (62%)	16 (73%)	
Starry-sky				0.42 (Fischer's exact test)
Assessable	120	90	22	
Present	30 (25%)	26 (29%)	4 (18%)	
Cytomorphology				0.28 (Fischer's exact test)
Assessable	119	89	22	
Centroblastic	52 (44%)	37 (42%)	12 (55%)	
Immunoblastic	14 (12%)	9 (10%)	4 (18%)	
Anaplastic	4 (3%)	4 (5%)	0 (0%)	
Mixed	49 (41%)	39 (44%)	6 (27%)	
Mortality				0.17 (Chi-square test)
Data available	76	60	16	
Demised	40 (53%)	34 (57%)	6 (38%)	

Abbreviations: HIV – human immunodeficiency virus, IPI – International Prognostic Index, LDL – lower than detectable limit, DLBCL – diffuse large B-cell lymphoma.

4.2.3 DLBCL: Gender of patients

The gender was specified for 123 patients. Of the HIV seropositive and seronegative patients, males comprised 55% and 59%, respectively. The male to female ratios were 1.2:1 in the HIV seropositive patients and 1.4:1 in the HIV seronegative patients.

4.2.4 DLBCL: HIV status

Eight patients had an unknown HIV status. Of 115 patients, the HIV status was seropositive for 93 (81%) and seronegative for 22 (19%) patients. The viral load was available for 78 patients and this was documented within 1-18 months of the lymphoma diagnosis. The median viral load was 217 (IQR 182 981) copies/mL. The minimum HIV viral load was LDL and the maximum was

10 000 000 copies/mL. The viral load was LDL in 30% (23 of 78) of the patients and for purposes of statistical analysis LDL was assigned a numerical value of 19 copies/mL.

4.2.5 DLBCL: CD4 count and immunosuppression

The CD4 counts were available for 86 patients and the CD4 counts were documented within 1-18 months of the lymphoma diagnosis. The median CD4 count was 162 cells/mm^3 (IQR was 215 cells/mm^3. The minimum and maximum CD4 counts were 6 cells/mm^3 and 1429 cells/mm^3. The CD4 count was <100 cells/mm^3 for 33% (28/86) of the patients. The impact of the CD4 counts on the survival outcome of HIV+ DLBCL patients is presented in the subsection 4.2.18.

4.2.6 DLBCL: Concomitant conditions

CCs were documented in 42 DLBCL patients. There were 27 patients with CC infections (CCI) and three patients had more than one infection (Table 4.8). Non-infective CCs were documented in sixteen patients and six thereof had more than one non-infective CC. A significant association between the overall CCs and the HIV status was not evident (P=0.94).

CCIs were documented in 24 HIV seropositive patients and CCIs were not significantly associated with CD4 counts <100 or ≥100 cells/mm^3 (P=0.61 Chi-square test). The impact of CCIs on the survival outcome of DLBCL patients is presented in the subsection 4.2.18.

Table 4.8: Concomitant conditions documented for DLBCL patients

No.	Concomitant conditions
	Infections
16	Sepsis (*Pseudomonas* spp. and/or other bacteria)
3	Hepatitis B infection
4	Herpes viral infection: cytomegalovirus, herpes simplex and/or varicella zoster
3	Pneumonia: *Pneumocystis* spp. or other
3	Tuberculosis
1	Gastroenteritis (*Clostridium difficile*)
	Non-infective
6	Renal failure
5	Deep venous thrombosis (subclavian or other)
4	Hypertension and/or diabetes mellitus
2	Neoplasia: squamous cell carcinoma or prostate carcinoma
1	Lymphoepithelial cyst
1	Gastrointestinal haemorrhage
3	Other: cardiomyopathy, hypothyroidism or obstructive jaundice.

4.2.7 DLBCL: Stage of lymphoma

The Ann Arbor stage of NHL was available for 69 patients who were referred to the Clinical Haematology Department at CHBAH for treatment of the lymphoma. Compared with the HIV seronegative group, the HIV seropositive patients demonstrated a significant predominance of an advanced stage at presentation (48 of 55, 87% P=0.04). The stage at presentation was not significantly associated with CD4 counts <100 cells/mm^3 or ≥ 100 cells/mm^3 in the HIV seropositive patients (P=0.40, Fischer's exact test). The stage was not significantly associated with the topographic site of biopsy (P=0.37, Chi square test). There was no significant difference in the median OS when advanced stage was compared with early-stage disease in the HIV+ group [(III-IV 228 days 95% CI 35-421, I-II 109 days 95% CI 53-165, respectively), P=0.95 Log rank test].

4.2.8 DLBCL: Topographic site of biopsy

The topographic origin of the diagnostic specimen was specified or microscopically discernible for 122 cases. In the HIV+ and HIV- DLBCLs, extranodal topographic sites of biopsy accounted for 62% (57 of 92) and 73% (16 of 22), respectively. The topographic site of biopsy was not significantly associated with the stage of lymphoma, irrespective of the HIV status [HIV+ P=0.37, Chi square test and HIV- P=0.58, Fischer's exact test].
Bone marrow infiltration by DLBCL occurred in 7% (6 of 87) of the patients and this was detected at the initial diagnosis or during staging of the lymphoma.

4.2.9 DLBCL: Starry-sky appearance and cytomorphology

SS appearance was noted in 29% (26/90) of the HIV+ DLBCLs and 18% (4/22) of the HIV- DLBCLs.

The cytomorphology of 119 DLBCLs was assessable. There was limited and partially crushed diagnostic tissue in four tumours, which precluded the reliable assessment of the cytomorphology. In the overall DLBCLs, centroblastic morphology (Figure 4.11 A) comprised 44% (52/119), immunoblastic morphology (Figure 4.11 B) which included plasmacytic differentiation comprised 12% (14/119), anaplastic morphology (Figure 4.11 C) comprised 3% (4/119) and mixed morphology comprised 41% (49/119). HIV- DLBCL demonstrated a 55% predominance of centroblastic morphology and the HIV+ DLBCL demonstrated mixed morphology predominantly (44%). A significant association between the cytomorphology of DLBCLs and the HIV status was not identified (P=0.28, Fischer's exact test). When the cytomorphology of DLBCL and the IHC-defined COO were cross tabulated, a significant association was not demonstrated (P=0.13). When the DLBCLs displayed anaplastic morphology, CD30 and CD15 were not expressed in the tumour cells. Hereby, CHL and B-cell lymphoma unclassifiable, with features intermediate between DLBCL and CHL, were excluded.

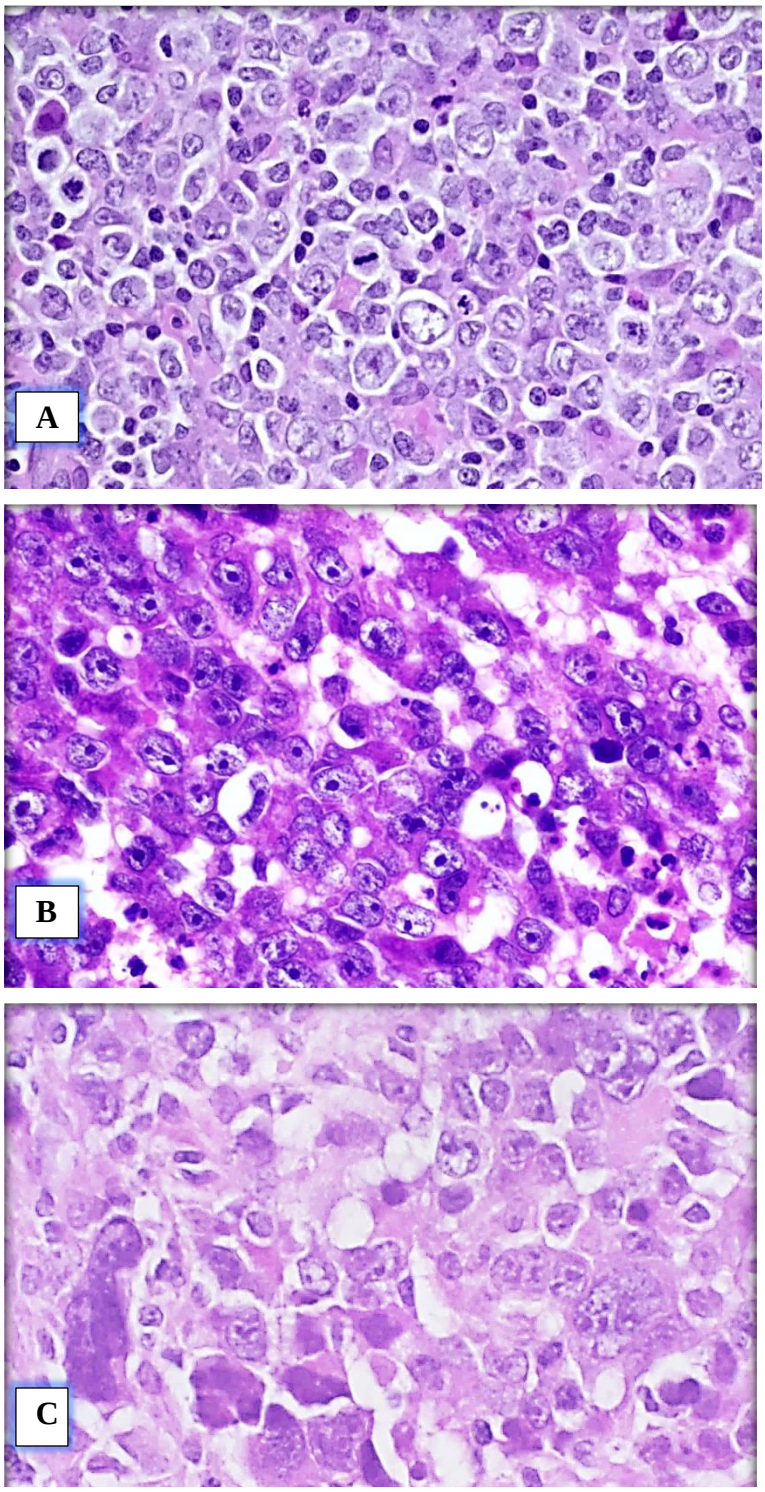


Figure 4.11: Centroblastic morphology (A), immunoblastic morphology (B) and anaplastic morphology (C) in DLBCL (H&E, x200 magnification).

4.2.10 DLBCL: Immunophenotype

The immunophenotype of HIV+ DLBCL was characterised by diffuse expression of CD20 in 99% of the cases. One tumour displayed limited expression of CD20, i.e., 20%, in association with diffuse expression of CD79a and PAX5.

Positive expression of CD10, bcl-6 and MUM1 was detected when at least 30% of the tumour cells displayed appropriate membranous or nuclear immunoreactivity. Accordingly, positive immunoexpression of these markers was 44%, 85% and 66%, respectively within the HIV+ DLBCLs.

Co-expression of MUM1 and bcl-6 occurred in 53% and 48% of HIV+ and HIV- DLBCLs, respectively.

BCL2 was deemed positive when at least 50% of the tumour displayed cytoplasmic immunoreactivity. Positive BCL2 immunoexpression was identified in 41% of the HIV+ DLBCLs and 59% of the HIV- DLBCLs.

c-MYC IHC was successful on 94% (116 of 123) of the DLBCLs. c-MYC was deemed positive when at least 40% of the tumour cells displayed nuclear immunoreactivity, irrespective of the staining intensity, as shown in Figure 4.12. c-MYC expression was detected in 40% of the HIV- DLBCLs and 58% of HIV+ DLBCLs as shown in Table 4.9.

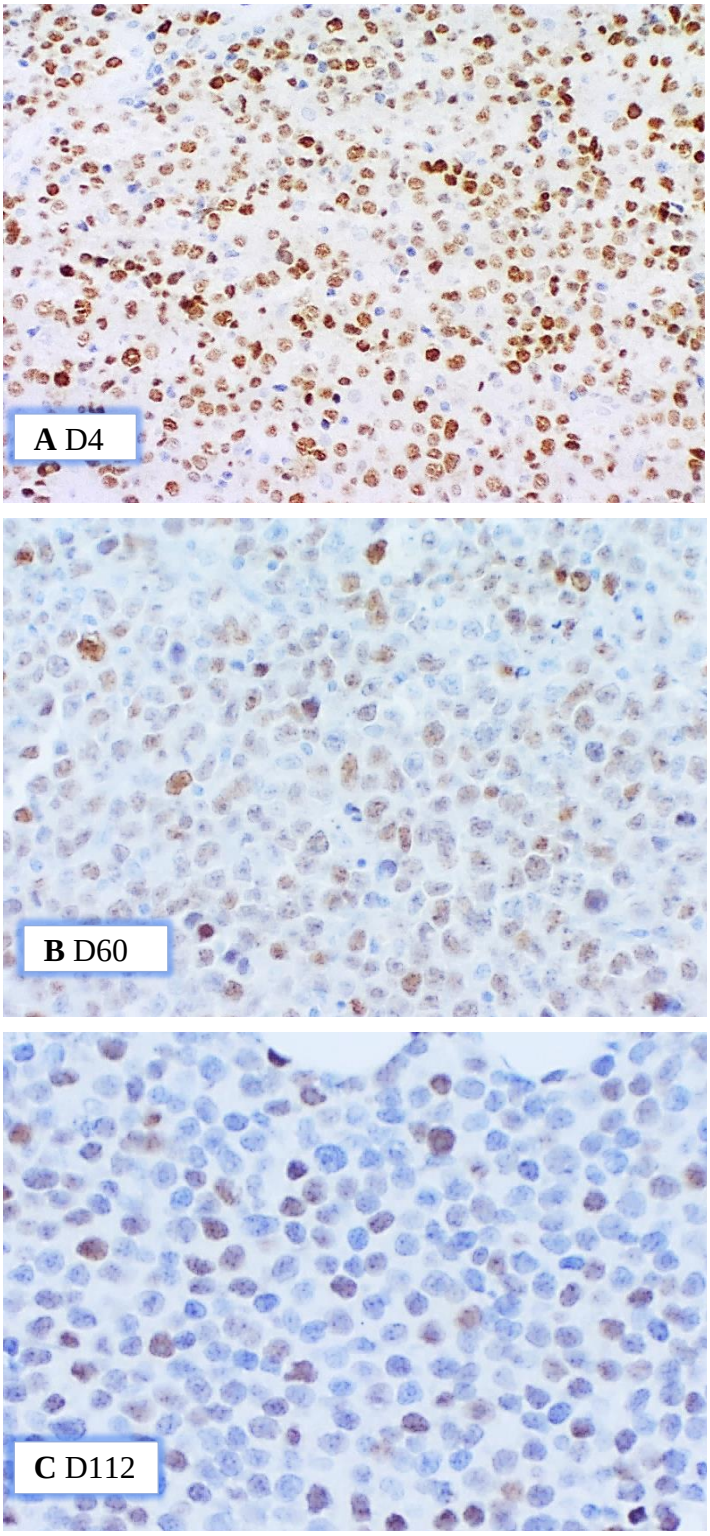


Figure 4.12: Positive nuclear immunoreactivity for c-MYC in DLBCL (D4 and D60 at x200, D112 at x400).

Table 4.9: Immunophenotypic analysis of DLBCL

Immunomarker	**DLBCL**	**HIV+ DLBCL**	**HIV-DLBCL**	***P*-value**
CD20+ +proportion (min-max) average proportion+	99% (122/123) 80-100% 99%	99% (92/93) 80-100% 99%	100% (22/22) 100% 100%	1.00 (Chi-square test)
CD10+ +proportion (min-max) average proportion+	45% (54/121) 30-100% 69%	44% (40/91) 30-100% 68%	46% (10/22) 40-90% 63%	0.83 (Chi-square test)
bcl-6+ +proportion (min-max) average proportion+	82% (98/119) 30-90% 69%	85% (76/89) 30-90% 67%	73% (16/22) 40-90% 76%	0.16 (Chi-square test)
MUM1+ +proportion (min-max) average proportion+	67% (81/121) 30-90% 61%	66% (61/92) 30-90% 59%	71% (15/21) 30-90% 63%	0.65 (Chi-square test)
BCL2+ +proportion (min-max) average proportion+	43% (51/118) 50-100% 75%	41% (36/88) 50-100 73%	59% (13/22) 60-100% 82%	0.13 (Chi-square test)
Ki-67 <90 ≥90%) min-max average proportion+	 20% (25/122) 80% (97/122) 70 - ≥95% 89%	 15% (14/92) 85% (78/92) 70 - ≥95% 90%	 41% 9/22 59% (13/22) 70-95% 86%	**0.01** (Chi-square test)
c-MYC+ +proportion (min-max) average proportion+	55% (64/116) 40-90% 56%	58% (52/89) 40-80% 56%	40% (8/20) 40-70% 54%	0.13 (Chi-square test)

Abbreviations: CD – cluster of differentiation, HIV – human immunodeficiency virus, DLBCL – diffuse large B-cell lymphoma.

HIV+ DLBCLs demonstrated a significant predominance of Ki-67 proliferation indices that were ≥90% as shown in Figure 4:13.

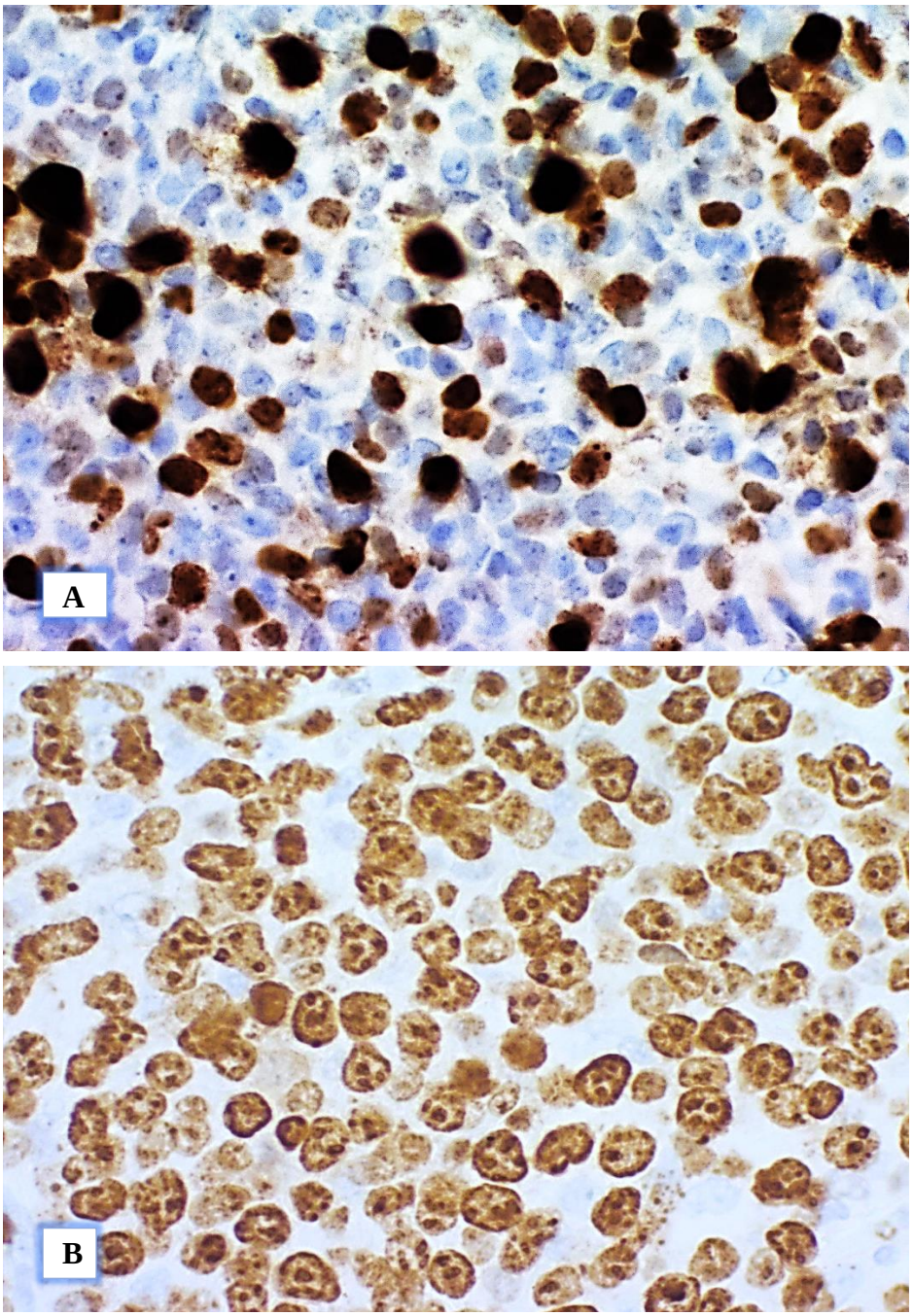


Figure 4.13: Ki-67 immunohistochemistry demonstrating a lower proliferation index in HIV- DLBCL (A) and a higher proliferation index in (B) HIV+ DLBCL (x400 magnification).

Bivariate analysis of c-MYC expression in the HIV+ DLBCL, as shown in Table 4.10, revealed significant associations with a SS appearance (P=0.04) and a Ki-67 proliferation index of ≥90% (P<0.01).

When c-MYC protein was expressed, no significant differences in the median OS were demonstrated in the HIV+ DLBCLs (c-MYC+ 325 days 95% CI 45-605 and c-MYC- 228 days 95% CI 143-313, P=0.86) and the HIV- DLBCLs (c-MYC+ 825 days 95% CI 158-1492 and c-MYC- 750 days 95% CI 150-1000, P=0.81).

HIV+ DLBCLs demonstrated significantly higher proliferation indices in the context of c-MYC protein expression (P<0.01). The median overall survival when Ki-67 ≥90% was 216 days (95% CI 95-337) in the HIV+ DLBCLs and 593 days (95% CI 197-989) in the HIV- DLBCLs (P=0.14, Log rank test).

Table 4.10: c-MYC protein expression in HIV+ and HIV- DLBCL.

c-MYC ≥40% and clinicopathological factors:	HIV+ DLBCL (c-MYC+ n=52)	***P*-value**	HIV- DLBCL (c-MYC+ n=8)	***P*-value**
Age median (yrs.)	43	*P*=0.83 (Mann-Whitney U test)	59	*P*=0.35 (Mann-Whitney U test)
Biopsy topography Nodal Extranodal	 17/52 (33%) 35/52 (67%)	*P*=0.18 (Chi-Square test)	 2/8 (25%) 6/8 (75%)	*P*=1.00 (Fischer's exact test)
SS appearance + **-**	20/26 (77%) 6/26 (23%)	***P*=0.04 (**Chi-Square test)	2/4 (50%) 2/4 (50%)	*P*=0.65 (Fischer's exact test)
Cytomorphology Centroblastic Immunoblastic Anaplastic Mixed	 22/51 (43%) 4/51 (8%) 2/51 (4%) 23/51 (45%)	*P*=0.77 (Chi-square test)	 4/8 (50%) 2/8 (25%) 0 (0%) 2/8 (25%)	*P*=0.89 (Chi-square test)
IHC COO GC NCG	 28/50 (56%) 22/50 (44%)	*P*=1.0 (Chi-Square test)	 4/8 (50%) 4/8 (50%)	*P*=0.38 (Fischer's exact test)
Ki-67 ≥90% <90%	 50/52 (96%) 2/52 (4%)	***P*<0.01** (Fischer's exact test)	 5/8 (63%) 3/8 (38%)	*P*=1.00 (Fischer's exact test)
***MYC* translocation +**	4/19 (21%)	*P*=0.08 (Fischer's exact test)	0/6 (0%)	-
Increased *MYC* copies + **-**	 20/34 (59%) 14/34 (41%)	*P*=0.71 (Chi-square test)	 3/6 (50%) 3/6 (50%)	*P*=1.00 (Fischer's exact test)
***MYC* aberrations +** **-**	23/42 (55%) 19/42 (45%)	*P*=0.13 (Chi-square test)	3/7 (43%) 4/7 (57%)	*P*=1.00 (Fischer's exact test)
IPI 0-2 3-5	 6/30 (20%) 24/30 (80%)	*P*=0.39 (Chi square test)	 0% 5/5 (100%)	-
Stage Early (I-II) Advanced (III-IV)	 3/33 (9%) 30/33 (91%)	*P*=0.66 (Fischer's exact test)	 1/6 (17%) 5/6 (83%)	*P*=1.00 (Fischer's exact test)
Median OS (days) c-MYC+ c-MYC-	325 (95% CI 45-605) 228 (95% CI 143-313)	*P*=0.86 (Log rank test)	825 (95% CI 158-1492) 750 (95% CI 150-1000)	*P*=0.81 (Log rank test)

Abbreviations: DLBCL – diffuse large B-cell lymphoma, COO – cell of origin, GC – germinal centre, NGC – nongerminal centre, IPI – International Prognostic Index, SS – starry-sky, IHC – immunohistochemistry, OS – overall survival.

4.2.11 DLBCL: IHC-defined COO

The cell of origin of DLBCL was based the Hans et al. (2004) defined IHC algorithm. GC and NGC immunophenotypic subtypes were evident in 53% (48 of 90) and 47% (42 of 90) of the HIV+ DLBCLs, respectively. GC and NGC immunophenotypic subtypes accounted for 57% (12 of 21) and 43% (9 of 21) in the HIV- DLBCLs. The HIV status was not significantly associated with the IHC COO (P=0.81). The COO was not significantly associated with the proliferation index (i.e., Ki-67 <90% or ≥90%) in the HIV+ DLBCLs (P=0.77, Chi Square test) and the HIV- DLBCLs (P=0.70, Chi Square test). Although the median OS of the GC subtype was 398 days (95% CI 0-1083) and the median OS of the NGC subtype was 105 days (95% CI 44-166) in the HIV+ DLBCL, this difference was not statistically significant (P=0.10, Log rank test) as shown in Figure 4.14.

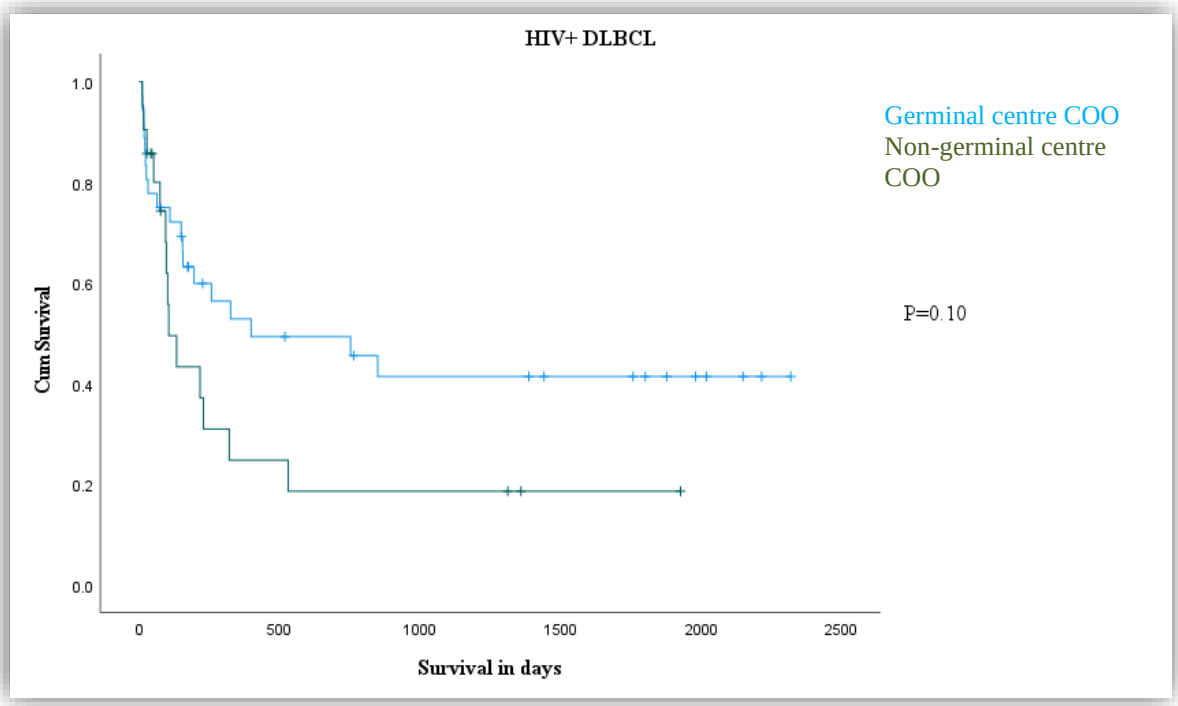


Figure 4.14: Kaplan Meier survival estimates for HIV+ DLBCL by COO.

4.2.12 DLBCL: Double expression of c-MYC and BCL2 proteins

Double expression (DE) of c-MYC (i.e., ≥40%) and BCL2 (i.e., ≥50%) proteins as shown in Figure 4.15 was detected within 25% (21 of 83) of the HIV+ DLBCLs and within 25% (5 of 20) of the HIV- DLBCLs (P=0.91 Chi-Square test) as shown in Table 4.11. *BCL2* and *BCL6* gene rearrangements were not detected in these tumours by utilising FISH.

DE in the HIV+ DLBCLs was significantly associated with NGC COO immunophenotype (15 of 20, 75%, [P<0.01 Chi-Square test]).

DE did not significantly influence the median OS in the HIV+ and HIV- DLBCLs (P=0.56). Although DE demonstrated an increased mortality hazard (HR 9.48, 95% CI 0.23-10.77) in the multivariate regression analysis, this did not approach significance (P=0.24).

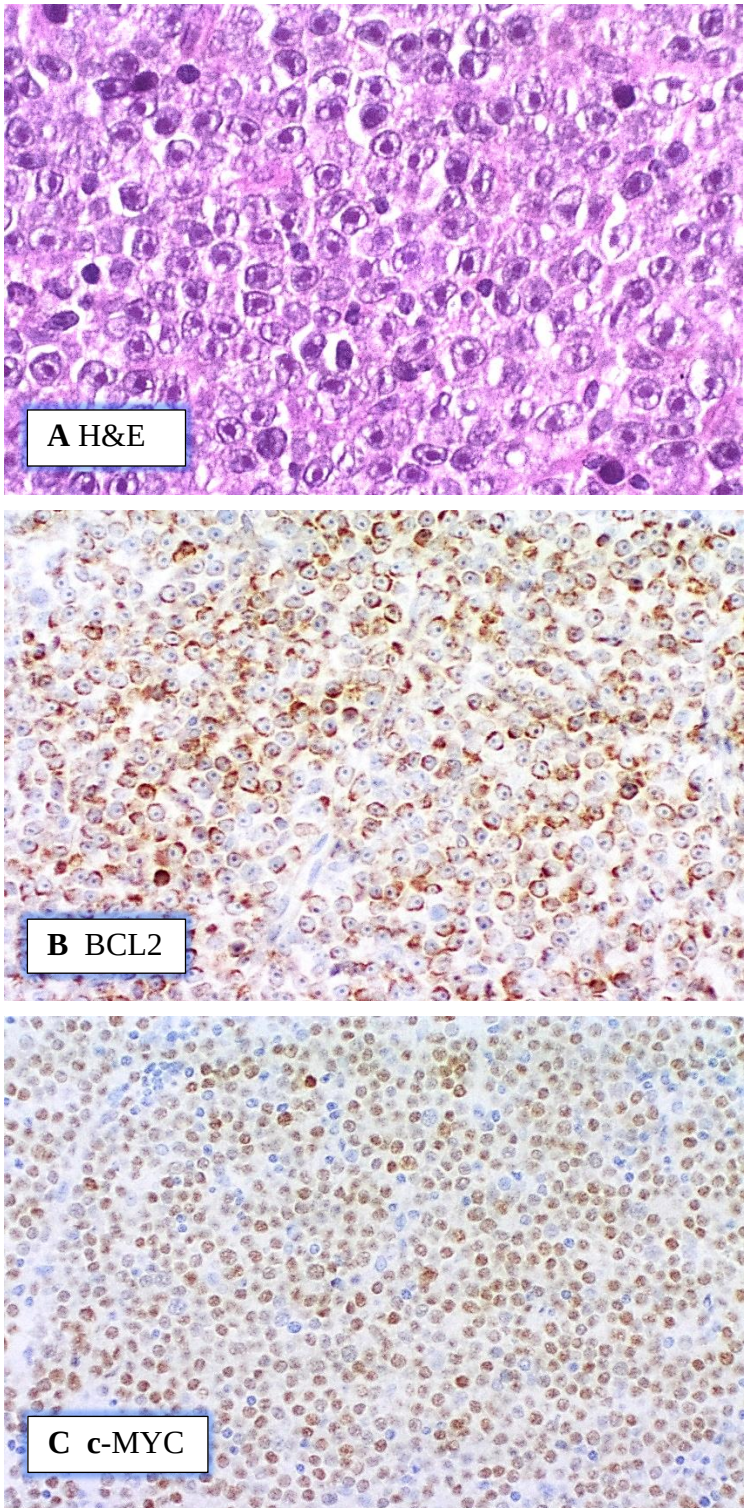


Figure 4.15: Double expression of c-MYC and BCL2 proteins in DLBCL [case D10] (x200 magnification).

Table 4.11: Analysis of c-MYC and BCL2 co-expression in HIV+ and HIV- DLBCL.

Clinicopathologic factors	**HIV+ DE**	**HIV- DE**	***P*-value**
	n= 21/83 (25%)	n=5/20 (25%)	0.98 Chi-Square test
Age in years median (IQR)	39 (12)	48 (29)	0.32 Mann-Whitney U test
Stage I-II III-IV	 2/13 (15%) 11/13 (85%)	 1/5 (20%) 4/5 (80%)	1.00 (Fischer's exact test)
IPI 0-2 3-5	 3/12 (25%) 9/12 (75%)	 0/5 (0%) 5/5/ (100%)	0.52 (Fischer's exact test)
R-IPI 1-2 3-5	 3/12 (25%) 9/12 (75%)	 0/5 (0%) 5/5 (100%)	0.52 (Fischer's exact test)
Topography Nodal Extranodal	 7/21 (33%) 14/21 (67%)	 1/5 (20%) 4/5 (80%)	1.00 (Fischer's exact test)
Starry-sky +	8/21 (38%)	1/5 (20%)	0.63 (Fischer's exact test)
COO GC NGC	 5/20 (25%) 15/20 (75%)	 3/5 (60%) 2/5 (40%)	HIV+ 0.002 (Chi-square test) HIV- 1.00 (Fischer's exact test)
Ki-67 <90% ≥90%	 2/21 (10%) 19/21 (90%)	 2/5 (40%) 3/5 (60%)	0.16 (Fischer's exact test)
MYC rearrangement +	1/3 (33%)	0/3 (0%)	0.36 (Fischer's exact test)
MYC copies increased	9/13 (69%)	1/3 (33%)	0.32 (Fischer's exact test)
MYC aberration +	9/14 (64%)	1/5 (20%)	0.15 (Fischer's exact test)
Mortality	8/16 (50%)	3/5 (60%)	1.00 (Fischer's exact test)
Median OS DE+ DE-	320 days (95% CI 0-783) 257 days (95% CI 0-681)	825 days (95% CI 252-1398) 825 days (95% CI 328-1323)	0.56 (Log rank test) HIV+ 0.93 (Log rank test) HIV- 1.00 (Log rank test)

Abbreviations: COO – cell of origin, GC – germinal centre, NGC – nongerminal centre, IPI – International Prognostic Index, OS – overall survival.

4.2.13 Increased *MYC* copy numbers detected using FISH and CISH

Fifty-one (n=51) DLBCLs, which had sufficient residual tumour cells, were subjected to dual-colour CISH staining for evaluation of *MYC* and CEN8 signals. When dual-colour CISH was assessed and interpreted, the internal positive control cells included squamous epithelium, glandular epithelium, fibroblasts, endothelial cells and non-neoplastic lymphocytes as shown in Figure 4.16.

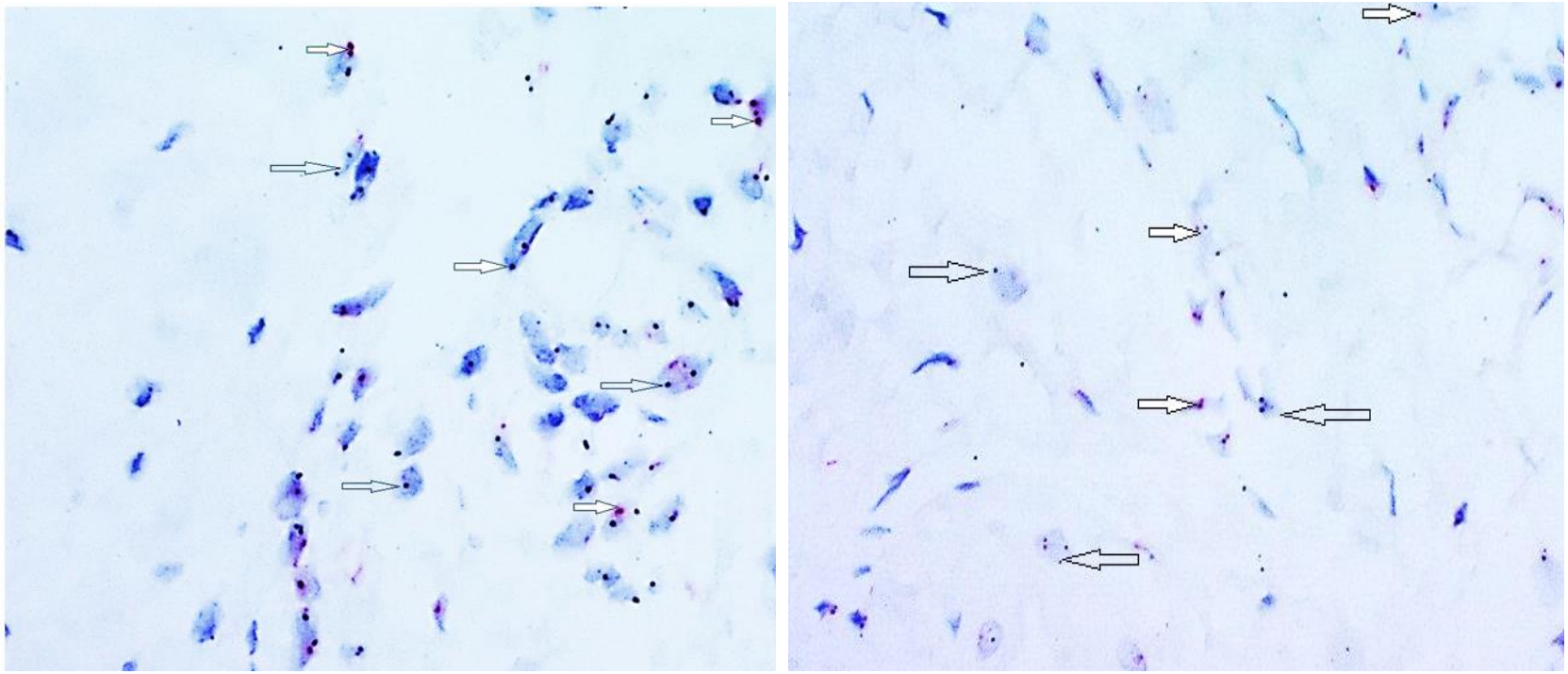


Figure 4.16: Dual-colour CISH demonstrating intranuclear *MYC* signals (black dots and transparent arrows) and CEN8 signals (red dots and white arrows) in the internal control endothelial cells and fibroblasts (x400 magnification).

CISH was successful on 46 tumours. In addition, *MYC* gene copy numbers were also assessed in 4 tumours by utilising FISH at the time of initial diagnosis. The HIV status was seropositive for 42, seronegative for 7 and unknown for 1 case that underwent *MYC* copy number enumeration. Overall, increased *MYC* copy numbers were detected in 28 tumours (56%, 28/50), inclusive of the four cases that were detected using FISH. Low-level increase in *MYC* gene copy numbers (i.e., 2.22-–3.6) occurred in 24 of the HIV+ DLBCLs (57%, 24/42) and 4 of the HIV- DLBCLs (57%, 4/7) as shown in Figure 4.17 and Table 4.12.

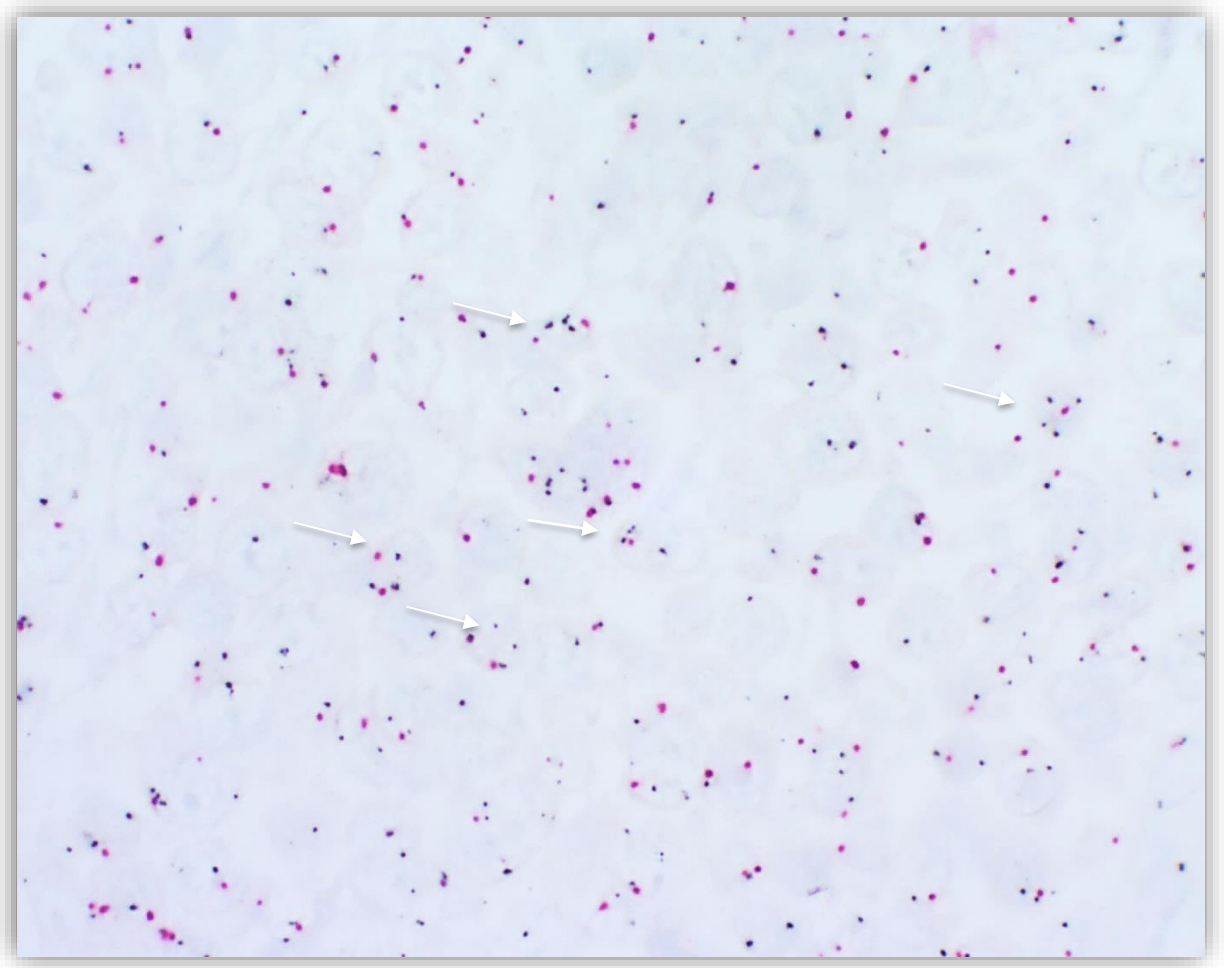


Figure 4.17: Case D60 displaying increased *MYC* gene signals (black dots/white arrows) and not increased CEN8 signals (red dots) [dual-colour CISH at x400 magnification].

Table 4.12: Increased *MYC* gene copy numbers and c-MYC protein expression in DLBCL

No.	DLBCL study no.	Age (yrs) Gender(M/F) Topography (lymph node -LN /extranodal - EN)	*MYC* signals per 50 nuclei; per nucleus of tumour	CEN8 signals per 50 nuclei; per nucleus of tumour	c-MYC IHC (proportion+)
1.	D1	39/M/LN	116; 2.32	89; 1.78	50%
2.	D4[a]	32/F/EN	128; 2.56	89; 1.78	80%
3.	D5	45/F/LN	113; 2.26	100; 2.00	70%
4.	D8[d]	38/F/EN	114; 2.28	92; 1.84	70%
5.	D12	48/F/EN	122; 2.44	99; 1.98	70%
6.	D18	23/F/LN	116; 2.32	94; 1.88	60%
7.	D19	49/F/EN	137; 2.74	95; 1.90	50%
8.	D20	38/F/EN	116; 2.32	94; 1.88	40%
9.	D22	57/M/LN	116; 2.32	72; 1.44	15%
10.	D29	48/M/LN	111; 2.22	94; 1.88	70%
11.	D33	44/M/LN	126; 2.52	92; 1.84	60%
12.	D40	32/M/EN	135; 2.70	94; 1.88	50%
13.	D41	55/F/EN	112; 2.24	96; 1.92	0%
14.	D42	49/M/EN	122; 2.44	93; 1.86	50%
15.	D50[d]	77/M/LN	111; 2.22	103; 2.06	0%
16.	D52[e]	38/F/EN	Clusters	100; 2.00	80%
17.	D60	31/F/LN	155; 3.10	81; 1.62	40%
18.	D61[b]	55/M/EN	150; 3.00	-	30%
19.	D70[e]	37/M/LN	Clusters	103; 2.06	70%
20.	D71[bd]	32/M/EN	150; 3.00	-	40%
21.	D85	43/F/EN	113; 2.26	85; 1.70	80%
22.	D86	45/M/EN	117; 2.34	75; 1.50	40%
23.	D87[c]	46//M/LN	132; 2.64	122; 2.44	50%
24.	D89[b]	47/M/LN	150; 3.00	-	70%
25.	D90	61/F//LN	118; 2.36	91; 1.82	40%
26.	D111[b]	17/M/LN	150; 3.00	-	10%
27.	D112[cd]	48/F/EN	144; 2.88	117; 2.34	50%
28.	D115	28/M/LN	181; 3.62	78; 1.56	50%

Abbreviations: DLBCL – diffuse large B-cell lymphoma, CEN8 – centromere of chromosome 8.

[a]D4 concurrently harboured *MYC* rearrangement and increased *MYC* copy numbers.

[b] Increased copies detected using FISH: 4 DLBCLs.

[c] C8 polysomy: 2 DLBCLs, [d] DLBCL with increased *MYC* gene copies occurred in 4 HIV seronegative patients and [e] *MYC* clusters: 2 DLBCLs.

There were two DLBCLs (HIV+ and HIV-) with C8 polysomy (Figure 4.18).

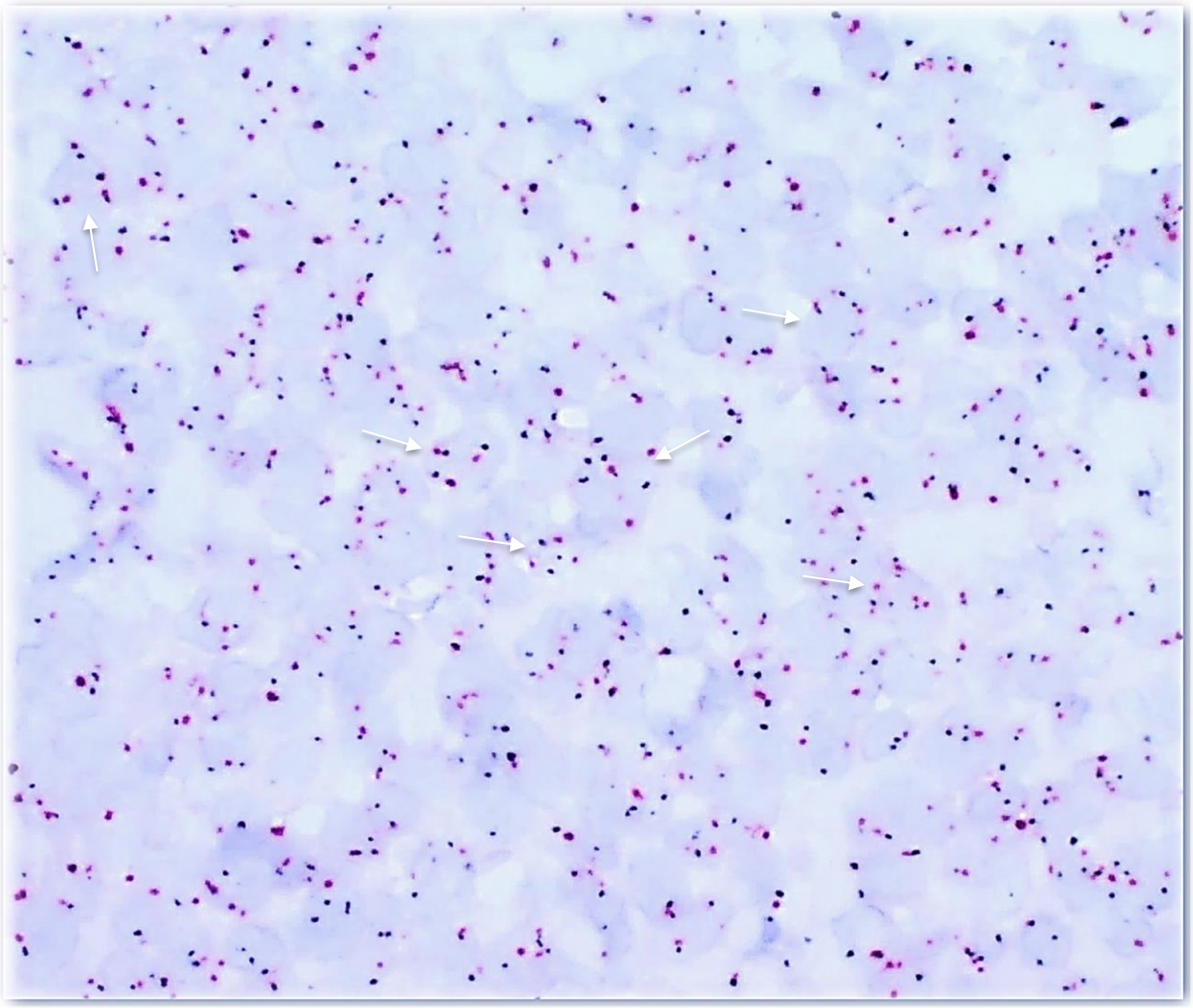


Figure 4.18: Case D112 displaying increased *MYC* gene signals (black dots) and increased CEN8 signals (red dots) denoted by white arrows [dual-colour CISH at x400 magnification].

There were also two cases of HIV+ DLBCLs with *MYC* gene clusters (Figure 4.19).

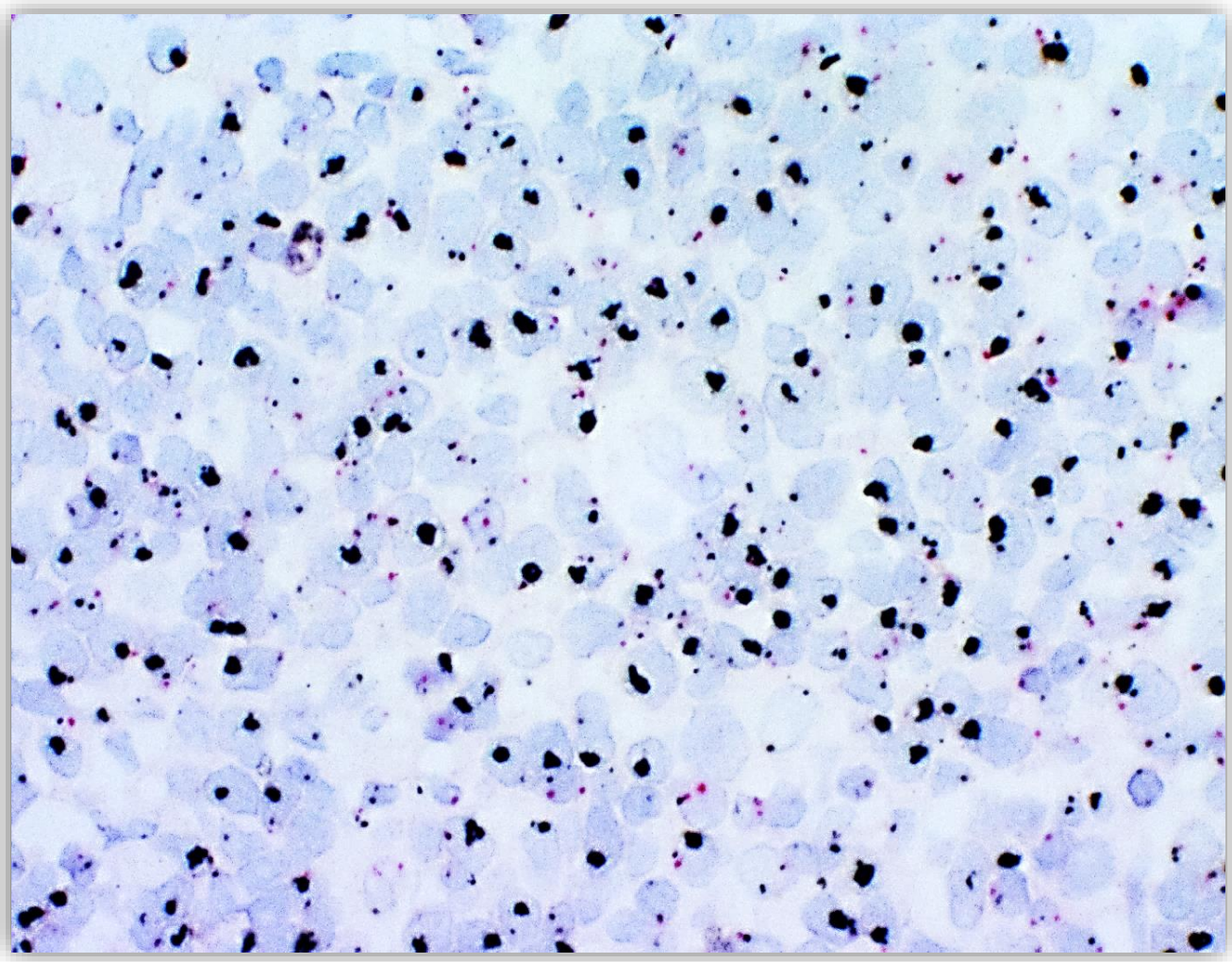


Figure 4.19: *MYC* gene clusters in case D52 (dual-colour CISH at x400 magnification).

CISH was deemed unsuccessful on 5 DLBCLs due to insufficient or absent *MYC* signals in the internal control cells or the tumour cells.

Increased *MYC* copy numbers did not adversely impact the median OS of the HIV seropositive and seronegative groups (Table 4.13). The survival outcome of the patients with *MYC* clusters was not known.

Table 4.13: Bivariate analysis of clinicopathological factors and *MYC* gene copies.

Clinicopathological factors	**Overall DLBCL increased *MYC* gene copies**	**HIV+ DLBCL Increased *MYC* gene copies**	**HIV- DLBCL Increased *MYC* gene copies**	***P*-value**
Increased *MYC* gene copy numbers Minimum Maximum Mean (SD)	n=28/50 (56%) 111 181 129 (18)	n=24/42 (57%) 111 181 129 (18)	n= 4/7 (57%) 111 150 130 (20)	1.00 (Fischer's exact test)
Age (median, IQR) yrs	44 years (16)	44 (16)	43 (36)	0.62 Mann Whitney U test
Gender F/M	F 13/28 (46%) M 15/28 (54%)	F 11/24 (46%) M 13/24 (54%)	F 2/4 (50%) M 2/4 (50%)	1.00 (Fischer's exact test)
IPI 0-2 3-5	 4/18 (22%) 14/18 (78%)	 4/16 (25%) 12/16 (75%)	 0/2 (0%) 2/2 (100%)	1.00 (Fischer's exact test)
Stage I-II III-IV	 1/21 (5%) 20/21 (95%)	 1/17 (6%) 16/17 (94%)	 0/4 (0%) 4/4 (100%)	1.00 (Fischer's exact test)
COO GC NGC	 13/27 (48%) 14/27 (52%)	 11/23 (48%) 12/23 (52%)	 2/4 (50%) 2/4 (50%)	1.00 (Fischer's exact test)
c-MYC ≥40% <40%	 23/28 (82%) 5/28 (18%)	 20/24 (83%) 4/24 (17%)	 3/4 (75%) 1/4 (25%)	1.00 (Fischer's exact test)
DE+ DE-	12/28 (43%) 16/28 (57%)	10/24 (42%) 14/24 (58%)	2/4 (50%) 2/4 (50%)	1.00 (Fischer's exact test)
Ki-67 <90% ≥90%	 4/28 (14%) 24/28 (86%)	 4/24 (17%) 20/24 (83%)	 0/4 (0%) 4/4 (100%)	1.00 (Fischer's exact test)
Median OS Increased *MYC* copies Not increased *MYC* copies	 257 days (95% CI 0-540) 418 days (95% CI 0-914)	 105 days (95% CI 0-391) 752 days (95% CI 0-1635)	 825 (95% 0-914) 134 (95% CI 0-914)	0.50 HIV+ 0.52 HIV- 0.22 (Log rank test)

Abbreviations: DLBCL – diffuse large B-cell lymphoma, COO – cell of origin, GC – germinal centre, NGC – nongerminal centre, IPI – International Prognostic Index, DE – double expression, OS – overall survival.

4.2.14 DLBCL: FISH for *MYC* rearrangement and *MYC* copy numbers

MYC break-apart or t(8;14) FISH was performed on 33 HIV+ DLBCLs and 6 HIV- DLBCLs at the time of the initial diagnosis. *MYC* rearrangement was detected in 12% (4/33) of HIV+ DLBCLs and was not detected in HIV- DLBCLs. *MYC* rearrangement was documented in one HIV+ DLBCL patient (D4) that concurrently demonstrated increased copies of the *MYC* gene. This patient received an intensified BL treatment protocol and survival of 1314 days was documented. *BCL2* and *BCL6* rearrangements were not evident.

4.2.15 DLBCL: *MYC* aberrations

MYC aberrations (rearrangement and/or increased *MYC* copies) were present in 47% (27/57) of the HIV+ DLBCL and 44% (4/9) of the HIV- DLBCLs (P=1.00). Bivariate analysis of clinicopathological factors and *MYC* aberrations is presented in Table 4.14. *MYC* aberrations did not significantly impact the median OS of the HIV+ and HIV- DLBCL patients (P=0.67 and P=0.94, respectively). In the multivariate regression analysis, although *MYC* aberrations demonstrated a hazard ratio of 1.23 (95% CI 0.05-5.67), this was also not statistically significant (p = 0.89).

Table 4.14: *MYC* aberrations in DLBCL.

Clinicopathologic factors	**Overall DLBCL + *MYC* aberrations**	**HIV+ DLBCL + *MYC* aberrations**	**HIV- DLBCL +*MYC* aberrations**	***P*-value**
MYC aberrations +	n=32/70 (46%)	n=27/57 (47%)	n= 4/9 (44%)	1.00 (Fischer's exact test)
Median age in years (IQR)	44 years (13)	44 (13)	43 (36)	0.21 Mann Whitney U test
Gender	F 14/32 (44%) M 18/32 (56%)	F 12/27 (44%) M 15/27 (56%)	F 2/4 (50%) M 2/4 (50%)	1.00 (Fischer's exact test)
IPI 0-2 3-5	 4/20 (20%) 16/20 (80%)	 4/18 (22%) 14/18 (78%)	 0/2 (0%) 2/2 (100%)	1.00 (Fischer's exact test)
Stage I-II III-IV	 1/23 (4%) 22/23 (96%)	 1/19 (5%) 18/19 (95%)	 0/4 (0%) 4/4 (100%)	1.00 (Fischer's exact test)
COO GC NGC	 17/31 (55%) 14/31 (45%)	 14/26 (54%) 12/26 (46%)	 2/4 (50%) 2/4 (50%)	1.00 (Fischer's exact test)
c-MYC ≥40% <40%	 27/32 (84%) 5/32 (16%)	 23/27 (85%) 4/27 (15%)	 3/4 (75%) 1/4 (25%)	0.53 (Fischer's exact test)
DE+ DE-	13/32 (41%) 19/32 (59%)	10/27 (37%) 17/27 (63%)	2/4 (50%) 2/4 (50%)	0.63 (Fischer's exact test)
Ki-67 <90% ≥90%	 5/32 (16%) 27/32 (84%)	 4/27 (15%) 23/27 (85%)	 0/4 (0%) 4/4 (100%)	1.00 (Fischer's exact test)
Median OS *+MYC* *-MYC*	 257 days (95% CI 18-496) 154 days (95% CI 47-261)	 155 days (95% CI 0-356) 154 days (95% CI 53-256)	 825 (95% 0-914) 418 (95% CI 0-873)	0.45 HIV+ 0.67 HIV- 0.94 (Log rank test)

Abbreviations: DLBCL – diffuse large B-cell lymphoma, IPI – International Prognostic Index, COO – cell of origin, GC – germinal centre, NGC – nongerminal centre, DE – double expression, OS – overall survival.

4.2.16 DLBCL: Treatment

During the study period, at the Clinical Haematology Department of CHBAH, DLBCL patients received CHOP, CHOEP, R-CHOP or R-CHOEP regimens with or without methotrexate, bleomycin or radiation. Other salvage regimens including platinum compounds, dexamethasone and cytosine arabinoside were used in refractory patients. Infrequently, the chemotherapy regimen was intensified by using a BL protocol.

In the context of HIV DLBCL, rituximab is not routinely used as the first line therapy because of the potential risk of infection in patients who have very low CD4 counts. If these patients did not respond to CHOP or CHOEP, rituximab was added to their treatment regimen.

Notably, if patients were included in the Non-Hodgkin Lymphoma 001 (SA) study, randomisation would have occurred such that CHOEP or R-CHOEP were administered as first line therapy. c-ARV therapy was commenced in the context of HIV seropositivity prior to or soon after the diagnosis of lymphoma occurred. When CCs were present, medical or surgical treatment occurred accordingly.

A limited number of patients (22 HIV+ and 12 HIV-) received rituximab immunotherapy. Rituximab immunotherapy significantly improved the median OS in the overall HIV+ DLBCL group from 109 days (95% CI 37–181) to 325 days (95% CI 0–673) [p = 0.002, Log rank]. Five HIV+ patients with CD4 counts <100 cells/mm^3, received rituximab and the median OS outcome in this limited subgroup was 530 days (95% CI 0-1110). When this was compared with the median OS [825 days (95% CI 384–1266)] of the 12 HIV- DLBCL patients that received rituximab, a statistically significant difference in the median OS was not demonstrated (p = 0.63 Log rank).

At the Paediatric Oncology Department at CHBAH, the 12-year-old patient in this study received the Berlin Frankfurt Munster (BFM) NHL1995 treatment protocol.

4.2.17 DLBCL: IPI score

IPI scores were available for 48 HIV+ and 7 HIV- patients. There were no significant differences in the distribution of the IPI scores in the HIV+ and HIV- groups (P=1.00). IPI scores of 3-5 were associated with an inferior median OS in the HIV+ DLBCL patients, i.e., 155 days (95% CI 37-273) compared with the median OS of 228 days (95% CI 0-460) which occurred when the IPI scores were 0-2 (P=0.01), as shown in Figure 4.20.

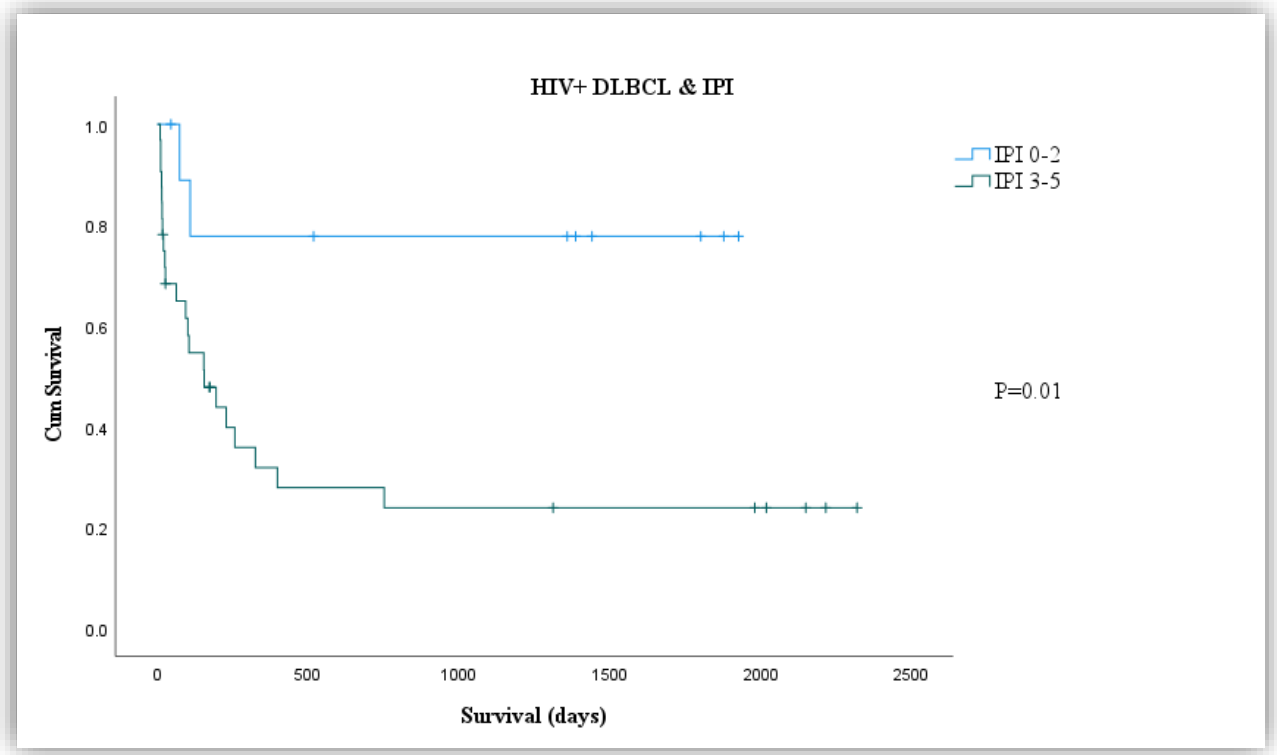


Figure 4.20: Kaplan Meier survival curves depicting HIV+ DLBCL with IPI 0-2 and 3-5.

4.2.18 DLBCL: Survival outcome

Survival outcome data were available for 76 DLBCL patients, who received treatment at the Clinical Haematology Department at CHBAH. The median follow-up time in this study was 1359 days [3.7 years] (95% CI 692-2026 days). The median OS was 228 days (95% CI 54-402) in the HIV+ DLBCL group and 825 days (95% CI 309-1341) in the HIV- DLBCL group (P=0.08) as shown in Figure 4.21.

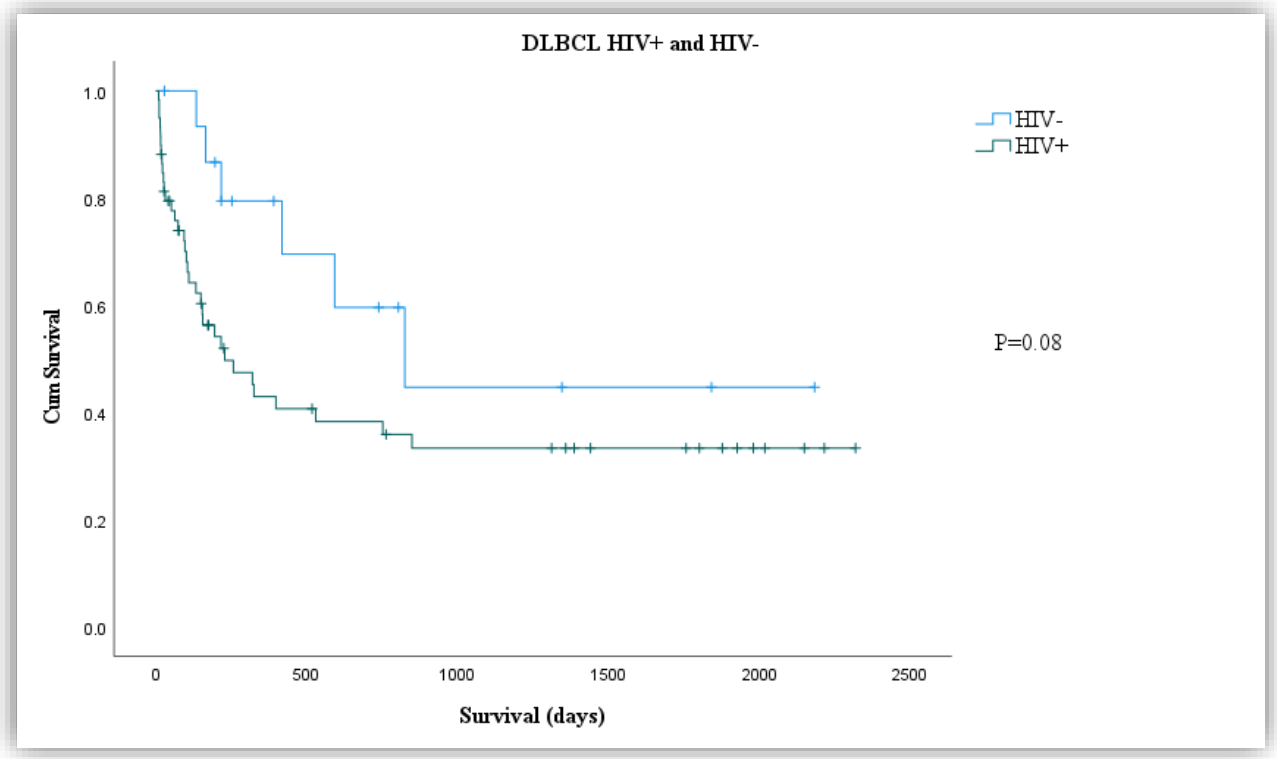


Figure 4.21: Kaplan Meier survival curves depicting HIV+ DLBCL and HIV- DLBCL.

The HIV+ DLBCL subgroup with CD4 counts <100 cells/mm^3 experienced a significantly inferior median OS (149 days [95% CI 44-254]) compared to the HIV- DLBCL group (825 days [95% CI 309-1341]), (p = 0.04) as shown in Figure 4.22.

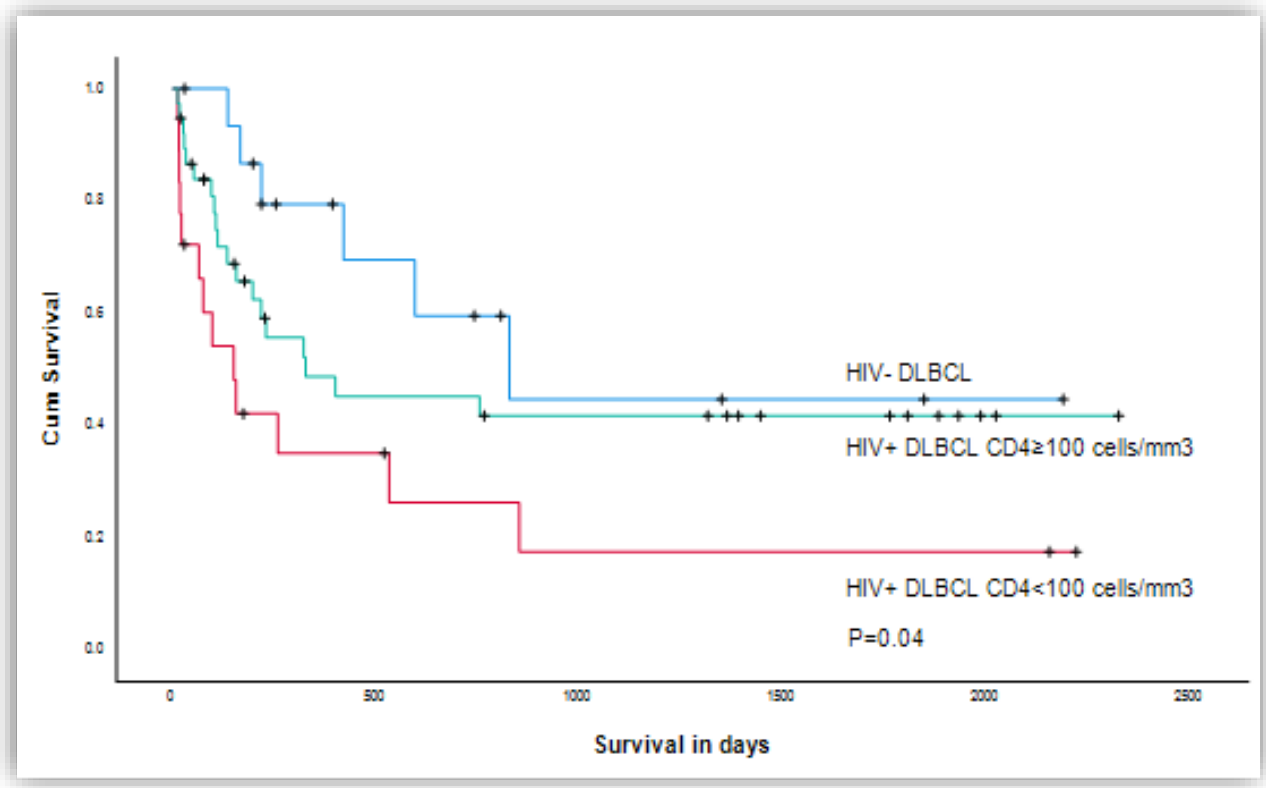


Figure 4.22: Kaplan Meier survival curves of DLBCL by HIV status, CD4 counts <100 cells/mm^3 and CD4 counts ≥100 cells/mm^3.

When CCIs were present, an inferior median OS was demonstrated in the HIV+ DLBCL group [+CCI 154 days (95% CI 85–223 and -CCI 228 days (95% CI 54-402), p =0.01], Figure 4.23.

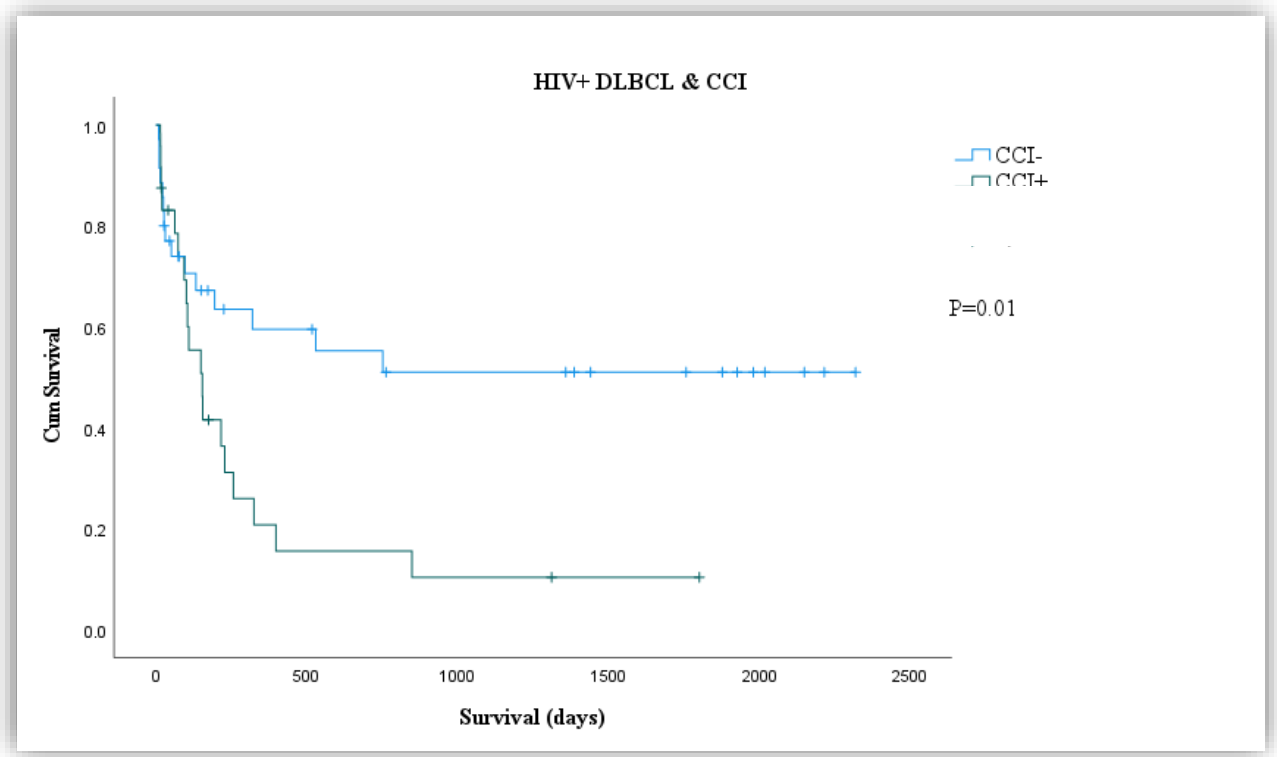


Figure 4.23: Kaplan Meier survival curves of HIV+ DLBCL with and without CCI.

Inferior median OS was also demonstrated in the HIV- DLBCL group when CCIs were present [+CCI 217 days and -CCI 825 days (95% CI 309-1341), P= 0.04].

Median OS analyses of the clinicopathological factors of DLBCL are presented in Table 4.15

Table 4.15: Clinicopathological factors of DLBCL and median overall survival outcome

	HIV+ DLBCL	**HIV- DLBCL**	***P*-value**
Median overall survival (days)	228 (95% CI 54 - 402)	825 (95% CI 309 – 1341)	0.08 (Log rank)
Age			0.80 (Log rank)
<60 years patients	257 days (95% CI 103 – 411)	825 days (95% CI 349 – 1301)	
≥60 years patients	154 (95% CI 0 – 377)	-	
Rituximab therapy			
+	325 days (95% CI 0-673)	825 days (95% CI 384-1266)	**<0.01 (HIV-)** **0.002 (HIV+)**
-	109 days (95% CI 37-181)	165 days (95% CI 115-215)	(Log rank)
Stage			
Early (I-II)	109 days (95% CI 53-165)	593 (95% CI 313-873)	0.96 (Log rank)
Advanced (III-IV)	228 days (95% CI 35-421)	825 (95% CI 0-1972)	
Biopsy topography			0.50 (Log rank)
Nodal	320 days (95% CI 0-868)	165 days (95% CI 84-246)	
Extranodal	216 days (95% CI 91-341)	825 days (95% CI undefined)	
Ki-67			0.14 (Log rank)
≥90%	216 days (95% CI 95-337)	593 days (95% CI 197-989)	
c-MYC			0.86 (Log rank)
<40%	228 days (95% CI 143-313)	-	
≥40%	325 days (95% CI 45-605)	825 days (95% CI 158-1492)	
***MYC* rearrangements**			0.46 (Log rank)
Present	155 days (95% CI undefined)	418 days (95% CI undefined)	
HIV+			0.07 (Log rank)
CD4<100 cells/mm^3	149 days (95% CI 44-254)		
CD4≥100 cells/mm^3	325 days (95% CI 0-981)		

	HIV+ DLBCL	**HIV- DLBCL**	***P*-value**
Rituximab & HIV+ CD4<100 cells/mm^3	530 days (95% CI 0-1110)	**HIV-** 825 days (95% CI 384-1266)	0.63 (Log rank)
HIV+ CD4<100 cells/mm^3 Rituximab+ CCI +	257 days (95% CI 0-764)		0.06 (Log rank)
CD4<100 cells/mm^3 Rituximab+ CCI -	530 days (95% CI 0-764)		
HIV+ **CD4**<150 cells/mm^3	257 days (95% CI 16-498)		0.49 (Log rank)
CD4≥150 cells/mm^3	320 days (95% CI 87-553)		
HIV+ **CD4**<150 cells/mm^3	257 days (95% CI 16-498)	**HIV-** 825 days (95% CI 384-1266)	0.26 (Log rank)
CD4≥150 cells/mm^3	320 days (95% CI 87-553)		
HIV+ **CD4**<200 cells/mm^3	257 days (95% CI 35-479)		0.63 (Log rank)
CD4≥200 cells/mm^3	320 days (95% CI 130-510)		
HIV+ **CD4**<200 cells/mm^3	257 days (95% CI 35-479)	**HIV-** 825 days (95% CI 384-1266)	0.22 (Log rank)
CD4≥200 cells/mm^3	320 days (95% CI 130-510)		

Abbreviations: DLBCL – diffuse large B-cell lymphoma, IHC – immunohistochemistry, IPI – International Prognostic Index, HIV – human immunodeficiency virus, CI – confidence interval.

Multivariate regression analysis demonstrated a significant HR of 4.01 (95% CI 1.86–12.20, *p* =0.02) when CCIs were present. IPI 3-5, *MYC* aberrations and DE in DLBCL demonstrated HR >1, as shown in Table 4.16 which were not statistically significant by multivariate regression analysis. Multivariate regression analysis demonstrated proclivity towards a favourable survival outcome (HR 0.04, 95% CI 0.001–1.66, *p* =0.09) when rituximab immunotherapy was administered.

Table 4.16: Univariate and multivariate Cox regression analysis of selected clinicopathological factors associated with overall survival

	Univariate analysis			**Multivariate analysis**		
Clinicopathological factors	**HR**	**95% CI**	***P* value**	**HR**	**95% CI**	***P* value**
HIV+ CD4<100 cells/mm^3 and HIV- DLBCL	3.08	1.16 – 8.17	0.02	1.96	0.02 – 2.17	0.78
CC Infections	2.93	1.55 – 5.51	<0.001	4.01	1.86 - 12.20	0.02
IPI (3-5)	5.72	1.35 – 24.29	0.02	4.44	0.00 - 5.66	0.99
Rituximab	0.27	0.13 – 0.55	<0.001	0.04	0.00 - 1.66	0.09
DE in DLBCL	1.07	0.53 – 2.19	0.84	9.48	0.23 - 10.77	0.24
MYC aberration	0.84	0.40 – 1.77	0.64	1.23	0.05 – 5.67	0.89

Abbreviations: HIV – human immunodeficiency virus, + - positive, - negative, CC – concomitant conditions, DE – double expression of c-MYC and BCL2 proteins, HR – hazard ratio.

5 CHAPTER FIVE

DISCUSSION

The survival outcome of aggressive B-cell NHL patients is often influenced by a diverse array of clinicopathological factors. Several clinicopathological factors of DLBCL, NOS, HIV-associated DLBCL and HIV-associated PBL were woven into the texture of this thesis and the influence thereof will now be discussed.

5.1 Age and gender

PBL: Age and gender of patients

HIV PBL has a propensity to develop in the 39 to 49 year age group and a male predominance is extensively reported (Castillo et al., 2010b; Morscio et al., 2014; Tchernonog et al., 2017; Rodrigues-Fernandes et al., 2018). Herein, the mean age of the PBL patients was 40 (SD ±10.2) years and there was a relatively equal male to female ratio. The latter aligns with other reports of HIV PBL in southern African countries (Zuze et al., 2018; Meer et al., 2020) regarding a relatively equal gender distribution. This likely reflects the dominant heterosexual mode of transmission of HIV within the southern African region (World Health Organisation, 2012). In contrast, a homosexual male predominance was documented in the sentinel report of PBL by Delecluse et al. (1997) and subsequent reports from the northern regions of the world aligned therewith (Loghavi et al., 2015; Witte et al., 2020).

DLBCL: Age and gender of patients

The age at presentation of DLBCL, NOS is approximately 59 to 70 years (Ott et al., 2010; Gascoyne et al., 2017b) and the median age at which HIV-associated DLBCL occurs is 36 to 41 years (Patel et al., 2015; Machailo, 2016; Cassim et al., 2020). Herein, the HIV seropositive patients were significantly younger, i.e., mean age of 42 (SD ±10.8) years, at presentation with lymphoma than the HIV seronegative patients who demonstrated a mean age of 57 (SD ±16.7) years ($P<0.01$). This finding substantiates that HIV- associated DLBCL tends to manifest 1.5

decades earlier than the HIV seronegative counterpart. A male predominance of 59% and 55% was present in the HIV seronegative and seropositive DLBCL patients, respectively (P=0.72). This gender distribution aligns with the general trend of DLBCL occurring mainly in male patients (Mounier et al., 2006; Ott et al., 2010; Chihara et al., 2015).

5.2 HIV status and severity of immunosuppression depicted by CD4 counts

SA currently has the largest population of people who are living with HIV infection (Human Sciences Research Council 2018). Accordingly, in this study, a predominance of HIV seropositivity and severe immunosuppression were evident among several of the PBL and DLBCL patients.

PBL: HIV status and severity of immunosuppression

In the PBL group, the HIV status was confirmed to be seropositive in 98% of the patients and the median viral load was 55 587 (IQR 273 582) copies/mL. The median CD4 count was 170 (IQR 249) cells/mm^3 and within one to five months of the PBL diagnosis, the CD4 count was <200 cells/mm^3 for 57% and <100 cells/mm^3 for 37% of the PBL patients. This degree of severity of immunosuppression among HIV PBL patients is congruent with that reported by Arora et al. (2019) and Ibrahim et al. (2014). In the current study the PBL patients received c-ART prior to the lymphoma diagnosis or they commenced c-ART shortly after PBL was diagnosed.

DLBCL: HIV status and severity of immunosuppression

A high HIV seropositivity rate of 81% was identified in the DLBCL patients with a median viral load of 217 (IQR 182 981) copies/mL and a median CD4 count of 162 (IQR 215) cells/mm^3. The HIV seropositivity of 81% mirrors that which was documented in a preceding DLBCL study at CHBAH by Machailo (2016) which included 139 patients from 2008 to 2012. Therein the median CD4 count was 144 cells/mm^3. In the current study, the seropositive DLBCL patients received c-ART prior to the lymphoma diagnosis or they commenced c-ART after the lymphoma diagnosis was confirmed. Within 1-18 months of the lymphoma diagnosis, the CD4 counts were <200 cells/mm^3 for 62%, <150 cells/mm^3 for 45% and <100 cells/mm^3 for 33% of the HIV seropositive DLBCL patients. When severe immunosuppression was evident in the HIV seropositive patients, i.e., CD4 counts <100 cells/mm^3, there was a significantly inferior median OS outcome of 149

days (95% CI 44-254) in contrast to the median OS of 825 days (95% CI 309-1341) which occurred in the HIV seronegative group [P=0.04, Log rank test]. When the CD4 count is severely compromised in HIV seropositive patients, restoration to normal values does not occur consistently after ART is implemented. Approximately 33% of patients who receive effective ART may experience persistently low levels of CD4 lymphocytes, despite the presence of virological suppression and long-term duration of therapy (Battegay et al., 2006). Incomplete CD4 recovery may be predicted by the presence of a profoundly low CD4 count (<200 cells/mm^3) at the time of initiating ART (Braitstein et al., 2006; Kelley et al., 2009). This may be a manifestation of HIV-induced exhaustion or destruction of lymphoid tissue (Mauser et al., 2021), loss of regenerative potential in the T-lymphocytic lineage and thymic dysfunction (Moir et al., 2011). Moreover, the cumulative viraemia that occurs during ARV therapy, is proven to be a strong independent risk factor for developing HIV-associated lymphoma (Zoufaly et al., 2009).

International HIV treatment guidelines have evolved to recommend the implementation of c-ART as soon as HIV infection is confirmed, irrespective of the baseline CD4 count (Kitahata et al., 2009; Sterne et al., 2009; World Health Organisation, 2016). In SA, adherence to the global c-ART guidelines has proven to be a strong contributor to the 53% reduction in the incidence of HIV since 2010 (Human Sciences Research Council 2018; UNAIDS, 2021). The positive influence of c-ART is furthermore reflected in this research by the presence of a LDL viral load for 30% of the HIV seropositive DLBCL patients and 15% of the HIV PBL patients. SA has the largest c-ART program worldwide and this country is striving to effectively rollout c-ART to its seropositive patients. The implementation of c-ART has led to a noteworthy reduction in the incidence of HIV-associated NHL in many regions of the world (Besson et al., 2001; Engels et al., 2008; Franceschi et al., 2010; Hleyhel et al., 2013). Accordingly, a decline in the incidence of aggressive HIV-associated B-cell NHL in SA is optimistically anticipated. Notwithstanding that other factors, independent of HIV-related immunosuppression, may also contribute to driving the aetiopathogenesis of NHL in SA.

5.3 Concomitant conditions

CCs included infections, neoplasia and other medical or surgical conditions. Due to the presence of HIV infection, iatrogenic immune suppression from immunotherapy, chemotherapy, radiation

and combinations hereof, concomitant infections (CCI) may develop as complicating factors, amid chronic CCs, in the setting of B-cell NHL (de Witt et al., 2013).

PBL and concomitant conditions

Herein, CCs were evident in 23% of PBL and majority thereof were infections. Although these conditions may have contributed to morbidity and confounded the clinical management of the PBL patients, CCs were not shown to be significantly associated with mortality (P=0.88). Moreover, CCs did not significantly impact the median OS (CCs+ 65 [95% CI 0-134] and CCs- 122 days [95% CI 27-217], P=0.74, Log rank test).

DLBCL and concomitant conditions

CCIs such as sepsis, tuberculosis, hepatitis B infection and herpes viral infections (simplex or cytomegalovirus) occurred predominantly in the HIV seropositive patients and CCIs were not significantly associated with CD4 counts <100 or ≥100 cells/mm^3 (P = 0.61). When CCIs were present, an inferior median OS occurred in the HIV seropositive patients (CCI+ 154 days 95% CI 85-223 versus CCI-228 days (95% CI 54-402, P = 0.01) and CCIs also predicted an inferior OS by multivariate regression analysis (HR 4.01, 95% CI 1.86-12.20, P = 0.02).

The treatment of HIV-associated NHL continues to evolve (Kaplan et al., 2005; Dunleavy and Wilson, 2006; Dunleavy et al., 2010; Dunleavy and Wilson, 2012; Kimani et al., 2021). Only 34 of the DLBCL patients, of which 22 were HIV+ and 5 had CD4 counts <100 cells/mm^3, received immunotherapy due to cost-limiting factors and lack of clarity regarding the role of rituximab in HIV+ DLBCL patients, given the increased risk of infection in patients with low CD4 counts. Rituximab immunotherapy had significantly improved the median OS in the HIV seropositive DLBCL group from 109 days (95% CI 37–181) to 325 days (95% CI 0–673) [P<0.01, Log rank]. Multivariate regression analysis demonstrated proclivity towards a favourable survival outcome (HR 0.04, 95% CI 0.001-–1.66, P=0.09) when rituximab immunotherapy was administered. The impact of rituximab on the survival of HIV seropositive DLBCL patients requires further in-depth evaluation within prospective clinical trials which should include patients with CD4 counts <100 cells/mm^3 who are receiving c-ART.

5.4 IPI score

Since the pentad of factors which constitute the IPI score was published in 1993, this model has proven to be accurate in predicting the long-term survival outcome of patients with aggressive NHLs, in the absence of HIV infection. The sentinel publication demonstrated that high IPI scores were predictive of a three-year overall survival of 59% (International Non-Hodgkin's Lymphoma Prognostic Factors Project, 1993). Twenty-seven years later, studies continue to substantiate the predictive value of the IPI with high scores predicting a five-year overall survival of 54% (Ruppert et al., 2020). In this study, there were no significant differences in the distribution of the IPI scores in the HIV seropositive and HIV seronegative DLBCL groups (P=1.00). Although the predictive value of IPI scores in HIV+ DLBCL is deemed controversial (Kimani et al., 2021; Dunleavy and Wilson, 2012), herein IPI scores of 3-5 demonstrated a significantly inferior median OS, i.e., 155 days (95% CI 37-273) in comparison with the median OS of 228 days (95% CI 0-460) when IPI scores were 0-2 (P=0.01 Log rank test). However, in the multivariate analysis, IPI of 3–5 did not retain significance [HR 4.44, 95% CI 0-–5.66, (P = 0.99)].

5.5 Topographic sites of biopsy

PBL: Topographic sites of biopsy

In the sentinel report of PBL, this tumour was documented within the oral cavity of 16 patients who were predominantly HIV seropositive males (Delecluse et al., 1997). Thereafter, a plethora of publications emerged as this tumour was histopathologically confirmed in various oronasal and extra-oronasal sites (Castillo et al., 2010a; Bibas and Castillo, 2014). Herein, HIV PBL was documented predominantly in extra-oronasal sites (76%) such as the gastrointestinal tract and lymph nodes. Unusual topographic sites of involvement by PBL included the cervicovaginal region of two patients, the breast of four patients and the urinary bladder of one patient.

DLBCL: Topographic sites of biopsy

Based on the topographic origin of the diagnostic biopsy specimen, DLBCL was confirmed predominantly in extranodal regions of the HIV seropositive (62%) and the seronegative (73%) patients. In contrast, Cassim et al. (2020) reported a predominance of nodal primary biopsy sites, while Magangane et al. (2020) reported a fairly even distribution of nodal and extranodal DLBCL

in HIV seropositive and seronegative patients. In the current study, topographic sites of biopsy were not associated with an advanced stage of lymphoma at presentation in the HIV seropositive (P=0.44) and seronegative subgroups (P=0.58). It is noteworthy that an extranodal site of biopsy does not necessarily imply the absence of nodal disease. Rather, it may reflect the high proportion of patients who have extranodal disease, which is amenable to biopsy, based on HIV seropositivity and an advanced stage of disease.

5.6 Starry-sky appearance

A SS appearance is depicted by the presence of several pale-staining tingible body macrophages resembling stars, which are dispersed among sheets of tumour cells which resemble a dark blue night-sky. The SS appearance was classically described in Burkitt lymphoma due to the presence of rapid tumour proliferation and turnover, apoptosis and macrophage phagocytic activity of the cellular debris (Burkitt, 1958; O'Conor and Davies, 1960; Andrade-Filho, 2014). Albeit less frequently, SS also occurs in other aggressive NHLs such as DLBCL and PBL.

SS appearance in PBL

SS was identified within 33% of HIV PBLs and this was significantly associated with monomorphic morphology (P=0.03) and *MYC* aberrations (P=0.01).

SS appearance in DLBCL

SS was identified within 25% of the overall DLBCLs and in 29% of HIV seropositive DLBCLs. In the latter group, SS was significantly associated with c-MYC protein expression of ≥40% (P=0.04).

These forementioned findings are supportive of a SS appearance as a morphological hallmark of an aggressive B-cell NHL which has enhanced proliferative potential, which is most likely due to c-MYC protein expression and/or *MYC* gene aberrations.

5.7 Cytomorphology

Cytomorphology of PBL

PBL may display blastic monomorphic morphology reminiscent of immunoblastic differentiation or it may display more advanced differentiation with plasmacytic cytomorphology. The former was classically described in HIV PBL that occurred in the oronasal regions and the latter in the extra-oronasal regions (Colomo et al., 2004; Campo et al., 2017). In this study, no significant association between PBL morphology and oronasal or extra-oronasal topography was evident (P=0.82). There was a negligible difference in the frequencies of blastic monomorphic morphology (49%) and plasmacytic morphology (51%). Notably however, *MYC* aberrations were significantly associated with blastic morphology of PBL (P=0.02). Hereupon, it appears that blastic morphology may be a morphological clue to the presence of *MYC* aberrations in HIV PBL. This finding has semblance to the significance of immunoblastic morphology in DLBCL which Ott et al. (2010) reported as an adverse prognostic factor in a large prospective trial. Subsequently, it was proposed that the immunoblastic variant may be a morphological clue and reservoir for the presence of *MYC* rearrangement which was demonstrated in 33% of the immunoblastic morphological variant (Horn et al., 2015).

Cytomorphology of DLBCL

HIV seropositive DLBCLs demonstrated mixed morphology (44%) predominantly and the HIV seronegative DLBCLs demonstrated a predominance of centroblastic morphology (55%). Cytomorphology was not significantly associated with the immunophenotypic COO (HIV+ DLBCL P=0.26 and HIV-DLBCL P=0.23). Cytomorphology was also not significantly associated with *MYC* aberrations (HIV+ DLBCLs P=0.68 and HIV- DLBCLs P=0.96) or c-MYC protein expression (HIV+ DLBCLs P=0.77 and HIV- DLBCLs P=0.89). Based on the cytomorphology, the median OS was not significantly different within the HIV seropositive DLBCL group (P=0.52) and the HIV seronegative DLBCL group (P=0.91).

5.8 Immunophenotype

Immunophenotype of PBL

The immunohistochemical profile of PBL is usually characterised by diffuse expression of markers of terminal B-cell differentiation, variable to absent expression of pan B-cell immunomarkers, limited to absent expression of leukocyte common antigen and a very high proliferation index, (Campo et al., 2017; Arora et al., 2019). Aligned herewith, the average expression of CD138, MUM1 and Ki-67 were 74%, 97% and 93%, respectively in PBL. Limited CD20 expression, i.e., 10-30%, was detected in 5% of the overall PBLs herein. c-MYC expression of ≥40% was identified in 81% of PBLs, with a maximum positive expression of 95%. c-MYC expression was significantly associated with extra-oronasal topography (P=0.03) and with blastic monomorphic morphology (P=0.06) in PBL. Chapman et al. (2015) reported that in HIV-associated PBLs and other subtypes, there was a high correlation of *MYC* RNA expression with c-MYC protein expression. In support thereof, the reliability of the 40% cut-off to denote positive expression in the current study was supported by a significant association of c-MYC protein expression with the presence of *MYC* aberrations, i.e., increased *MYC* gene copy numbers and/or *MYC* rearrangement (P=0.01). However, c-MYC expression in HIV PBL did not significantly influence the median OS [c-MYC+ 121 days (95% CI 0-360 days) and c-MYC- 153 days (95% CI 77-229 days), Log rank test (P=0.89)].

Immunophenotype of DLBCL

The immunohistochemical profile of DLBCL is characterised by diffuse expression of the pan-B-cell markers such as CD20, CD79a, PAX5, CD19 and/or CD22 (Gascoyne et al., 2017b). When CD20 immunoexpression is lacking from a DLBCL that displays immunoblastic or anaplastic features, the diagnostic confirmation thereof becomes challenging and costly. In such a context, two or more pan-B-cell markers, LCA and *in situ* hybridisation investigations may be required to reliably differentiate DLBCL, PBL and myeloma with plasmablastic features. Herein, diffuse CD20 expression was confirmed in 99% of the DLBCLs. A case of HIV+ DLBCL demonstrated limited expression of CD20 (i.e., 20%), coupled with diffuse expression of CD79a and PAX5. The IHC-defined COO distribution, according to the Hans algorithm, was similar in the HIV+ DLBCLs (GC 53%, NGC 47%) and the HIV- DLBCLs (GC 57%, NGC 43%), [P=0.81]. Significant differences were not evident in the distribution of the COO, when *MYC* aberrations were present

in the HIV+ and HIV- DLBCLs (P=0.32 and P=0.52, respectively). Moreover, the IHC-defined COO did not significantly influence the survival outcome of the HIV seropositive and seronegative patients (P=0.21 and P=0.08, respectively). The similarity in the COO distribution and the lack influence thereof on the survival outcome aligns with the findings of Chadburn et al. (2009); Pather et al. (2013b); Cassim et al. (2020).

Expression of c-MYC protein tends to correlate with cellular proliferation, as an immediate early response to mitogenic influences. By virtue of its ability to activate transcription, a gain of c-MYC function is associated with enhanced cell growth and proliferation (Kato et al., 1990; Eilers et al., 1991; Dang, 1999a; Dang, 2013). c-MYC protein expression occurs in 13-64% of DLBCL. In HIV+ DLBCLs c-MYC expression occurs more frequently than in HIV- DLBCL and is associated with increased mortality (Chao et al., 2015). In tandem herewith, in this study expression of c-MYC protein (i.e., ≥40%) was detected in 58% of the HIV+ DLBCLs and in 40% of the HIV- DLBCLs (P=0.13). In the HIV+ DLBCLs, positive c-MYC expression was significantly associated with a SS appearance (P=0.04) and Ki-67 proliferation indices ≥90% (P<0.01). Collectively, these findings substantiate the influential role of c-MYC protein on the proliferative potential of HIV-associated DLBCL. Notably however, c-MYC protein expression did not significantly influence the median OS outcome in the HIV seropositive group (P=0.86) and the HIV seronegative group of DLBCL (P=0.81).

Ki-67 proliferation indices

The proliferation index of an aggressive B-cell NHL is usually assessed by utilising Ki-67 IHC. The proliferation index often exceeds 70% (Broyde et al., 2009), particularly in the context of HIV infection (Grogan et al., 1988; Said et al., 2017). Herein, the average Ki-67 expression in HIV PBL was 93% with minimum and maximum values of 80% and 95%, respectively. The proliferation index of HIV PBL was not significantly associated with c-MYC protein expression (P=0.57), *MYC* translocation (P=0.19), increased *MYC* copy numbers (P=0.79) and *MYC* aberrations (P=1.00). The proliferation index also did not significantly influence the median OS of HIV PBL (P=0.88).

The HIV+ DLBCLs demonstrated significantly higher proliferation indices (i.e., Ki-67 ≥ 90%) than the HIV- DLBCLs (P=0.01). Notably, the significantly higher proliferation indices occurred in tandem with c-MYC protein expression in the HIV+ DLBCLs (P<0.01). However, Ki-67 ≥90%

did not significantly influence the median overall survival when the HIV+ DLBCLs [216 days (95% CI 95-337)] were compared with the HIV- DLBCLs [593 days (95% CI 197-989)], (*P*=0.14).

5.9 Double expression (DE) of c-MYC and BCL2 in DLBCL

The presence of DE is confirmed by c-MYC and BCL2 protein co-expression of ≥40% and ≥50%, respectively (Johnson et al., 2012; Horn et al., 2013; Perry et al., 2014; Wang et al., 2015; Rosenwald et al., 2019). Ten to 40% of de novo DLBCLs may demonstrate co-expression of c-MYC and BCL2 proteins, in the absence of *MYC* and *BCL2* gene translocations, hereby constituting DE tumours (Wang et al., 2015; Herrera et al., 2017; Rosenwald et al., 2019). Herein, DE was evident in 25% of the HIV+ DLBCLs and 25% of the HIV- DLBCLs (*P*=0.98). DE has a propensity to occur in the ABC subtype of DLBCL and is associated with an inferior survival outcome (Johnson et al., 2012; Hu et al., 2013; Jesionek-Kupnicka et al., 2019). Attuned herewith, DE in HIV+ DLBCL was significantly associated with the NGC COO immunophenotype (*P*=0.002). However, an adverse impact on the median OS was not demonstrated [*P*=0.84]. Although, DE demonstrated an increased mortality hazard (HR 9.48, 95% CI 0.23-10.77) in the multivariate analysis, this did not approach significance (*P*=0.24).

5.10 *MYC* rearrangement

MYC rearrangement in PBL

MYC rearrangements are identified in approximately 50% of PBL, most often with an *IgH* partner in association with a complex karyotype. *MYC* translocation tends to occur more frequently in HIV PBL and EBV-positive tumours (Dawson et al., 2007; Valera et al., 2010; Laurent et al., 2016; Miao et al., 2020). Herein, *MYC* rearrangement was identified in 70% of the HIV PBLs. It is noteworthy that 49% of these tumours harboured concurrent *MYC* rearrangement and increased *MYC* gene copy numbers. *MYC* rearrangement was not significantly associated with mortality (*P*=0.47) and *MYC* rearrangement did not exert a negative influence on the survival outcome (*P*=0.91).

MYC rearrangement in DLBCL

Approximately 4-16% of DLBCL may harbour *MYC* translocations (Yoon et al., 2008; Savage et al., 2009; Aukema et al., 2011) and *MYC* translocations may occur as a secondary event in DLBCL, in the setting of complex karyotypic aberrations (Nguyen et al., 2017). In support thereof, *MYC* rearrangement was detected in 12% of the HIV+ DLBCLs and was not detected in the HIV- DLBCLs. *MYC* translocations are frequently documented along with a GC COO subtype (Klapper et al., 2008; Yoon et al., 2008; Horn et al., 2013; Visco et al., 2013; Copie-Bergman et al., 2015; Rosenwald et al., 2019). However, herein *MYC* rearrangement was not significantly associated with the IHC COO in the HIV+ DLBCLs (P=0.97). *MYC* translocations tend to correlate with advancing age of patients, high-grade phenotype, progression of the lymphoma, poor response to CHOP/R-CHOP treatment regimens and an inferior overall survival (Yano et al., 1992; Akasaka et al., 2000; Yoon et al., 2008; Boerma et al., 2009; Barrans et al., 2010; Savage et al., 2009; Horn et al., 2013; Copie-Bergman et al., 2015). This study did not substantiate the negative influence of *MYC* rearrangement on the median OS of the HIV seropositive DLBCL patients [+*MYC* rearranged 155 days (95% CI 88-222) and -*MYC* 154 days (95% CI 34-274)], (P=0.30).

5.11 *MYC* gene copy number increases

The evaluation of *MYC* gene copy numbers may occur by FISH analysis, dual-colour CISH or comparative genomic hybridisation techniques.

MYC gene copy number increases in PBL

MYC gene copy numbers are rarely explored in HIV PBL (Ramburan et al., 2022) and gains of the *MYC* gene are reported infrequently in a PBL which harbours *MYC* translocation (Valera et al., 2010; Montes-Moreno et al., 2017; Miao et al., 2020; Witte et al., 2020). Herein, by utilising FISH and dual-colour CISH on FFPE tissue, increased *MYC* gene copy numbers were detected in 43% of HIV PBL and 6% demonstrated C8 polysomy. In the HIV PBL, the minimum, maximum and mean *MYC* gene copy number increases were 112, 173 and 132 per 50 tumour cells, respectively. Increased *MYC* gene copy numbers were not significantly associated with SS appearance, tumour morphology, positive EBV ISH status, c-MYC IHC positivity, Ki-67 ≥90%, stage, mortality or the median overall survival. Notably, 16 (of 33, 49%) HIV PBLs concurrently harboured *MYC*

rearrangement and increased *MYC* gene copies. The tumours that displayed *MYC* copy increases and/or *MYC* rearrangement were subsequently grouped as *MYC* aberrations and the clinicopathological significance thereof is further elaborated on in the subsection 5.13.

MYC gene copy number increases in DLBCL

Predominantly by utilising FISH or dual-colour CISH techniques, increased copies of the *MYC* gene have been demonstrated in 3-83% of DLBCLs (Yoon et al., 2008; Stasik et al., 2010; Testoni et al., 2011; Kluk et al., 2012; Valentino et al., 2013; Tzankov et al., 2014; Wang et al., 2015). *MYC* copy number aberrations, i.e., gains (3-4 copies) or amplification (≥5 copies), in DLBCL confer an inferior median OS and an inferior progression free survival (Yoon et al., 2008; Lu et al., 2015). Valentino et al. (2013) demonstrated that increased *MYC* gene copy number in DLBCLs correlated with c-MYC protein expression, which correlated with mRNA and poor outcome. While *MYC* amplification is documented infrequently in DLBCLs, low-level gains tend to occur frequently (Wang et al., 2015) and may result in higher levels of mRNA (Stasik et al., 2010). While *MYC* amplification tends to negatively impact the survival outcome, it is questionable whether *MYC* gains in DLBCL exert a negative impact on the overall survival (Valentino et al., 2013; Ott et al., 2013). Herein, low-level increases in *MYC* gene copy numbers (i.e., 2.22-–3.6 per tumour nucleus) occurred in 57% of the HIV+ DLBCLs. Although the median OS was shorter when increased *MYC* copy numbers were present (105 days, 95% CI 0-39) in the HIV+ DLBCL group, a statistically significant difference was not evident (P=0.52) when compared with the median OS when *MYC* copy numbers were not increased (752 days, 95% CI 0-1635). Approximately 2-15% of DLBCLs may concurrently harbour *MYC* translocation and *MYC* copy number aberrations (Stasik et al., 2010; Valentino et al., 2013; Lu et al., 2015). Herein only one HIV+ DLBCL, in a 31-year-old female, concurrently harboured *MYC* rearrangement and increased *MYC* gene copy numbers, with c-MYC immunoexpression of 80%. This patient received an intensified BL treatment protocol and survival of 1314 days was documented.

5.12 Dual-colour CISH on FFPE specimens

In this project, optimisation of the dual-staining CISH protocol was challenging. While red signals of CEN8 were consistently discernible, the delicate silver signals were not discernible during the initial phases of the optimisation process. Following several local troubleshooting attempts and international intervention by the supplier, an optimised automated staining procedure was subsequently achieved and implemented.

By mapping the regions of highest c-MYC IHC expression, targeted areas of the tumours were selected for *MYC* gene signal enumeration. When IHC was negative, random fields were selected for CISH signal enumeration. Consistency in the method of signal enumeration was implemented by using the diagrammatic visual approach for each HPF of tumour and the CISH interpretation tool (Appendix V). The interpretation of the dual-colour CISH sections was significantly influenced by the thickness of the tissue sections and optimal bluing of nuclei during the staining procedure. When the sections were reasonably thin, i.e. 2µm, minimal nuclear overlapping occurred. When thin sections were present in unison with clearly visible light blue nuclear contours, interpretation and enumeration of the signals proceeded well. The CISH sections were interpretable by using conventional light microscopy and the signals were enumerated at a magnification of x400. Several months after CISH staining occurred, the signals had not faded within the tissue sections. Storage of the stained sections occurred away from direct sunlight. Unsuccessful dual-colour CISH was mainly due to technical challenges encountered with the autostainer instrument or limited residual tumour cells in the tissue sections.

5.13 *MYC* aberrations in DLBCL and PBL

MYC aberrations in PBL

MYC aberrations, which are reported in 57-100% of HIV PBL, comprise *MYC* rearrangements predominantly with infrequent reports of *MYC* copy number alterations (Taddesse-Heath et al., 2010; Boy et al., 2011; Morscio et al., 2014; Loghavi et al., 2015; Meer et al., 2020; Ramburan et al., 2022). In the current study, *MYC* aberrations in HIV PBL included *MYC* rearrangement (70%), low-level *MYC* gene copy number increases (43%) with low-level chromosome 8 polysomy (6%) and concurrent *MYC* rearrangement with increased *MYC* gene copy numbers (49%). *MYC*

aberrations in HIV PBLs were significantly associated with SS appearance (P=0.01), monomorphic morphology (P=0.03), c-MYC protein expression of ≥40% (P=0.03) and mortality (P=0.03). Collectively, these clinicopathological characteristics are supportive of the influential role that *MYC* exerts in the pathogenesis of HIV PBL.

MYC aberrations in DLBCL

MYC aberrations in HIV+ DLBCL are associated with less favourable survival outcome (Ramos et al., 2020). In the current study, the spectrum of *MYC* aberrations included *MYC* rearrangement, increased *MYC* gene copy numbers, inclusive of *MYC* gene clusters, C8 polysomy and concurrent rearrangement with increased *MYC* copies. *MYC* aberrations were identified in 47% of the HIV+ DLBCLs and 44% of the HIV- DLBCLs (P= 1.00). However, *MYC* aberrations did not significantly impact the median OS of the HIV seropositive and HIV seronegative DLBCL patients (P=0.67 and P=0.94, respectively). In the multivariate analysis, although *MYC* aberrations demonstrated a hazard ratio of 1.23 (95% CI 0.05-5.67), this was also not significant (P= 0.89).

5.14 Stage of lymphoma

The Ann Arbor staging classification, and the Cotswold modification, are the platforms from which the stage of lymphoma is gauged. These are the globally adopted method for the anatomic staging of NHL (Carbone et al., 1971; Lister et al., 1989; Armitage, 2005). HIV-associated NHLs have a strong tendency towards an advanced stage, i.e., III to IV, at presentation (Patel, 2007; Lu et al., 2014; Patel et al., 2015; Chen et al., 2019).

PBL stage at presentation

In this study, 77% of the PBL patients presented with an advanced stage of III or IV. This aligns with the global trend regarding the propensity of HIV PBL patients to present with advanced stage of disease (Bibas and Castillo, 2014; Arora et al., 2019).

DLBCL stage at presentation

An advanced stage of lymphoma, i.e., III or IV, at presentation occurred predominantly in the HIV+ DLBCL patients (87%), compared with the HIV- patients (64%, P=0.04). However, in the HIV+ group, there was no significant difference in the median OS when advanced-stage was

compared with early-stage disease [(stage III-IV 228 days 95% CI 35-421 versus stage I-II 109 days 95% CI 53-165, respectively), P=0.95 Log rank test). Moreover, advanced stage of DLBCL at presentation was not significantly associated with the severity of immunosuppression [(CD4 counts <100 cells/mm^3 or ≥ 100 cells/mm^3) P=0.40]. When advanced stage occurred in HIV+ DLBCL, there was also no significant difference in the median OS when the CD4 counts were <100 cells/mm^3 or ≥100 cells/mm^3 (P=0.91, Log rank test). The stage was not significantly associated with the topographic site of the biopsy specimen (P=0.38)

5.15 Survival outcome

Survival outcome with PBL

The median OS for HIV PBL was 75 days [95% confidence interval (CI) 14-136 days]. No significant difference was demonstrated in the median OS regarding HIV PBL with *MYC* aberrations [65 days (95% CI 0-143 days)] and HIV PBL without *MYC* aberrations [71 days (95% CI 11-131 days)] (Log rank test P=0.61).

The HIV seronegative PBL patient was an immunocompetent 24-year-old male who presented with a nasal-based tumour. The tumour demonstrated mixed blastic and plasmacytic morphology with c-MYC protein expression of 60%, positive EBER ISH status, and increased *MYC* gene copy numbers i.e. 181 per 50 nuclei, without *MYC* rearrangement. This patient had stage IV lymphoma, without bone marrow involvement. This patient received CHOEP and further second line chemotherapy. Death ensued 695 days after the PBL diagnosis was confirmed, due to disease progression.

Survival outcome with DLBCL

In the developing regions of the world, the survival outcome of HIV+ DLBCL is progressively evolving. Reports from the southern regions of Africa have attested that when ART and CHOP treatment regimens are used for HIV-DLBCL, the overall survival outcome might not be influenced by HIV infection. Moreover, the survival outcome might be similar to that achieved in the USA and Europe (de Witt et al., 2013; Painschab et al., 2019). It is further suggested that HIV DLBCL may be associated with longer or similar disease-free survival (Baptista et al., 2015) to that of HIV negative DLBCL and possibly an excellent overall survival (Coutinho et al.,

2014). Herein, when the CD4 counts were <100 cells/mm^3 the HIV seropositive patients experienced a significantly inferior median OS outcome of 149 days (95% CI 44-254), compared with the median OS of 825 days (95% CI 309-1341) of the HIV seronegative patients (P=0.04). An inferior median OS was also demonstrated in the HIV+ DLBCL group when the IPI scores were 3-–5 [155 days (95% CI 37-–273)] compared with 228 days (95% CI 0-460) when IPI scores were 1-2 (P =0.01). When CCIs were present, an inferior median OS occurred in the HIV seropositive patients (154 days 95% CI 85-223, P=0.01) and the HIV seronegative patients (217 days, 95% CI 200-1341, P=0.01). CCIs furthermore predicted a significantly inferior overall survival outcome in the multivariate regression analysis (HR 4.01, 95% CI 1.86 -12.20, P=0.02).

5.16 DLBCL in a paediatric patient

Rarely, DLBCL may occur in paediatric patients and it tends to display a germinal centre immunophenotype in this age group (Oschlies et al., 2006). Herein, DLBCL was confirmed within skeletal muscle of the diaphragm of a 12-year-old male patient, who was HIV seropositive. The tumour demonstrated diffuse CD20 expression, centroblastic morphology and a germinal centre immunophenotype. The Ki-67 proliferation index exceeded 90% and c-MYC protein expression was 40%. The tumour lacked *MYC* rearrangement and was negative for translocation t(8;14). Dual-colour CISH demonstrated 103 *MYC* gene signals and 84 CEN8 signals per 50 tumour cells. There was stage III disease at the presentation of the lymphoma and the patient received the BFM NHL 1995 treatment protocol. Unfortunately, death ensued 22 days after the lymphoma was confirmed.

5.17 Latent EBV infection in PBL

The hallmarks of EBV infection include B-lymphocytic tropism, latent infection and B-lymphocytic transforming capacity (Ok et al., 2015). Lifelong EBV latent infection is linked to this virus' unique interaction with resting memory B-lymphocytes which serve as a viral reservoir (Babcock et al., 1998; Linke-Serinsoz et al., 2017). By utilising EBER ISH, latent infection has been detected in 70-93% of HIV PBL (Loghavi et al., 2015; Tchernonog et al., 2017; Meer et al., 2020). Recently, (Ramburan et al., 2022) demonstrated EBV latency 0 in 73% of PBLs. Therefore,

the presence of EBER positivity may be considered a defining feature of HIV PBL. Herein, EBV latent infection was detected in 90% of the HIV PBLs and there were diffuse intranuclear EBER ISH signals within the tumour cells. In HIV PBL, latent EBV infection often occurs in association with *MYC* rearrangement (Castillo and Reagan, 2011a; Laurent et al., 2016; Ramburan et al., 2022). It is likely that within *MYC*-rearranged EBV-positive PBL, oncogenic *MYC* prevents cellular apoptosis while plasmablastic differentiation of B-cells is driven by EBV (Castillo et al., 2015). In the current study, 67% of HIV PBL were EBER ISH positive and *MYC* rearranged, 41% were EBER ISH positive with increased *MYC* copies, 52% were EBER ISH positive with *MYC* aberrations and 73% demonstrated dual positivity for EBER ISH and c-MYC protein expression. The positive EBER ISH status in did not significantly influence mortality ($P=0.66$) and the median OS ($P=0.63$).

5.18 Limitations of this study

- The delayed presentation of patients to healthcare facilities or the lack of timeous referral of the patients may have contributed to the advanced stage of lymphoma at presentation.
- Due to the retrospective nature of this study, clinical data were not available for all the patients. This was likely due to the loss of follow up or the demise of patients prior to their referral to the Clinical Haematology Department at CHBAH.
- During the study timeframe, there was variation in the treatment regimens for PBL and DLBCL. Only a limited number of patients received rituximab immunotherapy.
- Non-compliance on c-ART and other therapeutic agents may have been limiting factors.
- There were limited numbers of HIV seronegative DLBCL patients in this study.
- During the study timeframe, FISH for *MYC* rearrangement was not routinely performed on all the DLBCLs.
- Due to technical challenges with the autostainer instrument and the presence of limited residual tumour within tissue blocks after c-MYC IHC occurred, it was not possible to conduct CISH on all the tumours in this study.

- Cyclin D1 and CD5 IHC, for pleomorphic mantle cell lymphoma, were not performed routinely during the diagnostic confirmation of all the DLBCLs in this study.

6 CHAPTER SIX

CONCLUSION

Herein, an in-depth exploration was conducted of the clinicopathological features of PBL and DLBCL patients at the largest hospital in Africa. HIV-associated PBL demonstrated a mean age of 41 (SD ±10.1) years with a 54% female predominance. Advanced stage of disease, i.e., stage III-IV occurred in 77% of the patients and extra-oronasal topographic involvement predominated. Expression of c-MYC protein (≥40%) occurred in 81% and latent EBV infection was detected in 90% of these tumours. *MYC* gene aberrations included *MYC* rearrangement (70%), low-level increase in *MYC* gene copy numbers (43%), concurrent *MYC* rearrangement with increased *MYC* gene copy numbers (49%) and low-level chromosome 8 polysomy (6%). *MYC* aberrations in HIV PBLs were significantly associated with a SS appearance (P=0.01), monomorphic morphology (P=0.03) and c-MYC expression (P=0.03). The median overall survival for HIV PBL was 75 days (95% CI 14–136).

HIV-associated DLBCL was typified by a mean age of 42 (SD ±10.8) years, a male predominance of 55%, an advanced stage of disease, i.e., stage III-IV at presentation and intermediate to high IPI scores. GC and NGC immunophenotypic COO were evident in 53% and 47%, respectively. Expression of c-MYC protein (≥40%), occurred in 58% of these tumours, and was significantly associated with a SS appearance and high tumour proliferation indices (i.e., Ki-67 ≥90%). Double expression of c- MYC and BCL2 proteins were significantly associated with the NGC COO immunophenotype (P=0.002). *MYC* aberrations included a low-level increase of *MYC* gene copy numbers (57%) and *MYC* rearrangements (12%). Infrequently, C8 polysomy, *MYC* gene clusters and concurrent *MYC* rearrangement with increased *MYC* gene copies were also detected. In the HIV seropositive and seronegative DLBCL patients, the median overall survival was 228 days (95% CI 54–402) and 825 days (95% CI 309–1341) , respectively (P=0.08, Log rank). When compared with the median OS of the HIV seronegative DLBCL patients, an inferior median survival outcome occurred when the CD4 counts were <100 cells/mm^3 and when the IPI was 3–5 in the HIV seropositive patients. In the multivariate analysis, the presence of concomitant infections negatively impacted the overall survival.

Greater awareness of these aggressive tumours, early and accurate diagnosis, timeous referral and appropriate treatment, may improve the outcome of the patients who tend to present with advanced stage disease and an array of adverse prognostic factors.

FUTURE RESEARCH

HIV-associated DLBCL and HIV-associated PBL frequently harbour *MYC* aberrations. Evaluation for *MYC* rearrangement is now routinely performed on all DLBCLs at our institute, irrespective of the immunophenotypic COO distribution. The evaluation of *MYC* copy numbers may also occur concurrently to detect tumours with *MYC* gene amplification, as the presence thereof may negatively impact the survival outcome.

TP53 gene mutation is recognised as a negative prognostic factor of DLBCL and investigation thereof is currently under scientific exploration at our institute.

Plasma cell-free DNA, which is also referred to as cell-free liquid biopsy, from HIV seropositive patients with and without lymphoma at our institute, and clonal immunoglobulin next generation sequencing (NGS) are currently being investigated in collaboration with researchers at Johns Hopkins University, Maryland, USA.

NGS, that simultaneously identifies multiple genomic biomarkers for B-cell NHL, may contribute significantly to the diagnostic and prognostic advancement of DLBCL and PBL. The application of NGS methodologies to minimally-invasive liquid biopsies creates opportunities for early-stage diagnoses, real-time monitoring, timeous detection of relapse and adaptive therapeutic approaches.

The influence of rituximab immunotherapy, in combination with conventional chemotherapy and c-ART, on the survival outcome of HIV-associated aggressive B-cell NHL is currently being investigated within prospective clinical trials at our institute.

REFERENCES

Abayomi E.A., Somers A., Grewal R., et al. (2011) Impact of the HIV epidemic and anti-retroviral treatment policy on lymphoma incidence and subtypes seen in the Western Cape of South Africa, 2002-2009: preliminary findings of the Tygerberg Lymphoma Study Group. *Transfusion and Apheresis Science* 44(2): 161-166.

Adams J.M., Gerondakis S., Webb E., et al. (1983) Cellular myc oncogene is altered by chromosome translocation to an immunoglobulin locus in murine plasmacytomas and is rearranged similarly in human Burkitt lymphomas. *Proceedings of the National Academy of Sciences of the United States of America* 80(7): 1982-1986.

Adams J.M., Harris A.W., Pinkert C.A., et al. (1985) The c-myc oncogene driven by immunoglobulin enhancers induces lymphoid malignancy in transgenic mice. *Nature* 318(6046): 533-538.

Adhikary S. and Eilers M. (2005) Transcriptional regulation and transformation by Myc proteins. *Nature Reviews: Molecular Cell Biology* 6(8): 635-645.

Akasaka T., Akasaka H., Ueda C., et al. (2000) Molecular and clinical features of non-Burkitt's, diffuse large-cell lymphoma of B-cell type associated with the c-MYC/immunoglobulin heavy-chain fusion gene. *Journal of Clinical Oncology* 18(3): 510-518.

Alizadeh A.A., Eisen M.B., Davis R.E., et al. (2000) Distinct types of diffuse large B-cell lymphoma identified by gene expression profiling. *Nature* 403(6769): 503-511.

Allday M.J. (2009) How does Epstein–Barr virus (EBV) complement the activation of Myc in the pathogenesis of Burkitt's lymphoma? *Seminars in Cancer Biology* 19(6): 366-376.

Alli N. and Meer S. (2017) Head and neck lymphomas: A 20-year review in an Oral Pathology Unit, Johannesburg, South Africa, a country with the highest global incidence of HIV/AIDS. *Oral Oncology* 67: 17-23.

Amati B., Littlewood T.D., Evan G.I., et al. (1993) The c-Myc protein induces cell cycle progression and apoptosis through dimerization with Max. *European Molecular Biology Organization Journal* 12(13): 5083-5087.

Ambinder R.F. and Mann R.B. (1994) Epstein-Barr-encoded RNA in situ hybridization: Diagnostic applications. *Human Pathology* 25(6): 602-605.

Anagnostopoulos I., Hummel M., Kreschel C., et al. (1995) Morphology, immunophenotype, and distribution of latently and/or productively Epstein-Barr virus-infected cells in acute infectious mononucleosis: implications for the interindividual infection route of Epstein-Barr virus. *Blood* 85(3): 744-750.

Anderson J.R., Armitage J.O. and Weisenburger D.D. (1998) Epidemiology of the non-Hodgkin's lymphomas: distributions of the major subtypes differ by geographic locations. Non-Hodgkin's Lymphoma Classification Project. *Annals of Oncology* 9(7): 717-720.

Andrade-Filho J. (2014) Analogies in medicine: starry-sky appearance. *Revista do Instituto de Medicina Tropical de São Paulo* 56(6): 541-542.

Armitage J.O. (2005) Staging non-Hodgkin lymphoma. *CA: A Cancer Journal for Clinicians* 55(6): 368-376.

Armitage J.O. and Weisenburger D.D. (1998) New Approach to Classifying Non-Hodgkin's Lymphomas: Clinical Features of the Major Histologic Subtypes. *Journal of Clinical Oncology* 16(8): 2780-2795.

Arnould L., Denoux Y., MacGrogan G., et al. (2003) Agreement between chromogenic in situ hybridisation (CISH) and FISH in the determination of HER2 status in breast cancer. *British Journal of Cancer* 88(10): 1587-1591.

Arora N., Eule C., Gupta A., et al. (2019) Clinicopathologic features, management, and outcomes of plasmablastic lymphoma: A 10-year experience. *American Journal of Hematology* 94(5): E127-E129.

Arvanitis C. and Felsher D.W. (2006) Conditional transgenic models define how MYC initiates and maintains tumorigenesis. *Seminars in Cancer Biology* 16(4): 313-317.

Aukema S.M., Siebert R., Schuuring E., et al. (2011) Double-hit B-cell lymphomas. *Blood* 117(8): 2319-2331.

Babcock G.J., Decker L.L., Volk M., et al. (1998) EBV persistence in memory B cells in vivo. *Immunity* 9(3): 395-404.

Bahram F., von der Lehr N., Cetinkaya C., et al. (2000) c-Myc hot spot mutations in lymphomas result in inefficient ubiquitination and decreased proteasome-mediated turnover. *Blood* 95(6): 2104-2110.

Banks P.M., Keller R.H., Li C.Y., et al. (1978) Malignant lymphoma of plasmablastic identity. A neoplasm with both "immunoblastic" and plasma cellular features. *American Journal of Medicine* 64(5): 906-909.

Baptista M.J., Garcia O., Morgades M., et al. (2015) HIV-infection impact on clinical-biological features and outcome of diffuse large B-cell lymphoma treated with R-CHOP in the combination antiretroviral therapy era. *AIDS* 29(7): 811-818.

Barrans S., Crouch S., Smith A., et al. (2010) Rearrangement of MYC is associated with poor prognosis in patients with diffuse large B-cell lymphoma treated in the era of rituximab. *Journal of Clinical Oncology* 28(20): 3360-3365.

Barre-Sinoussi F., Chermann J.C., Rey F., et al. (1983) Isolation of a T-lymphotropic retrovirus from a patient at risk for acquired immune deficiency syndrome (AIDS). *Science* 220(4599): 868-871.

Barta S.K., Xue X., Wang D., et al. (2013) Treatment factors affecting outcomes in HIV-associated non-Hodgkin lymphomas: a pooled analysis of 1546 patients. *Blood* 122(19): 3251-3262.

Basta D., Latinovic O., Lafferty M.K., et al. (2015) Angiogenic, lymphangiogenic and adipogenic effects of HIV-1 matrix protein p17. *Pathogens and Disease* 73(8): 1-8.

Battegay M., Nuesch R., Hirschel B., et al. (2006) Immunological recovery and antiretroviral therapy in HIV-1 infection. *Lancet Infectious Diseases* 6(5): 280-287.

Battey J., Moulding C., Taub R., et al. (1983) The human c-myc oncogene: structural consequences of translocation into the IgH locus in Burkitt lymphoma. *Cell* 34(3): 779-787.

Bauer K.D., Merkel D.E., Winter J.N., et al. (1986) Prognostic Implications of Ploidy and Proliferative Activity in Diffuse Large Cell Lymphomas. *Cancer Research* 46(6): 3173.

Beer S., Zetterberg A., Ihrie R.A., et al. (2004) Developmental context determines latency of MYC-induced tumorigenesis. *PLoS Biology* 2(11): e332.

Beral V., Peterman T., Berkelman R., et al. (1991) AIDS-associated non-Hodgkin lymphoma. *Lancet* 337(8745): 805-809.

Bertrand P., Bastard C., Maingonnat C., et al. (2007) Mapping of MYC breakpoints in 8q24 rearrangements involving non-immunoglobulin partners in B-cell lymphomas. *Leukemia* 21: 515-523.

Besson C., Goubar A., Gabarre J., et al. (2001) Changes in AIDS-related lymphoma since the era of highly active antiretroviral therapy. *Blood* 98(8): 2339-2344.

Bibas M. and Castillo J.J. (2014) Current knowledge on HIV-associated Plasmablastic Lymphoma. *Mediterranean Journal of Hematology and Infectious Diseases* 6(1): e2014064.

Bigras G. (2016) MYC immunohistochemistry assessment in high-grade lymphomas hit or miss? *American Journal of Clinical Pathology* 145(2): 155-157.

Bishop J.M. (1978) Retroviruses. *Annual Review of Biochemistry* 47(1): 35-88.

Black C.L., Foster-Smith E., Lewis I.D., et al. (2013) Post-transplant plasmablastic lymphoma of the skin. *Australasian Journal of Dermatology* 54(4): 277-282.

Blackwell T.K., Kretzner L., Blackwood E.M., et al. (1990) Sequence-specific DNA binding by the c-Myc protein. *Science* 250(4984): 1149-1151.

Blackwood E.M. and Eisenman R.N. (1991) Max: a helix-loop-helix zipper protein that forms a sequence-specific DNA-binding complex with Myc. *Science* 251(4998): 1211-1217.

Boerma E.G., Siebert R., Kluin P.M., et al. (2009) Translocations involving 8q24 in Burkitt lymphoma and other malignant lymphomas: a historical review of cytogenetics in the light of todays knowledge. *Leukemia* 23: 225–234.

Bogusz A.M., Seegmiller A.C., Garcia R., et al. (2009) Plasmablastic lymphomas with MYC/IgH rearrangement: report of three cases and review of the literature. *American Journal of Clinical Pathology* 132(4): 597-605.

Borenstein J., Pezzella F. and Gatter K.C. (2007) Plasmablastic lymphomas may occur as post-transplant lymphoproliferative disorders. *Histopathology* 51(6): 774-777.

Bouchla A., Papageorgiou S.G., Tsakiraki Z., et al. (2018) Plasmablastic lymphoma in an immunocompetent patient with MDS/MPN with ring sideroblasts and thrombocytosis- a case report. *Case Reports in Hematology* 2018: 2525070.

Bouvard V., Baan R., Straif K., et al. (2009) A review of human carcinogens-Part B: Biological agents. *Lancet Oncology* 10(4): 321-322.

Bower M., Fisher M., Hill T., et al. (2009) CD4 counts and the risk of systemic non-Hodgkin's lymphoma in individuals with HIV in the UK. *Haematologica* 94(6): 875-880.

Boy S., van Heerden M., Pool R., et al. (2015) Plasmablastic lymphoma versus diffuse large B cell lymphoma with plasmablastic differentiation: proposal for a novel diagnostic scoring system. *Journal of Hematopathology* 8(1): 3-11.

Boy S.C., van Heerden M.B., Babb C., et al. (2011) Dominant genetic aberrations and coexistent EBV infection in HIV-related oral plasmablastic lymphomas. *Oral Oncology* 47(9): 883-887.

Boy S.C., van Heerden M.B., Raubenheimer E.J., et al. (2010) Plasmablastic lymphomas with light chain restriction - plasmablastic extramedullary plasmacytomas? *Journal of Oral Pathology and Medicine* 39(5): 435-439.

Brahmania M., Sylwesterowic T. and Leitch H. (2011) Plasmablastic lymphoma in the ano-rectal junction presenting in an immunocompetent man: a case report. *Journal of Medical Case Reports* 5: 168.

Braitstein P., Brinkhof M.W., Dabis F., et al. (2006) Mortality of HIV-1-infected patients in the first year of antiretroviral therapy: comparison between low-income and high-income countries. *Lancet* 367(9513): 817-824.

Bray F., Ferlay J., Soerjomataram I., et al. (2018) Global cancer statistics 2018: GLOBOCAN estimates of incidence and mortality worldwide for 36 cancers in 185 countries. *CA: A Cancer Journal for Clinicians* 68(6): 394-424.

Brown D.C. and Gatter K.C. (2002) Ki67 protein: the immaculate deception? *Histopathology* 40(1): 2-11.

Broyde A., Boycov O., Strenov Y., et al. (2009) Role and prognostic significance of the Ki-67 index in non-Hodgkin's lymphoma. *American Journal of Hematology* 84(6): 338-343.

Burkitt D. (1958) A sarcoma involving the jaws in African children. *British Journal of Surgery* 46: 218–223.

Burkitt D. and O'Conor G.T. (1961) Malignant lymphoma in African children. I. A clinical syndrome. *Cancer* 14: 258-269.

Caccuri F., Giagulli C., Bugatti A., et al. (2012) HIV-1 matrix protein p17 promotes angiogenesis via chemokine receptors CXCR1 and CXCR2. *Proceedings of the National Academy of Sciences of the United States of America* 109(36): 14580-14585.

Caccuri F., Rueckert C., Giagulli C., et al. (2014) HIV-1 matrix protein p17 promotes lymphangiogenesis and activates the endothelin-1/endothelin B receptor axis. *Arteriosclerosis, Thrombosis, and Vascular Biology* 34(4): 846-856.

Campo E., Stein H. and Harris N.L. (2017) Plasmablastic lymphoma. In: Swerdlow SH, Campo E, Harris NL, et al. (eds) *WHO classification of tumours of the haematopoietic and lymphoid tissues*. Revised 4th ed. IARC: Lyon, pp. 321-322.

Carbone A. (2002) AIDS-related non-Hodgkin's lymphomas: from pathology and molecular pathogenesis to treatment. *Human Pathology* 33(4): 392-404.

Carbone A., Vaccher E., Gloghini A., et al. (2014) Diagnosis and management of lymphomas and other cancers in HIV-infected patients. *Nature Reviews. Clinical Oncology* 11(4): 223-238.

Carbone P.P., Kaplan H.S., Musshoff K., et al. (1971) Report of the Committee on Hodgkin's Disease Staging Classification. *Cancer Research* 31(11): 1860-1861.

Carroll V. and Garzino-Demo A. (2015) HIV-associated lymphoma in the era of combination antiretroviral therapy: shifting the immunological landscape. *Pathogens and Disease* 73(7).

Cassim S., Antel K., Chetty D.R., et al. (2020) Diffuse large B-cell lymphoma in a South African cohort with a high HIV prevalence: an analysis by cell-of-origin, Epstein–Barr virus infection and survival. *Pathology* 52(4): 453-459.

Castillo J., Pantanowitz L. and Dezube B.J. (2008) HIV-associated plasmablastic lymphoma: lessons learned from 112 published cases. *American Journal of Hematology* 83(10): 804-809.

Castillo J.J., Bibas M. and Miranda R.N. (2015) The biology and treatment of plasmablastic lymphoma. *Blood* 125(15): 2323-2330.

Castillo J.J. and Reagan J.L. (2011a) Plasmablastic lymphoma: a systematic review. *Scientific World Journal* 11: 687-696.

Castillo J.J., Reagan J.L., Bishop K.D., et al. (2014) Viral lymphomagenesis: from pathophysiology to the rationale for novel therapies. *British Journal of Haematology* 165(3): 300-315.

Castillo J.J., Winer E.S., Stachurski D., et al. (2010a) Clinical and pathological differences between human immunodeficiency virus-positive and human immunodeficiency virus-negative patients with plasmablastic lymphoma. *Leukemia and Lymphoma* 51(11): 2047-2053.

Castillo J.J., Winer E.S., Stachurski D., et al. (2010b) Prognostic factors in chemotherapy-treated patients with HIV-associated Plasmablastic lymphoma. *Oncologist* 15(3): 293-299.

Castillo J.J., Winer E.S., Stachurski D., et al. (2011b) HIV-negative plasmablastic lymphoma: not in the mouth. *Clinical Lymphoma, Myeloma & Leukemia* 11(2): 185-189.

Cattaneo C., Re A., Ungari M., et al. (2015) Plasmablastic lymphoma among human immunodeficiency virus-positive patients: results of a single center's experience. *Leukemia and Lymphoma* 56(1): 267-269.

Centre for disease control. (1981) Kaposi's sarcoma and Pneumocystis pneumonia among homosexual men--New York City and California. *Morbidity and Mortality Weekly Report* 30(25): 305-308.

Chabay P., De Matteo E., Lorenzetti M., et al. (2009) Vulvar plasmablastic lymphoma in a HIV-positive child: a novel extraoral localisation. *Journal of Clinical Pathology* 62(7): 644-646.

Chadburn A., Chiu A., Lee J.Y., et al. (2009) Immunophenotypic analysis of AIDS-related diffuse large B-cell lymphoma and clinical implications in patients from AIDS Malignancies Consortium clinical trials 010 and 034. *Journal of Clinical Oncology* 27(30): 5039-5048.

Chang C.C., Zhou X., Taylor J.J., et al. (2009) Genomic profiling of plasmablastic lymphoma using array comparative genomic hybridization (aCGH): revealing significant overlapping genomic lesions with diffuse large B-cell lymphoma. *Journal of Hematology and Oncology* 2: 47.

Chang T., Yu D., Lee Y., et al. (2008) Widespread microRNA repression by Myc contributes to tumorigenesis. *Nature Genetics* 40: 43–50.

Chao C., Silverberg M.J., Xu L., et al. (2015) A comparative study of molecular characteristics of diffuse large B-cell lymphoma from patients with and without human immunodeficiency virus infection. *Clinical cancer research : an official journal of the American Association for Cancer Research* 21(6): 1429-1437.

Chapman J., Gentles A.J., Sujoy V., et al. (2015) Gene expression analysis of plasmablastic lymphoma identifies downregulation of B-cell receptor signaling and additional unique transcriptional programs. *Leukemia* 29(11): 2270-2273.

Chapuy B., Stewart C., Dunford A.J., et al. (2018) Molecular subtypes of diffuse large B cell lymphoma are associated with distinct pathogenic mechanisms and outcomes. *Nature Medicine* 24(5): 679-690.

Chen B.J., Fend F., Campo E., et al. (2019) Aggressive B-cell lymphomas-from morphology to molecular pathogenesis. *Annals of Lymphoma* 3(1).

Chen H., Liu H. and Qing G. (2018) Targeting oncogenic Myc as a strategy for cancer treatment. *Signal Transduction and Targeted Therapy* 3(1): 5.

Chen Y., Liu Y., Luo D., et al. (2015) Clinicopathologic analysis of HIV-negative plasmablastic lymphoma. *Zhonghua Bing Li Xue Za Zhi. Chinese Journal of Pathology* 44(8): 548-552.

Chen Y.B., Yu H., Gillani A., et al. (2007) AIDS-associated plasmablastic lymphoma presenting at the insertion site of a peritoneal dialysis catheter. *Journal of Clinical Oncology* 25(21): 3176-3178.

Chetty R., Hlatswayo N., Muc R., et al. (2003) Plasmablastic lymphoma in HIV+ patients: an expanding spectrum. *Histopathology* 42(6): 605-609.

Chihara D., Nastoupil L.J., Williams J.N., et al. (2015) New insights into the epidemiology of non-Hodgkin lymphoma and implications for therapy. *Expert Review of Anticancer Therapy* 15(5): 531-544.

Chisholm K.M., Bangs C.D., Bacchi C.E., et al. (2015) Expression profiles of MYC protein and MYC gene rearrangement in lymphomas. *American Journal of Surgical Pathology* 39(3): 294-303.

Choi W.W., Weisenburger D.D., Greiner T.C., et al. (2009) A new immunostain algorithm classifies diffuse large B-cell lymphoma into molecular subtypes with high accuracy. *Clinical Cancer Research* 15(17): 5494-5502.

Coakley D. (2006) Denis Burkitt and his contribution to haematology/oncology. *British Journal of Haematology* 135(1): 17-25.

Cohen J.I. (2000) Epstein-Barr virus infection. *New England Journal of Medicine* 343(7): 481-492.

Collins S. and Groudine M. (1982) Amplification of endogenous myc-related DNA sequences in a human myeloid leukaemia cell line. *Nature* 298(5875): 679-681.

Colombat P., Salles G., Brousse N., et al. (2001) Rituximab (anti-CD20 monoclonal antibody) as single first-line therapy for patients with follicular lymphoma with a low tumor burden: clinical and molecular evaluation. *Blood* 97(1): 101-106.

Colomo L., Loong F., Rives S., et al. (2004) Diffuse large B-cell lymphomas with plasmablastic differentiation represent a heterogeneous group of disease entities. *American Journal of Surgical Pathology* 28(6): 736-747.

Cook J.R., Goldman B., Tubbs R.R., et al. (2014) Clinical significance of MYC expression and/or "high-grade" morphology in non-Burkitt, diffuse aggressive B-cell lymphomas: a SWOG S9704 correlative study. *American Journal of Surgical Pathology* 38(4): 494-501.

Copie-Bergman C., Cuillière-Dartigues P., Baia M., et al. (2015) MYC-IG rearrangements are negative predictors of survival in DLBCL patients treated with immunochemotherapy: a GELA/LYSA study. *Blood* 126(22): 2466-2474.

Coutinho R., Pria A.D., Gandhi S., et al. (2014) HIV status does not impair the outcome of patients diagnosed with diffuse large B-cell lymphoma treated with R-CHOP in the cART era. *AIDS* 28(5): 689-697.

Croce C.M. (1993) Molecular biology of lymphomas. *Seminars in Oncology* 20: 31–46.

Dalla-Favera R., Bregni M., Erikson J., et al. (1982a) Human *c-myc onc* gene is located on the region of chromosome 8 that is translocated in Burkitt lymphoma cells. *Proceedings of the National Academy of Sciences of the United States of America* 79(24): 7824.

Dalla-Favera R., Gelmann E.P., Martinotti S., et al. (1982b) Cloning and characterization of different human sequences related to the onc gene (v-myc) of avian myelocytomatosis virus (MC29). *Proceedings of the National Academy of Sciences of the United States of America* 79(21): 6497-6501.

Dang C.V. (1999a) c-Myc target genes involved in cell growth, apoptosis and metabolism. *Molecular and Cellular Biology* 19(1): 1-11.

Dang C.V. (2012) MYC on the Path to Cancer. *Cell* 149(1): 22-35.

Dang C.V. (2013) MYC, metabolism, cell growth and tumorigenesis. *Cold Spring Harbor Perspectives in Medicine* 3: a014217.

Dang C.V., O'Donnell K.A., Zeller K.I., et al. (2006) The c-Myc target gene network. *Seminars in Cancer Biology* 16(4): 253-264.

Dang C.V., O'Donnell K.A. and Juopperi T. (2005) The great MYC escape in tumorigenesis. *Cancer Cell* 8(3): 177-178.

Dang C.V., Resar L.M.S., Emison E., et al. (1999b) Function of the c-Myc oncogenic transcription factor. *Experimental Cell Research* 253: 63–77.

Davis R.E., Ngo V.N., Lenz G., et al. (2010) Chronic active B-cell-receptor signalling in diffuse large B-cell lymphoma. *Nature* 463(7277): 88-92.

Dawson M.A., Schwarer A.P., McLean C., et al. (2007) AIDS-related plasmablastic lymphoma of the oral cavity associated with an IGH/MYC translocation--treatment with autologous stem-cell transplantation in a patient with severe haemophilia-A. *Haematologica* 92(1): 11-12.

de Witt P., Maartens D.J., Uldrick T.S., et al. (2013) Treatment outcomes in AIDS-related diffuse large B-cell lymphoma in the setting roll-out of combination antiretroviral therapy in South Africa. *Journal of Acquired Immune Deficiency Syndromes* 64(1): 66-73.

Del Rio C. (2017) The global HIV epidemic: What the pathologist needs to know. *Seminars in Diagnostic Pathology* 34(4): 314-317.

Delecluse H.J., Anagnostopoulos I., Dallenbach F., et al. (1997) Plasmablastic lymphomas of the oral cavity: a new entity associated with the human immunodeficiency virus infection. *Blood* 89(4): 1413-1420.

Dittus C., Grover N., Ellsworth S., et al. (2018) Bortezomib in combination with dose-adjusted EPOCH (etoposide, prednisone, vincristine, cyclophosphamide, and doxorubicin) induces long-term survival in patients with plasmablastic lymphoma: a retrospective analysis. *Leukemia and Lymphoma* 59(9): 2121-2127.

Dolcetti R., Gloghini A., Caruso A., et al. (2016) A lymphomagenic role for HIV beyond immune suppression? *Blood* 127(11): 1403-1409.

Dong H.Y., Scadden D.T., de Leval L., et al. (2005) Plasmablastic lymphoma in HIV-positive patients: an aggressive Epstein-Barr virus-associated extramedullary plasmacytic neoplasm. *American Journal of Surgical Pathology* 29(12): 1633-1641.

Douek D.C., Roederer M. and Koup R.A. (2009) Emerging concepts in the immunopathogenesis of AIDS. *Annual Review of Medicine* 60: 471-484.

Dunleavy K., Little R.F., Pittaluga S., et al. (2010) The role of tumor histogenesis, FDG-PET, and short-course EPOCH with dose-dense rituximab (SC-EPOCH-RR) in HIV-associated diffuse large B-cell lymphoma. *Blood* 115(15): 3017-3024.

Dunleavy K., Pittaluga S., Czuczman M.S., et al. (2009) Differential efficacy of bortezomib plus chemotherapy within molecular subtypes of diffuse large B-cell lymphoma. *Blood* 113(24): 6069-6076.

Dunleavy K. and Wilson W.H. (2006) The case for rituximab in AIDS-related lymphoma. *Blood* 107(7): 3014-3015.

Dunleavy K. and Wilson W.H. (2012) How I treat HIV-associated lymphoma. *Blood* 119(14): 3245-3255.

Egger M., May M., Chene G., et al. (2002) Prognosis of HIV-1-infected patients starting highly active antiretroviral therapy: a collaborative analysis of prospective studies. *Lancet* 360(9327): 119-129.

Eilers M., Schirm S. and Bishop J.M. (1991) The MYC protein activates transcription of the alpha-prothymosin gene. *European Molecular Biology Organization Journal* 10(1): 133-141.

Elyamany G., Alzahrani A.M., Aljuboury M., et al. (2015) Clinicopathologic features of plasmablastic lymphoma: Single-center series of 8 cases from Saudi Arabia. *Diagnostic Pathology* 10: 78.

Endl E. and Gerdes J. (2000) The Ki-67 protein: fascinating forms and an unknown function. *Experimental Cell Research* 257(2): 231-237.

Engels E.A., Biggar R.J., Hall H.I., et al. (2008) Cancer risk in people infected with human immunodeficiency virus in the United States. *International Journal of Cancer* 123(1): 187-194.

Engels E.A., Pfeiffer R.M., Landgren O., et al. (2010) Immunologic and virologic predictors of AIDS-related non-hodgkin lymphoma in the highly active antiretroviral therapy era. *Journal of Acquired Immune Deficiency Syndromes* 54(1): 78-84.

Epeldegui M., Breen E.C., Hung Y.P., et al. (2007) Elevated expression of activation induced cytidine deaminase in peripheral blood mononuclear cells precedes AIDS-NHL diagnosis. *AIDS* 21(17): 2265-2270.

Epstein M.A., Achong B.G. and Barr Y.M. (1964) Virus particles in cultured lymphoblasts from Burkitt's lymphoma. *Lancet* 1: 702–703.

Erikson J., Finan J., Nowell P.C., et al. (1982) Translocation of immunoglobulin VH genes in Burkitt lymphoma. *Proceedings of the National Academy of Sciences of the United States of America* 79(18): 5611-5615.

Felsher D. and Bishop J. (1999) Reversible tumorigenesis by MYC in hematopoietic lineages. *Molecular Cell* 4: 199–207.

Fingeroth J.D., Weis J.J., Tedder T.F., et al. (1984) Epstein-Barr virus receptor of human B lymphocytes is the C3d receptor CR2. *Proceedings of the National Academy of Sciences of the United States of America* 81(14): 4510-4514.

Fisher F., Crouch D.H., Jayaraman P.S., et al. (1993) Transcription activation by Myc and Max: flanking sequences target activation to a subset of CACGTG motifs in vivo. *European Molecular Biology Organization Journal* 12(13): 5075-5082.

Franceschi S., Lise M., Clifford G.M., et al. (2010) Changing patterns of cancer incidence in the early- and late-HAART periods: the Swiss HIV Cohort Study. *British Journal of Cancer* 103(3): 416-422.

Gabay M., Yulin L. and Felsher D. (2014) MYC activation is a hallmark of cancer initiation and maintenance. *Cold Spring Harbor Perspectives in Medicine* 4: a014241.

Gaidano G., Cerri M., Capello D., et al. (2002) Molecular histogenesis of plasmablastic lymphoma of the oral cavity. *British Journal of Haematology* 119(3): 622-628.

Gallo R.C., Sarin P.S., Gelmann E.P., et al. (1983) Isolation of human T-cell leukemia virus in acquired immune deficiency syndrome (AIDS). *Science* 220(4599): 865-867.

Galvao Ferreira P.A., Gomes Luna C., Silva M.F., et al. (2017) Vulvar and gastric involvement in plasmablastic lymphoma. *European Journal of Gynaecological Oncology* 38(2): 308-310.

Gao F., Bailes E., Robertson D.L., et al. (1999) Origin of HIV-1 in the chimpanzee Pan troglodytes troglodytes. *Nature* 397(6718): 436-441.

Gao J., Kong X., Zhong D., et al. (2013) An uncommon case of epidural plasmablastic lymphoma presents as spinal cord compression. *Clinical Neurology and Neurosurgery* 115(10): 2301-2303.

Gao P., Tchernyshyov I., Chang T.C., et al. (2009) c-Myc suppression of miR-23a/b enhances mitochondrial glutaminase expression and glutamine metabolism. *Nature* 458: 762–765.

Gascoyne D.M., Lyne L., Spearman H., et al. (2017a) Vitamin D receptor expression in plasmablastic lymphoma and myeloma cells confers susceptibility to vitamin D. *Endocrinology* 158(3): 503-515.

Gascoyne R.D., Campo E., Jaffe E.S., et al. (2017b) Diffuse large B-cell lymphoma, NOS. In: Swerdlow SH, Campo E, Harris NL, et al. (eds) *WHO classification of tumours of haematopoietic and lymphoid tissues*. Revised 4th ed. IARC: Lyon, pp. 291-297.

Gerdes J., Dallenbach F., Lennert K., et al. (1984) Growth fractions in malignant non-Hodgkin's lymphomas (NHL) as determined in situ with the monoclonal antibody Ki-67. *Hematological Oncology* 2(4): 365-371.

Gerdes J., Li L., Schlueter C., et al. (1991) Immunobiochemical and molecular biologic characterization of the cell proliferation-associated nuclear antigen that is defined by monoclonal antibody Ki-67. *American Journal of Pathology* 138(4): 867-873.

Gerdes J., Schwab U., Lemke H., et al. (1983) Production of a mouse monoclonal antibody reactive with a human nuclear antigen associated with cell proliferation. *International Journal of Cancer* 31(1): 13-20.

Gerdes J., Stein H., Pileri S., et al. (1987) Prognostic relevance of tumour-cell growth fraction in malignant non-Hodgkin's lymphomas. *Lancet* 2(8556): 448-449.

Ghasemi A. and Zahediasl S. (2012) Normality tests for statistical analysis: a guide for non-statisticians. *International Journal of Endocrinology and Metabolism* 10(2): 486-489.

Giagulli C., Marsico S., Magiera A.K., et al. (2011) Opposite effects of HIV-1 p17 variants on PTEN activation and cell growth in B cells. *PloS One* 6(3): e17831.

Gibson T.M., Morton L.M., Shiels M.S., et al. (2014) Risk of non-Hodgkin lymphoma subtypes in HIV-infected people during the HAART era: a population-based study. *AIDS* 28(15): 2313-2318.

Goedert J.J., Cote T.R., Virgo P., et al. (1998) Spectrum of AIDS-associated malignant disorders. *Lancet* 351(9119): 1833-1839.

Goedhals J., Beukes C.A. and Cooper S. (2006) The ultrastructural features of plasmablastic lymphoma. *Ultrastructural Pathology* 30(6): 427-433.

Goedhals J., Stones D. and Botha M. (2014) Plasmablastic lymphoma in childhood: A report of two cases. *South African Journal of Child Health* 8: 39.

Goff S.P. (2001) Retroviridae : the retroviruses and their replication. In: Knipe DM HP (ed) *Fields Virology*. 4th ed. Philadelphia: Lippincott Williams & Wilkins, pp.1871–1939.

Gopal S., Patel M.R., Yanik E.L., et al. (2013) Temporal trends in presentation and survival for HIV-associated lymphoma in the antiretroviral therapy era. *Journal of the National Cancer Institute* 105(16): 1221-1229.

Goto H., Hagiwara S., Hirai R., et al. (2011) Case of relapsed AIDS-related plasmablastic lymphoma treated with autologous stem cell transplantation and highly active antiretroviral therapy. *Rare Tumors* 3(1): 33-35.

Gottlieb M.S., Schroff R., Schanker H.M., et al. (1981) Pneumocystis carinii pneumonia and mucosal candidiasis in previously healthy homosexual men: evidence of a new acquired cellular immunodeficiency. *New England Journal of Medicine* 305(24): 1425-1431.

Graham J.P., Arcipowski K.M. and Bishop G.A. (2010) Differential B-lymphocyte regulation by CD40 and its viral mimic, latent membrane protein 1. *Immunological Reviews* 237(1): 226-248.

Grandori C., Cowley S.M., James L.P., et al. (2000) The MYC/MAX/MAD network and the transcriptional control of cell behavior. *Annual Review of Cell and Developmental Biology* 16: 653–699.

Green T.M., Nielsen O., de Stricker K., et al. (2012a) High levels of nuclear MYC protein predict the presence of MYC in diffuse large B-cell lymphoma. *American Journal of Surgical Pathology* 36: 612-619.

Green T.M., Young K.H., Visco C., et al. (2012b) Immunohistochemical double-hit score is a strong predictor of outcome in patients with diffuse large B-cell lymphoma treated with rituximab plus cyclophosphamide, doxorubicin, vincristine, and prednisone. *Journal of Clinical Oncology* 30(28): 3460-3467.

Grogan T.M., Lippman S.M., Spier C.M., et al. (1988) Independent prognostic significance of a nuclear proliferation antigen in diffuse large cell lymphomas as determined by the monoclonal antibody Ki-67. *Blood* 71(4): 1157-1160.

Grogg K.L., Miller R.F. and Dogan A. (2007) HIV infection and lymphoma. *Journal of Clinical Pathology* 60(12): 1365-1372.

Grossman Z., Feinberg M.B. and Paul W.E. (1998) Multiple modes of cellular activation and virus transmission in HIV infection: a role for chronically and latently infected cells in sustaining viral replication. *Proceedings of the National Academy of Sciences of the United States of America* 95(11): 6314-6319.

Grulich A.E. (1999) AIDS-associated non-Hodgkin's lymphoma in the era of highly active antiretroviral therapy. *Journal of Acquired Immune Deficiency Syndromes* 21 (Suppl 1): S27-30.

Guadalupe M., Reay E., Sankaran S., et al. (2003) Severe CD4+ T-cell depletion in gut lymphoid tissue during primary human immunodeficiency virus type 1 infection and substantial delay in restoration following highly active antiretroviral therapy. *Journal of Virology* 77(21): 11708-11717.

Guan B., Zhang X., Ma H., et al. (2010) A meta-analysis of highly active anti-retroviral therapy for treatment of plasmablastic lymphoma. *Hematology Oncology and Stem Cell Therapy* 3(1): 7-12.

Guerrero-Garcia T.A., Mogollon R.J. and Castillo J.J. (2017) Bortezomib in plasmablastic lymphoma: a glimpse of hope for a hard-to-treat disease. *Leukemia Research* 62: 12-16.

Gui L., He X.H., Liu P., et al. (2016) Clinical features and outcomes: analysis of 9 cases of HIV-negtive plasmablastic lymphoma. *Zhonghua Xue Ye Xue Za Zhi. Chinese Journal of Hematology.* 37(9): 762-767. [Abstract only].

Gujral S., Shet T.M. and Kane S.V. (2008) Morphological spectrum of AIDS-related plasmablastic lymphomas. *Indian Journal of Pathology and Microbiology* 51(1): 121-124.

Gupta M., Maurer M.J., Wellik L.E., et al. (2012) Expression of Myc, but not pSTAT3, is an adverse prognostic factor for diffuse large B-cell lymphoma treated with epratuzumab/R-CHOP. *Blood* 120(22): 4400-4406.

Haase A.T. (2005) Perils at mucosal front lines for HIV and SIV and their hosts. *Nature Reviews: Immunology* 5(10): 783-792.

Hadzisejdic I., Babarovic E., Vranic L., et al. (2017) Unusual presentation of plasmablastic lymphoma involving ovarian mature cystic teratoma: a case report. *Diagnostic Pathology* 12(1): 83.

Hahn B.H., Shaw G.M., De Cock K.M., et al. (2000) AIDS as a zoonosis: scientific and public health implications. *Science* 287(5453): 607-614.

Han X., Duan M., Hu L., et al. (2017) Plasmablastic lymphoma: review of 60 Chinese cases and prognosis analysis. *Medicine* 96(9): 1-5.

Hans C.P., Weisenburger D.D., Greiner T.C., et al. (2004) Confirmation of the molecular classification of diffuse large B-cell lymphoma by immunohistochemistry using a tissue microarray. *Blood* 103(1): 275-282.

Harmon C.M. and Smith L.B. (2016) Plasmablastic lymphoma: a review of clinicopathologic features and differential diagnosis. *Archives of Pathology and Laboratory Medicine* 140(10): 1074-1078.

Hasselblom S., Ridell B., Sigurdardottir M., et al. (2008) Low rather than high Ki-67 protein expression is an adverse prognostic factor in diffuse large B-cell lymphoma. *Leukemia and Lymphoma* 49(8): 1501-1509.

He L., Thomson J.M., Hemann M.T., et al. (2005) A microRNA polycistron as a potential human oncogene. *Nature* 435(7043): 828-833.

He X., Chen Z., Fu T., et al. (2014) Ki-67 is a valuable prognostic predictor of lymphoma but its utility varies in lymphoma subtypes: evidence from a systematic meta-analysis. *BMC Cancer* 14: 153-153.

Held G., Pöschel V. and Pfreundschuh M. (2006) Rituximab for the treatment of diffuse large B-cell lymphomas. *Expert Review of Anticancer Therapy* 6(8): 1175-1186.

Hellerstein M., Hanley M.B., Cesar D., et al. (1999) Directly measured kinetics of circulating T lymphocytes in normal and HIV-1-infected humans. *Nature Medicine* 5(1): 83-89.

Hemann M.T., Bric A., Teruya-Feldstein J., et al. (2005) Evasion of the p53 tumour surveillance network by tumour-derived MYC mutants. *Nature* 436(7052): 807-811.

Herrera A.F., Mei M., Low L., et al. (2017) Relapsed or refractory double-expressor and double-hit lymphomas have inferior progression-free survival after autologous stem-cell transplantation. *Journal of Clinical Oncology* 35(1): 24-31.

Hirosawa M., Morimoto H., Shibuya R., et al. (2015) A striking response of plasmablastic lymphoma of the oral cavity to bortezomib: a case report. *Biomarker Research* 3: 28.

Hleyhel M., Belot A., Bouvier A.M., et al. (2013) Risk of AIDS-defining cancers among HIV-1-infected patients in France between 1992 and 2009: results from the FHDH-ANRS CO4 cohort. *Clinical Infectious Diseases* 57(11): 1638-1647.

Horn H., Staiger A.M., Vöhringer M., et al. (2015) Diffuse large B-cell lymphomas of immunoblastic type are a major reservoir for MYC-IGH translocations. *American Journal of Surgical Pathology* 39(1): 61-66.

Horn H., Ziepert M., Becher C., et al. (2013) MYC status in concert with BCL2 and BCL6 expression predicts outcome in diffuse large B-cell lymphoma. *Blood* 121(12): 2253-2263.

Hu S., Xu-Monette Z.Y. and Tzankov A. (2013) MYC/BCL2 protein coexpression contributes to the inferior survival of activated B-cell subtype of diffuse large B-cell lymphoma and demonstrates high-risk gene expression signatures: a report from The International DLBCL Rituximab-CHOP Consortium Program. *Blood* 121(20): 4021-4031.

Huang X., Zhang Y. and Gao Z. (2015) Plasmablastic lymphoma of the stomach with c-MYC rearrangement in an immunocompetent young adult: a case report. *Medicine* 94(4): 1-3.

Human Sciences Research Council (2018) The fifth South African national HIV prevalence, incidence, behaviour and communication survey, 2017: HIV impact assessment summary report. Cape town. HSRC Press.

Hummel M., Bentink S., Berger H., et al. (2006) A biologic definition of Burkitt's lymphoma from transcriptional and genomic profiling. *New England Journal of Medicine* 354(23): 2419-2430.

Hurlin P.J., Quéva C. and Eisenman R.N. (1997) Mnt, a novel Max-interacting protein is coexpressed with Myc in proliferating cells and mediates repression at Myc binding sites. *Genes and Development* 11(1): 44-58.

Hwang J.P., Jeong S.H., Kim H.K., et al. (2017) Human immunodeficiency virus (HIV)-negative uterine plasmablastic lymphoma on 18F-FDG PET/CT. *British Journal of Radiology Case Reports* 3(2): 20160124.

Ibrahim I.F., Shapiro G.A. and Naina H.V.K. (2014) Treatment of HIV-associated plasmablastic lymphoma: A single-center experience with 25 patients. *Journal of Clinical Oncology* 32(15_suppl): 8583-8583.

Igawa T., Sato Y., Kawai H., et al. (2015) Spontaneous regression of plasmablastic lymphoma in an elderly human immunodeficiency virus (HIV)-negative patient. *Diagnostic Pathology* 10: 183.

Iliadis A., Koletsa T. and Kostopoulos I. (2016) Aberrant expression of T-cell marker CD7 in HIV negative intestinal plasmablastic lymphoma. *Pathology* 48(7): 731-733.

Imbeault M., Ouellet M., Giguere K., et al. (2011) Acquisition of host-derived CD40L by HIV-1 in vivo and its functional consequences in the B-cell compartment. *Journal of Virology* 85(5): 2189-2200.

International Non-Hodgkin's Lymphoma Prognostic Factors Project (1993) A predictive model for aggressive non-Hodgkin's lymphoma. *New England Journal of Medicine* 329(14): 987-994.

Ise M., Kageyama H., Ikebe D., et al. (2018) Transformation of double-hit follicular lymphoma to plasmablastic lymphoma: a partial role of MYC gene rearrangement. *Journal of Clinical and Experimental Hematopathology* 58(3): 128-135.

Ivanov X., Mladenov Z., Nedyalkov S., et al. (1964) Experimental investigations into avian leucoses. Transmission, haematology and morphology of avian myelocytomatosis. *Bulletin de Institut de Pathology Comparative Animaux* 10: 5–38.

Jaffe E. and Pittaluga S. (2011) Aggressive B-Cell Lymphomas: A review of new and old entities in the WHO classification. *Hematology: The Education Program of the American Society of Hematology* 2011: 506-514.

Jaffe E.S., Campo E., Harris N.L., et al. (2017) Introduction and overview of the classification of lymphoid neoplasms. In: Swerdlow SH, Campo E, Harris NL, et al. (eds) *WHO classification of tumours of haematopoietic and lymphoid tissues*. IARC: Lyon, pp.190-198.

Jarrett R.F. (2006) Viruses and lymphoma/leukaemia. *Journal of Pathology* 208(2): 176-186.

Jazirehi A.R. and Bonavida B. (2005) Cellular and molecular signal transduction pathways modulated by rituximab (rituxan, anti-CD20 mAb) in non-Hodgkin's lymphoma: implications in chemosensitization and therapeutic intervention. *Oncogene* 24(13): 2121-2143.

Jerkeman M., Anderson H., Dictor M., et al. (2004) Assessment of biological prognostic factors provides clinically relevant information in patients with diffuse large B-cell lymphoma--a Nordic Lymphoma Group study. *Annals of Hematology* 83(7): 414-419.

Jesionek-Kupnicka D., Braun M., Robak T., et al. (2019) A large single-institution retrospective analysis of aggressive B-cell lymphomas according to the 2016/2017 WHO classification. *Advances in Clinical and Experimental Medicine* 28(10): 1359-1365.

Johnson N.A., Slack G.W., Savage K.J., et al. (2012) Concurrent expression of MYC and BCL2 in diffuse large B-cell lymphoma treated with rituximab plus cyclophosphamide, doxorubicin, vincristine, and prednisone. *Journal of Clinical Oncology* 30(28): 3452-3459.

Junttila M.R. and Westermarck J. (2008) Mechanisms of MYC stabilization in human malignancies. *Cell Cycle* 7: 592–596.

Kane S., Khurana A., Parulkar G., et al. (2009) Minimum diagnostic criteria for plasmablastic lymphoma of oral/sinonasal region encountered in a tertiary cancer hospital of a developing country. *Journal of Oral Pathology and Medicine* 38(1): 138-144.

Kaplan L.D., Lee J.Y., Ambinder R.F., et al. (2005) Rituximab does not improve clinical outcome in a randomized phase 3 trial of CHOP with or without rituximab in patients with HIV-associated non-Hodgkin lymphoma: AIDS-Malignancies Consortium Trial 010. *Blood* 106(5): 1538-1543.

Karn J., Watson J., Lowe A., et al. (1989) Regulation of cell cycle duration by c-myc levels. *Oncogene* 4: 773–787.

Karpathiou G., Batistatou A., Forest F., et al. (2016) Basic molecular pathology and cytogenetics for practicing pathologists: correlation with morphology and with a focus on aspects of diagnostic or therapeutic utility. *Advances in Anatomic Pathology* 23(6): 368-380.

Kato G.J., Barrett J., Villa-Garcia M., et al. (1990) An amino-terminal c-Myc domain required for neoplastic transformation activates transcription. *Molecular and Cellular Biology* 10(11): 5914–5920.

Kelley C.F., Kitchen C.M., Hunt P.W., et al. (2009) Incomplete peripheral CD4+ cell count restoration in HIV-infected patients receiving long-term antiretroviral treatment. *Clinical Infectious Diseases* 48(6): 787-794.

Kharsany A.B. and Karim Q.A. (2016) HIV infection and AIDS in sub-Saharan Africa: current status, challenges and opportunities. *Open AIDS Journal* 10: 34-48.

Kim J., Tchernyshyov I., Semenza G., et al. (2006) HIF-1-mediated expression of pyruvate dehydrogenase kinase: a metabolic switch required for cellular adaptation to hypoxia. *Cell Metabolism* 3: 177–185.

Kimani S., Painschab M.S., Kaimila B., et al. (2021) Safety and efficacy of rituximab in patients with diffuse large B-cell lymphoma in Malawi: a prospective, single-arm, non-randomised phase 1/2 clinical trial. *The Lancet Global Health* 9(7): 1008-1016.

Kinra P. and Malik A. (2020) Ki 67: Are we counting it right? *Indian Journal of Pathology and Microbiology* 63(1): 98-99.

Kitahata M.M., Gange S.J., Abraham A.G., et al. (2009) Effect of early versus deferred antiretroviral therapy for HIV on survival. *New England Journal of Medicine* 360(18): 1815-1826.

Klapper W., Stoecklein H., Zeynalova S., et al. (2008) Structural aberrations affecting the MYC locus indicate a poor prognosis independent of clinical risk factors in diffuse large B-cell lymphomas treated within randomized trials of the German High-Grade Non-Hodgkin's Lymphoma Study Group (DSHNHL). *Leukemia* 22(12): 2226-2229.

Klapproth K. and Wirth T. (2010) Advances in the understanding of MYC-induced lymphomagenesis. . *British Journal of Haematolgy* 149(4): 484-497.

Kluin P.M., Harris N.l., Stein H., et al. (2017) High-grade B-cell lymphoma with MYC and BCL2 and/or BCL6 rearrangements. In: Swerdlow SH, Campo E, Harris NL, et al. (eds) *WHO classification of tumours of haematopoietic and lymphoid tissues*. Revised 4th ed. International Agency for Research on Cancer: Lyon, pp.335-340.

Kluk M., Chapuy B., Sinha P., et al. (2012) Immunohistochemical detection of MYC-driven diffuse large B-cell lymphomas. *PloS One* 7(4): e33813.

Kluk M.J., Ho C., Pinkus G.S., et al. (2016) MYC immunohistochemistry to identify MYC-driven B-cell lymphomas in clinical practice. *American Journal of Clinical Pathology* 145(2): 166-179.

Knowles D. (2003) Etiology and pathogenesis of AIDS-related non-Hodgkin's lymphoma. . *Hematology/Oncology Clinics of North America* 17: 785–820.

Kobayashi H. and Miyagi N. (2017) HIV-negative plasmablastic lymphoma attaining sustained remission with bortezomib-combined dose-adjusted EPOCH therapy. *Rinsho Ketsueki. Japanese Journal of Clinical Hematology* 58(5): 443-448. [Abstract only].

Koh Y.W., Hwang H.S., Park C.S., et al. (2015) Prognostic effect of Ki-67 expression in rituximab, cyclophosphamide, doxorubicin, vincristine and prednisone-treated diffuse large B-cell lymphoma is limited to non-germinal center B-cell-like subtype in late-elderly patients. *Leukemia and Lymphoma* 56(9): 2630-2636.

Koizumi Y., Uehira T., Ota Y., et al. (2016) Clinical and pathological aspects of human immunodeficiency virus-associated plasmablastic lymphoma: analysis of 24 cases. *International Journal of Hematology* 104(6): 669-681.

Kroemer G. and Pouyssegur J. (2008) Tumor cell metabolism: cancer's Achilles' heel. *Cancer Cell* 13(6): 472–482.

Kundu R.K., Sangiorgi F., Wu L.Y., et al. (1999) Expression of the human immunodeficiency virus-Tat gene in lymphoid tissues of transgenic mice is associated with B-cell lymphoma. *Blood* 94(1): 275-282.

Lacy S.E., Barrans S.L., Beer P.A., et al. (2020) Targeted sequencing in DLBCL, molecular subtypes, and outcomes: a Haematological Malignancy Research Network report. *Blood* 135(20): 1759-1771.

Lane H.C., Masur H., Edgar L.C., et al. (1983) Abnormalities of B-cell activation and immunoregulation in patients with the acquired immunodeficiency syndrome. *New England Journal of Medicine* 309(8): 453-458.

Laurent C., Fabiani B., Do C., et al. (2016) Immune-checkpoint expression in Epstein-Barr virus positive and negative plasmablastic lymphoma: a clinical and pathological study in 82 patients. *Haematologica* 101(8): 976-984.

Lautenberger J.A., Schulz R.A., Garen C.F., et al. (1981) Molecular cloning of myelocytomatosis virus (MC29) transforming sequences. *Proceedings of the National Academy of Sciences of the United States of America* 78(3): 1518-1522.

Lazzi S., Bellan C., De Falco G., et al. (2002) Expression of RB2/p130 tumor-suppressor gene in AIDS-related non-Hodgkin's lymphomas: implications for disease pathogenesis. *Human Pathology* 33(7): 723-731.

Leoncini L., Raphaël M., Stein H., et al. (2008) Burkitt lymphoma. In: Swerdlow SH, Campo E, Harris NL, et al. (eds) *WHO classification of tumours of the haematopoietic and lymphoid tissues* 4th ed. Lyon: IARC, pp.262-264.

Leucci E., Cocco M., Onnis A., et al. (2008) MYC translocation-negative classical Burkitt lymphoma cases: An alternative pathogenetic mechanism involving miRNA deregulation. *Journal of Pathology* 216: 440-450.

Levine A.M. (1993) AIDS-related malignancies: the emerging epidemic. *Journal of the National Cancer Institute* 85(17): 1382-1397.

Li F., Ding W., Zuo Z., et al. (2016) Plasmablastic lymphoma: a clinicopathologic analysis of 11 cases with review of literature. *Zhonghua Bing Li Xue Za Zhi. Chinese Journal of Pathology* 45(1): 37-42. [Abstract only].

Li Q, Spriggs MK, Kovats S, et al. (1997) Epstein-Barr virus uses HLA class II as a cofactor for infection of B lymphocytes. *Journal of Virology* 71(6): 4657-4662.

Li S., Lin P., Fayad L.E., et al. (2012a) B-cell lymphomas with MYC/8q24 rearrangements and IGH@BCL2/t(14;18)(q32;q21): an aggressive disease with heterogeneous histology, germinal center B-cell immunophenotype and poor outcome. *Modern Pathology* 25(1): 145-156.

Li Z.M., Huang J.J., Xia Y., et al. (2012b) High Ki-67 expression in diffuse large B-cell lymphoma patients with non-germinal center subtype indicates limited survival benefit from R-CHOP therapy. *European Journal of Haematology* 88(6): 510-517.

Liang R., Wang Z., Chen X.Q., et al. (2014) Treatment of plasmablastic lymphoma with multiple organ involvement. *Singapore Medical Journal* 55(12): 194-197.

Lin C.Y., Loven J., Rahl P.B., et al. (2012) Transcriptional amplification in tumor cells with elevated c-Myc. *Cell* 151(1): 56-67.

Linke-Serinsoz E., Fend F. and Quintanilla-Martinez L. (2017) Human immunodeficiency virus (HIV) and Epstein-Barr virus (EBV) related lymphomas, pathology view point. *Seminars in Diagnostic Pathology* 34(4): 352-363.

Lipstein M., O'Connor O., Montanari F., et al. (2010) Bortezomib-induced tumor lysis syndrome in a patient with HIV-negative plasmablastic lymphoma. *Clinical Lymphoma, Myeloma & Leukemia* 10(5): 43-46.

Lister T.A., Crowther D., Sutcliffe S.B., et al. (1989) Report of a committee convened to discuss the evaluation and staging of patients with Hodgkin's disease: Cotswolds meeting. *Journal of Clinical Oncology* 7(11): 1630-1636.

Liu F., Asano N., Tatematsu A., et al. (2012) Plasmablastic lymphoma of the elderly: a clinicopathological comparison with age-related Epstein-Barr virus-associated B cell lymphoproliferative disorder. *Histopathology* 61(6): 1183-1197.

Liu M., Liu B., Liu B., et al. (2015) Human immunodeficiency virus-negative plasmablastic lymphoma: a comprehensive analysis of 114 cases. *Oncology Reports* 33(4): 1615-1620.

Liu Z., Filip I., Gomez K., et al. (2020) Genomic characterization of HIV-associated plasmablastic lymphoma identifies pervasive mutations in the JAK–STAT pathway. *Blood Cancer Discovery* 1(1): 112.

Loghavi S., Alayed K., Aladily T.N., et al. (2015) Stage, age, and EBV status impact outcomes of plasmablastic lymphoma patients: a clinicopathologic analysis of 61 patients. *Journal of Hematology & Oncology* 8: 65-65.

Lopez A. and Abrisqueta P. (2018) Plasmablastic lymphoma: current perspectives. *Blood and Lymphatic Cancer* 8: 63-70.

Lu C.H., Lee K.F., Chen C.C., et al. (2014) Clinical characteristics and treatment outcome in a Taiwanese population of patients with Epstein-Barr virus-positive diffuse large B-cell lymphoma. *Japanese Journal of Clinical Oncology* 44(12): 1164-1171.

Lu T.X., Fan L., Wang L., et al. (2015) MYC or BCL2 copy number aberration is a strong predictor of outcome in patients with diffuse large B-cell lymphoma. *Oncotarget* 6(21): 18374-18388.

Ma H., Wei M.H., Qin H.M., et al. (2017) Long-term survival of primary intracranial plasmablastic lymphoma: case report and review of the literature. *World Neurosurgery* 97: 750 e5750.

Ma Z., Niu J., Cao Y., et al. (2020) Clinical significance of 'double-hit' and 'double-expression' lymphomas. *Journal of Clinical Pathology* 73(3): 126-138.

Machailo J.T. (2016) Diffuse large B-cell lymphoma in adults at Chirs Hani Baragwanath Academic Hospital, Master of Medicine research report. Faculty of Health Sciences, University of the Witwatersrand.

Madden S.K., de Araujo A.D., Gerhardt M., et al. (2021) Taking the Myc out of cancer: toward therapeutic strategies to directly inhibit c-Myc. *Molecular Cancer* 20(1): 3.

Magangane P.S., Mohamed Z. and Naidoo R. (2020) Diffuse large B-cell lymphoma in a high human immunodeficiency virus (HIV) prevalence, low-resource setting. *South African Journal of Oncology* 4(0): a104.

Marini C., Baldaia H., Trigo F., et al. (2016) Transformation of a previously diagnosed diffuse large B-cell lymphoma to plasmablastic lymphoma. *American Journal of Hematology* 91(8): E324.

Marrero W.D., Cruz-Chacon A., Castillo C., et al. (2018) Successful use of bortezomib-lenalidomide combination as treatment for a patient with plasmablastic lymphoma. *Clinical Lymphoma, Myeloma & Leukemia* 18(7): 275-277.

Martin G., Roy J., Barat C., et al. (2007) Human immunodeficiency virus type 1-associated CD40 ligand transactivates B lymphocytes and promotes infection of CD4+ T cells. *Journal of Virology* 81(11): 5872-5881.

Martinez D., Valera A., Perez N.S., et al. (2013) Plasmablastic transformation of low-grade B-cell lymphomas: report on 6 cases. *American Journal of Surgical Pathology* 37(2): 272-281.

Mateyak M., Obaya A. and Sedivy J. (1999) c-Myc regulates cyclin D-Cdk4 and Cdk6 activity but affects cell cycle progression at multiple independent points. *Molecular and Cellular Biology* 19(7): 4672–4683.

Mathews Griner L.A., Guha R., Shinn P., et al. (2014) High-throughput combinatorial screening identifies drugs that cooperate with ibrutinib to kill activated B-cell-like diffuse large B-cell lymphoma cells. *Proceedings of the National Academy of Sciences of the United States of America* 111(6): 2349-2354.

Matikas A., Kanellis G., Papadimitriou C., et al. (2014) Plasmablastic lymphoma of the breast in an immunocompetent patient: long-lasting complete response induced by chemotherapy and autologous stem cell trasplantation. *Anticancer Research* 34(9): 5111-5115.

Matsuki E., Miyakawa Y., Asakawa S., et al. (2011) Identification of loss of p16 expression and upregulation of MDR-1 as genetic events resulting from two novel chromosomal translocations found in a plasmablastic lymphoma of the uterus. *Clinical Cancer Research* 17(8): 2101-2109.

Mauser M., Kruger D., Pather S., et al. (2021) Compromised gut associated lymphoid tissue is a risk factor for postoperative septic complications in HIV-seropositive trauma patients. *World Journal of Surgery* 45(4): 1006-1013.

McLaughlin P., Grillo-López A.J., Link B.K., et al. (1998) Rituximab chimeric anti-CD20 monoclonal antibody therapy for relapsed indolent lymphoma: half of patients respond to a four-dose treatment program. *Journal of Clinical Oncology* 16(8): 2825-2833.

Meer S., Perner Y., McAlpine E.D., et al. (2020) Extraoral plasmablastic lymphomas in a high human immunodeficiency virus endemic area. *Histopathology* 76(2): 212-221.

Meyer P.N., Fu K., Greiner T.C., et al. (2011) Immunohistochemical methods for predicting cell of origin and survival in patients with diffuse large B-cell lymphoma treated with rituximab. *Journal of Clinical Oncology* 29(2): 200-207.

Miao L., Guo N., Feng Y., et al. (2020) High incidence of MYC rearrangement in human immunodeficiency virus-positive plasmablastic lymphoma. *Histopathology* 76(2): 201-211.

Mihashi Y., Mizoguchi M., Takamatsu Y., et al. (2017) c-MYC and its main ubiquitin ligase, FBXW7, influence cell proliferation and prognosis in adult T-cell leukemia/lymphoma. *American Journal of Surgical Pathology* 41(8): 1139-1149.

Miller D., Thomas S., Islam A., et al. (2012) c-Myc and cancer metabolism. *Clinical Cancer Research* 18(20): 5546-5553.

Miller D.V., Mookadam F., Mookadam M., et al. (2007) Primary cardiac plasmablastic (diffuse large B-cell) lymphoma mimicking left ventricular aneurysm with mural thrombus. *Cardiovascular Pathology* 16(2): 111-114.

Miller T.P., Grogan T.M., Dahlberg S., et al. (1994) Prognostic significance of the Ki-67-associated proliferative antigen in aggressive non-Hodgkin's lymphomas: a prospective Southwest Oncology Group Trial. *Blood* 83(6): 1460-1466.

Mine S., Hishima T., Suganuma A., et al. (2017) Interleukin-6-dependent growth in a newly established plasmablastic lymphoma cell line and its therapeutic targets. *Scientific Reports* 7(1): 10188.

Mishra P., Kakri S. and Gujral S. (2017) Plasmablastic transformation of plasma cell myeloma with heterotropic expression of CD3 and CD4: a case report. *Acta Clinica Belgica* 72(4): 250-253.

Mishra P., Pandey C.M., Singh U., et al. (2019) Descriptive statistics and normality tests for statistical data. *Annals of Cardiac Anaesthesia* 22(1): 67-72.

Misra A., Bakhshi S., Kumar R., et al. (2017) Pediatric plasmablastic lymphoma: diagnostic and therapeutic dilemma. *Indian Journal of Pathology and Microbiology* 60(2): 303-304.

Moir S., Chun T.W. and Fauci A.S. (2011) Pathogenic mechanisms of HIV disease. *Annual Review of Pathology* 6: 223-248.

Montes-Moreno S., Gonzalez-Medina A.R., Rodriguez-Pinilla S.M., et al. (2010) Aggressive large B-cell lymphoma with plasma cell differentiation: immunohistochemical characterization of plasmablastic lymphoma and diffuse large B-cell lymphoma with partial plasmablastic phenotype. *Haematologica* 95(8): 1342-1349.

Montes-Moreno S., Martinez-Magunacelaya N., Zecchini-Barrese T., et al. (2017) Plasmablastic lymphoma phenotype is determined by genetic alterations in MYC and PRDM1. *Modern Pathology* 30(1): 85-94.

Morscio J., Dierickx D., Nijs J., et al. (2014) Clinicopathologic comparison of plasmablastic lymphoma in HIV-positive, immunocompetent, and posttransplant patients: single-center series of 25 cases and meta-analysis of 277 reported cases. *American Journal of Surgical Pathology* 38(7): 875-886.

Morton L.M., Kim C.J., Weiss L.M., et al. (2014) Molecular characteristics of diffuse large B-cell lymphoma in human immunodeficiency virus-infected and -uninfected patients in the pre-highly active antiretroviral therapy and pre-rituximab era. *Leukemia and Lymphoma* 55(3): 551-557.

Mounier N., Briere J., Gisselbrecht C., et al. (2003) Rituximab plus CHOP (R-CHOP) overcomes bcl-2--associated resistance to chemotherapy in elderly patients with diffuse large B-cell lymphoma (DLBCL). *Blood* 101(11): 4279-4284.

Mounier N., Spina M., Gabarre J., et al. (2006) AIDS-related non-Hodgkin lymphoma: final analysis of 485 patients treated with risk-adapted intensive chemotherapy. *Blood* 107(10): 3832-3840.

Muris J.J., Meijer C.J., Vos W., et al. (2006) Immunohistochemical profiling based on Bcl-2, CD10 and MUM1 expression improves risk stratification in patients with primary nodal diffuse large B cell lymphoma. *Journal of Pathology* 208(5): 714-723.

Mwazha A., Nhlonzi G.B. and Mazengenya P. (2020) Gastrointestinal tract plasmablastic lymphoma in HIV-infected adults: a histopathological review. *International Journal of Surgical Pathology* 28(7): 735-748.

NAM AIDS map (2021) *HIV-1 and HIV-2*. Available at: https://www.aidsmap.com/about-hiv/hiv-1-and-hiv-2 (accessed 24 January 2021).

Nasta S.D., Carrum G.M., Shahab I., et al. (2002) Regression of a plasmablastic lymphoma in a patient with HIV on highly active antiretroviral therapy. *Leukemia and Lymphoma* 43(2): 423-426.

National Health Laboratory Service (2018) *National Cancer Registry: Cancer in South Africa 2017 - Full report*. Available at: https://www.nicd.ac.za/centres/national-cancer-registry/ (accessed 19 January 2021).

Nguyen L., Papenhausen P. and Shao H. (2017) The role of c-MYC in B-cell lymphomas: diagnostic and molecular aspects. *Genes* 8(4): 116.

Niedobitek G., Agathanggelou A., Herbst H., et al. (1997) Epstein-Barr virus (EBV) infection in infectious mononucleosis: virus latency, replication and phenotype of EBV-infected cells. *Journal of Pathology* 182(2): 151-159.

Nitta H., Hauss-Wegrzyniak B., Lehrkamp M., et al. (2008) Development of automated brightfield double in situ hybridization (BDISH) application for HER2 gene and chromosome 17 centromere (CEN 17) for breast carcinomas and an assay performance comparison to manual dual color HER2 fluorescence in situ hybridization (FISH). *Diagnostic Pathology* 3(1): 41.

Noy A., Lensing S.Y., Moore P.C., et al. (2016) Plasmablastic lymphoma is treatable in the HAART era. A 10 year retrospective by the AIDS Malignancy Consortium. *Leukemia and Lymphoma* 57(7): 1731-1734.

Nwanze J., Siddiqui M.T., Stevens K.A., et al. (2017) MYC immunohistochemistry predicts MYC rearrangements by FISH. *Frontiers in Oncology* 7: 209-209.

Nyman H., Adde M., Karjalainen-Lindsberg M.L., et al. (2007) Prognostic impact of immunohistochemically defined germinal center phenotype in diffuse large B-cell lymphoma patients treated with immunochemotherapy. *Blood* 109(11): 4930-4935.

O'Conor G.T. (1961) Malignant lymphoma in African children. II. A pathological entity. *Cancer* 14: 270-283.

O'Conor G.T. and Davies J.N. (1960) Malignant tumors in African children. With special reference to malignant lymphoma. *Journal of Pediatrics* 56: 526-535.

O'Donnell K.A., Wentzel E.A., Zeller K.I., et al. (2005) c-Myc-regulated microRNAs modulate E2F1 expression. *Nature* 435(7043): 839-843.

Ok C.Y., Li L. and Young K.H. (2015) EBV-driven B-cell lymphoproliferative disorders: from biology, classification and differential diagnosis to clinical management. *Experimental and Molecular Medicine* 47: 1-14.

Olszewski A.J., Winer E.S. and Castillo J.J. (2015) Validation of clinical prognostic indices for diffuse large B-cell lymphoma in the National Cancer Data Base. *Cancer Causes and Control* 26(8): 1163-1172.

Oschlies I., Klapper W., Zimmermann M., et al. (2006) Diffuse large B-cell lymphoma in pediatric patients belongs predominantly to the germinal-center type B-cell lymphomas: a clinicopathologic analysis of cases included in the German BFM (Berlin-Frankfurt-Münster) Multicenter Trial. *Blood* 107(10): 4047-4052.

Ott G., Rosenwald A. and Campo E. (2013) Understanding *MYC*-driven aggressive B-cell lymphomas: pathogenesis and classification. *Blood* 122: 575-583.

Ott G., Ziepert M., Klapper W., et al. (2010) Immunoblastic morphology but not the immunohistochemical GCB/nonGCB classifier predicts outcome in diffuse large B-cell lymphoma in the RICOVER-60 trial of the DSHNHL. *Blood* 116(23): 4916-4925.

Ouansafi I., He B., Fraser C., et al. (2010) Transformation of follicular lymphoma to plasmablastic lymphoma with c-myc gene rearrangement. *American Journal of Clinical Pathology* 134(6): 972-981.

Painschab M.S., Kasonkanji E., Zuze T., et al. (2019) Mature outcomes and prognostic indices in diffuse large B-cell lymphoma in Malawi: a prospective cohort. *British Journal of Haematology* 184(3): 364-372.

Pan Z., Chen M., Zhang Q., et al. (2018) CD3-positive plasmablastic B-cell neoplasms: a diagnostic pitfall. *Modern Pathology* 31(5): 718-731.

Pan Z., Xie Q., Repertinger S., et al. (2013) Plasmablastic transformation of low-grade CD5+ B-cell lymphoproliferative disorder with MYC gene rearrangements. *Human Pathology* 44(10): 2139-2148.

Parkin D.M., Sitas F., Chirenje M., et al. (2008) Part I: Cancer in Indigenous Africans--burden, distribution, and trends. *Lancet Oncology* 9(7): 683-692.

Pasqualucci L., Bhagat G., Jankovic M., et al. (2008) AID is required for germinal center-derived lymphomagenesis. *Nature Genetics* 40(1): 108-112.

Pasqualucci L., Trifonov V., Fabbri G., et al. (2011) Analysis of the coding genome of diffuse large B-cell lymphoma. *Nature Genetics* 43(9): 830-837.

Patel M. (2007) The impact of HIV on non-Hodgkin's lymphoma at Chris Hani Baragwanath Hospital. *Haematologica* 92(273).

Patel M., Philip V., Omar T., et al. (2015) The impact of human immunodeficiency virus infection (HIV) on lymphoma in South Africa. *Journal of Cancer Therapy* 6: 527-535.

Pather S., MacKinnon D. and Padayachee R.S. (2013a) Plasmablastic lymphoma in pediatric patients: clinicopathologic study of three cases. *Annals of Diagnostic Pathology* 17(1): 80-84.

Pather S., Mohamed Z., McLeod H., et al. (2013b) Large cell lymphoma: correlation of HIV status and prognosis with differentiation profiles assessed by immunophenotyping. *Pathology Oncology Research* 19(4): 695-705.

Pather S., Philip V., Lakha A., et al. (2015) An expanded spectrum of high-grade B-cell non-Hodgkin lymphomas Involving the cervicovaginal region. *International Journal of Gynecological Pathology* 34: 1.

Perez-Roger I., Solomon D., Sewing A., et al. (1997) Myc activation of cyclin E/Cdk2 kinase involves induction of cyclin E gene transcription and inhibition of p27(Kip1) binding to newly formed complexes. *Oncogene* 14: 2373–2381.

Perry A.M., Alvarado-Bernal Y., Laurini J.A., et al. (2014) MYC and BCL2 protein expression predicts survival in patients with diffuse large B-cell lymphoma treated with rituximab. *British Journal of Haematology* 165(3): 382-391.

Persson H. and Leder P. (1984) Nuclear localization and DNA binding properties of a protein expressed by human c-myc oncogene. *Science* 225(4663): 718.

Philipp A., Schneider A., Vasrik I., et al. (1994) Repression of cyclin D1: a novel function of MYC. *Molecular and Cellular Biology* 14(6): 4032-4043.

Pinnix C.C., Shah J.J., Chuang H., et al. (2016) Doxorubicin-based chemotherapy and radiation therapy produces favorable outcomes in limited-stage plasmablastic lymphoma: a single-institution review. *Clinical Lymphoma, Myeloma & Leukemia* 16(3): 122-128.

Popovic M., Tenner-Racz K., Pelser C., et al. (2005) Persistence of HIV-1 structural proteins and glycoproteins in lymph nodes of patients under highly active antiretroviral therapy. *Proceedings of the National Academy of Sciences of the United States of America* 102(41): 14807-14812.

Powles T., Matthews G. and Bower M. (2000) AIDS related systemic non-Hodgkin's lymphoma. *Sexually Transmitted Infections* 76(5): 335-341.

Pretscher D., Kalisch A., Wilhelm M., et al. (2017) Refractory plasmablastic lymphoma-a review of treatment options beyond standard therapy. *Annals of Hematology* 96(6): 967-970.

Qing X., Enbom E., Qing A., et al. (2016) Plasmablastic lymphoma presenting as a large intracardiac mass and bilateral pleural effusions. *Experimental and Molecular Pathology* 100(1): 79-81.

Rabkin C. (1994) Epidemiology of AIDS-related malignancies. *Current Opinion in Oncology* 6: 492–496.

Radhakrishnan R., Suhas S., Kumar R.V., et al. (2005) Plasmablastic lymphoma of the oral cavity in an HIV-positive child. *Oral Surgery, Oral Medicine, Oral Pathology, Oral Radiology and Endodontics* 100(6): 725-731.

Rafaniello Raviele P., Pruneri G. and Maiorano E. (2009) Plasmablastic lymphoma: a review. *Oral Diseases* 15(1): 38-45.

Ramalingam P., Nayak-Kapoor A., Reid-Nicholson M., et al. (2008) Plasmablastic lymphoma with small lymphocytic lymphoma: clinico-pathologic features, and review of the literature. *Leukemia and Lymphoma* 49(10): 1999-2002.

Ramburan A., Kriel R. and Govender D. (2022) Plasmablastic lymphomas show restricted EBV latency profile and MYC gene aberrations. *Leukemia and Lymphoma* 63(2): 370-376.

Ramos J.C., Sparano J.A., Chadburn A., et al. (2020) Impact of Myc in HIV-associated non-Hodgkin lymphomas treated with EPOCH and outcomes with vorinostat (AMC-075 trial). *Blood* 136(11): 1284-1297.

Regidor D.L., Detels R., Breen E.C., et al. (2011) Effect of highly active antiretroviral therapy on biomarkers of B-lymphocyte activation and inflammation. *AIDS* 25(3): 303-314.

Ribera J.M., Oriol A., Morgades M., et al. (2008) Safety and efficacy of cyclophosphamide, adriamycin, vincristine, prednisone and rituximab in patients with human immunodeficiency virus-associated diffuse large B-cell lymphoma: results of a phase II trial. *British Journal of Haematology* 140(4): 411-419.

Robak T., Urbanska-Rys H., Strzelecka B., et al. (2001) Plasmablastic lymphoma in a patient with chronic lymphocytic leukemia heavily pretreated with cladribine (2-CdA): an unusual variant of Richter's syndrome. *European Journal of Haematology* 67(5-6): 322-327.

Robbiani D.F., Bothmer A., Callen E., et al. (2008) AID is required for the chromosomal breaks in c-myc that lead to c-myc/IgH translocations. *Cell* 135(6): 1028-1038.

Robbiani D.F., Bunting S., Feldhahn N., et al. (2009) AID produces DNA double-strand breaks in non-Ig genes and mature B cell lymphomas with reciprocal chromosome translocations. *Molecular Cell* 36(4): 631-641.

Rodrigues-Fernandes C.I., de Souza L.L., Santos-Costa S.F.D., et al. (2018) Clinicopathological analysis of oral plasmablastic lymphoma: A systematic review. *Journal of Oral Pathology and Medicine* 47(10): 915-922.

Romero M., Gonzalez-Fontal G.R., Saavedra C., et al. (2016) Primary CNS plasmablastic lymphoma in an HIV/EBV negative patient: A case report. *Diagnostic Cytopathology* 44(1): 61-65.

Rosenwald A., Bens S., Advani R., et al. (2019) Prognostic significance of MYC rearrangement and translocation partner in diffuse large B-cell lymphoma: A study by the Lunenburg Lymphoma Biomarker Consortium. *Journal of Clinical Oncology* 37(35): 3359-3368.

Rosenwald A., Wright G., Chan W.C., et al. (2002) The use of molecular profiling to predict survival after chemotherapy for diffuse large-B-cell lymphoma. *New England Journal of Medicine* 346(25): 1937-1947.

Rosenwald A., Wright G., Leroy K., et al. (2003) Molecular diagnosis of primary mediastinal B cell lymphoma identifies a clinically favorable subgroup of diffuse large B cell lymphoma related to Hodgkin lymphoma. *Journal of Experimental Medicine* 198(6): 851-862.

Rudresha A.H., Lakshmaiah K.C., Agarwal A., et al. (2017) Plasmablastic lymphoma in immunocompetent and in immunocompromised patients: Experience at a regional cancer centre in India. *South Asian Journal of Cancer* 6(2): 69-71.

Ruppert A.S., Dixon J.G., Salles G., et al. (2020) International prognostic indices in diffuse large B-cell lymphoma: a comparison of IPI, R-IPI, and NCCN-IPI. *Blood* 135(23): 2041-2048.

Ryan K.M. and Birnie G.D. (1996) Myc oncogenes: the enigmatic family. *Biochemical Journal* 314(Pt 3): 713-721.

Saba N.S., Dang D., Saba J., et al. (2013) Bortezomib in plasmablastic lymphoma: a case report and review of the literature. *Onkologie* 36(5): 287-291.

Said J., Cesarman E., Rosenwald A., et al. (2017) Lymphomas associated with HIV infection. In: Swerdlow SH, Campo E, Harris NL, et al. (eds) *WHO classification of tumours of haematopoietic and lymphoid tissues*. Revised 4th ed. IARC: Lyon, pp. 440-452.

Sakamuro D. and Prendergast G.C. (1999) New Myc-interacting proteins: a second Myc network emerges. *Oncogene* 18(19): 2942-2954.

Salghetti S.E., Kim S.Y. and Tansey W.P. (1999) Destruction of Myc by ubiquitin-mediated proteolysis: cancer-associated and transforming mutations stabilize Myc. *European Molecular Biology Organization Journal* 18(3): 717-726.

Salles G., de Jong D., Xie W., et al. (2011) Prognostic significance of immunohistochemical biomarkers in diffuse large B-cell lymphoma: a study from the Lunenburg Lymphoma Biomarker Consortium. *Blood* 117(26): 7070-7078.

Sander S., Bullinger L., Klapproth K., et al. (2008) MYC stimulates EZH2 expression by repression of its negative regulator miR-26a. *Blood* 112: 4202–4212.

Sarode S.C., Sarode G.S. and Patil A. (2010) Plasmablastic lymphoma of the oral cavity: a review. *Oral Oncology* 46(3): 146-153.

Savage K.J., Johnson N.A., Ben-Neriah S., et al. (2009) MYC gene rearrangements are associated with a poor prognosis in diffuse large B-cell lymphoma patients treated with R-CHOP chemotherapy. *Blood* 114(17): 3533-3537.

Scala G, Ruocco MR, Ambrosino C, et al. (1994) The expression of the interleukin 6 gene is induced by the human immunodeficiency virus 1 TAT protein. *Journal of Experimental Medicine* 179(3): 961-971.

Schmit J.M., DeLaune J., Norkin M., et al. (2017) A Case of Plasmablastic Lymphoma Achieving Complete Response and Durable Remission after Lenalidomide-Based Therapy. *Oncology Research and Treatment* 40(1-2): 46-48.

Schmitz R., Wright G.W., Huang D.W., et al. (2018) Genetics and pathogenesis of diffuse large B-cell lymphoma. *New England Journal of Medicine* 378(15): 1396-1407.

Scholzen T. and Gerdes J. (2000) The Ki-67 protein: from the known and the unknown. *Journal of Cellular Physiology* 182(3): 311-322.

Schommers P., Hentrich M., Hoffmann C., et al. (2015) Survival of AIDS-related diffuse large B-cell lymphoma, Burkitt lymphoma, and plasmablastic lymphoma in the German HIV Lymphoma Cohort. *British Journal of Haematology* 168(6): 806-810.

Scott D.W., Wright G.W., Williams P.M., et al. (2014) Determining cell-of-origin subtypes of diffuse large B-cell lymphoma using gene expression in formalin-fixed paraffin-embedded tissue. *Blood* 123(8): 1214-1217.

Sehn L.H. (2012) Paramount prognostic factors that guide therapeutic strategies in diffuse large B-cell lymphoma. *Hematology American Society Hematology Education Program.* 2012(1): 402-409.

Sehn L.H., Berry B., Chhanabhai M., et al. (2006) The revised International Prognostic Index (R-IPI) is a better predictor of outcome than the standard IPI for patients with diffuse large B-cell lymphoma treated with R-CHOP. *Blood* 109(5): 1857-1861.

Shah B.K., Bista A. and Shafii B. (2014) Survival in advanced diffuse large B-cell lymphoma in pre- and post-rituximab eras in the United States. *Anticancer Research* 34(9): 5117-5120.

Sharp P.M. and Hahn B.H. (2011) Origins of HIV and the AIDS pandemic. *Cold Spring Harbor Perspectives in Medicine* 1(1): 6841.

Sheiness D. and Bishop J.M. (1979) DNA and RNA from uninfected vertebrate cells contain nucleotide sequences related to the putative transforming gene of avian myelocytomatosis virus. *Journal of Virology* 31(2): 514-521.

Shi J., Bodo J., Zhao X., et al. (2019) SLAMF7 (CD319/CS1) is expressed in plasmablastic lymphoma and is a potential diagnostic marker and therapeutic target. *British Journal of Haematology* 185(1): 145-147.

Shiels M.S., Islam J.Y., Rosenberg P.S., et al. (2018) Projected cancer incidence rates and burden of incident cancer cases in HIV-infected adults in the United States through 2030. *Annals of Internal Medicine* 168(12): 866-873.

Shim H., Chun Y., Lewis B., et al. (1998) A unique glucose-dependent apoptotic pathway induced by c-Myc. *Proceedings of the National Academy of Sciences of the United States of America* 95(4): 1511–1516.

Shim H., Dolde C., Lewis B., et al. (1997) c-Myc transactivation of LDH-A: implications for tumor metabolism and growth. *Proceedings of the National Academy of Sciences of the United States of America* 94: 6658–6663.

Shponka V., Reveles C.Y., Alam S., et al. (2020) Frequent expression of activation-induced cytidine deaminase in diffuse large B-cell lymphoma tissues from persons living with HIV. *AIDS* 34(14): 2025-2035.

Shuangshoti S., Assanasen T., Lerdlum S., et al. (2008) Primary central nervous system plasmablastic lymphoma in AIDS. *Neuropathology and Applied Neurobiology* 34(2): 245-247.

Siegel R.L., Miller K.D. and Jemal A. (2020) Cancer statistics, 2020. *CA: A Cancer Journal for Clinicians* 70(1): 7-30.

Sixbey J.W., Nedrud J.G., Raab-Traub N., et al. (1984) Epstein-Barr virus replication in oropharyngeal epithelial cells. *New England Journal of Medicine* 310(19): 1225-1230.

Smith C.J., Ryom L., Weber R., et al. (2014) Trends in underlying causes of death in people with HIV from 1999 to 2011 (D:A:D): a multicohort collaboration. *Lancet* 384(9939): 241-248.

Snuderl M., Kolman O.K., Chen Y.B., et al. (2010) B-cell lymphomas with concurrent IGH-BCL2 and MYC rearrangements are aggressive neoplasms with clinical and pathologic features distinct from Burkitt lymphoma and diffuse large B-cell lymphoma. *American Journal of Surgical Pathology* 34(3): 327-340.

Sonet A. and Bosly A. (2009) Rituximab and chemotherapy in diffuse large B-cell lymphoma. *Expert Review of Anticancer Therapy* 9(6): 719-726.

Soucek L., Whitfield J., Martins C.P., et al. (2008) Modelling Myc inhibition as a cancer therapy. *Nature* 455: 679–683.

Spencer C.A. and Groudine M. (1991) Control of c-myc regulation in normal and neoplastic cells. *Advances in Cancer Research* 56: 1-48.

Staiger A.M., Ziepert M., Horn H., et al. (2017) Clinical impact of the cell-of-origin classification and the MYC/ BCL2 dual expresser status in diffuse large B-cell lymphoma treated within prospective clinical trials of the German High-Grade Non-Hodgkin's Lymphoma Study Group. *Journal of Clinical Oncology* 35(22): 2515-2526.

Stasik C.J., Nitta H., Zhang W., et al. (2010) Increased MYC gene copy number correlates with increased mRNA levels in diffuse large B-cell lymphoma. *Haematologica* 95(4): 597-603.

Sterne J.A., May M., Costagliola D., et al. (2009) Timing of initiation of antiretroviral therapy in AIDS-free HIV-1-infected patients: a collaborative analysis of 18 HIV cohort studies. *Lancet* 373(9672): 1352-1363.

Sugimoto K., Koike H. and Esa A. (2011) Plasmablastic lymphoma of the right testis. *International Journal of Urology* 18(1): 85-86.

Sun J., Medeiros L.J., Lin P., et al. (2011) Plasmablastic lymphoma involving the penis: a previously unreported location of a case with aberrant CD3 expression. *Pathology* 43(1): 54-57.

Suzuki Y., Yoshida T., Nakamura N., et al. (2010) CD3- and CD4-positive plasmablastic lymphoma: a literature review of Japanese plasmablastic lymphoma cases. *Internal Medicine* 49(16): 1801-1805.

Swerdlow S.H., Campo E., Pileri S.A., et al. (2016) The 2016 revision of the World Health Organization classification of lymphoid neoplasms. *Blood* 127(20): 2375-2390.

Sylla B. and Wild C. (2012) A million Africans a year dying from cancer by 2030: what can cancer research and control offer to the continent? *International Journal of Cancer* 130: 245-250.

Taddesse-Heath L., Meloni-Ehrig A., Scheerle J., et al. (2010) Plasmablastic lymphoma with MYC translocation: evidence for a common pathway in the generation of plasmablastic features. *Modern Pathology* 23(7): 991-999.

Tan C.R., Barta S.K., Lensing S.Y., et al. (2019) A multicenter, open-label feasibility study of daratumumab with dose-adjusted EPOCH in newly diagnosed plasmablastic lymphoma: AIDS Malignancy Consortium 105. *Blood* 134(Supplement_1): 1595-1595.

Tan Q., Zhu Y., Li J., et al. (2013) Structure of the CCR5 chemokine receptor-HIV entry inhibitor maraviroc complex. *Science* 341(6152): 1387-1390.

Tansey W.P. (2014) Mammalian MYC Proteins and Cancer. *New Journal of Science* 2014: 27.

Taub R., Kirsch I., Morton C., et al. (1982) Translocation of the c-myc gene into the immunoglobulin heavy chain locus in human Burkitt lymphoma and murine plasmacytoma cells. *Proceedings of the National Academy of Sciences of the United States of America* 79(24): 7837.

Tchernonog E., Faurie P., Coppo P., et al. (2017) Clinical characteristics and prognostic factors of plasmablastic lymphoma patients: analysis of 135 patients from the LYSA group. *Annals of Oncology* 28(4): 843-848.

Teruya-Feldstein J., Chiao E., Filippa D.A., et al. (2004) CD20-negative large-cell lymphoma with plasmablastic features: a clinically heterogenous spectrum in both HIV-positive and -negative patients. *Annals of Oncology* 15(11): 1673-1679.

Testoni M., Kwee I., Greiner T.C., et al. (2011) Gains of MYC locus and outcome in patients with diffuse large B-cell lymphoma treated with R-CHOP. *British Journal of Haematology* 155(2): 274-277.

Todorović-Raković N., Jovanović D., Nesković-Konstantinović Z., et al. (2007) Prognostic value of HER2 gene amplification detected by chromogenic in situ hybridization (CISH) in metastatic breast cancer. *Experimental and Molecular Pathology* 82(3): 262-268.

Totonchy J. and Cesarman E. (2016) Does persistent HIV replication explain continued lymphoma incidence in the era of effective antiretroviral therapy? *Current Opinion in Virology* 20: 71-77.

Tzankov A., Brunhuber T., Gschwendtner A., et al. (2005) Incidental oral plasmablastic lymphoma with aberrant expression of CD4 in an elderly HIV-negative patient: how a gingival polyp can cause confusion. *Histopathology* 46(3): 348-350.

Tzankov A., Xu-Monette Z.Y., Gerhard M., et al. (2014) Rearrangements of MYC gene facilitate risk stratification in diffuse large B-cell lymphoma patients treated with rituximab-CHOP. *Modern Pathology* 27(7): 958-971.

UNAIDS (2016) *Prevention Gap Report.* Available at: www.unaids.org/en/resources/documents/2016/prevention-gap (accessed 7 August 2017).

UNAIDS (2021) *AIDS 2020 report*. Available at: https://aids2020.unaids.org/report/ (accessed 23 January 2021).

Urrego P.A., Smethurst M., Fowkes M., et al. (2011) Primary CNS plasmablastic lymphoma: report of a case with CSF cytology, flow cytometry, radiology, histological correlation, and review of the literature. *Diagnostic Cytopathology* 39(8): 616-620.

Ustun C., Reid-Nicholson M., Nayak-Kapoor A., et al. (2009) Plasmablastic lymphoma: CNS involvement, coexistence of other malignancies, possible viral etiology, and dismal outcome. *Annals of Hematology* 88(4): 351-358.

Valdez H. and Lederman M.M. (1997) Cytokines and cytokine therapies in HIV infection. *AIDS Clinical Review*. 187-228.

Valentino C., Kendrick S., Johnson N., et al. (2013) Colorimetric in situ hybridization identifies MYC gene signal clusters correlating with increased copy number, mRNA, and protein in diffuse large B-cell lymphoma. *American Journal of Clinical Pathology* 139(2): 242-254.

Valera A., Balague´ O., Colomo L., et al. (2010) IG/MYC rearrangements are the main cytogenetic alteration in plasmablastic lymphomas. *American Journal of Surgical Pathology* 34: 1686-1694.

Vardhana S.A., Sauter C.S., Matasar M.J., et al. (2017) Outcomes of primary refractory diffuse large B-cell lymphoma (DLBCL) treated with salvage chemotherapy and intention to transplant in the rituximab era. *British Journal of Haematology* 176(4): 591-599.

Vaubell J.I., Sing Y., Ramburan A., et al. (2014) Pediatric plasmablastic lymphoma: a clinicopathologic study. *International Journal of Surgical Pathology* 22(7): 607-616.

Vega F., Chang C.C., Medeiros L.J., et al. (2005) Plasmablastic lymphomas and plasmablastic plasma cell myelomas have nearly identical immunophenotypic profiles. *Modern Pathology* 18(6): 806-815.

Vendrame E., Hussain S.K., Breen E.C., et al. (2014) Serum levels of cytokines and biomarkers for inflammation and immune activation, and HIV-associated non-Hodgkin B-cell lymphoma risk. *Cancer Epidemiology, Biomarkers and Prevention* 23(2): 343-349.

Vennstrom B., Sheiness D., Zabielski J., et al. (1982) Isolation and characterization of c-myc, a cellular homolog of the oncogene (v-myc) of avian myelocytomatosis virus strain 29. *Journal of Virology* 42(3): 773-779.

Visco C., Tzankov A., Xu-Monette Z.Y., et al. (2013) Patients with diffuse large B-cell lymphoma of germinal center origin with BCL2 translocations have poor outcome, irrespective of MYC status: a report from an International DLBCL rituximab-CHOP Consortium Program Study. *Haematologica* 98(2): 255-263.

Wang D., Zheng Y., Zeng D., et al. (2017) Clinicopathologic characteristics of HIV/AIDS-related plasmablastic lymphoma. *International Journal of STD and AIDS* 28(4): 380-388.

Wang J., Hernandez O.J. and Sen F. (2008) Plasmablastic lymphoma involving breast: a case diagnosed by fine-needle aspiration and core needle biopsy. *Diagnostic Cytopathology* 36(4): 257-261.

Wang X.J., Medeiros L.J., Lin P., et al. (2015) MYC cytogenetic status correlates with expression and has prognostic significance in patients with MYC/BCL2 protein double-positive diffuse large B-cell lymphoma. *American Journal of Surgical Pathology* 39(9): 1250-1258.

Wise D.R., Deberardinis R.J., Mancuso A., et al. (2008) Myc regulates a transcriptional program that stimulates mitochondrial glutaminolysis and leads to glutamine addiction. *Proceedings of the National Academy of Sciences of the United States of America* 105(48): 18782–18787.

Witte H.M., Hertel N., Merz H., et al. (2020) Clinicopathological characteristics and MYC status determine treatment outcome in plasmablastic lymphoma: a multi-center study of 76 consecutive patients. *Blood Cancer Journal* 10(5): 63.

Wolff A.C., Hammond M.E.H., Allison K.H., et al. (2018) Human epidermal growth factor receptor 2 testing in breast cancer: American Society of Clinical Oncology/College of American Pathologists clinical practice guideline focused update. *Journal of Clinical Oncology* 36(20): 2105-2122.

World Health Organisation (2012) *Understanding the modes of transmission model of new HIV infection and its use in prevention planning*. Available at: https://www.who.int/bulletin/volumes/90/11/12-102574/en/ (accessed 15 August 2020).

World Health Organisation (2016) *Progress report 2016: Prevent HIV, test and treat all*. Available at: http://www.who.int/hiv/pub/progressreports/2016-progress-report/en/ (accessed 6 October 2017).

World Health Organisation (2017) *Global Health Observatory (GHO) data HIV/AIDS*. Available at: http://www.who.int/gho/hiv/en/ (accessed 3 August 2017).

World Health Organization (2018) *Cancer*. Available at: https://www.who.int/news-room/fact-sheets/detail/cancer (accessed 19 January 2021).

World Health Organization (2020) *The Global Cancer Observatory: All cancers fact sheet*. Available at: https://gco.iarc.fr/today/data/factsheets/cancers/39-All-cancers-fact-sheet.pdf (accessed 19 January 2021).

Wright G.W., Huang D.W., Phelan J.D., et al. (2020) A Probabilistic Classification Tool for Genetic Subtypes of Diffuse Large B Cell Lymphoma with Therapeutic Implications. *Cancer Cell* 37(4): 551-568.e514.

Yan M., Dong Z., Zhao F., et al. (2014) CD20-positive plasmablastic lymphoma with excellent response to bortezomib combined with rituximab. *European Journal of Haematology* 93(1): 77-80.

Yanamandra U., Sahu K.K., Jain N., et al. (2016) Plasmablastic lymphoma: successful management with CHOP and lenalidomide in resource constraint settings. *Annals of Hematology* 95(10): 1715-1717.

Yano T., Jaffe E.S., Longo D.L., et al. (1992) MYC rearrangements in histologically progressed follicular lymphoma. *Blood* 80: 758–767.

Yao Q.Y., Rickinson A.B. and Epstein M.A. (1985) A re-examination of the Epstein-Barr virus carrier state in healthy seropositive individuals. *International Journal of Cancer* 35(1): 35-42.

Ye Q., Xu-Monette Z.Y., Tzankov A., et al. (2016) Prognostic impact of concurrent MYC and BCL6 rearrangements and expression in de novo diffuse large B-cell lymphoma. *Oncotarget* 7(3): 2401-2416.

Yoon D.H., Choi D.R., Ahn H.J., et al. (2010) Ki-67 expression as a prognostic factor in diffuse large B-cell lymphoma patients treated with rituximab plus CHOP. *European Journal of Haematology* 85(2): 149-157.

Yoon S.O., Jeon Y.K., Paik J.H., et al. (2008) MYC translocation and an increased copy number predict poor prognosis in adult diffuse large B-cell lymphoma (DLBCL), especially in germinal centre-like B cell (GCB) type. *Histopathology* 53(2): 205-217.

Zaiem F., Jerbi R., Albanyan O., et al. (2020) High Ki67 proliferation index but not cell-of-origin subtypes is associated with shorter overall survival in diffuse large B-cell lymphoma. *Avicenna Journal of Medicine* 10(4): 241-248.

Zarifi C., Deutsch S., Dullet N., et al. (2018) An enlarging pacemaker pocket: A case report of a plasmablastic lymphoma arising as a primary tumor around a cardiac pacemaker and systematic literature review of various malignancies arising at the pacemaker pocket. *Journal of Cardiology Cases* 17(2): 41-43.

Zech L., Haglund U., Nilsson K., et al. (1976) Characteristic chromosomal abnormalities in biopsies and lymphoid-cell lines from patients with Burkitt and non-Burkitt lymphomas. *International Journal of Cancer* 17(1): 47-56.

Zhang L.Y., Lin H.Y., Gao L.X., et al. (2012) Primary central nervous system plasmablastic lymphoma presenting in human immunodeficiency virus-negative but Epstein-Barr virus-positive patient: a case report. *Diagnostic Pathology* 7: 51.

Zhou F., Xu D., Cao Y., et al. (2014) c-MYC aberrations as prognostic factors in diffuse large B-cell lymphoma: A meta-analysis of epidemiological studies. *PloS One* 9(4): e95020.

Zhu T., Korber B.T., Nahmias A.J., et al. (1998) An African HIV-1 sequence from 1959 and implications for the origin of the epidemic. *Nature* 391(6667): 594-597.

Ziepert M., Hasenclever D., Kuhnt E., et al. (2010) Standard International prognostic index remains a valid predictor of outcome for patients with aggressive CD20+ B-cell lymphoma in the rituximab era. *Journal of Clinical Oncology* 28(14): 2373-2380.

Zimmermann H., Oschlies I., Fink S., et al. (2012) Plasmablastic posttransplant lymphoma: cytogenetic aberrations and lack of Epstein-Barr virus association linked with poor outcome in the prospective German Posttransplant Lymphoproliferative Disorder Registry. *Transplantation* 93(5): 543-550.

Zoufaly A., Stellbrink H.J., Heiden M.A., et al. (2009) Cumulative HIV viremia during highly active antiretroviral therapy is a strong predictor of AIDS-related lymphoma. *Journal of Infectious Diseases* 200(1): 79-87.

Zuze T., Painschab M.S., Seguin R., et al. (2018) Plasmablastic lymphoma in Malawi. *Infectious Agents and Cancer* 13: 22.

APPENDICES

I: Ethics certificates

R14/49 Dr Sugeshnee Pather et al

HUMAN RESEARCH ETHICS COMMITTEE (MEDICAL)

CLEARANCE CERTIFICATE NO. M151017

NAME: (Principal Investigator)	Dr Sugeshnee Pather et al
DEPARTMENT:	Anatomical Pathology Chris Hani Baragwanath Academic Hospital National Health Laboratory Service
PROJECT TITLE:	Prognostic Influence of MYC Aberrations and other Clinicopathological Factors of High Grade B-Cell Non-Hodgkin Lymphomas in Adult and Paediatric Patients
DATE CONSIDERED:	30/10/2015
DECISION:	Approved unconditionally
CONDITIONS:	
SUPERVISOR:	Prof Moosa Patel and Prof Martin Hale
APPROVED BY:	Professor P Cleaton-Jones, Chairperson, HREC (Medical)
DATE OF APPROVAL:	02/03/2016

This clearance certificate is valid for 5 years from date of approval. Extension may be applied for.

DECLARATION OF INVESTIGATORS

To be completed in duplicate and **ONE COPY** returned to the Research Office Secretary in Room 10004, 10th floor, Senate House/2nd Floor, Phillip Tobias Building, Parktown, University of the Witwatersrand. I/we fully understand the conditions under which I am/we are authorized to carry out the above-mentioned research and I/we undertake to ensure compliance with these conditions. Should any departure be contemplated, from the research protocol as approved, I/we undertake to resubmit the application to the Committee. **I agree to submit a yearly progress report**.

Principal Investigator Signature Date 10/03/2016

UNIVERSITY OF THE
WITWATERSRAND,
JOHANNESBURG

R14/49 Dr S Pather

HUMAN RESEARCH ETHICS COMMITTEE (MEDICAL)
CLEARANCE CERTIFICATE NO. M2010122

NAME: **(Principal Investigator)**	Dr S Pather
DEPARTMENT:	School of Pathology Department of Anatomical Pathology Medical School University
PROJECT TITLE:	The prognostic influence of c-MYC aberrations and other clinicopathological factors of high-grade B-cell non-Hodgkin lymphomas
DATE CONSIDERED:	Ad hoc
DECISION:	Approved unconditionally
CONDITIONS:	Renewal of M151017
SUPERVISOR:	Professor M Patel
APPROVED BY:	CB Penny Dr CB Penny, Chairperson, HREC (Medical)
DATE OF APPROVAL:	2020/11/11

This clearance certificate is valid for 5 years from the date of approval. Extension may be applied for.

II: Title amendments

UNIVERSITY OF THE WITWATERSRAND, JOHANNESBURG

Private Bag 3 Wits, 2050
Fax: 027117172119
Tel: 02711 7172076

Reference: Mrs Sandra Benn
E-mail: sandra.benn@wits.ac.za

04 January 2019
Person No: 9703787W
PAG

Dear Dr Sugeshnee Pather

Doctor of Philosophy: Approval of Title

We have pleasure in advising that your proposal entitled *The prognostic influence of c-MYC aberrations and other clinicopathological factors of high-grade B-cell non-Hodgkin lymphomas* has been approved. Please note that any amendments to this title have to be endorsed by the Faculty's higher degrees committee and formally approved.

Yours sincerely

Mrs Sandra Benn
Faculty Registrar
Faculty of Health Sciences

UNIVERSITY OF THE
WITWATERSRAND,
JOHANNESBURG

Private Bag 3 Wits, 2050
Fax: 027117172119
Tel: 02711 7172076

Reference: Mrs Sandra Benn
E-mail: sandra.benn@wits.ac.za

04 March 2022
Person No: 9703787W
TAA

Dear Dr Sugeshnee Pather

Doctor of Philosophy: Change of title of research

I am pleased to inform you that the following change in the title of your Thesis for the degree of **Doctor of Philosophy** has been approved:

From:	**Prognostic influence of c-MYC aberrations and other clinicopathological factors of high-grade B-cell non-Hodgkin lymphomas.**
To:	**Prognostic influence of MYC aberrations and other clinicopathological factors of aggressive B-cell non-Hodgkin lymphomas.**

Yours sincerely

Mrs Sandra Benn
Faculty Registrar
Faculty of Health Sciences

III. DLBCL data collection spreadsheet

DIFFUSE LARGE B-CELL LYMPHO	DLBCL		DATA CAPTURE SHEET												
Linked code	AGE at dx YEARS	GENDER MALE (M) FEMALE (F)	RVD Reactive (P) Non reactive(N) Unknown (U)	CD4 cour VIRAL LOAD		NHL STAGE	BONE MARROW INFILTRATION P+ N-	TREATMENT c-ART; CHOP; RCHOP; RCHOEP	IPI 0-2 / 3-5	DATE of LYMPHOMA DIAGNOSIS	FOLLOW UP DURATION	SURVIVAL OUTCOME DEMISED (D) ALIVE (A) UNKNOWN (U)	DURATION of SURVIVAL in DAYS	CONCOMITTANT CONDITIONS Clinical	
D1															
D2															

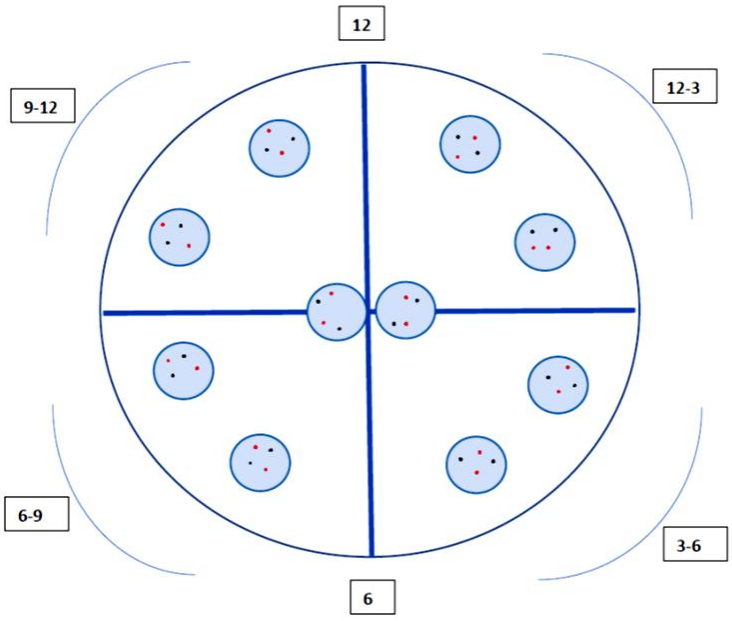
DLBCL										CHROMOGENIC IN SITU HYBRIDISATION			
LINKED CODE	TOPOGRAPHIC REGION OF BX	'STARRY-SKY' YES NO	CENTROBLASTIC	IMMUNOBLASTIC	ANAPLASTIC	PLASMACYTIC	MIXED	CONCOMITANT PATHOLOGY noted in tissue sections		Internal control positive (P) & negative (N)	External control positive (P) & negative (N)	*MYC* silver signals/ 50 tumour nuclei	CEN 8 red signals/ 50 tumour nuclei
D1													
D2													

DLBCL	IMMUNOHISTOCHEMISTR'	% of tumour cells immunoreactive (proportion)							FLUORESCENCE IN SITU HYBRIDISATION		
LINKED CODE	CD20 membranous proportion 0-100%	CD10 membranous porportion 0-100%	bcl-6 nuclear proportion 0-100%	BCL2 cytoplasmic proportion 0-100%	MUM1 nuclear proportion 0-100%	Ki-67 nuclear proportion 0-100%	MYC nuclear proportion 0-100%		*MYC* REARRANGEMENT Positive / Negative Not performed NP	*BCL2* Positive / Negative Not performed NP	*BCL6* Positive / Negative Not performed NP
D1											
D2											

IV: PBL data collection spreadsheet

PLASMABLASTIC LYMPHOMA				PBL	DATA CAPTURE SHEET											
Linked code		AGE at dx YEARS	GENDER MALE (M) FEMALE (F)	RVD Reactive (P) Non reactive(N) Unknown (U)		CD4 count	VIRAL LOAD	NHL STAGE	BONE MARROW INFILTRATION P+ N-	TREATMENT c-ART; CHOP; RCHOP; RCHOEP	DATE of LYMPHOMA DIAGNOSIS	FOLLOW UP DURATION	SURVIVAL OUTCOME DEMISED (D) ALIVE (A) UNKNOWN (U)	DURATION of SURVIVAL in DAYS	CONCOMITTANT CONDITIONS Clinical	
P1																
P2																
PBL																
			MORPHOLOGY :													
LINKED CODE	TOPOGRAPHIC REGION OF BX oral /extraoral		'STARRY-SKY' YES NO	BLASTIC/MONOMORPHIC YES NO				PLASMACYTIC YES NO	MIXED YES NO	CONCOMITANT PATHOLOGY noted in tissue sections						
P1																
P2																
PBL	IMMUNOHISTOCHEMISTRY			% of tumour cells immunoreactive				0-100%								
LINKED CODE	CONTROL Internal positive (P) negative (N)	external	CD20 membranous proportion	HHV8 nuclear Positive (P) Negative (N)				ALK1 cytoplasmic or nuclear Positive (P) Negative (N)		CD138 or CD38 membranous proportion		MUM1 nuclear proportion	KI-67 nuclear proportion	c-MYC nuclear proportion		
P1																
P2																
PBL	EPSTEIN-BARR VIRUS ENCODED SMALL RNA IN SITU HYBRIDISATION (EBER ISH)															
LINKED CODE	POSITIVE (P)		NEGATIVE (N)	not performed/tested												
P1																
P2																
PBL	CHROMOGENIC IN SITU HYBRIDISATION									FLUORESCENCE IN SITU HYBRIDISATION						
LINKED CODE	Internal control positive (P) & negative (N)		External control positive (P) & negative (N)	*MYC* silver signals/ 50 tumour nuclei				CEN 8 red signals/ 50 tumour nuclei		*MYC* Rearrangement Present/Not Present/Not Performed						
P1																
P2																

V: CISH interpretation tools



V(a): Selection of tumour cells per HPF.

LINKED CODE
EXTERNAL CONTROL P/N
INTERNAL CONTROL P/N

	FIELD 1		F2		F3		F4		F5		
	MYC	C8	MYC	C8	MYC	C8	MYC	C8	MYC	C8	
TUMOUR CELL 1											
C 2											
C 3											
C 4											
C 5											
C 6											
C 7											
C 8											
C 9											CLUSTERS/50
C 10											
TOTAL MYC SIGNALS/FIELD		0		0		0		0		0	….MYC/50CELLS
TOTAL C8 SIGNALS/FIELD	0		0		0		0		0		….C8/50CELLS

V(b): Data collection tool for dual-colour CISH signals noted in 50 tumour cells.

VI: Turn-it-in

UNIVERSITY OF THE WITWATERSRAND JOHANNESBURG

Division of Haematology, Department of Medicine, Chris Hani Baragwanath Academic Hospital, University of the Witwatersrand, Johannesburg

Chris Hani Road, Diepkloof, Soweto. Tel: +27 11 9339377, Fax: +27 11 9339449, email: moosa.patel@wits.ac.za

22 March 2022

The Chair

Postgraduate Committee

Faculty of Health Sciences

University of the Witwatersrand

Re: Turn-it-in report: Dr Sugeshnee Pather – postgraduate student number 9703787W. Title: 'Prognostic influence of *MYC* aberrations and other clinicopathological factors of aggressive B-cell Non-Hodgkin lymphomas'.

As the supervisor of Dr Sugeshnee Pather's PhD, I have reviewed the Turn-it-in report of her doctoral thesis. The Turn-it-in report identifies a similarity index of 28%, with 16% deriving from study publications. Much of the similarity relates to definitions, classifications and standardized lymphoma terminology. The other information which bears a similarity has been appropriately and correctly referenced.

Thank you

Yours sincerely

Moosa Patel MBChB, FCP(SA), MMed(Wits), FRCP(Lond.), PhD(Wits)

Emeritus Professor, Clinical Haematology Unit, Department of Medicine, Chris Hani Baragwanath Academic Hospital and the Faculty of Health Sciences, University of the Witwatersrand, Johannesburg, South Africa